NUREG/CR-6608
UCRL-ID-129211

Summary and Evaluation of Low-Velocity Impact Tests of Solid Steel Billet Onto Concrete Pads

Prepared by
M. C. Witte, J. Hovingh, G. C. Mok,
S. S. Mory, T. F. Chan, L. E. Fischer

Lawrence Livermore National Laboratory

Prepared for
U.S. Nuclear Regulatory Commission

AVAILABILITY NOTICE

Availability of Reference Materials Cited in NRC Publications

Most documents cited in NRC publications will be available from one of the following sources:

1. The NRC Public Document Room, 2120 L Street, NW., Lower Level, Washington, DC 20555–0001
2. The Superintendent of Documents, U.S. Government Printing Office, P. O. Box 37082, Washington, DC 20402–9328
3. The National Technical Information Service, Springfield, VA 22161–0002

Although the listing that follows represents the majority of documents cited in NRC publications, it is not intended to be exhaustive.

Referenced documents available for inspection and copying for a fee from the NRC Public Document Room include NRC correspondence and internal NRC memoranda; NRC bulletins, circulars, information notices, inspection and investigation notices; licensee event reports; vendor reports and correspondence; Commission papers; and applicant and licensee documents and correspondence.

The following documents in the NUREG series are available for purchase from the Government Printing Office: formal NRC staff and contractor reports, NRC-sponsored conference proceedings, international agreement reports, grantee reports, and NRC booklets and brochures. Also available are regulatory guides, NRC regulations in the *Code of Federal Regulations*, and *Nuclear Regulatory Commission Issuances*.

Documents available from the National Technical Information Service include NUREG-series reports and technical reports prepared by other Federal agencies and reports prepared by the Atomic Energy Commission, forerunner agency to the Nuclear Regulatory Commission.

Documents available from public and special technical libraries include all open literature items, such as books, journal articles, and transactions. *Federal Register* notices, Federal and State legislation, and congressional reports can usually be obtained from these libraries.

Documents such as theses, dissertations, foreign reports and translations, and non-NRC conference proceedings are available for purchase from the organization sponsoring the publication cited.

Single copies of NRC draft reports are available free, to the extent of supply, upon written request to the Office of Administration, Distribution and Mail Services Section, U.S. Nuclear Regulatory Commission, Washington, DC 20555–0001.

Copies of industry codes and standards used in a substantive manner in the NRC regulatory process are maintained at the NRC Library, Two White Flint North, 11545 Rockville Pike, Rockville, MD 20852–2738, for use by the public. Codes and standards are usually copyrighted and may be purchased from the originating organization or, if they are American National Standards, from the American National Standards Institute, 1430 Broadway, New York, NY 10018–3308.

DISCLAIMER NOTICE

NUREG/CR-6608
UCRL-ID-129211

Summary and Evaluation of Low-Velocity Impact Tests of Solid Steel Billet Onto Concrete Pads

Prepared by
M. C. Witte, J. Hovingh, G. C. Mok,
S. S. Murty, T. F. Chen, L. E. Fischer

Lawrence Livermore National Laboratory

Prepared for
U.S. Nuclear Regulatory Commission

D502/1

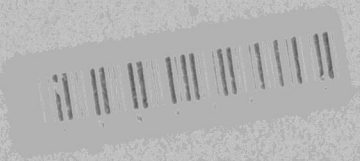

AVAILABILITY NOTICE

Availability of Reference Materials Cited in NRC Publications

Most documents cited in NRC publications will be available from one of the following sources:

1. The NRC Public Document Room, 2120 L Street, NW., Lower Level, Washington, DC 20555-0001
2. The Superintendent of Documents, U.S. Government Printing Office, P. O. Box 37082, Washington, DC 20402-9328
3. The National Technical Information Service, Springfield, VA 22161-0002

Although the listing that follows represents the majority of documents cited in NRC publications, it is not intended to be exhaustive.

Referenced documents available for inspection and copying for a fee from the NRC Public Document Room include NRC correspondence and internal NRC memoranda; NRC bulletins, circulars, information notices, inspection and investigation notices; licensee event reports; vendor reports and correspondence; Commission papers; and applicant and licensee documents and correspondence.

The following documents in the NUREG series are available for purchase from the Government Printing Office: formal NRC staff and contractor reports, NRC-sponsored conference proceedings, international agreement reports, grantee reports, and NRC booklets and brochures. Also available are regulatory guides, NRC regulations in the *Code of Federal Regulations*, and *Nuclear Regulatory Commission Issuances*.

Documents available from the National Technical Information Service include NUREG-series reports and technical reports prepared by other Federal agencies and reports prepared by the Atomic Energy Commission, forerunner agency to the Nuclear Regulatory Commission.

Documents available from public and special technical libraries include all open literature items, such as books, journal articles, and transactions. *Federal Register* notices, Federal and State legislation, and congressional reports can usually be obtained from these libraries.

Documents such as theses, dissertations, foreign reports and translations, and non-NRC conference proceedings are available for purchase from the organization sponsoring the publication cited.

Single copies of NRC draft reports are available free, to the extent of supply, upon written request to the Office of Administration, Distribution and Mail Services Section, U.S. Nuclear Regulatory Commission, Washington, DC 20555-0001.

Copies of industry codes and standards used in a substantive manner in the NRC regulatory process are maintained at the NRC Library, Two White Flint North, 11545 Rockville Pike, Rockville, MD 20852-2738, for use by the public. Codes and standards are usually copyrighted and may be purchased from the originating organization or, if they are American National Standards, from the American National Standards Institute, 1430 Broadway, New York, NY 10018-3308.

DISCLAIMER NOTICE

NUREG/CR-6608
UCRL-ID-129211

Summary and Evaluation of Low-Velocity Impact Tests of Solid Steel Billet Onto Concrete Pads

Manuscript Completed: December 1997
Date Published: February 1998

Prepared by
M. C. Witte, J. Hovingh, G. C. Mok,
S. S. Murty, T. F. Chen, L. E. Fischer

Lawrence Livermore National Laboratory
7000 East Avenue
Livermore, CA 94550

D. T. Tang, NRC Technical Monitor

Prepared for
Spent Fuel Project Office
Office of Nuclear Material Safety and Safeguards
U.S. Nuclear Regulatory Commission
Washington, DC 20555-0001
NRC Job Code A0293

Disclaimer

This work was supported by the United States Nuclear Regulatory commission under a Memorandum of Understanding with the United States Department of Energy, and performed under the auspices of the U.S. Department of Energy by Lawrence Livermore National Laboratory under Contract W-7405-Eng-48.

ABSTRACT

Spent fuel storage casks intended for use at independent spent fuel storage installations are evaluated during the application and review process for low-velocity impacts representative of possible handling accidents. In the past, the analyses involved in these evaluations have assumed that the casks dropped or tipped onto an unyielding surface—a conservative and simplifying assumption. Since 10 CFR Part 72, the regulation imposed by the Nuclear Regulatory Commission (NRC), does not require this assumption, applicants are currently seeking a more realistic model for the analyses to predict the effect of a cask dropping onto a reinforced concrete pad, including energy absorbing aspects such as cracking and flexure. To develop data suitable for benchmarking these analyses, the NRC has conducted several series of drop-test studies of a solid steel billet and of a near-full-scale empty cask.

This report contains a summary and evaluation of all steel billet testing conducted by Sandia National Laboratories and Lawrence Livermore National Laboratory. A series of finite element analyses of the billet testing is described and benchmarked against the test data. A method to apply the benchmarked finite element model of the soil and concrete pad to an analysis of a full-size storage cask is provided. In addition, an application to a "generic" full-size cask is presented for side and end drops, and tipover events.

The primary purpose of this report is to provide applicants for an NRC license under 10 CFR Part 72 with a method for evaluating storage casks for low-velocity impact conditions.

CONTENTS

TABLES

FIGURES

ACKNOWLEDGMENT

This work was funded by the Spent Fuel Technical Review Section, Spent Fuel Project Office, Office of Nuclear Material Safety and Safeguards, U. S. Nuclear Regulatory Commission (NRC). The authors would like to thank David T. Tang, technical monitor at the NRC, for his overall direction and specific contributions. The timely response and attention to detail by Lyssa Campbell during preparation of the manuscript are greatly appreciated.

SUMMARY AND EVALUATION OF LOW-VELOCITY IMPACT TESTS OF SOLID STEEL BILLET ONTO CONCRETE PADS

1. INTRODUCTION

Spent fuel storage casks intended for use at independent spent fuel storage installations (ISFSIs) typically are evaluated during the application and review process for low-velocity impacts representative of possible handling accidents. In the past, the analyses involved in these evaluations have assumed that the casks dropped or tipped onto an unyielding surface—a conservative and simplifying assumption. Since 10 CFR Part 72,[1] the regulation imposed by the Nuclear Regulatory Commission (NRC), does not require this assumption, applicants are currently seeking a more realistic model for the analyses to predict the effect of a cask dropping onto a reinforced concrete pad, including energy absorbing aspects such as cracking and flexure. To develop data suitable for benchmarking these analyses, the NRC has conducted several series of drop-test studies.

The first series, performed in March 1993 by Sandia National Laboratories (SNL), involved five end-drops of a solid steel billet, nominally 50.8 cm (20 inches) in diameter and 1.83 m (72 inches)long, onto pads of various stiffnesses from a height of 45.7 cm (18 inches.) The second series of tests, performed between July and October 1993, involved four end-drops of a near-full-scale empty Excellox 3A cask onto a full-scale concrete pad and foundation, and onto an essentially unyielding surface, from heights ranging from 45.7 cm (18 inches) to 1.52 m (60 inches.) These tests were conducted by British Nuclear Fuels Limited in Winfrith, England. (Two of the drops in the second series were sponsored jointly by Electric Power Research Institute and several storage cask user groups, vendors, and utilities.)* The third test series, performed in September 1993 by SNL, involved eight additional end-drop tests of the billet onto concrete pads. These pads were cast either on engineered fill or on undisturbed soil; the billet was dropped from heights ranging from 45.7 cm (18 inches) to 1.83 m (6 feet.) The first three series of tests are described in Reference 2.

The fourth test series included twelve drops of a solid steel cylindrical billet onto reinforced concrete pads resting on undisturbed soil. This series was conducted by Lawrence Livermore National Laboratory (LLNL) in February 1996. The size of the billet was selected to match the billet used in the Series 1 and 3 tests; it was a 1/3-scale model of a spent fuel storage cask (the linear dimension was scaled). The dimensions of the concrete pad were selected to match the concrete pads used in the Series 1 and 3 tests; however, the outside pad dimension was somewhat larger because tests in this series were primarily side drops and earlier tests were end-drops. The concrete pads were approximately 1/3-scale models of the symmetry section of a hypothetical ISFSI concrete storage pad, including the reinforcing steel and gravel within the concrete. Results and a preliminary evaluation of the side and tipover results from the fourth test series are provided in two reports[3,4] published by LLNL.

2. SCOPE AND PURPOSE

This report contains a summary and evaluation of all steel billet testing conducted by SNL and LLNL described above. A series of finite element analyses (FEA) of the billet testing is described and benchmarked against the test data. A method to apply the benchmarked finite element model of the soil and concrete pad to an analysis of a full-size storage cask is provided. In addition, an application to a "generic" full-size cask is presented for side and end drops, and tipover events.

---

* Note: The second series of tests is not discussed in this report.

The primary purpose of this report is to provide applicants for an NRC license under 10 CFR Part 72 with a method for evaluating storage casks for low-velocity impact conditions. The LLNL test data described in this report are directly available to applicants on diskettes from the NRC Public Document Room.[5]

3. SUMMARY OF THE BILLET TESTING

3.1 Series 1 Tests Conducted at Sandia in March 1993

Five drop tests were conducted in the first testing series at SNL. All five consisted of 45.7-cm (18-inch) end drops of a solid steel circular cylinder, 50.8 cm (20 inches) in diameter and 1.83 m (72 inches) long, weighing 2994 kg (6600 lb.)[2] The purpose of these tests was, in part, to characterize the effect of various foundation stiffnesses on the deceleration of the billet. In each case the billet was instrumented with four accelerometers attached as shown in Figure 1(a). The drop configurations are summarized in Table 1.

3.2 Series 3 Tests Conducted at Sandia in September 1993

Eight drop tests were conducted at SNL in the third test series.** All eight consisted of end drops of the same billet that was used in the Series 1 tests. The purpose of this third series was to further characterize the effect of various foundation stiffnesses on the deceleration of the billet. In each case the billet was dropped onto a concrete pad. The pad dimensions, rebar strength, substrate materials, and drop height were varied in this series. The billet was equipped with six accelerometers attached as shown in Figure 1(b). The drop configurations are summarized in Table 2.

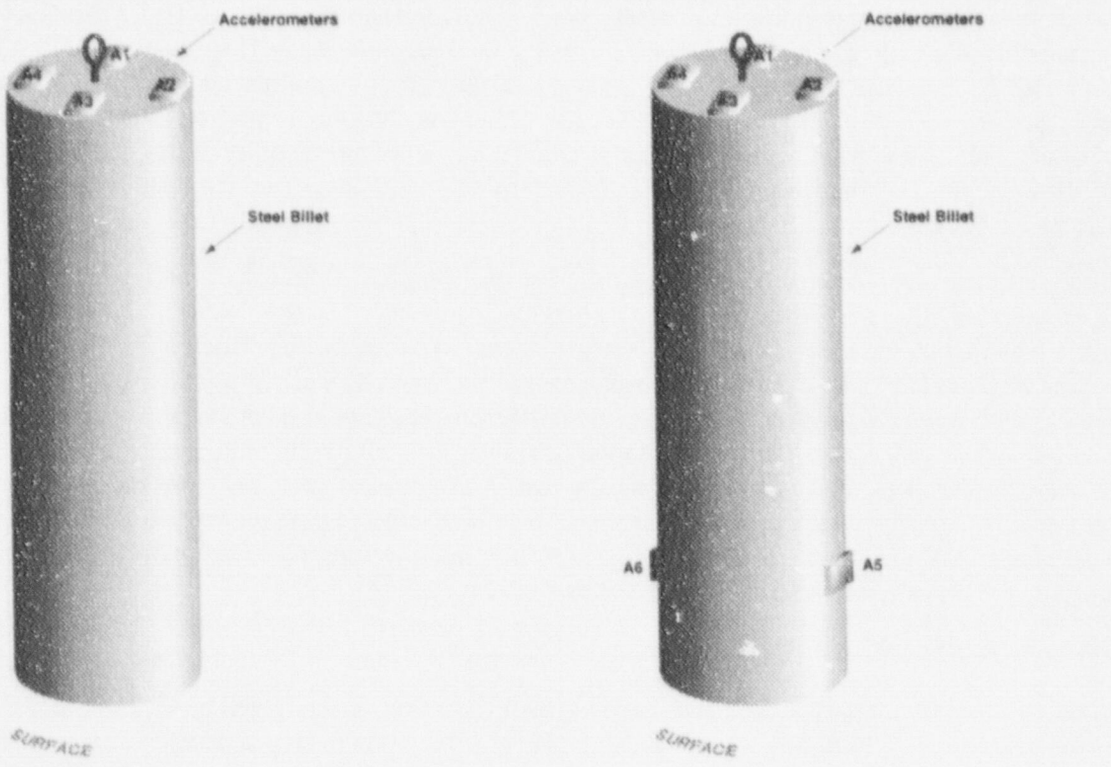

(a) SNL Series 1 End Drop Tests

(b) SNL Series 3 End Drop Tests

Figure 1. Accelerometer Locations for SNL End Drop Tests

** Note: The second series of tests of a near-full-scale empty cask is not discussed in this report.

Table 1. Billet Drop Tests Included in the Series 1 SNL Tests

Test Location / Date	Test ID	Pad Dimensions	Soil / engineered fill	Rebar	Drop Height
SNL/ March 1993	#166	N/A	unyielding surface	N/A	45.7 cm (18")
SNL/ March 1993	#167	1.83 m × 1.83 m × .3 m (6' × 6' × 1')	pad on unyielding surface	#3 on 45.7 cm (18") centers (yield strength = 4.14×10^5 kPa (60 ksi))	45.7 cm (18")
SNL/ March 1993	#168	1.83 m × 1.8 m × .3 m (6' × 6' × 1')	pad on .3m (1') fill on unyielding surface	#3 on 45.7 cm (18") centers (yield strength = 4.14×10^5 kPa (60 ksi))	45.7 cm (18")
SNL/ March 1993	#169	1.83 m × 1.83 m × .3 m (6' × 6' × 1')	unknown soil A / .3m (1') fill	#3 on 45.7 cm (18") centers (yield strength = 4.14×10^5 kPa (60 ksi))	45.7 cm (18")
SNL/ March 1993	#170	1.83 m × 1.83 m × .3 m (6' × 6' × 1') (reused the pad from test #169)	unknown soil A / .3m (1') fill	#3 on 45.7 cm (18") centers (yield strength = 4.14×10^5 kPa (60 ksi))	45.7 cm (18")

Table 2. Billet Drop Tests Included in the Series 3 SNL Tests

Test Location / Date	Test ID	Pad Dimensions	Soil / engineered fill	Rebar	Drop Height
SNL / Sept. 1993	#226, 1-A	1.83 m × 1.83 m × .3 m (6' × 6' × 1')	unknown soil B / .3 m (1') fill	#3 on 45.7 cm (18") centers (yield strength = 4.14×10^5 kPa (60 ksi))	45.7 cm (18")
SNL / Sept. 1993	#228, 2-B	1.83 m × 1.83 m × .3 m (6' × 6' × 1')	unknown soil B / .3 m (1') fill	#3 on 45.7 cm (18") centers (yield strength = 4.14×10^5 kPa (60 ksi))	45.7 cm (18")
SNL / Sept. 1993	#229, 3-C	1.83 m × 1.83 m × .23 m (6' × 6' × 9")	unknown soil B / .3 m (1') fill	#3 on 45.7 cm (18") centers (yield strength = 4.14×10^5 kPa (60 ksi))	45.7 cm (18")
SNL / Sept. 1993	#230, 4-D	1.83 m × 1.83 m × 45.7 cm (6' × 6' × 18")	unknown soil B / .3 m (1') fill	#3 on 45.7 cm (18") centers (yield strength = 4.14×10^5 kPa (60 ksi))	45.7 cm (18")
SNL / Sept. 1993	#231, 5-E	3 m × 3 m × .3 m (10' × 10' × 1')	unknown soil B / .3 m (1') fill	#3 on 45.7 cm (18") centers (yield strength = 4.14×10^5 kPa (60 ksi))	45.7 cm (18")
SNL / Sept. 1993	#232, 6-A	1.83 m × 1.83 m × .3 m (6' × 6' × 1')	unknown soil B, (pad on grade)	#3 on 45.7 cm (18") centers (yield strength = 4.14×10^5 kPa (60 ksi))	45.7 cm (18")
SNL / Sept. 1993	#233, 8-A	1.83 m × 1.83 m × .3 m (6' × 6' × 1')	unknown soil B / .3 m (1') fill	#3 on 45.7 cm (18") centers (yield strength = 4.14×10^5 kPa (60 ksi))	1.83 m (72")
SNL / Sept. 1993	#234, 9-A	1.83 m × 1.83 m × .3 m (6' × 6' × 1')	unknown soil B, (pad on grade)	#3 on 45.7 cm (18") centers (yield strength = 4.14×10^5 kPa (60 ksi))	1.83 m (72")

3.3 Series 4 Tests Conducted at LLNL in February 1996

Twelve drop tests were conducted at LLNL in the fourth test series. An almost identical billet was used for this series. The billet was 51.43 cm (20.25 inches) in diameter, 1.83 m (72 inches) long, and weighed 2937 kg (6475 lb.) The purpose of these tests was to characterize the effect of side drops and tipover events on the deceleration of the billet and to provide additional data for benchmarking finite element models. In each case the billet was dropped onto a reinforced concrete pad. The tests included two 45.7-cm (18-inch) end drops to provide a direct comparison with the SNL drop series, eight side drops from 45.7 cm (18 inches), 91.4 cm (36 inches), and 1.83 m (72 inches), and two tipovers, during which the billet was propped up to a center-of-gravity over corner position and then released. The pad dimensions, rebar strength, substrate materials, and drop height remained constant. The billet was instrumented with four or five accelerometers attached as shown in Figures 2a, b, and c. The drop configurations are summarized in Tables 3 through 5.

4. EVALUATION OF TEST DATA

4.1 Filtering Data to Determine Rigid Body Motion

Deceleration data were collected using Endevco piezoresistive accelerometers Model 7270A for both the SNL and the LLNL tests. The SNL tests used 7270A accelerometers rated for peak accelerations of 6000 and 20,000 g's. The accelerometers rated for up to 20,000 g's were considered unnecessary for the LLNL tests based on the SNL results. The sampling frequency for the SNL Series 1 data was 200 kHz, for the SNL Series 3 data it was 100 kHz. The SNL tests used an antialias filter with a frequency of 30 kHz. The LLNL data were sampled at 200 kHz and used a 100 kHz 6-pole Bessel analog antialias filter.

One characteristic of impact testing is the presence of vibratory motions or stress waves within the test article which are superimposed upon the rigid body deceleration, giving a high indication of the peak rigid body deceleration. To remove this vibratory component of the data, the raw accelerometer data described above were filtered at an appropriate frequency such that the remaining deceleration represented the rigid body motion of the billet.

To determine the appropriate filter frequency for this effort, several steps were taken. The lowest natural frequencies of the billet were analytically determined to be between 109 and 1406 Hz, as listed in Table 6. Fourier-spectrum analyses of the impact responses, were also performed to demonstrate the presence of those frequencies. The analyses showed that, in addition to the rigid body motion, the responses were dominated by a few modes of vibratory motion. These modes were longitudinal vibrations associated with the free-free and fixed-free end conditions for the end drop and bending vibrations associated with the free-free end conditions for the side drop and tipover. A low-pass Butterworth filter was chosen because it produced minimal amplitude distortions. The time delay or phase shift produced by the filter in the filtered signal was eliminated by performing a backward filtering after the normal forward filtering. An 8th order filter was used to provide an adequately sharp cutoff of the high-frequency response. Using the natural frequencies of the dominant vibrations of the billet as a guide, the cutoff frequency for filtering the billet drop test results was set at 450 Hz. The filtering was accomplished with the commercial software package DADiSP 4.0.[6] (The Fourier spectrum plots for each accelerometer trace for the SNL and LLNL tests are provided in References 2 and 3, respectively.) The cutoff frequency was located below the lowest dominant vibration frequency of the billet. The adequacy of the cutoff frequency was confirmed by comparing the Fourier spectrum of the filtered and unfiltered responses. The comparison showed that the filtering effectively removed vibratory motions associated with the billet free vibrations but preserved the rigid body response motion. An example of this comparison is provided in Figure 3. Raw deceleration time histories for each of the accelerometers for each drop, overlaid with the filtered data at 450 Hz, are provided in Appendices A and B.

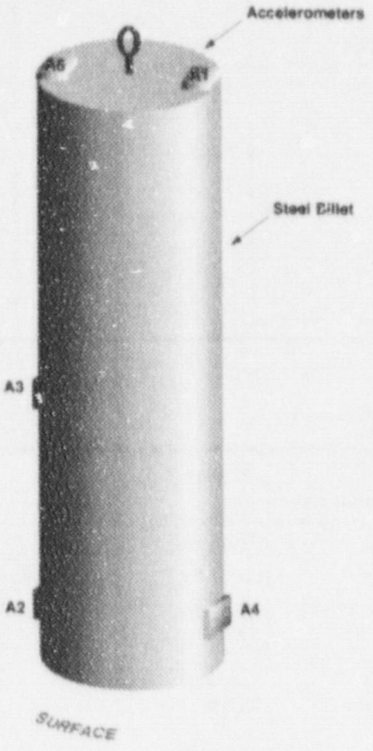

(a) LLNL End Drop Tests

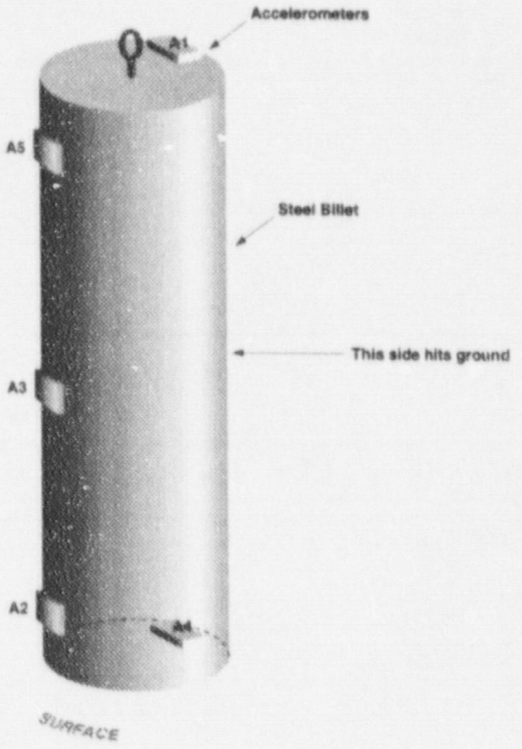

(b) LLNL Side Drop Tests

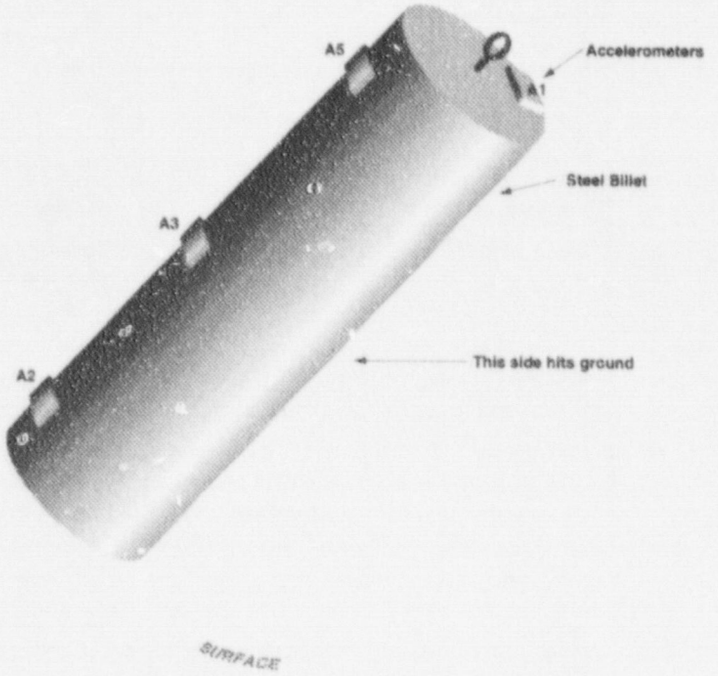

(c) LLNL Tipover Tests

Figure 2. Accelerometer Locations for LLNL Tests

Table 3. End Drop Billet Tests at LLNL

Test Location / Date	Test ID	Pad Dimensions	Soil / engineered fill	Rebar	Drop Height
LLNL / Feb. 1996	#1	3m × 3m × .3m (10' × 10' × 1')	approximately known soil C	#3 on 45.7 cm (18") centers (yield strength = 4.14 × 10^5 kPa (60 ksi))	45.7 cm (18")
LLNL / Feb. 1996	#2	3m × 3m × .3m (10' × 10' × 1') (reused the pad from test #1)	approximately known soil C	#3 on 45.7 cm (18") centers (yield strength = 4.14 × 10^5 kPa (60 ksi))	45.7 cm (18")

Table 4. Side Drop Billet Tests at LLNL

Test Location / Date	Test ID	Pad Dimensions	Soil / engineered fill	Rebar	Drop Height
LLNL / Feb. 1996	#3	3 m × 3 m × .3 m (10' × 10' × 1')	approximately known soil C	#3 on 45.7 cm (18") centers (yield strength = 4.14 × 10^5 kPa (60 ksi))	45.7 cm (18")
LLNL / Feb. 1996	#5	3 m × 3 m × .3 m (10' × 10' × 1')	approximately known soil C	#3 on 45.7 cm (18") centers (yield strength = 4.14 × 10^5 kPa (60 ksi))	45.7 cm (18")
LLNL / Feb. 1996	#10	3 m × 3 m × .3 m (10' × 10' × 1') (reused the pad from test #9)	approximately known soil C	#3 on 45.7 cm (18") centers (yield strength = 4.14 × 10^5 kPa (60 ksi))	45.7 cm (18")
LLNL / Feb. 1996	#4	3 m × 3 m × .3 m (10' × 10' × 1') (reused the pad from test #3)	approximately known soil C	#3 on 45.7 cm (18") centers (yield strength = 4.14 × 10^5 kPa (60 ksi))	91.4 cm (36")
LLNL / Feb. 1996	#7	3 m × 3 m × .3 m (10' × 10' × 1')	approximately known soil C	#3 on 45.7 cm (18") centers (yield strength = 4.14 × 10^5 kPa (60 ksi))	91.4 cm (36")
LLNL / Feb. 1996	#9	3 m × 3 m × .3 m (10' × 10' × 1')	approximately known soil C	#3 on 45.7 cm (18") centers (yield strength = 4.14 × 10^5 kPa (60 ksi))	91.4 cm (36")
LLNL / Feb. 1996	#6	3 m × 3 m × .3 m (10' × 10' × 1') (reused the pad from test #5)	approximately known soil C	#3 on 45.7 cm (18") centers (yield strength = 4.14 × 10^5 kPa (60 ksi))	1.83 m (72")
LLNL / Feb. 1996	#8	3 m × 3 m × .3 m (10' × 10' × 1') (reused the pad from test #7)	approximately known soil C	#3 on 45.7 cm (18") centers (yield strength = 4.14 × 10^5 kPa (60 ksi))	1.83 m (72")

Table 5. Tipover Billet Tests at LLNL

Test Location / Date	Test ID	Pad Dimensions	Soil / engineered fill	Rebar	Drop Height
LLNL / Feb. 1996	#11	3 m × 3 m × 3 m (10' × 10' × 1')	approximately known soil C	#3 on 45.7 cm (18") centers (yield strength = 4.14 × 10^5 kPa (60 ksi))	tip
LLNL / Feb. 1996	#12	3 m × 3 m × .3 m (10' × 10' × 1') (reused the pad from test #11)	approximately known soil C	#3 on 45.7 (18") centers (yield strength = 4.14 × 10^5 kPa (60 ksi))	tip

Table 6. Natural Frequencies of 1.83-meter (72-inch) Long, 50.8-cm (20-inch) Diameter Steel Billet

Longitudinal with both ends free	Longitudinal with one end free, one end fixed	Bending with both ends free	Bending with one end fixed, the other pinned	Bending with one end fixed, the other free
1406 Hz	703 Hz	696 Hz	477 Hz	109 Hz

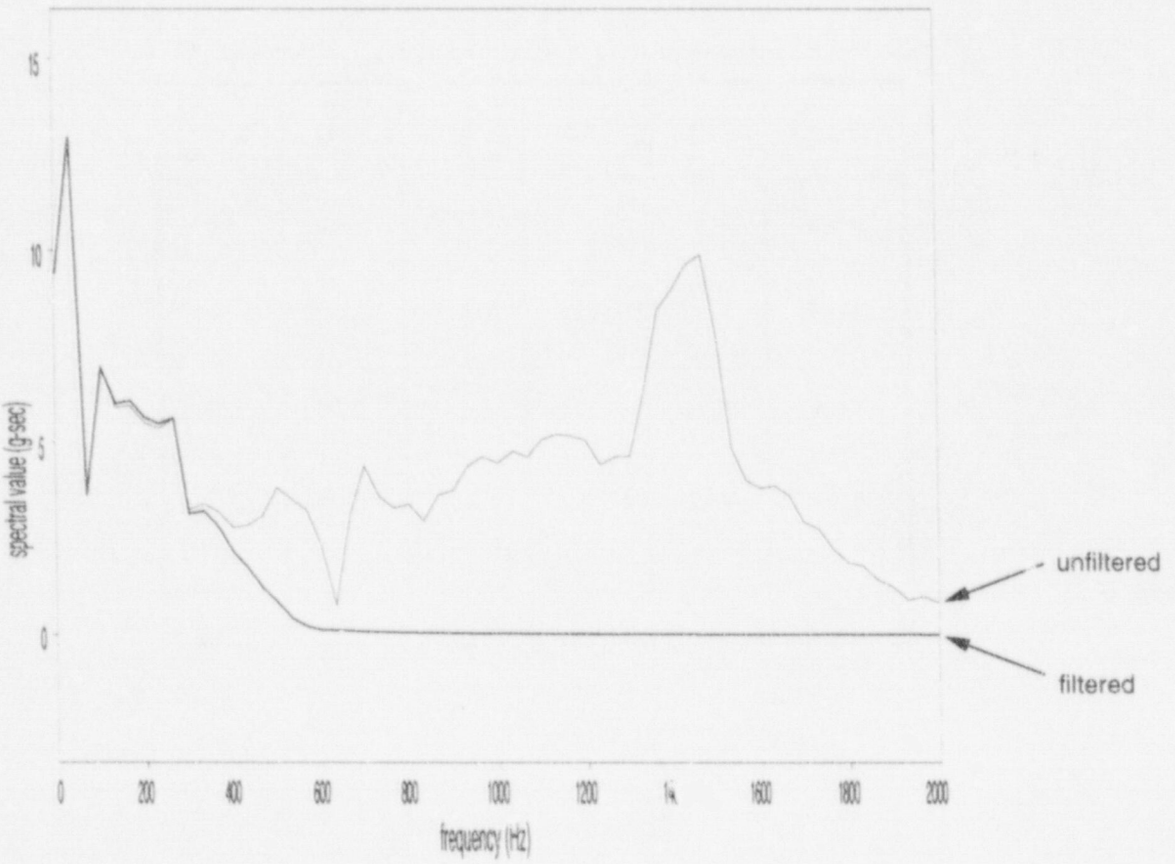

Figure 3. Comparison of the Filtered and Unfiltered Fourier Spectrum for LLNL Test #1, Accelerometer A1

4.2 Discussion of Billet Test Results

4.2.1 End Drop Tests

Maximum rigid body decelerations of the billet resulting from the end drop tests at SNL and LLNL for individual accelerometers are tabulated in Tables 7 through 9. Note that the mean is calculated only for those accelerometers located on the billet upper end: A1 through A4 for the SNL tests, and A1 and A5 for the LLNL tests, because these accelerometers provide data which are readily comparable.

4.2.1.1 Effect of Pad Dimensions on End Drop Results

It can be seen from SNL tests #226, 229, and 230 that the concrete pad thickness affects the deceleration, as expected.

4.2.1.2 Effect of Substrate Materials on End Drop Results

The SNL tests included a variety of substrate materials, including an unyielding surface with or without a concrete pad or engineered fill, and soil with or without engineered fill above it. Details on the engineered fill are limited. The fill conformed to Stone and Webster Specification 12911.54, which covers site preparation and foundation preparation. A small amount of dry cement was added to the fill. The effect of the thirty centimeters of fill was to increase the deceleration of the cask by roughly 33 and 53 percent in two cases, as can be seen in Figure 4.

Table 7. SNL Series 1
Maximum Deceleration at Each Accelerometer, g's, Filtered at 450 Hz

Test ID	A1	A2	A3	A4	Mean
#166	*	210.0	211.5	258.9	226.8
#167	183.4	188.8	206.0	189.4	191.7
#168	202.9	197.2	211.6	217.7	207.4
#169	98.3	*	134.7	115.8	116.3
#170	108.9	*	117.5	126.8	117.7

* Accelerometer failed

Table 8. SNL Series 3
Maximum Deceleration at Each Accelerometer, g's, Filtered at 450 Hz

Test ID	A1	A2	A3	A4	A5	A6	Mean
#226	131.3	103.2	107.6	131.3	*	106.4	118.4
#228	129.6	126.2	143.7	141.5	127.0	120.8	135.3
#229	121.4	99.2	105.6	123.4	107.3	100.5	112.4
#230	167.9	154.5	156.4	164.0	148.6	143.7	160.7
#231	134.8	117.1	122.7	140.2	123.2	116.8	128.7
#232	84.0	89.5	93.8	87.5	80.1	80.1	88.7
#233	205.2	205.7	210.2	202.4	191.0	187.4	205.9
#234	123.0	122.3	147.3	146.3	123.7	120.6	134.7

* Accelerometer failed

Table 9. Maximum Deceleration at Each Accelerometer, g's, Filtered at 450 Hz, LLNL End Drops

Test ID	A1	A2	A3	A4	A5	Mean
#1	70.8	80.7	109.5	87.2	103.8	87.8
#2	78.7	63.6	89.8	75.4	88.0	83.3

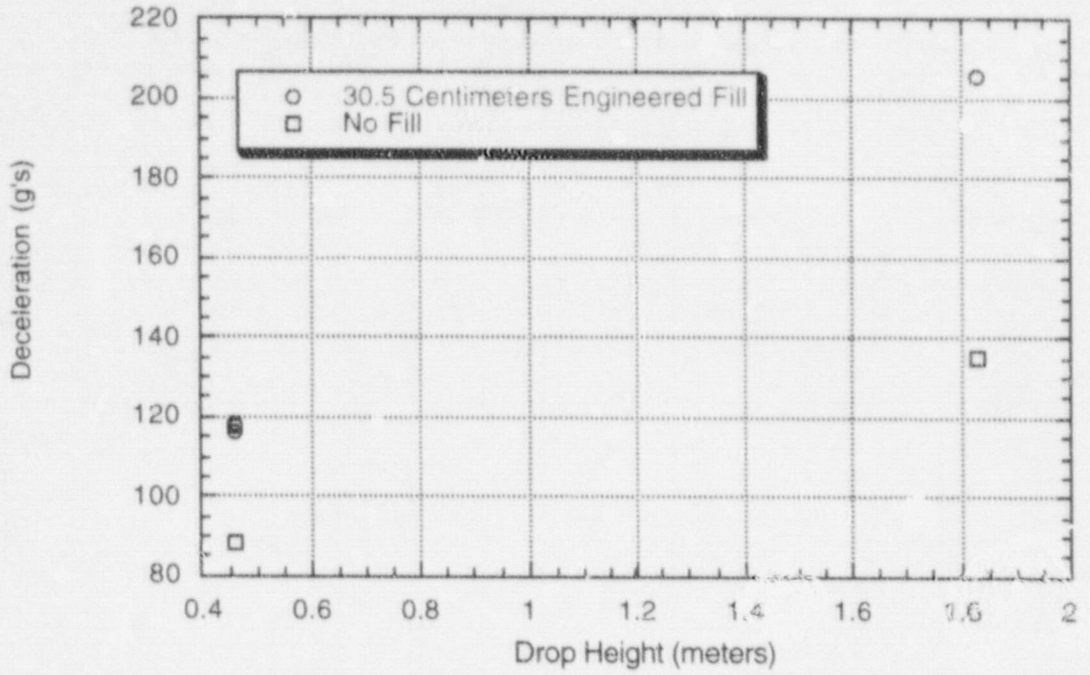

Figure 4. Effect of Engineered Fill on Decelerations, End Drops at SNL

4.2.1.3 Effect of Drop Height on End Drop Results

Again, limited SNL test data are available to measure the effect of the drop height on the deceleration results for the end drop cases, since only two drop heights were tested. Nevertheless, the trend of the results is the expected one—as the drop height is increased, the deceleration increases.

4.2.1.4 Comparison of SNL and LLNL End Drop Tests

Although no tests had identical configurations at SNL and LLNL, one SNL end drop test is similar to the two LLNL end drop tests. This is SNL test #232, an 45.7-m (18-inch) end drop onto a 1.83 m × 1.83 m × .3 m (6' × 6' × 1') thick concrete pad, without fill. The only differences between this test and LLNL tests #1 and #2 are that the SNL concrete pad is smaller than the LLNL pad, which was 3 m × 3 m × .3 m (10' × 10' × 1') thick, and the test was conducted in a different location with therefore different soil. Nevertheless, the decelerations are very comparable, with the SNL average for test #232 at 88.7 g's, and the LLNL averages at 87.8 g's and 83.3 g's for LLNL tests #1 and #2, respectively.

4.2.2 Results of LLNL Side Drop Tests

Maximum decelerations of the billet resulting from the side drop tests for individual accelerometers are tabulated in Table 10.

Table 10. Maximum Deceleration at Each Accelerometer, g's, Filtered at 450 Hz, LLNL Side Drops

Test ID	Drop Height	A1	A2	A3	A4	A5
#3	45.7 cm (18")	148.8	136.9	108.2	129.9	154.0
#4	1.83 m (72")	200.0	180.7	110.0	173.1	198.7
#5	45.7 cm (18")	145.8	172.4	86.0	171.2	164.4
#6	1.83 m (72")	246.3	225.7	206.7	227.0	251.5
#7	91.4 cm (36")	154.2	179.5	*	176.8	162.0
#8	1.83 m (72")	84.9	*	197.0	227.9	255.1
#9	1.83 m (72")	274.9	*	125.2	152.5	253.5
#10	45.7 cm (18")	120.6	*	125.5	107.0	135.3

* Accelerometer failed

4.2.2.1 Possible Obliqueness of Side Drops

A review of the deceleration time history plots shows that the billet did not hit squarely on its side for most of the drops (a summary of this is provided in Table 11). The effect of hitting the ground obliquely is more significant for a side drop than it is for an end drop since rotational motion is added to the vertical velocity as soon as the first end impacts. The time between one end hitting and then the other end hitting is usually less than 0.5 milliseconds, which at the impact velocity associated with a 91.44-cm (36-inch) drop indicates an out-of-alignment of about one quarter of a centimeter. This rotational motion, even though it was very slight, increased the deceleration at the ends of the billet, sometimes significantly. The billet center (accelerometer location A3) produced results which were more consistent with each other than the accelerometers which were located at the ends. A plot of deceleration vs. drop height for all of the side drops, for channel A3 only, is provided in Figure 5.

Table 11. Possible Obliqueness of Side Drops

	Test Identification	Drop level, yes or no?	Comment
45.7 cm (18") Side Drops)	Test #3	Yes	
	Test #5	No	Bottom end hit first
	Test #10	No	Bottom end hit first
91.4 cm (36") Side Drops	Test #4	No	Bottom end hit first
	Test #7	No	Bottom end hit first
	Test #9	No	Top end hit first
1.83 m (72") Side Drops	Test #6	No	Top end hit first
	Test #8	No	Top end hit first

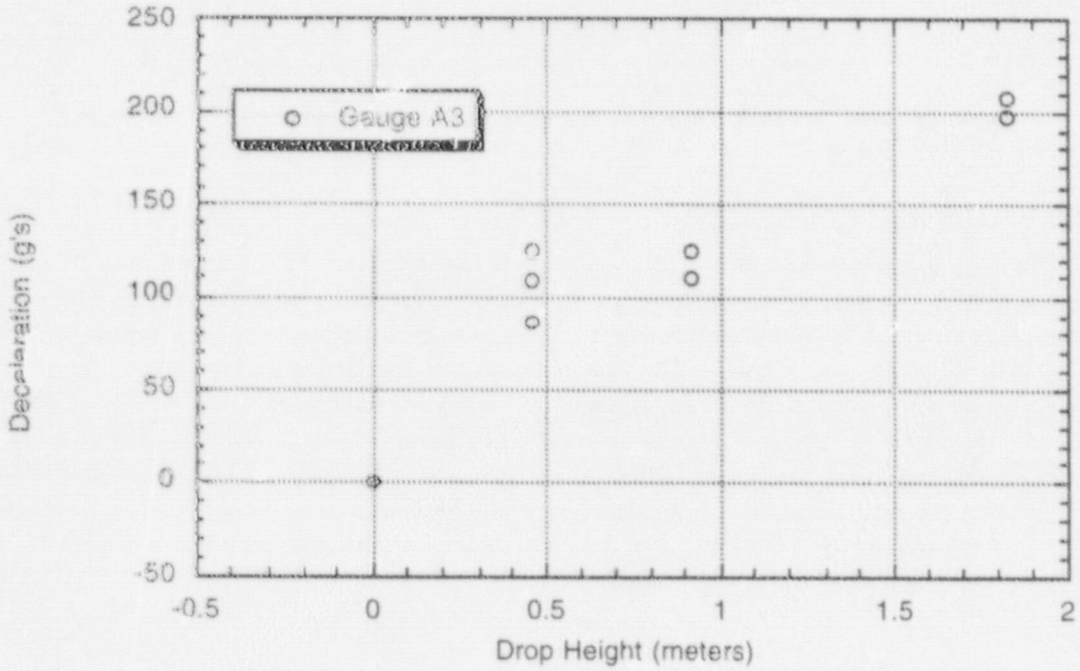

Figure 5. Deceleration vs. Drop Height for All of the Side Drops Tests, for Gauge A3 Only

4.2.3 Tipover Tests

Maximum decelerations of the billet resulting from the tipover tests at LLNL for individual accelerometers are tabulated in Table 12.

Table 12 Maximum Deceleration at Each Accelerometer, g's Filtered at 450 Hz, LLNL Tipover Tests

Test ID	A1	A2	A3	A5
#11	237.5	41.5	107.3	231.5
#12	213.6	17.1	107.8	213.0

5. DESCRIPTION OF FINITE ELEMENT MODEL REPRESENTATION OF BILLET TESTING

5.1 General Description of the Finite Element Model

A finite element model of the steel billet, concrete pad, and the subgrade soil was constructed using the TrueGrid[7] mesh generator. The model takes advantage of symmetry planes that exist in this drop orientation; thus, only a quarter model is needed for the billet side drop impact analysis. A half model was used for the billet tipover analysis. The quarter model included a 4.57 m × 4.57 m × 5.77 m (180" × 180" × 227") deep soil section, with a quarter section of the 3 m × 3 m × .3 m (10' × 10' × 1') thick pad. A half model is shown in Figure 6. The impact event was simulated with the nonlinear finite element code DYNA3D.[8] Slide surfaces with voids are placed between the steel billet and the concrete pad and between the concrete pad and the subgrade soil. A coefficient of friction of 0.25 was assumed for both slide surfaces. A non-reflecting boundary condition is also imposed on the embedded faces of the soil model, except on the symmetry face(s), to represent the true situation of infinite soil domain with no stress wave reflection from soil medium. The billet end and side impacts were simulated by imposing a uniform initial velocity on the billet; the tipover is simulated by applying an initial angular velocity to the billet.

5.2 Material Models Used in the Finite Element Model

5.2.1 Steel Billet Material Representation

The material of the test billet was ASTM 576 Grade 1045 steel, with a tensile strength of 6.69×10^5 kPa (97 ksi) and a yield strength of 4.14×10^5 kPa to 4.62×10^5 kPa (60 to 67 ksi), as specified by the supplier. The material can be represented by a perfectly elastic model with

$E = 2.0685 \times 10^8$ kPa (30.0×10^6 psi,) Young's modulus

$\upsilon = 0.29$, Poisson's ratio

density = 7819 kg/m^3 (488 lb./ft^3)

5.2.2 Subgrade Soil Representation

Soil properties vary widely from site to site; therefore, selecting a soil model to cover most situations is difficult. In light of this uncertainty, a simple elastic model was chosen to represent the subgrade soil. Representative ranges of soil values, provided in Table 13, vary significantly, even in the elastic range.

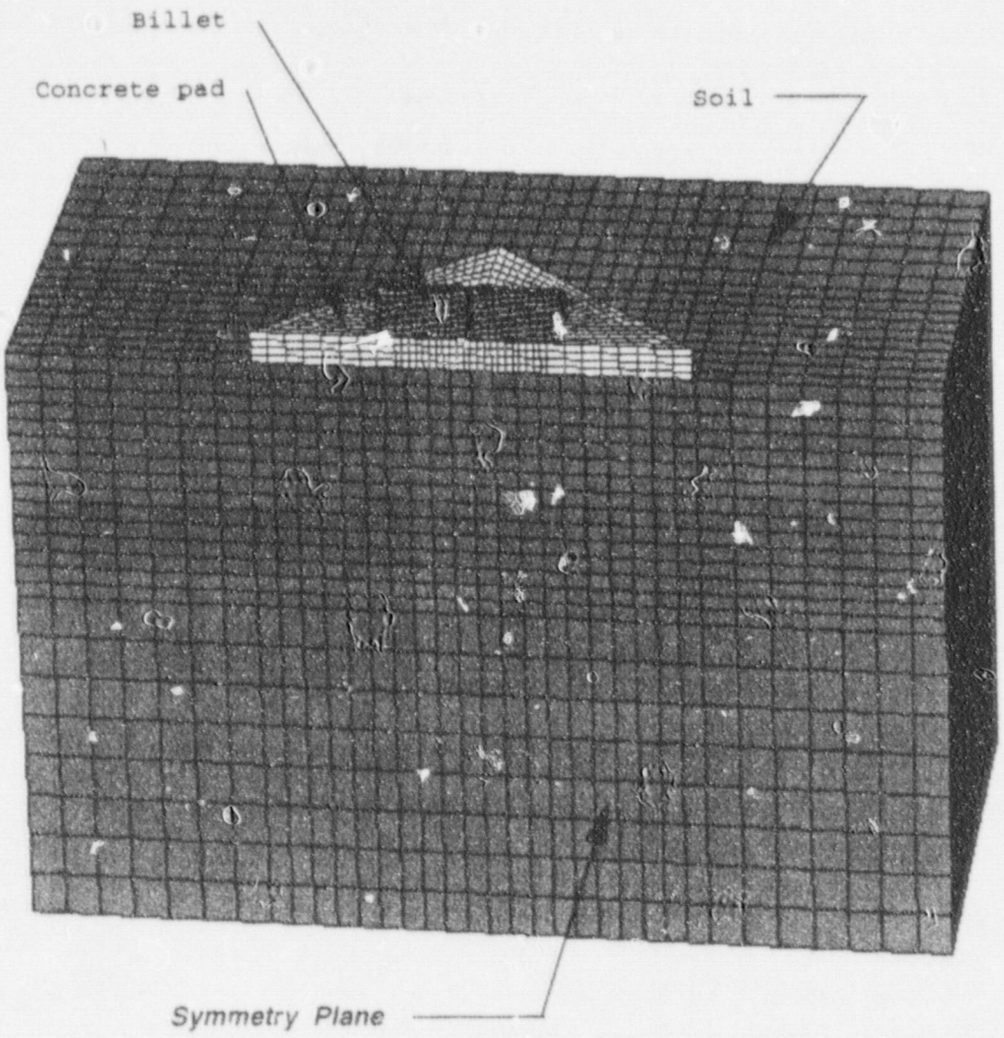

Figure 6. Finite Element Model of Steel Billet Side Drop and Tipover onto Concrete Pad and Soil

Table 13. Soil Elastic Parameters[9]

Subgrade	E	υ
Clay	345 kPa - 4.13×10^4 kPa (0.05 – 6.0 ksi)	0.1 – 0.5
Glacial fill	1.03×10^4 - 1.5×10^5 kPa (1.5 – 22.0 ksi)	
Sand	6.9×10^3 - 8.3×10^4 kPa (1.0 – 12.0 ksi)	0.2 – 0.4
Sand and Gravel	4.8×10^4 - 1.9×10^5 kPa (7.0 – 28.0 ksi)	0.1 – 0.4
Loess	1.8×10^4 - 5.5×10^4 kPa (2.0 – 8.0 ksi)	0.1 – 0.3
Shales	14×10^5 - 1.4×10^7 kPa (20.0 – 2000.0 ksi)	
Silt	2.1×10^3 - 2.1×10^4 kPa (0.3 – 3.0 ksi)	0.3 – 0.35

A few analytical simulations of the billet 1.83-meter (72-inch) side drop onto a concrete pad, on top of soil were made with varying soil elastic parameters. Young's Modulus for the soil was varied from a minimum of 3.4×10^4 kPa (5 ksi) to a maximum of 4.1×10^6 kPa (600 ksi,) and Poisson's ratio, υ, was varied from 0.1 to 0.45, even though some of these combinations are unrealistic. These variations in soil elastic properties produced little differences in the predicted initial 'peak' deceleration of the billet, as shown in Table 14.

A perfectly elastic soil model with

$E = 4.1 \times 10^4$ kPa (6 ksi)

$\upsilon = 0.45$

$\rho = 2179$ kg/m^3 (136 lb./ft.^{3})

was selected as most representative of the properties of the Livermore drop test site due to the saturated nature of the sandy clay ground during the testing in Livermore.

5.2.3 Concrete Representation

The concrete pad is modeled using a constitutive model based on a concrete which was developed by LLNL for the Shippingport Station Decommissioning Project in 1988.[10] The model was developed for the concrete fill in the reactor pressure vessel/neutron shield tank. At the time that the model was developed, Stanford Research Institute was contracted to measure the required properties of samples of the particular concrete grout used in the Shippingport project. Because the average compressive strengths of the Shippingport concrete grout and the concrete pads for this drop test study were similar, a modification to the Shippingport concrete model was used for the drop test concrete pad. In the present simulation, no steel reinforcement has been explicitly modeled even though the pads did in fact contain reinforcing steel. The model was judged to behave satisfactorily. Details of the concrete model used in the simulations described in this report are provided in Appendix C.

Table 14. Maximum g's for 1.83-meter (72-inch) Billet Side Drop Analysis Results Filtered at 450 Hz, for a Range of Elastic Soil Properties

	Poisson's ratio υ=0.1 (such as some rock) ρ = 1600 kg/m^3 (100 lb./ft.^{3})	Poisson's ratio υ=0.2 (such as unsaturated clay) ρ = 1600 kg/m^3 (100 lb./ft.^{3})	Poisson's ratio υ=0.3 (such as unsaturated clay) ρ = 1600 kg/m^3 (100 lb./ft.^{3})	Poisson's ratio υ=0.45 (such as saturated clay) ρ = 1600 kg/m^3 (100 lb./ft.^{3})	Poisson's ratio υ=0.45 (such as saturated sandy-clay) ρ = 2179 kg/m^3 (136 lb./ft.^{3})
Young's Modulus E=3.44 × 10^4 kPa (5 ksi) (such as some rock)	169	170	171	175	
Young's Modulus E=4.14 × 10^4 kPa (6 ksi)	170	170	171	177	190
Young's Modulus E=8.27 × 10^4 kPa (12 ksi) (such as dense sand)	170	170	172	184	198
Young's Modulus E=1.93 × 10^5 kPa (28 ksi) (such as dense gravel)	173	175	178	201	
Young's Modulus E=4.14 × 10^6 kPa (600 ksi) (such as shale)			296		

5.3. Steel Billet Impact Finite Element Simulation Results

The analysis results for the steel billet impact simulation include the response calculated by the finite element code at each calculational time step (3.7 × 10^{-6} seconds). The analysis results were filtered using the same filtering technique used for the test results, an eighth-order Butterworth low-pass filter with a cutoff frequency of 450 Hz. Both analysis data and test data were processed using DADiSP 4.0. Results are provided in Tables 15, 16, and 17. These tables show that the finite element simulation results of the billet impact event for end drop, side drop, and tipover using the material models described are in good agreement with test results. The comparison is also depicted graphically in Figure 7, for the side drops.

Table 15. Maximum Billet End Drop Deceleration Test vs. Simulation

Test # / Channel #	Test data, filtered at 450 Hz	Finite element analysis simulation, filtered at 450 Hz
Test #1/ Channel A1	70.8 g	
Test #2 / Channel A1	78.7 g	
Test #1 / Channel A5	103.8 g	99.5g
Test #2 / Channel A5	88.0 g	

Table 16. Maximum Billet Side Drop Deceleration Test vs. Simulation

Billet drop height / (Test #)	Test data from channel A3, filtered at 450 Hz	Finite element analysis simulation, filtered at 450 Hz
45.7 cm (18 inches) (Test #3)	108.2 g	105.0 g
45.7 cm (18 inches) (Test #5)	86.0 g	
45.7 cm (18 inches) (Test #10)	125.5 g	
91.4 cm (36 inches) (Test #4)	110.0 g	142.7 g
91.4 cm (36 inches) (Test #7)	not available	
91.4 cm (36 inches) (Test #9)	125.2 g	
1.83 cm (72 inches) (Test #6)	206.7	190.1 g
1.83 cm (72 inches) (Test #8)	197.0	

Table 17. Maximum Billet Tipover Deceleration Test vs. Simulation

Test # / Channel #	Test data, filtered at 450 Hz	Finite element analysis simulation, filtered at 450 Hz
Test #11/ Channel A1	237.5 g	244.7 g
Test #12 / Channel A1	213.6 g	
Test #11 / Channel A5	231.5 g	
Test #12 / Channel A5	213.0 g	

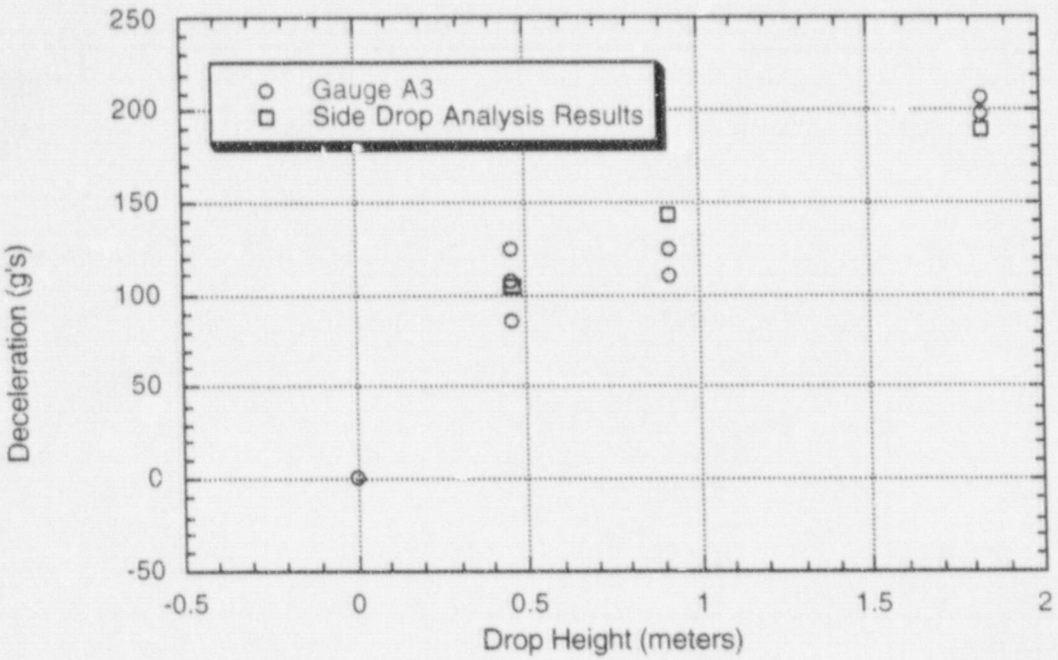

Figure 7. Comparison of Analysis and Test Results for Billet Side Drops

6. FULL SIZE "GENERIC" STORAGE CASK FINITE ELEMENT SIMULATIONS

6.1 Selection and Modeling of "Generic" Cask

A storage cask using representative dimensions, material properties, and cask weight was selected for this study. The cask selected is referred to in this report as a "generic" cask, and is shown in Figure 8. The "generic" storage cask end and side drops and tipover were simulated with the DYNA3D finite element code using the concrete and soil material property representations described in Section 5.

The finite element model for the "generic" cask is shown in Figure 9. Only the essential structural members of the cask are included in the model. Components such as trunions and an external neutron shield are neglected. The basket structure and fuel assemblies are modeled as a solid cylinder in the region within the cask cavity occupied by fuel. The weight distribution of the cylinder representing the basket structure is representative of a typical basket with fuel assemblies. The stiffness of the cylinder is set at $E = 1.9 \times 10^7$ kPa (2.8×10^6 psi) to reflect the flexible nature of the basket structure. As can be seen in Figure 9, the basket is modeled in sections to facilitate data reduction at various locations along the basket length.

Sliding interfaces are placed between the cask and the concrete pad, and between the concrete pad and the soil. The concrete pad dimensions used in the simulation are 4.06-meters wide, 5.08-meters long, and .91-meters thick (160-inches wide, 200-inches long, and 36-inches thick.) The full soil model (not accounting for symmetry) is 20.3-meters wide, 14.0-meters thick, and 11.9-meters deep into the ground (800-inches wide, 550-inches thick, and 470-inches deep.) The finite element model takes advantage of the symmetry plane along the axis of the cask. Non-reflecting boundary conditions are imposed on all faces of the soil model to prevent artificial stress wave reflections from the boundaries of the soil model.

The cask tipover impact is simulated with DYNA3D by imposing an angular velocity of 1.729 radians/sec (the angular velocity associated with a center-of-gravity over corner tip condition) to the entire cask body.

The center of rotation is set at the edge of the cask bottom. DYNA3D calculates the initial velocity components associated with each node for this rotational motion.

6.2 Additional Finite Element Analyses for End Drop

In order to verify that the end drop analysis correctly predicted the rigid body deceleration of the cask, two additional finite element analyses of the end drop were accomplished. In the first analysis, the cask contents were not included at all, and their total weight, including the basket, was added to the weight of the endcap by increasing the mass of the endcap. The results of this case are referred to as the "hollow model" in the results section below.

In the second additional analysis, the cask was modeled as a homogenous solid body with the density required to obtain the correct cask total weight, including the fuel assemblies and basket. The results of this case are referred to as the "solid homogeneous model" in the results section below.

6.3 Finite Element End Drop, Side Drop, and Tipover Simulation Results

The maximum rigid body decelerations are obtained from the simulations for end and side drops and tipover of the "generic" cask. The analysis results from these simulations have been filtered in a manner similar to the billet data filtering process. The cutoff frequency for filtering the generic cask analysis results was set at 350 Hz based on a review of the significant vibration response in the Fourier spectrum.

Maximum decelerations are listed in Table 18. Deceleration time histories for these analyses are included in Appendix D to this report. The results from the two additional analyses for the end drop are provided in Table 19. The adequacy of the cutoff frequency was confirmed by evaluating the Fourier spectra of the responses, averaged through the endcap for the "hollow model" and through the cask body for the "solid homogeneous model," as shown in Figures 10 and 11, respectively.

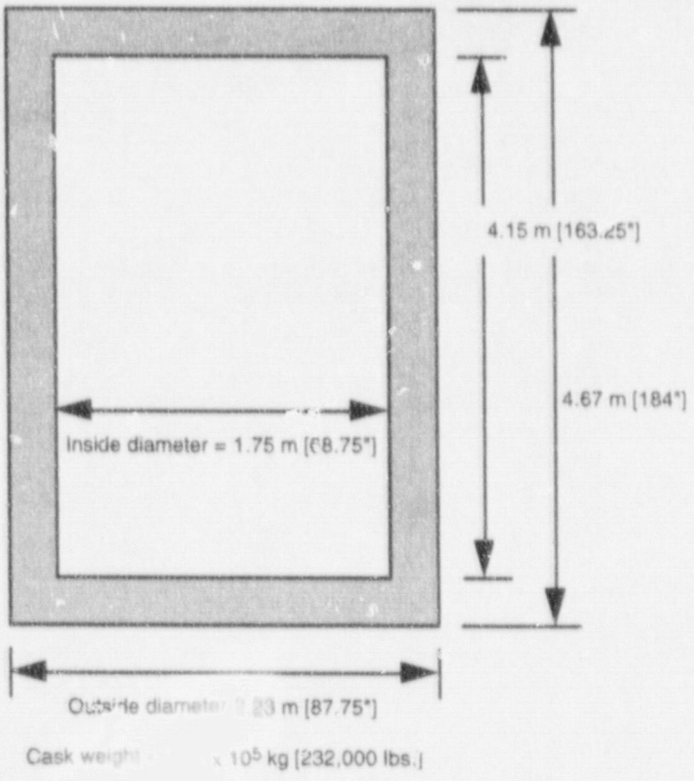

Figure 8. Generic Cask Dimensions

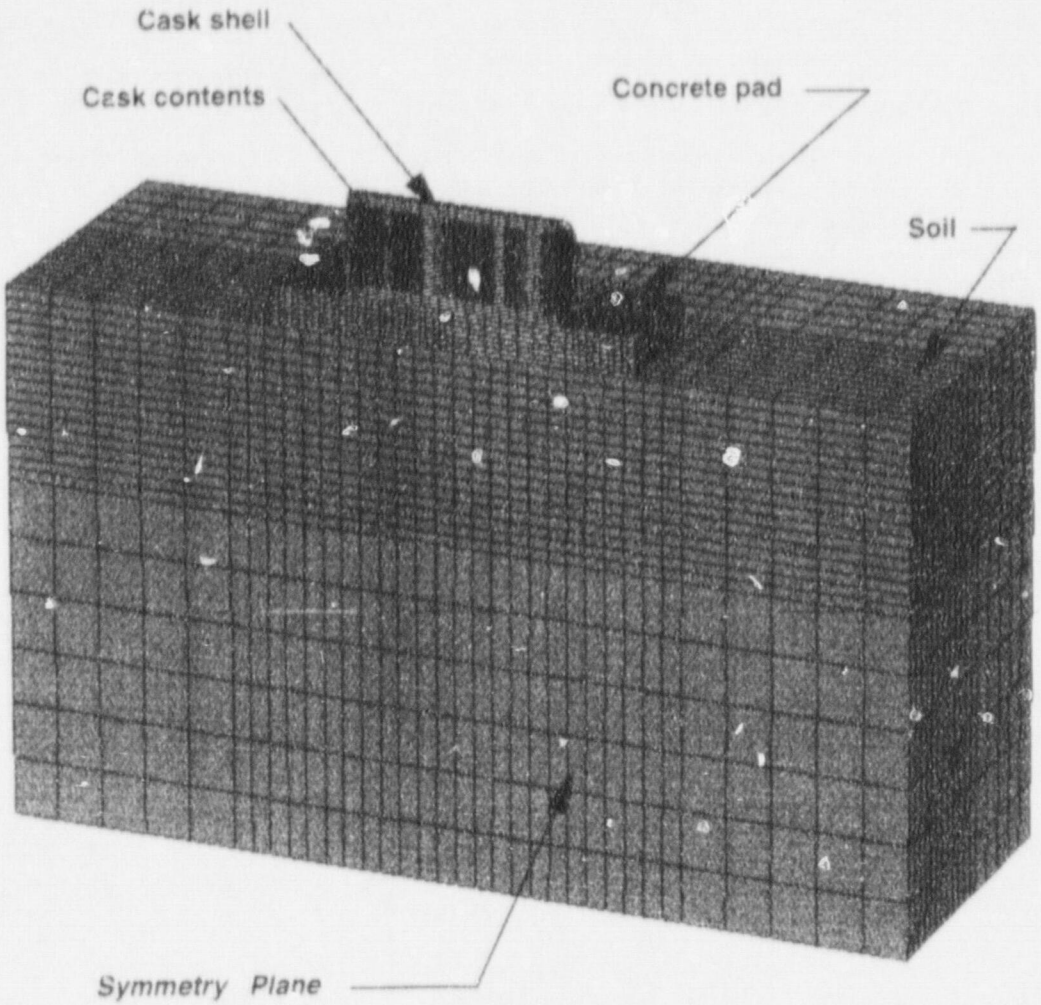

Figure 9. Finite Element Model of "Generic" Storage Cask, Side Drop and Tipover Onto Concrete Pad and Soil

Table 18. ISFSI Generic Cask End Drop, Side Drop, and Tipover Analysis Results

	Finite element analysis simulation, filtered at 350 Hz	Location of reported g's
45.7 cm (18") End Drop	47.3	Averaged through the cask wall
45.7 cm (18") Side Drop	23.2	Averaged through the cask wall
91.4 cm (36") Side Drop	36.5	Averaged through the cask wall
1.83 m (72") Side Drop	54.8	Averaged through the cask wall
3.66 m (144") Side Drop*	65.3 75.8	Averaged through the cask wall Averaged through the cask lid
Tipover	73.2	Averaged through the cask lid

*Plots not included

Table 19. ISFSI Generic Cask End Drop Results for Additional Analyses

	Finite element analysis simulation, filtered at 350 Hz	Location of reported g's
45.7 cm (18") End Drop Hollow Model	44.5	Averaged through the end cap
	37.1	Averaged through the cask wall
	78.0	Averaged through the cask lid
45.7 cm (18") End Drop Solid Homogeneous Model	38.6	Averaged through the cask body

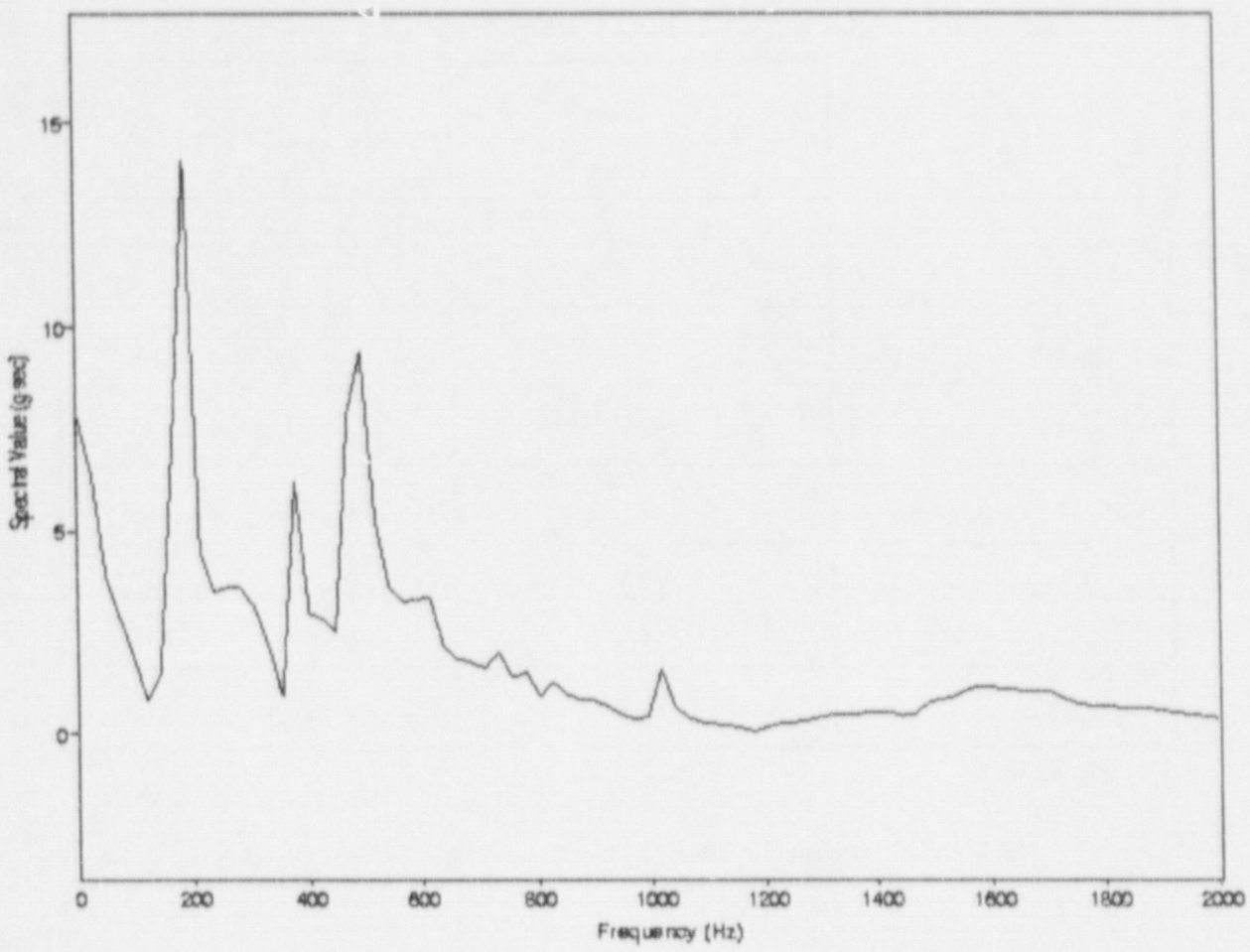

Figure 10. Fourier Spectrum for Hollow Model Finite Element Analysis Generic Cask End Drop Results, Averaged Through the Cask End Cap

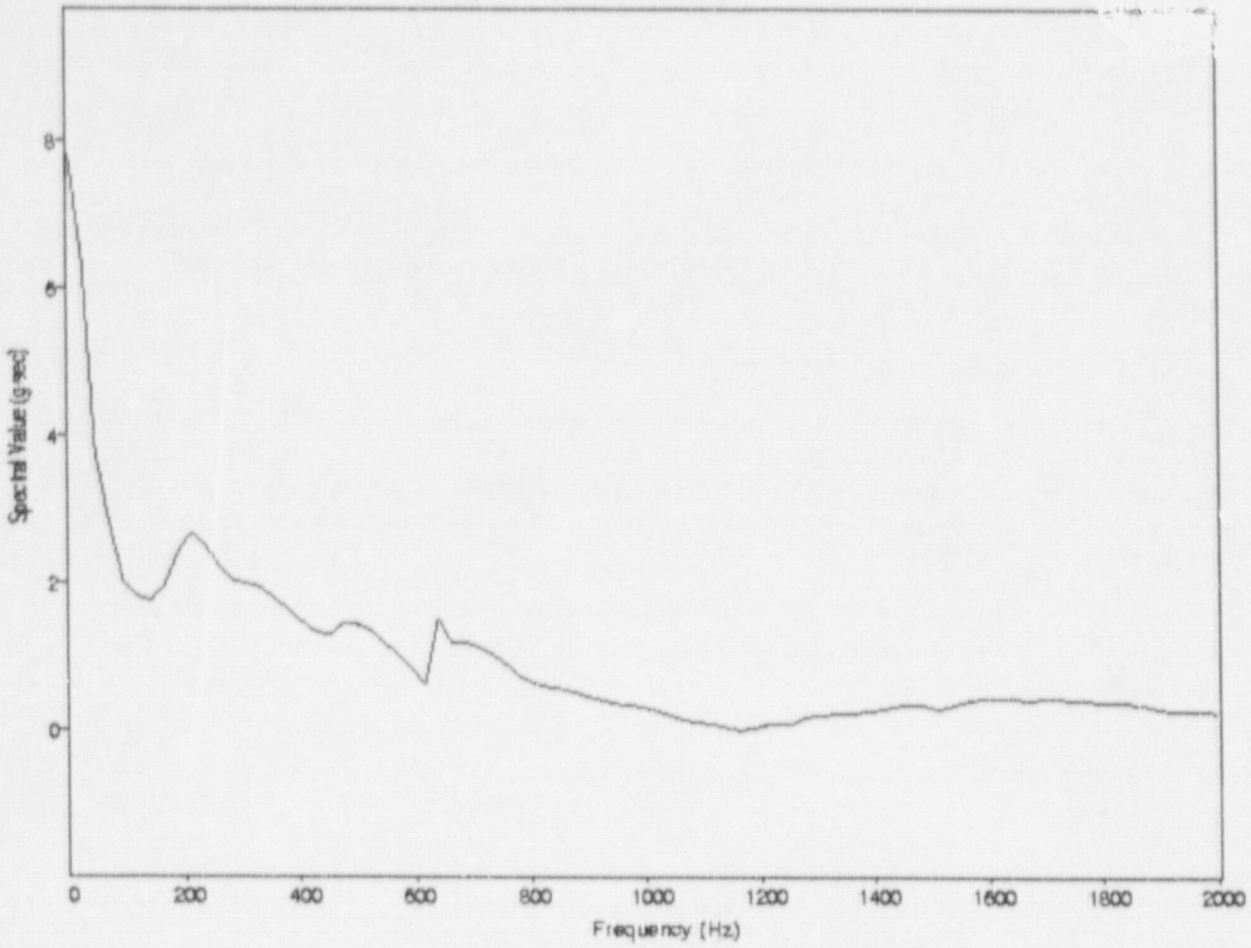

Figure 11. Fourier Spectrum for Solid Homogenous Finite Element Analysis of the Generic Cask End Drop Results, Averaged Through the Cask Body

7. APPLICATION OF METHODOLOGY

7.1 General Approach

In order to use the test data provided in References 2 and 3 to evaluate impact loads for a full-size storage cask, a series of steps needs to be taken. A brief summary is given here.

- Step 1: Rigid Body Motion of Billet Tests

  The accelerometer data collected and reported in References 2 and 3 include unfiltered data for twenty-five tests. The data must be filtered at an appropriate frequency to remove the vibratory components in the data such that the remaining deceleration represents the rigid body motion of the billet. A filter frequency of 450 Hz was used in this report.

- Step 2: Finite Element Model Representation of Billet Tests

  The data collected and filtered in Step 1 are then used to determine the response characteristics of the billet-pad-soil interaction system during impact in order to develop a material model of the concrete pad for analysis of low-velocity impact conditions. This task involves developing a finite element

model of the billet and pad to be used in a series of dynamic analyses simulating the billet test conditions. Based on the series of simulations, a model of the test condition is developed which characterizes the parameter of primary interest, that is, the rigid body g-loads corresponding to those determined in Step 1.

- Step 3: Full Size Storage Cask End Drop, Side Drop and Tipover Finite Element Simulations

  The constitutive model of the concrete pad and soil system developed for the finite element analysis in Step 2 is then utilized in a finite element simulation of a full-scale "generic" cask dropping onto a typical concrete storage pad.

7.2 Other Considerations to be Addressed

Once a benchmarked model of the impact test has been established, an analyst applying this method to the evaluation of a specific storage cask might be interested in a variety of aspects of the finite element results, such as stresses and strains in the cask body, or decelerations for possible application to a secondary structure. At this point, the analyst must ensure that he has captured the drop orientation of interest.

It was pointed out in Section 4.2.1.2 (Effect of Substrate Materials on End Drop Results) that the engineered fill significantly increased the deceleration resulting from a drop onto the concrete pad. The analyst must ensure that this effect is considered and, if necessary, accounted for in any analyses of the impact.

In order to apply the deceleration calculated for the storage cask body to a secondary internal structure such as a basket, several options are available. An analyst might take the calculated deceleration time history of the cask body and apply it directly to the secondary structure in a dynamic analysis. Or, an analyst might choose to perform a quasi-static analysis of the secondary structure, in which case a dynamic amplification factor needs to be applied to the static load. In the absence of information about the vibration period of the secondary structure, a dynamic amplification factor of two is appropriate for an impulse load to the secondary structure.[11]

8. SUMMARY AND CONCLUSIONS

Tests were performed at SNL and LLNL to assess loading conditions on a spent fuel storage cask for end drops, side drops and tipover events. The tests were performed with a 1/3-scale model billet and a 1/3-scale model concrete pad, and included a variety of substrate materials. This report was prepared to provide a summary and an evaluation of all of the billet testing conducted. Deceleration time histories were evaluated and discussed, and are included in Appendices A and B to this report. The billet and test pad were modeled with a general purpose finite element code, DYNA3D, using material properties and techniques provided in this report. The simulated analytical peak or maximum deceleration results were conservative for most cases, but in the worst case underpredicted the test result by less than 15%.

A "generic" or representative cask was modeled with the benchmarked finite element analysis approach and evaluated for ISFSI end and side drops and tipover events. The analytical method can be applied to similar casks to estimate deceleration loads on storage casks resulting from low-velocity drop or tip impacts onto concrete storage pads.

9. REFERENCES

1. United States Code of Federal Regulations Title 10, Part 72.

2. McConnell, P., et al. "Test Report, Drop Tests Onto Concrete Pads for Benchmarking Response of Interim Spent Fuel Storage Installations," Sandia National Laboratory, September 1993.

3. Witte, M., et al. "Low Velocity Impact Testing of Solid Steel Billet onto Concrete Pads," Lawrence Livermore National Laboratory, UCRL-ID 126274, March 1997.

4. Witte, M., et al. "Evaluation of Low Velocity Impact Tests of Solid Steel Billet onto Concrete Pads, and Application to Generic ISFSI Storage Cask for Tipover and Side Drop," Lawrence Livermore National Laboratory, UCRL-ID 126295, March 1997.

5. Witte, M. Lawrence Livermore National Laboratory, letter no. NTFS97-76/MW forwarding data diskettes to D. Tang, Nuclear Regulatory Commission, dated June 4, 1997.

6. DADiSP Data Analysis and Display Software. DSP Development Corporation, One Kendall Square, Cambridge MA, March 1996.

7. TrueGrid, XYZ Scientific Applications, Inc., 1324 Concannon Blvd., Livermore, CA, May 1997.

8. Whirley, R. G. "DYNA3D, A Nonlinear, Explicit, Three-Dimensional Finite Element Code for Solid and Structural Mechanics—User Manual," Lawrence Livermore National Laboratory, UCRL-MA-107254 , Rev. 1, 1993.

9. Bowles, J. E. *Foundation Analysis and Design*, 2nd ed., New York: McGraw Hill, 1977, p. 35.

10. Simons, J.W. and Gefkin, P.R. "Characterization of Grout for DYNA3D Model," SRI International, Final Report for SRI Project PYD-5077, April 1988.

11. Biggs, John M. *Introduction to Structural Dynamics*. New York: McGraw Hill, 1964.

APPENDIX A. ACCELERATION TRACES, FILTERED AND UNFILTERED, FOR SNL TESTS

SNL Test #166, Gauge A1. Accelerometer did not function.

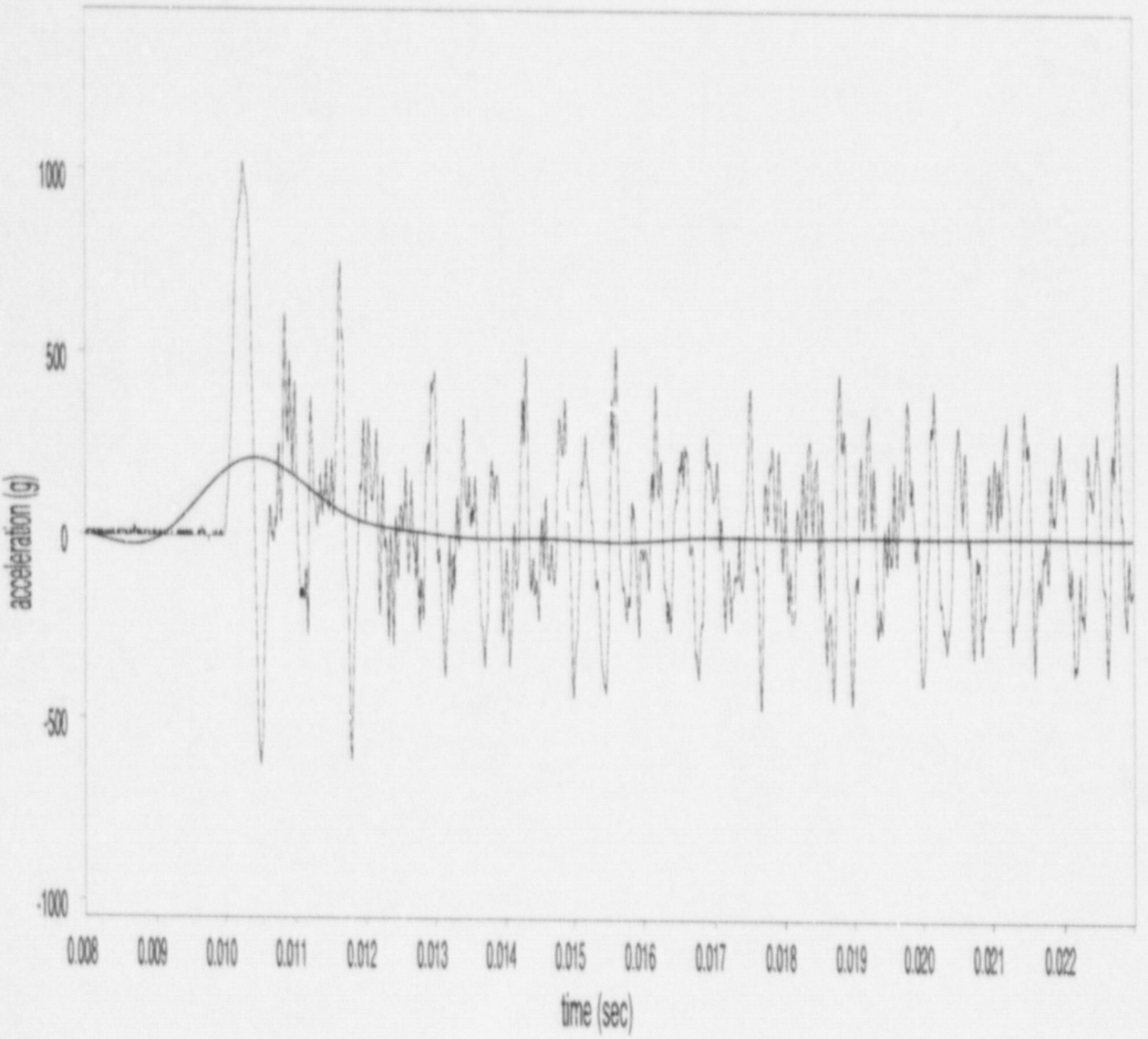

Figure A-1 SNL Test #166, Gauge A2 (45.7-cm (45.7-cm (18-inch)) end drop, filter cutoff: 450Hz, max. acceleration: 210.0g)

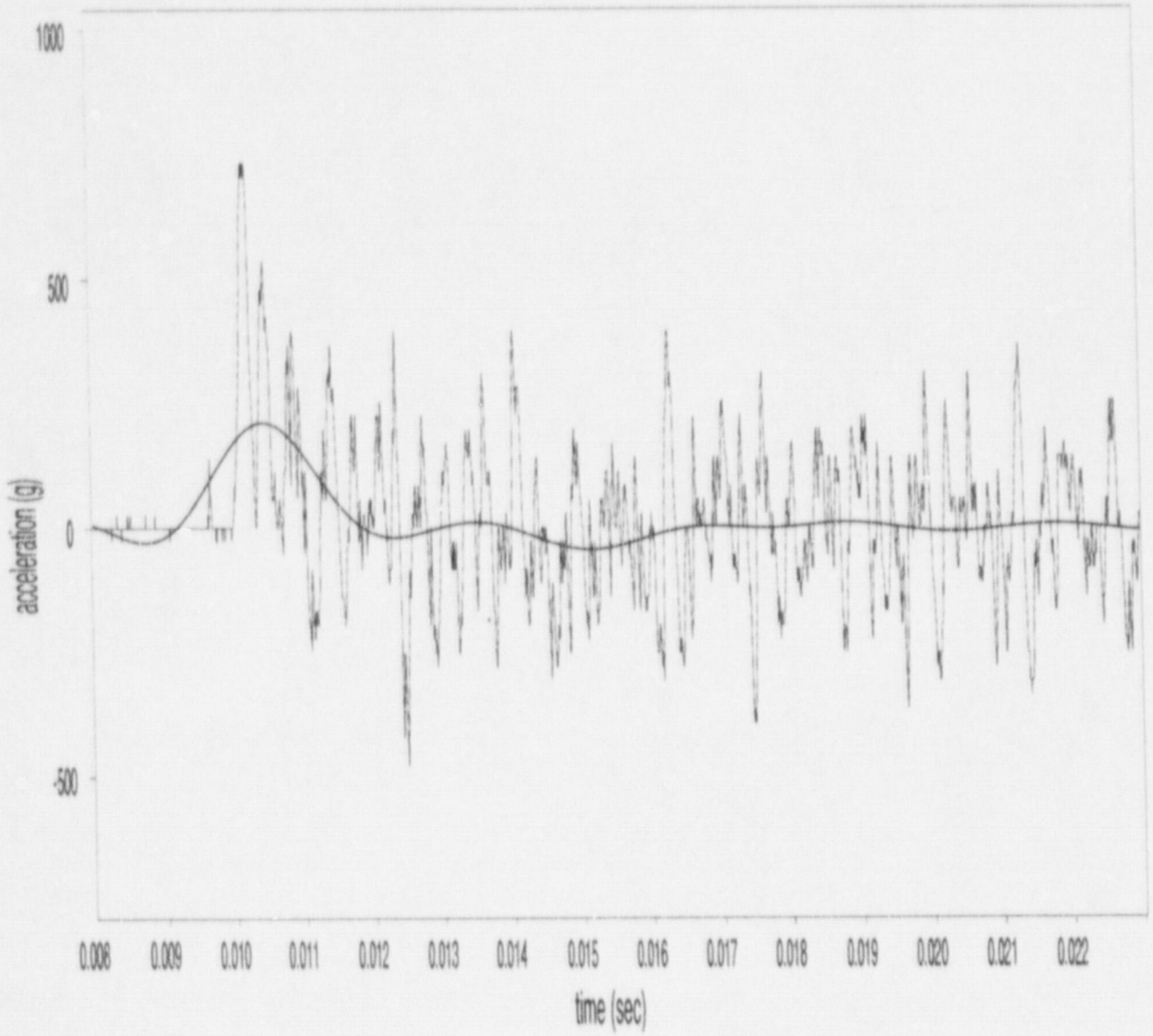

Figure A-2 SNL Test #166, Gauge A3 (45.7-cm (45.7-cm (18-inch)) end drop, filter cutoff: 450Hz, max. acceleration: 211.5g)

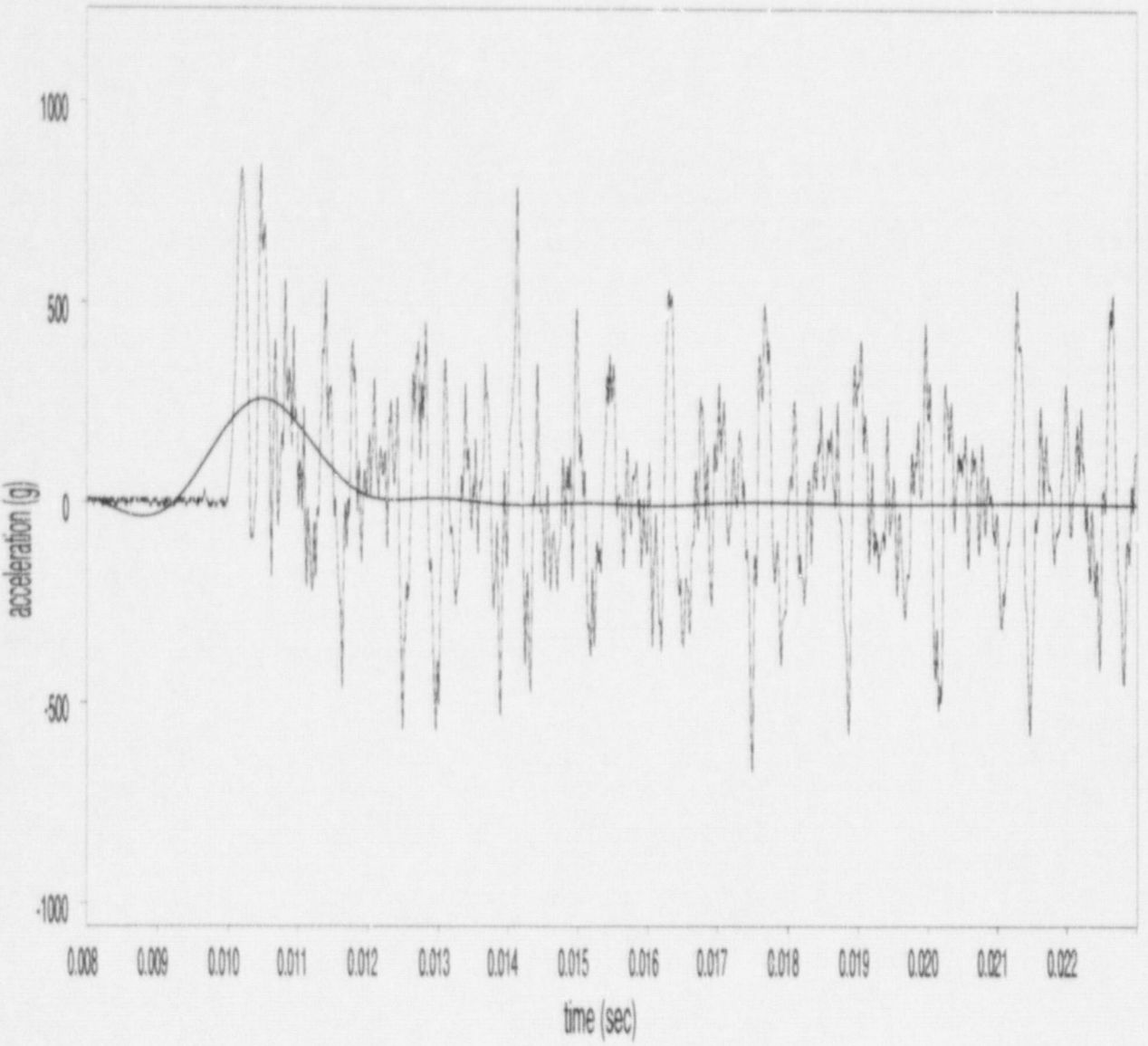

Figure A-3 SNL Test #166, Gauge A4 (45.7-cm (45.7-cm (18-inch)) end drop, filter cutoff: 450Hz, max. acceleration: 253.9g)

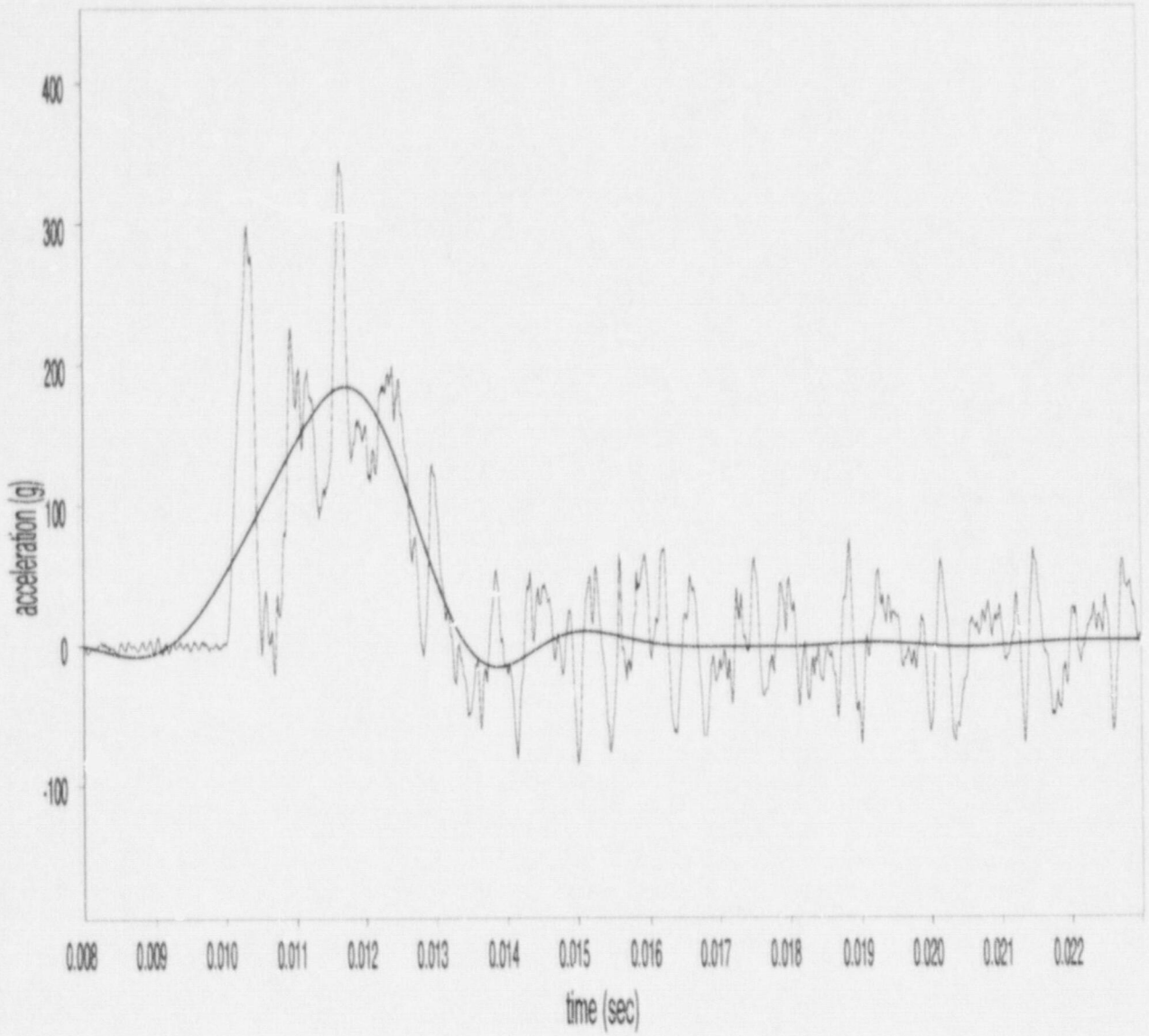

Figure A-4 SNL Test #167, Gauge A1 (45.7-cm (45.7-cm (18-inch)) end drop, filter cutoff: 450Hz, max. acceleration: 183.4g)

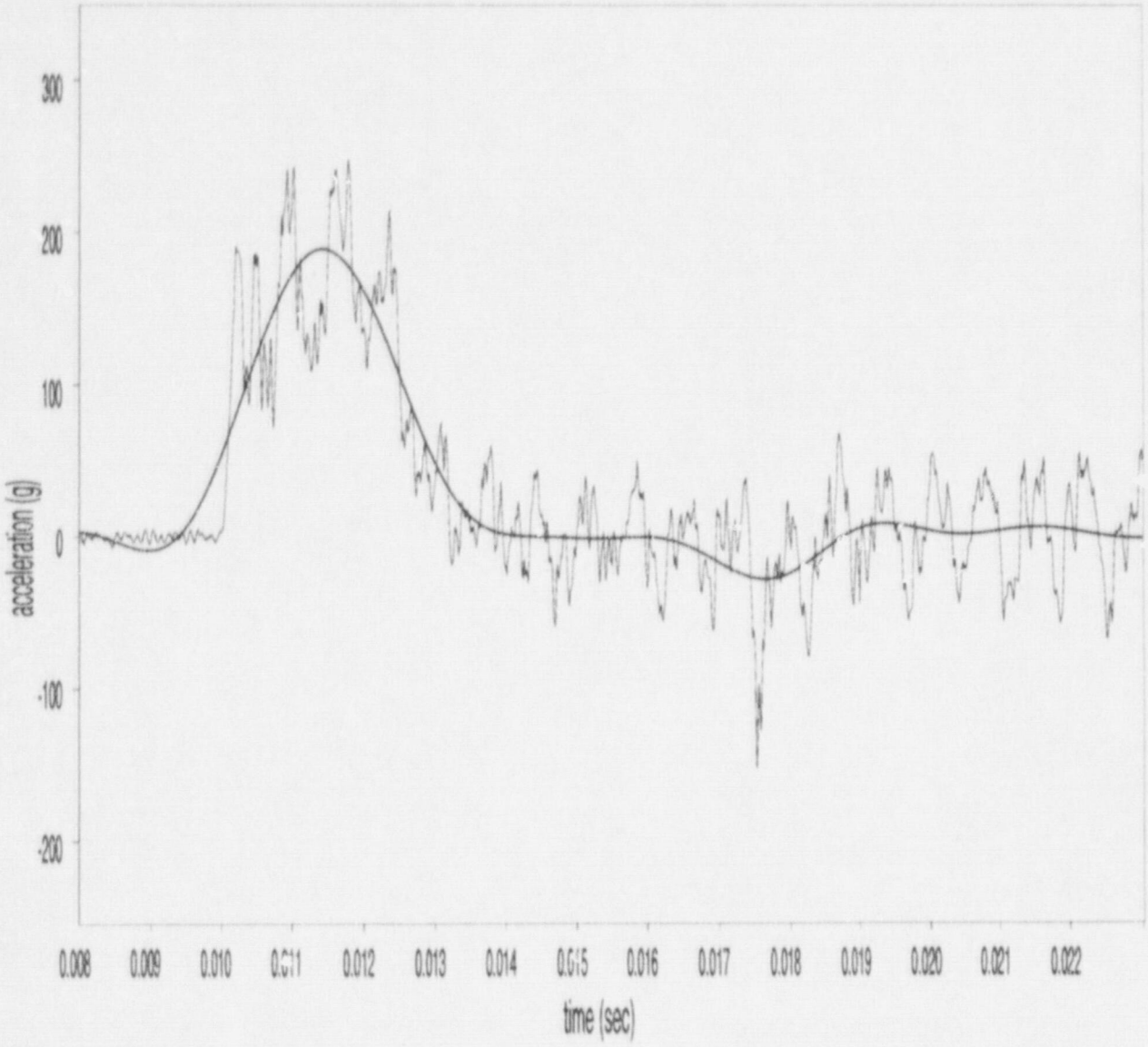

Figure A-5 SNL Test #167, Gauge A2 (45.7-cm (45.7-cm (18-inch)) end drop, filter cutoff: 450Hz, max. acceleration: 188.8g)

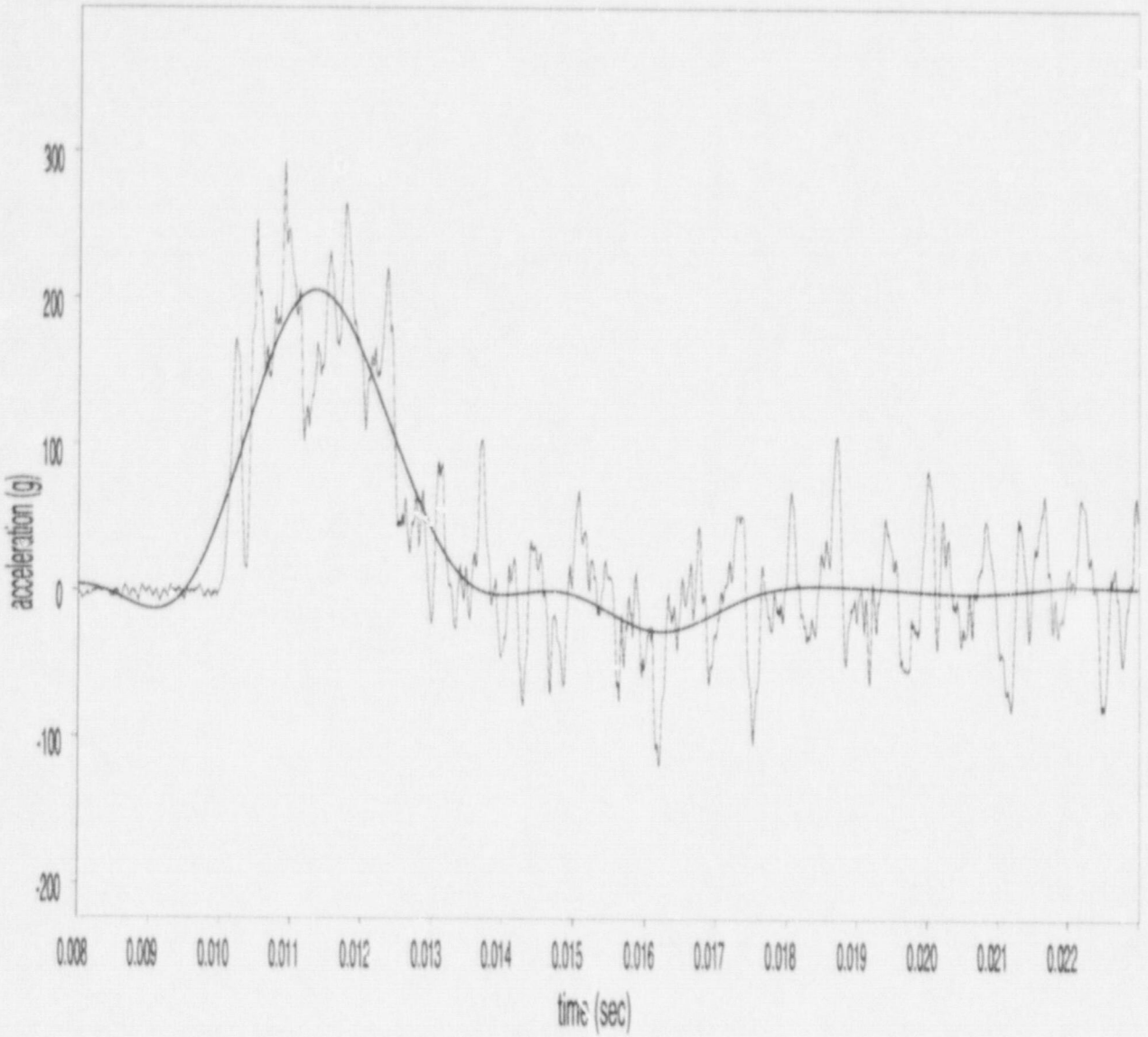

Figure A-6 SNL Test #167, Gauge A3 (45.7-cm (45.7-cm (18-inch)) end drop, filter cutoff: 450Hz, max. acceleration: 206g)

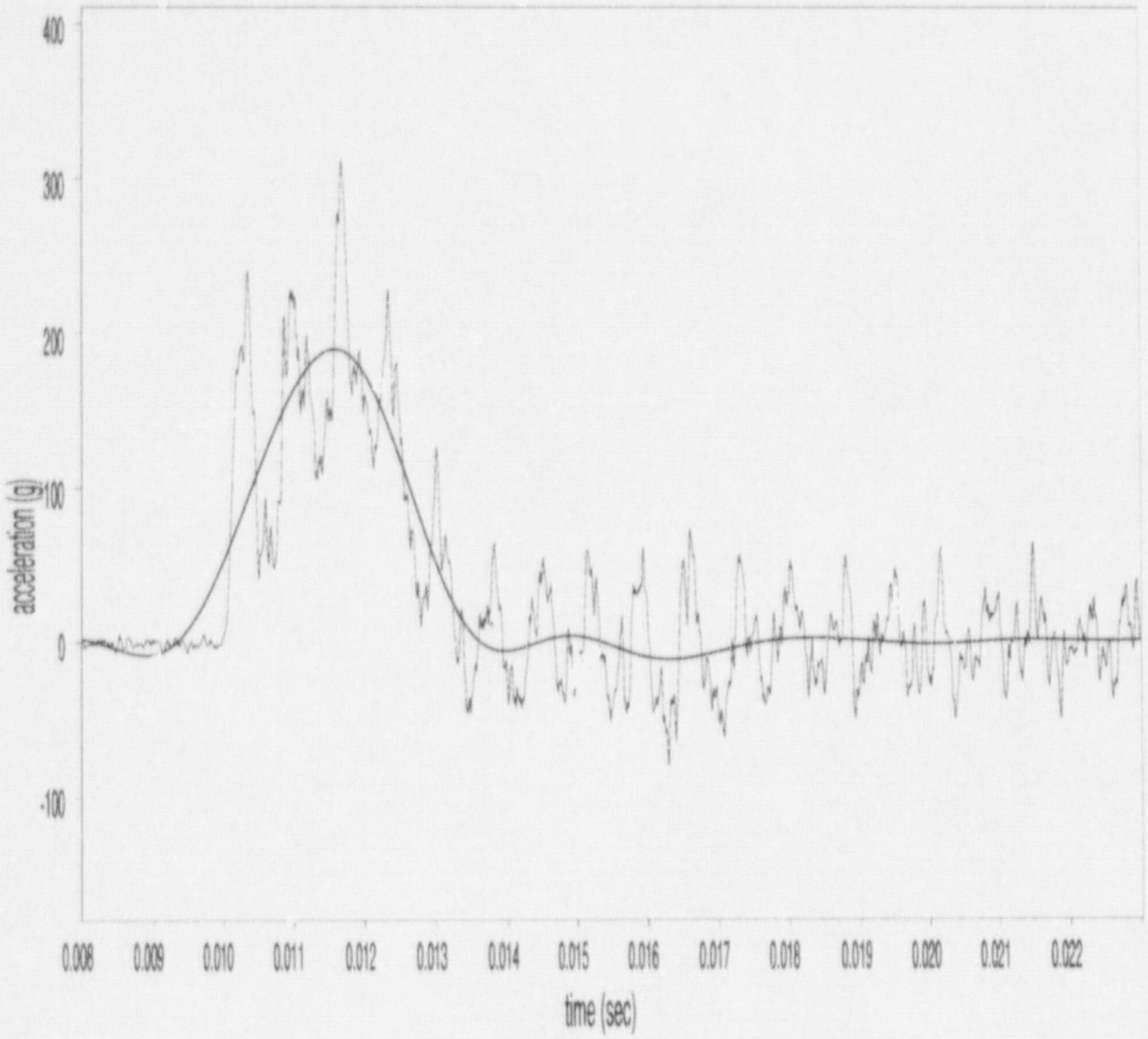

Figure A-7 SNL Test #167, Gauge A4 (45.7-cm (45.7-cm (18-inch)) end drop, filter cutoff: 450Hz, max. acceleration: 189.4g)

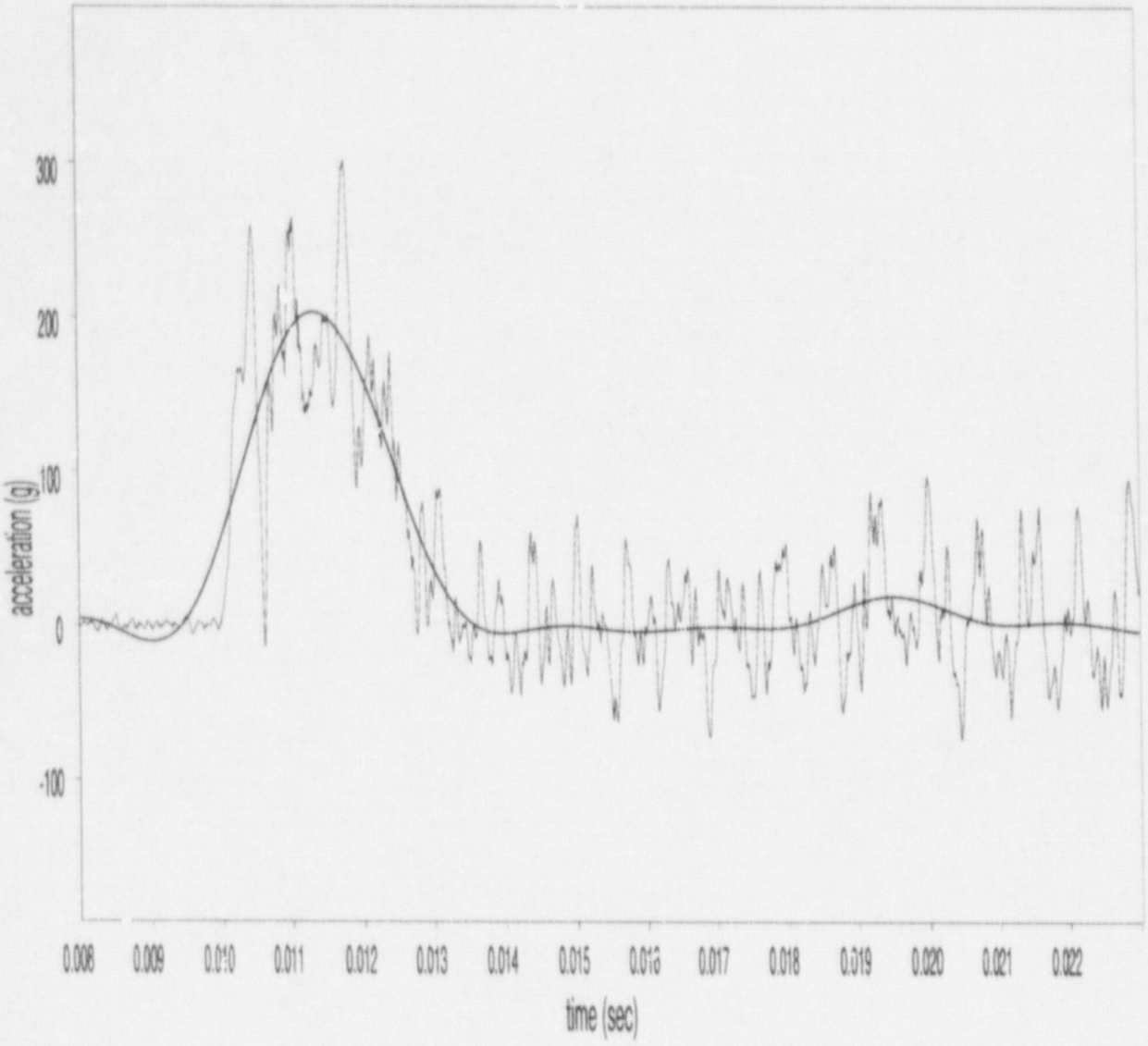

Figure A-8 SNL Test #168, Gauge A1 (45.7-cm (45.7-cm (18-inch)) end drop, filter cutoff: 450Hz, max. acceleration: 202.9g)

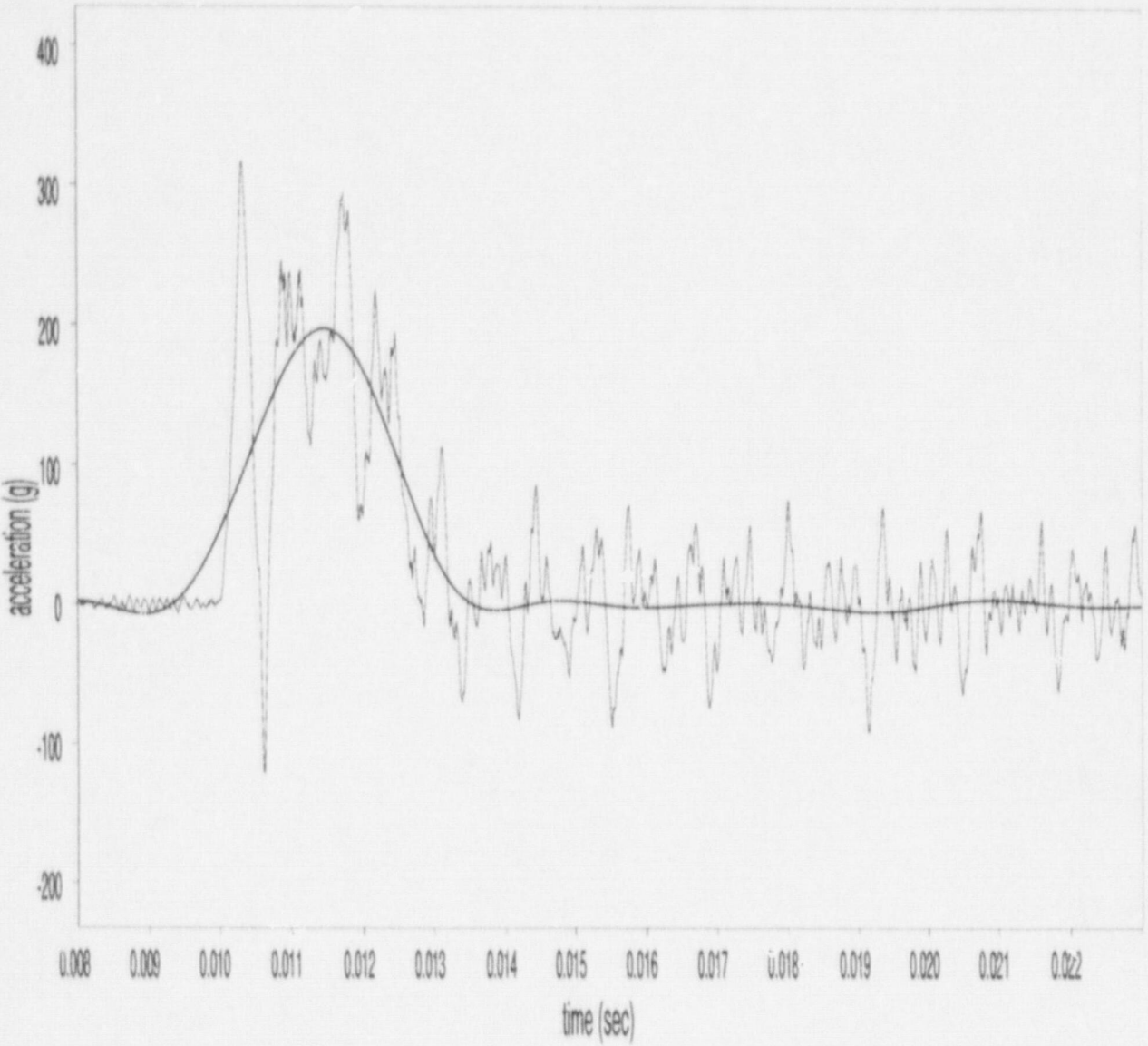

Figure A-9 SNL Test #168, Gauge A2 (45.7-cm (45.7-cm (18-inch)) end drop, filter cutoff: 450Hz, max. acceleration: 197.2g)

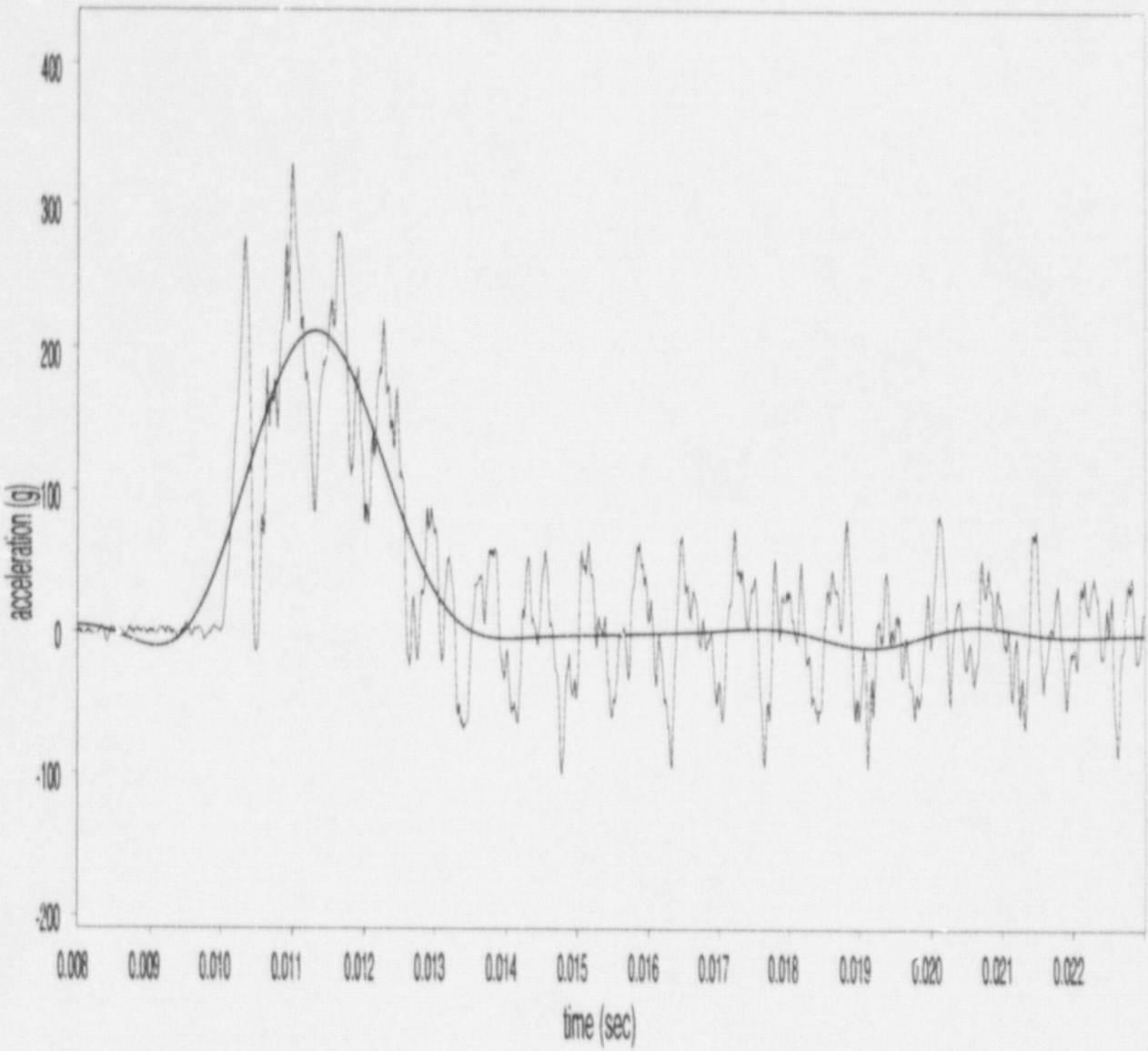

Figure A-10 SNL Test #168, Gauge A3 (45.7-cm (45.7-cm (18-inch)) end drop, filter cutoff: 450Hz, max. acceleration: 211.6g)

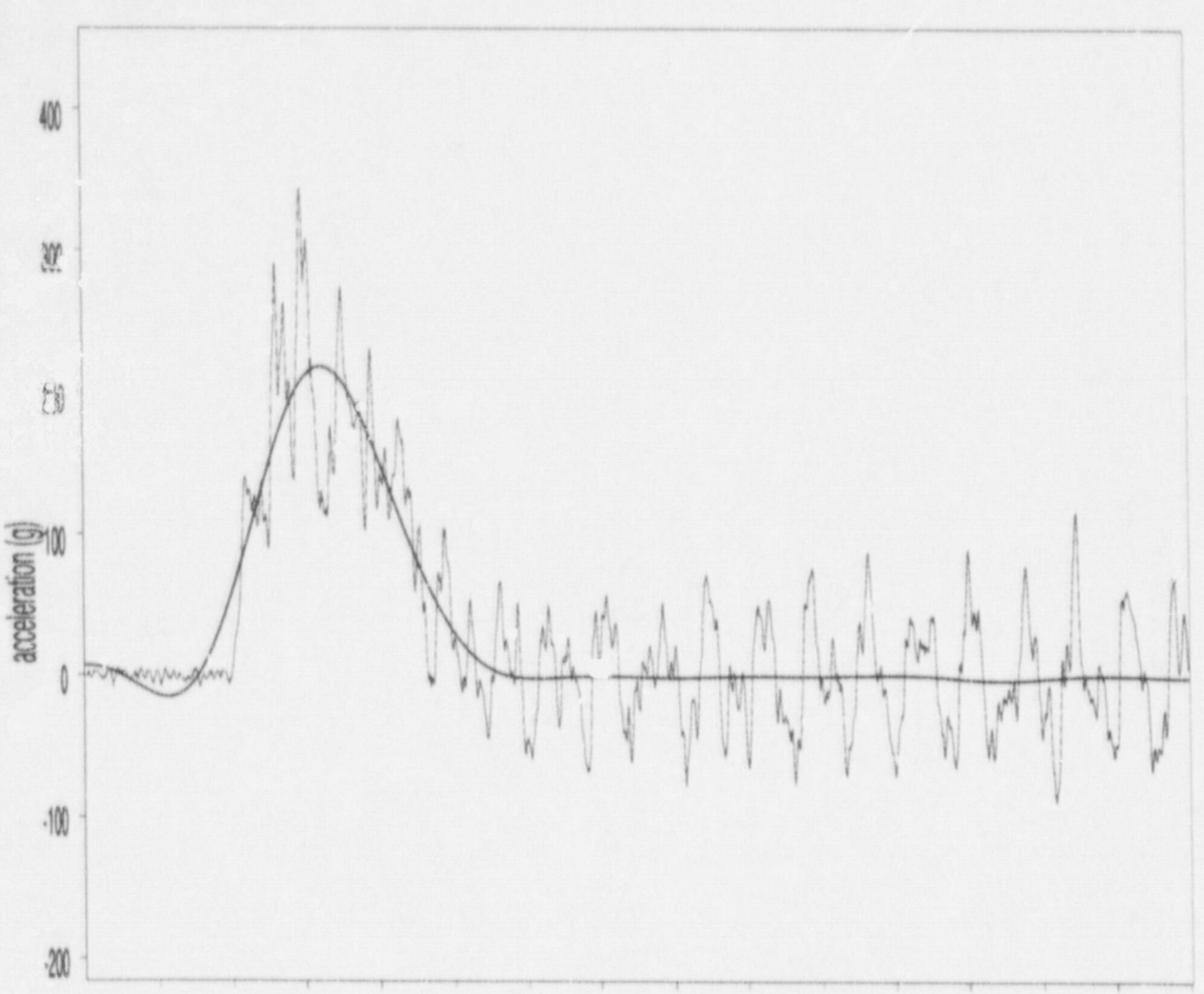

Figure A-11 SNL Test #168, Gauge A4 (45.7-cm (45.7-cm (18-inch)) end drop, filter cutoff: 450Hz, max. acceleration: 217.7g)

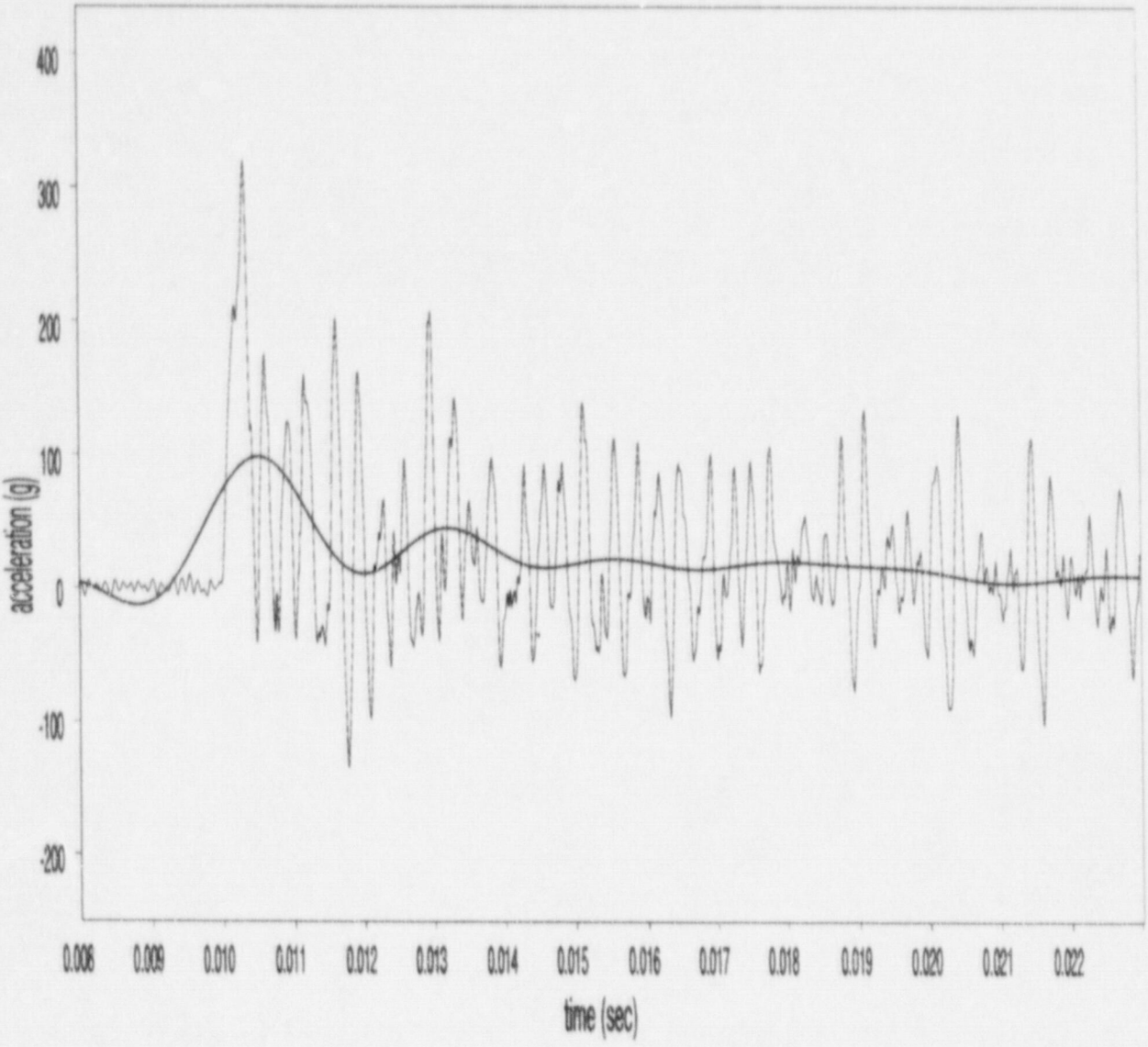

Figure A-12 SNL Test #169, Gauge A1 (45.7-cm (45.7-cm (18-inch)) end drop, filter cutoff: 450Hz, max. acceleration: 98.3g)

SNL Test #169, Gauge A2. Accelerometer did not function.

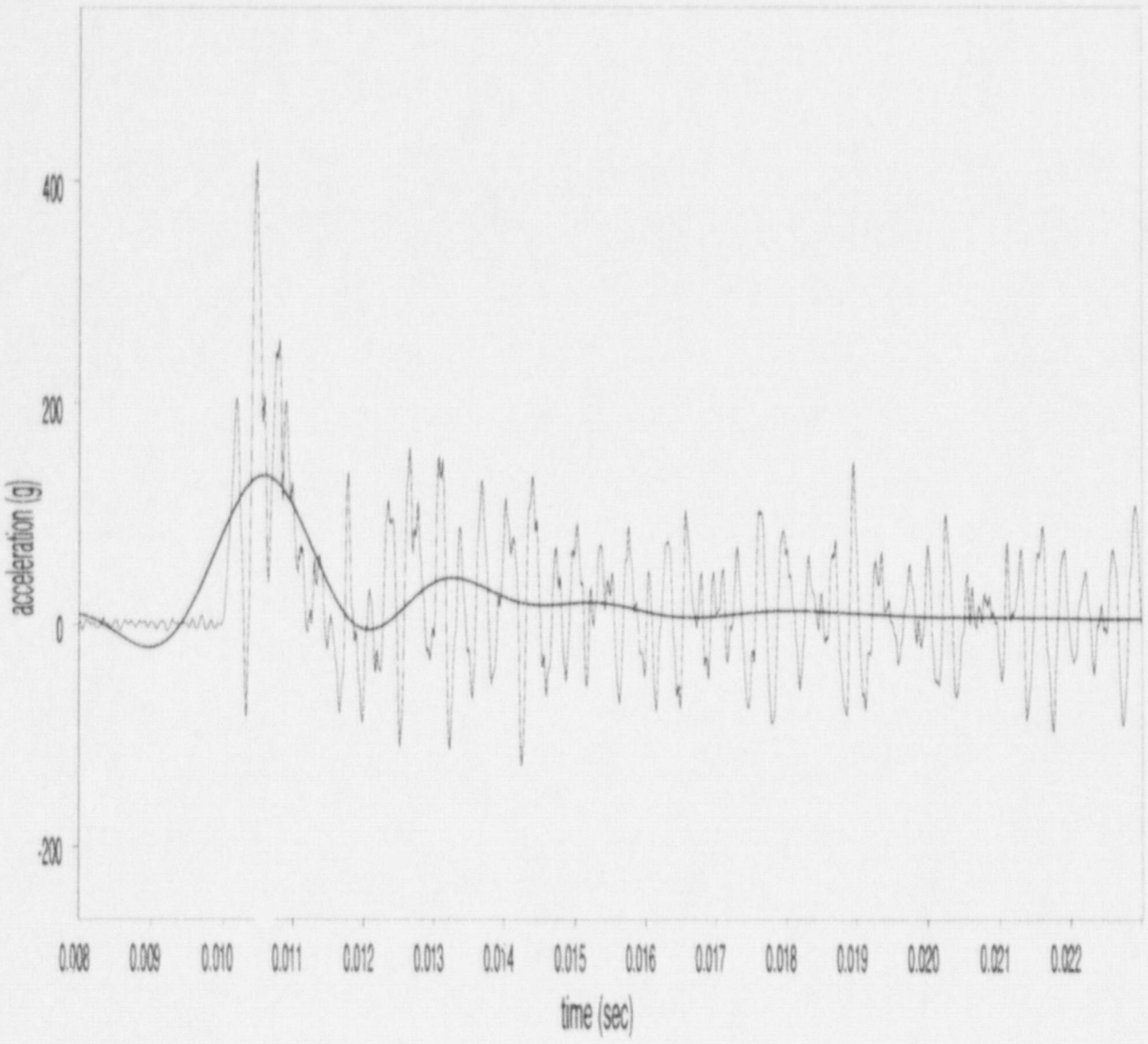

Figure A-13 SNL Test #169, Gauge A3 (45.7-cm (45.7-cm (18-inch)) end drop, filter cutoff: 450Hz, max. acceleration: 134.7g)

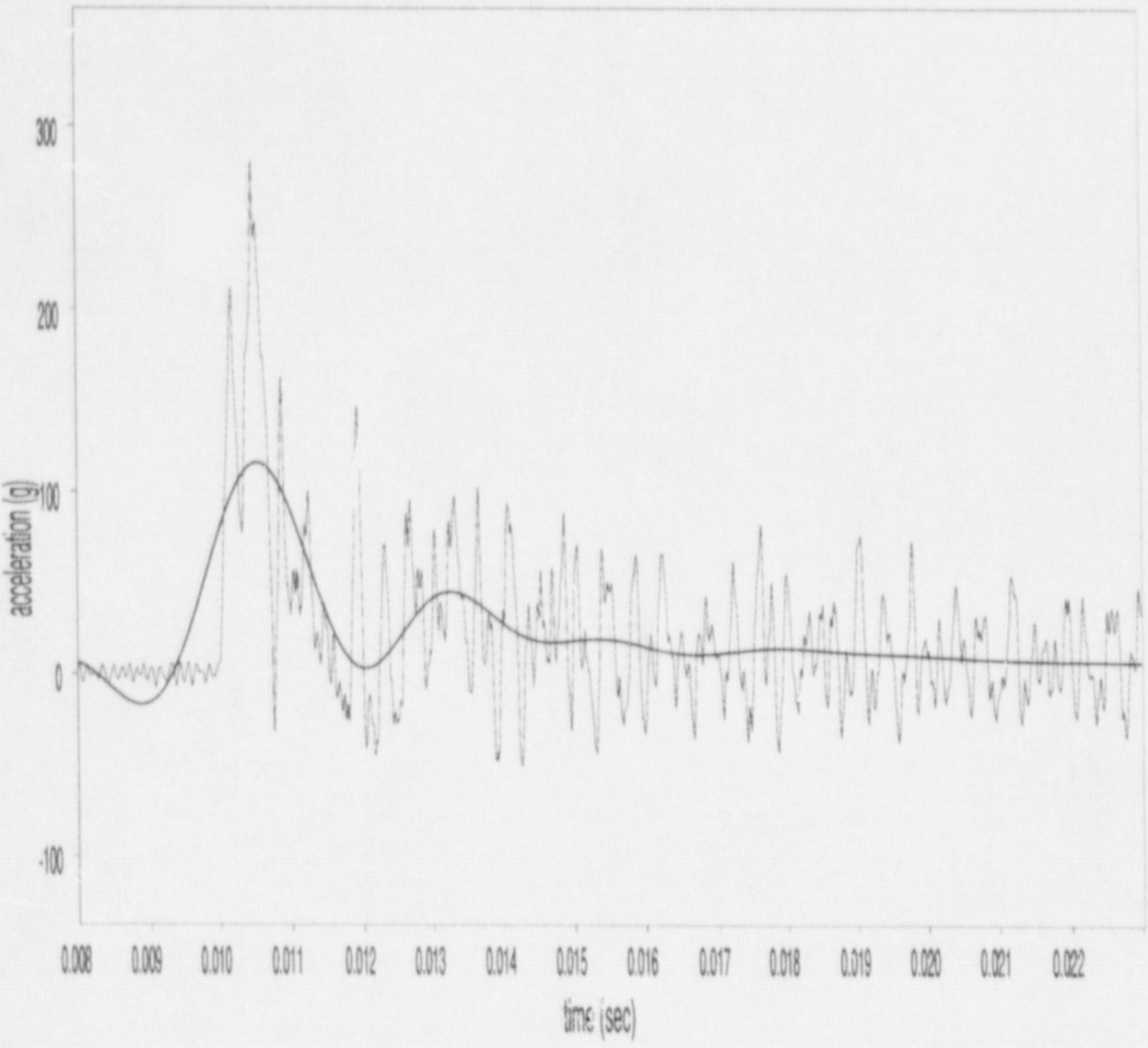

Figure A-14 SNL Test #169, Gauge A4 (45.7-cm (45.7-cm (18-inch)) end drop, filter cutoff: 450Hz, max. acceleration: 115.8g)

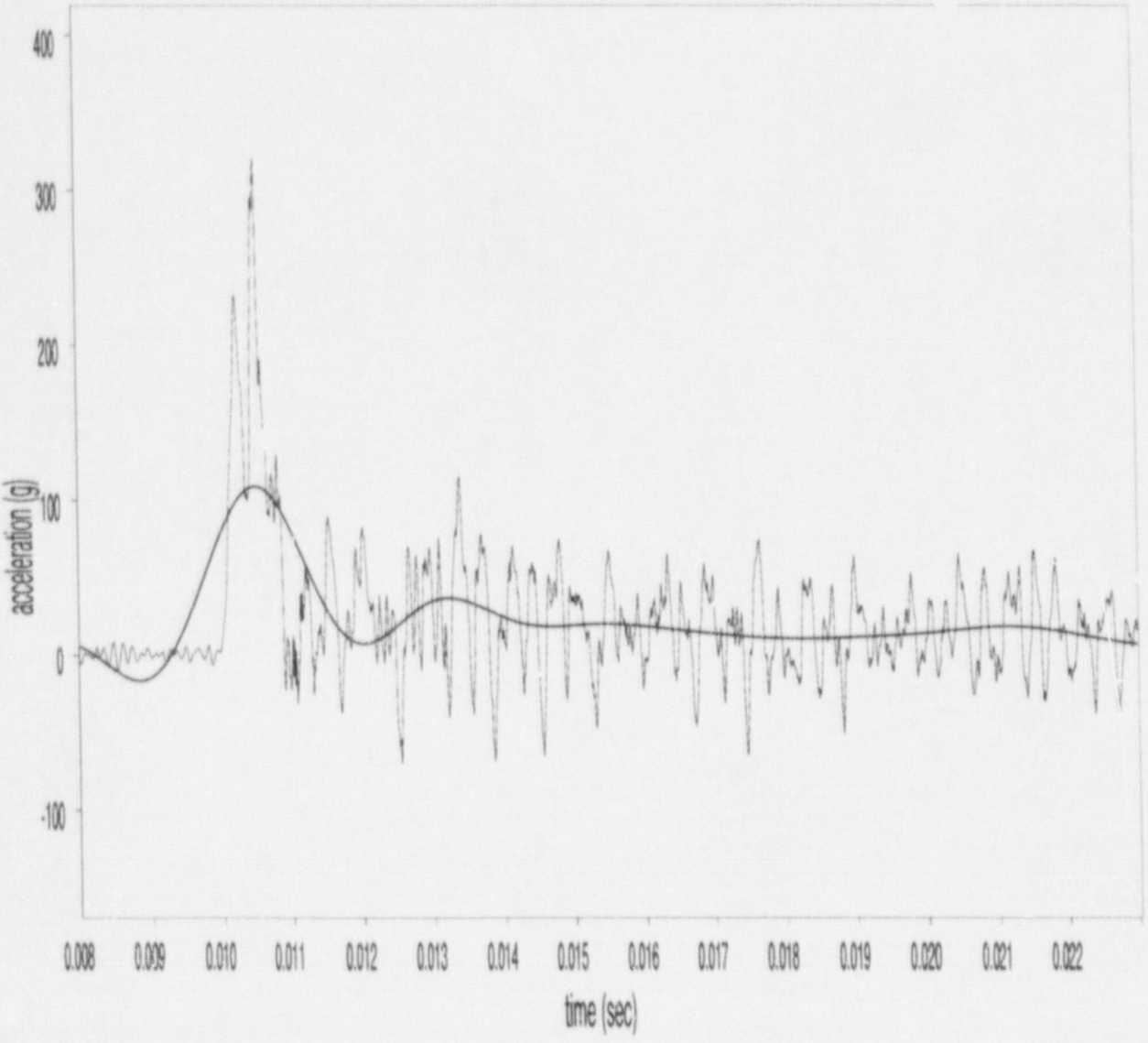

Figure A-15 SNL Test #170, Gauge A1 (45.7-cm (45.7-cm (18-inch)) end drop, filter cutoff: 450Hz, max. acceleration: 108.9g)

SNL Test #170, Gauge A2. Accelerometer did not function.

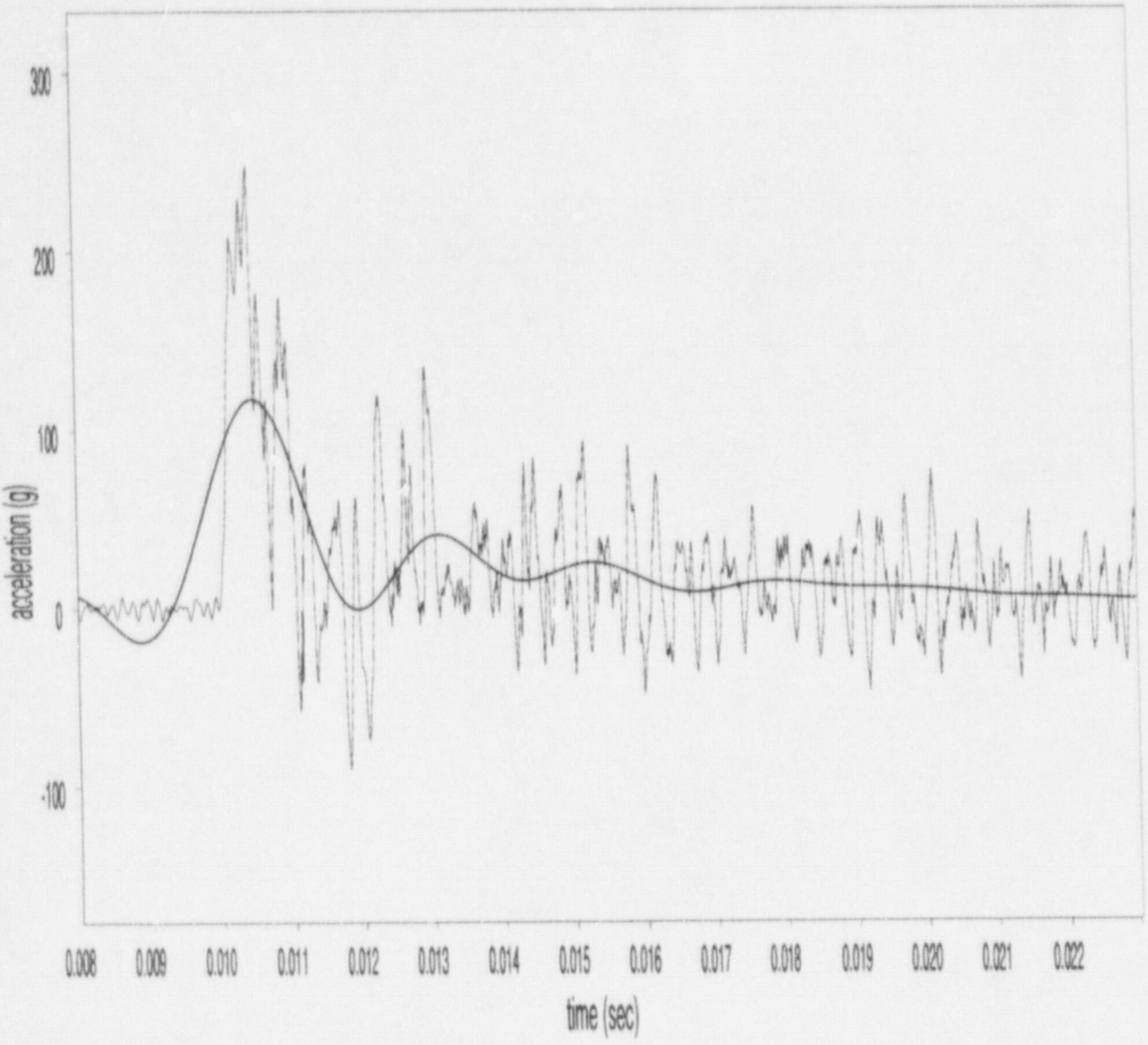

Figure A-16 SNL Test #170, Gauge A3 (45.7-cm (45.7-cm (18-inch)) end drop, filter cutoff: 450Hz, max. acceleration: 117.5g)

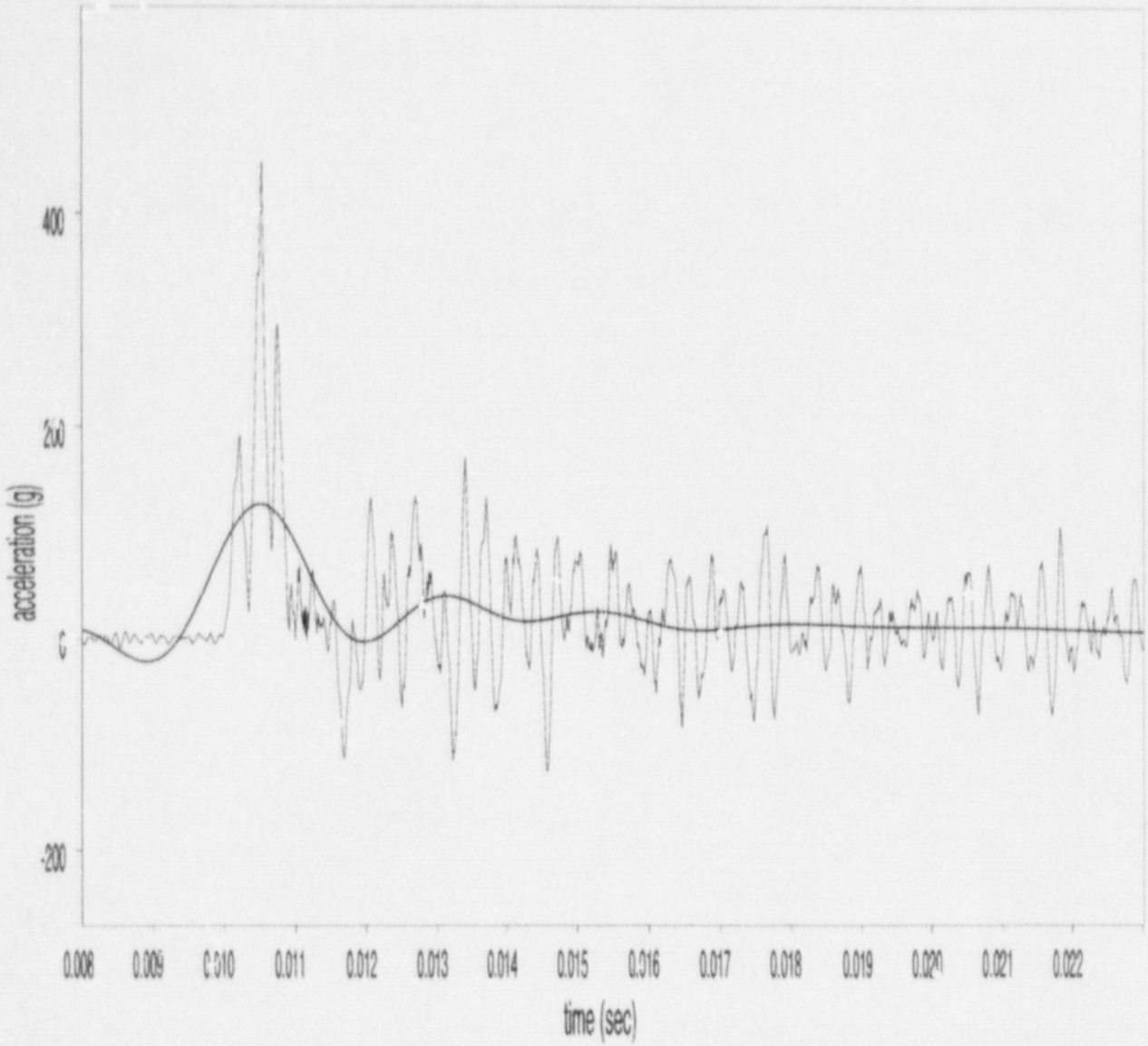

Figure A-17 SNL Test #170, Gauge A4 (45.7-cm (45.7-cm (18-inch)) end drop, filter cutoff: 450Hz, max. acceleration: 126.8g)

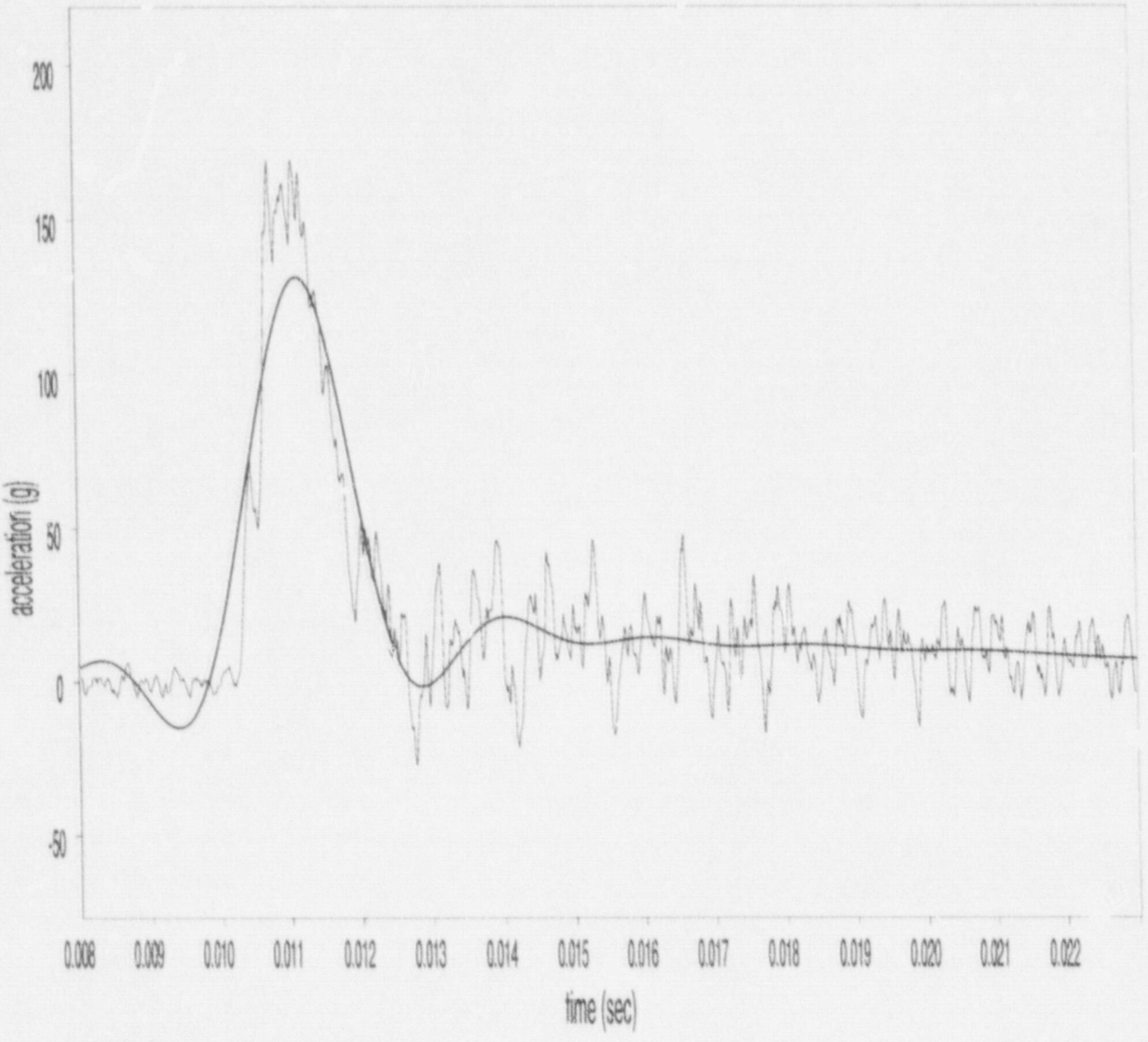

Figure A-18 SNL Test #226, Gauge A1 (45.7-cm (45.7-cm (18-inch)) end drop, filter cutoff: 450Hz, max. acceleration: 131.3g)

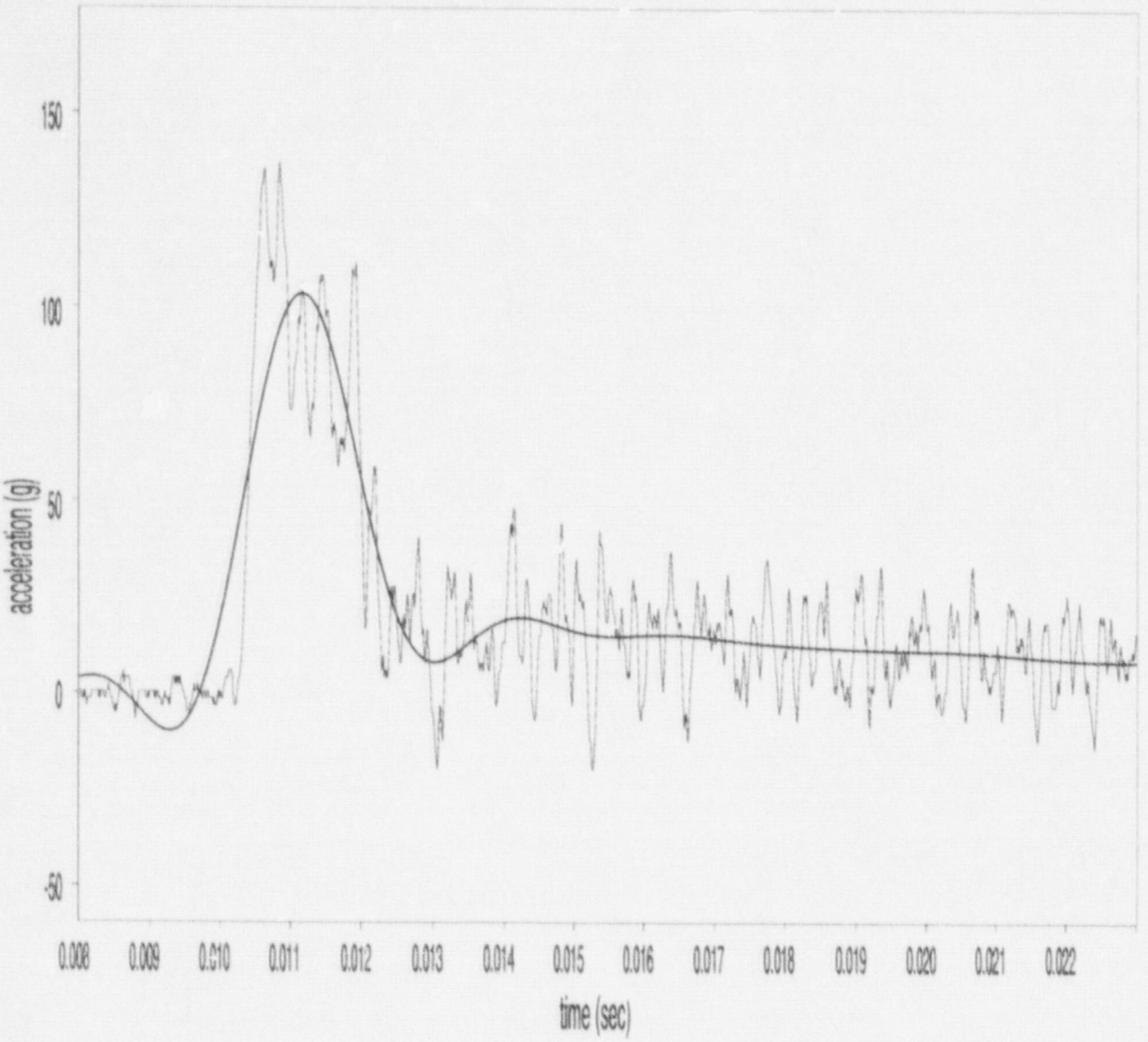

Figure A-19 SNL Test #226, Gauge A2 (45.7-cm (45.7-cm (18-inch)) end drop, filter cutoff: 450Hz, max. acceleration: 103.2g)

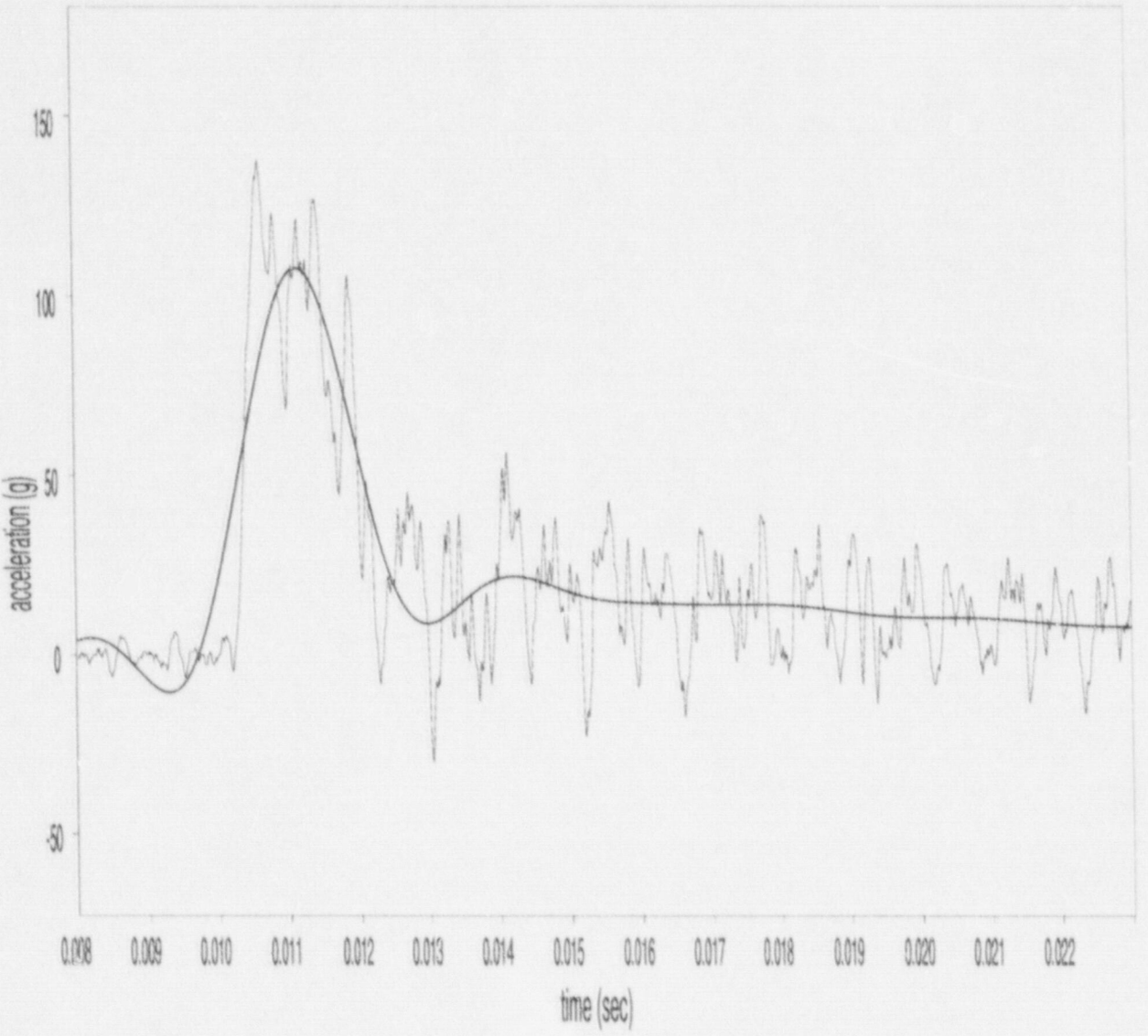

Figure A-20 SNL Test #226, Gauge A3 (45.7-cm (45.7-cm (18-inch)) end drop, filter cutoff: 450Hz, max. acceleration: 107.6g)

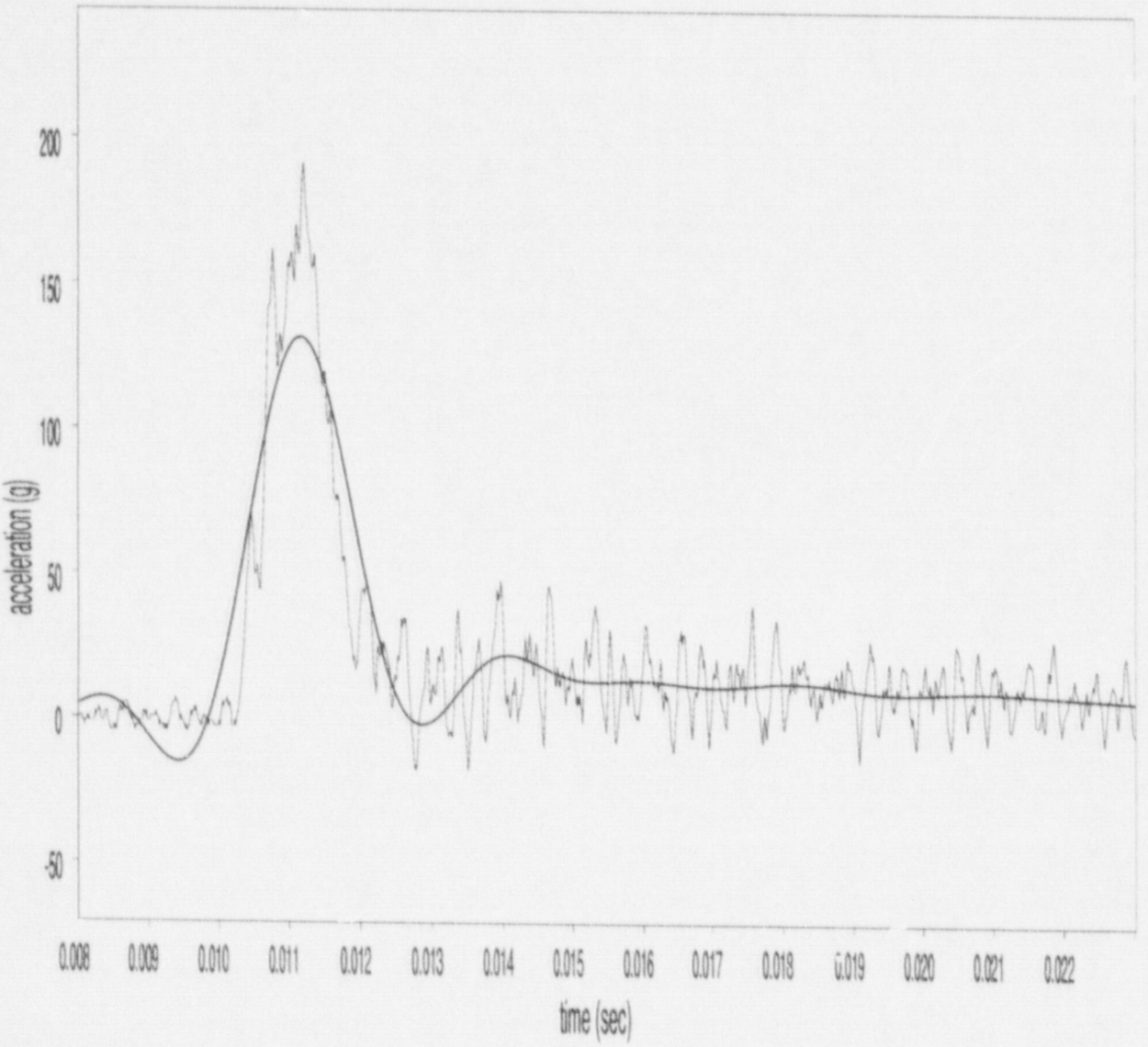

Figure A-21 SNL Test #226, Gauge A4 (45.7-cm (45.7-cm (18-inch)) end drop, filter cutoff: 450Hz, max. acceleration: 131.3g)

SNL Test #226, Gauge A5. Accelerometer did not function.

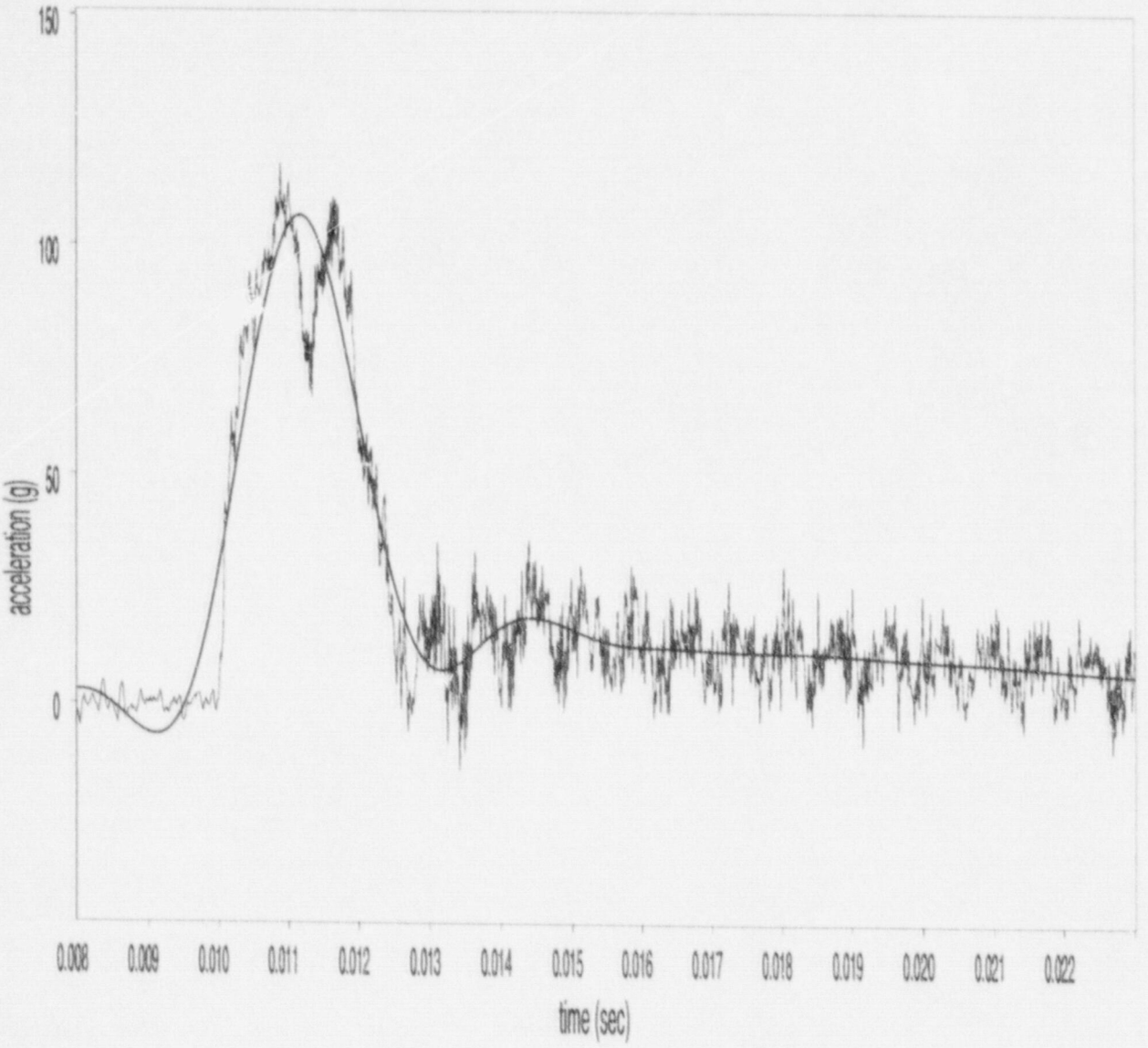

Figure A-22 SNL Test #226, Gauge A6 (45.7-cm (45.7-cm (18-inch)) end drop, filter cutoff: 450Hz, max. acceleration: 106.4g)

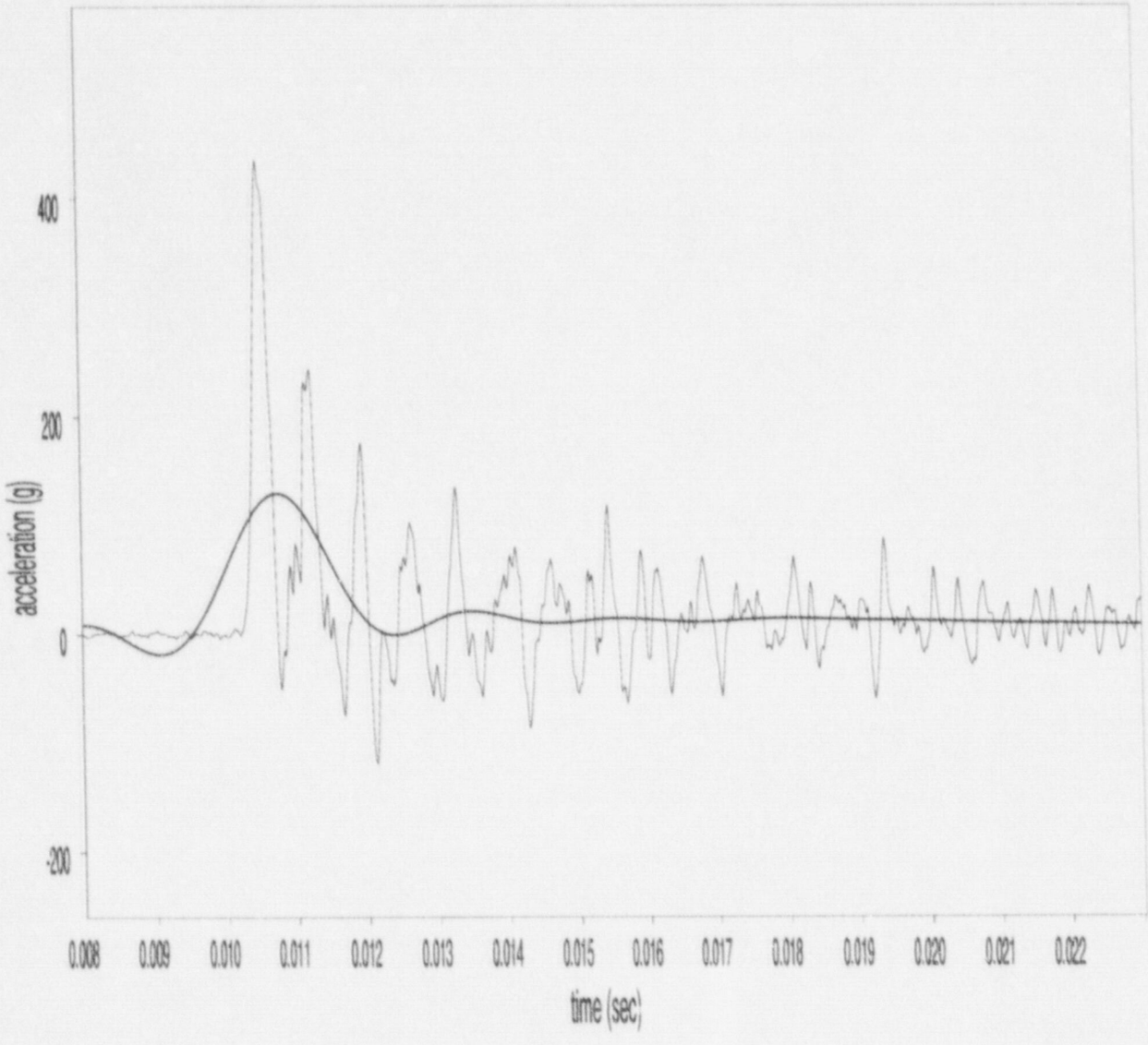

Figure A-23 SNL Test #228, Gauge A1 (45.7-cm (45.7-cm (18-inch)) end drop, filter cutoff: 450Hz, max. acceleration: 129.6g)

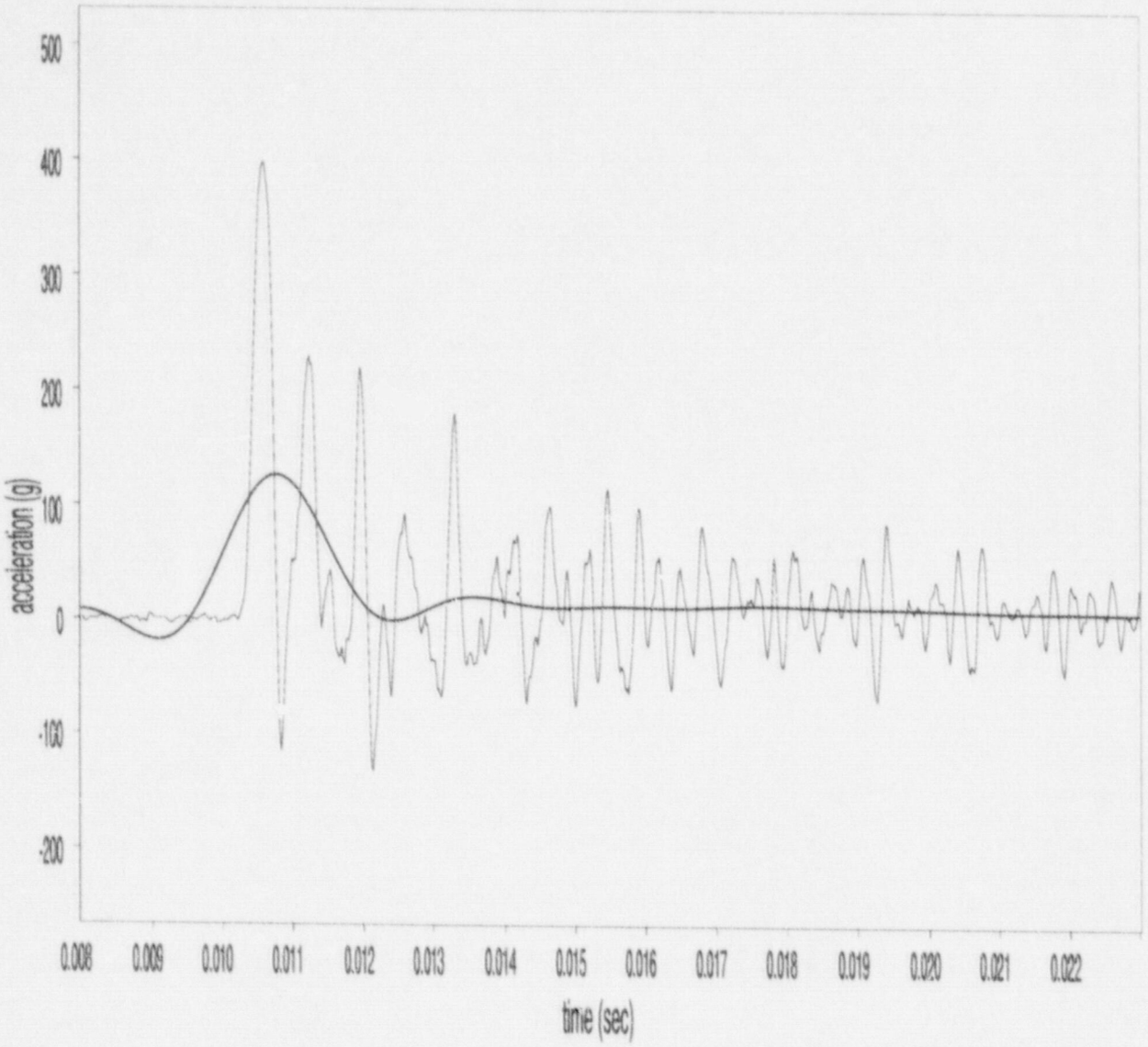

Figure A-24 SNL Test #228, Gauge A2 (45.7-cm (45.7-cm (18-inch)) end drop, filter cutoff: 450Hz, max. acceleration: 126.2g)

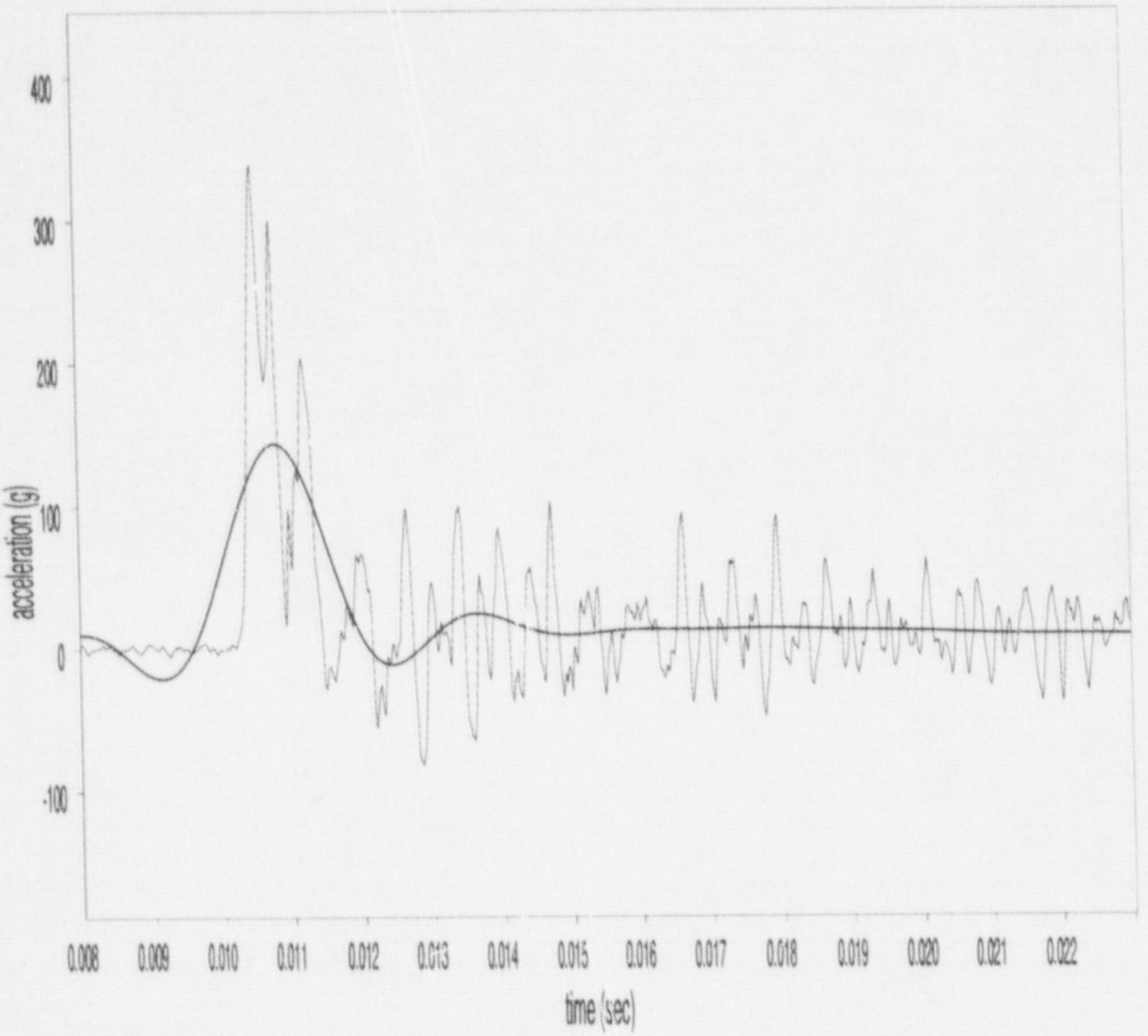

Figure A-25 SNL Test #228, Gauge A3 (45.7-cm (45.7-cm (18-inch)) end drop, filter cutoff: 450Hz, max. acceleration: 143.7g)

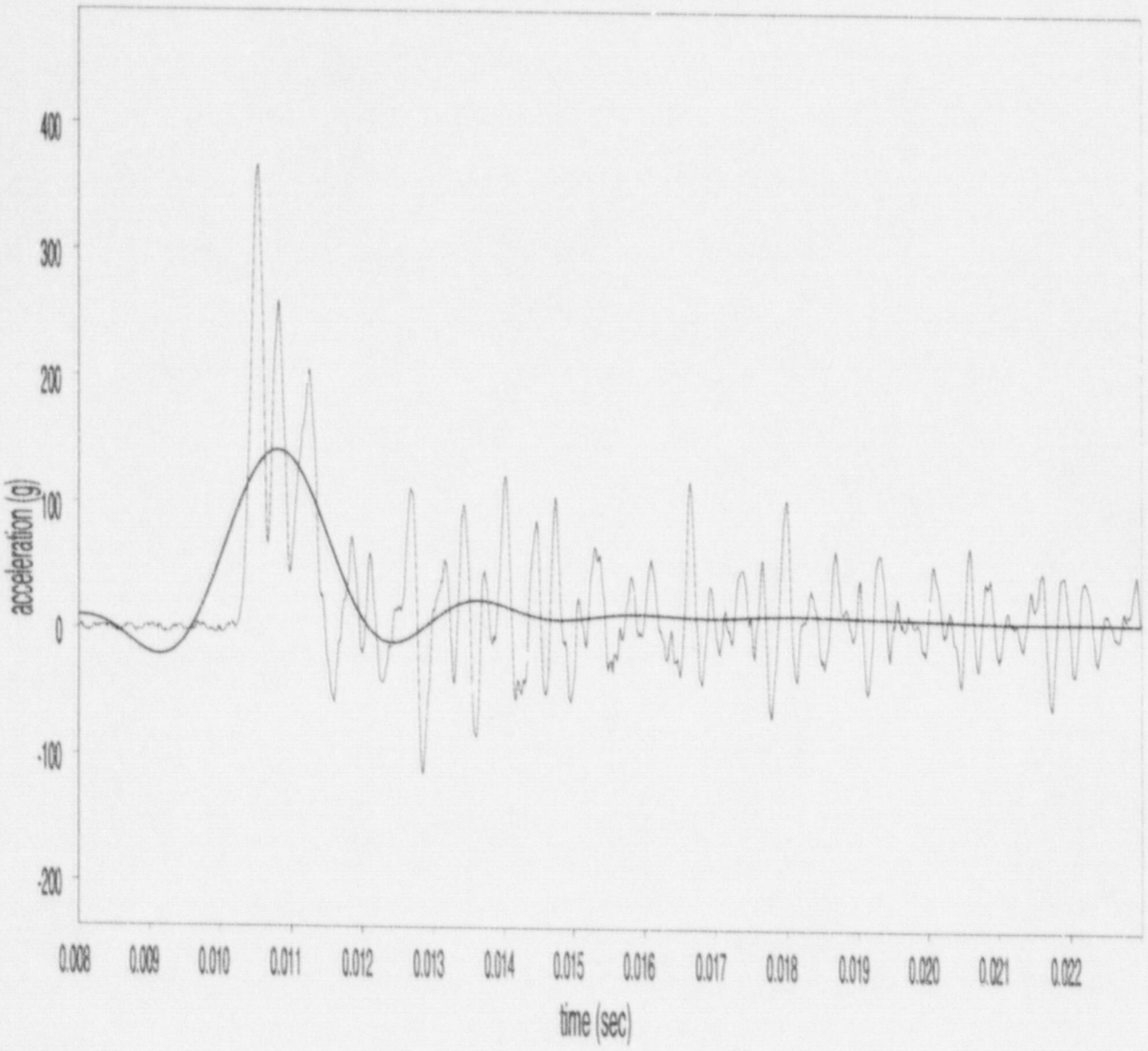

Figure A-26 SNL Test #228, Gauge A4 (45.7-cm (45.7-cm (18-inch)) end drop, filter cutoff: 450Hz, max. acceleration: 141.5g)

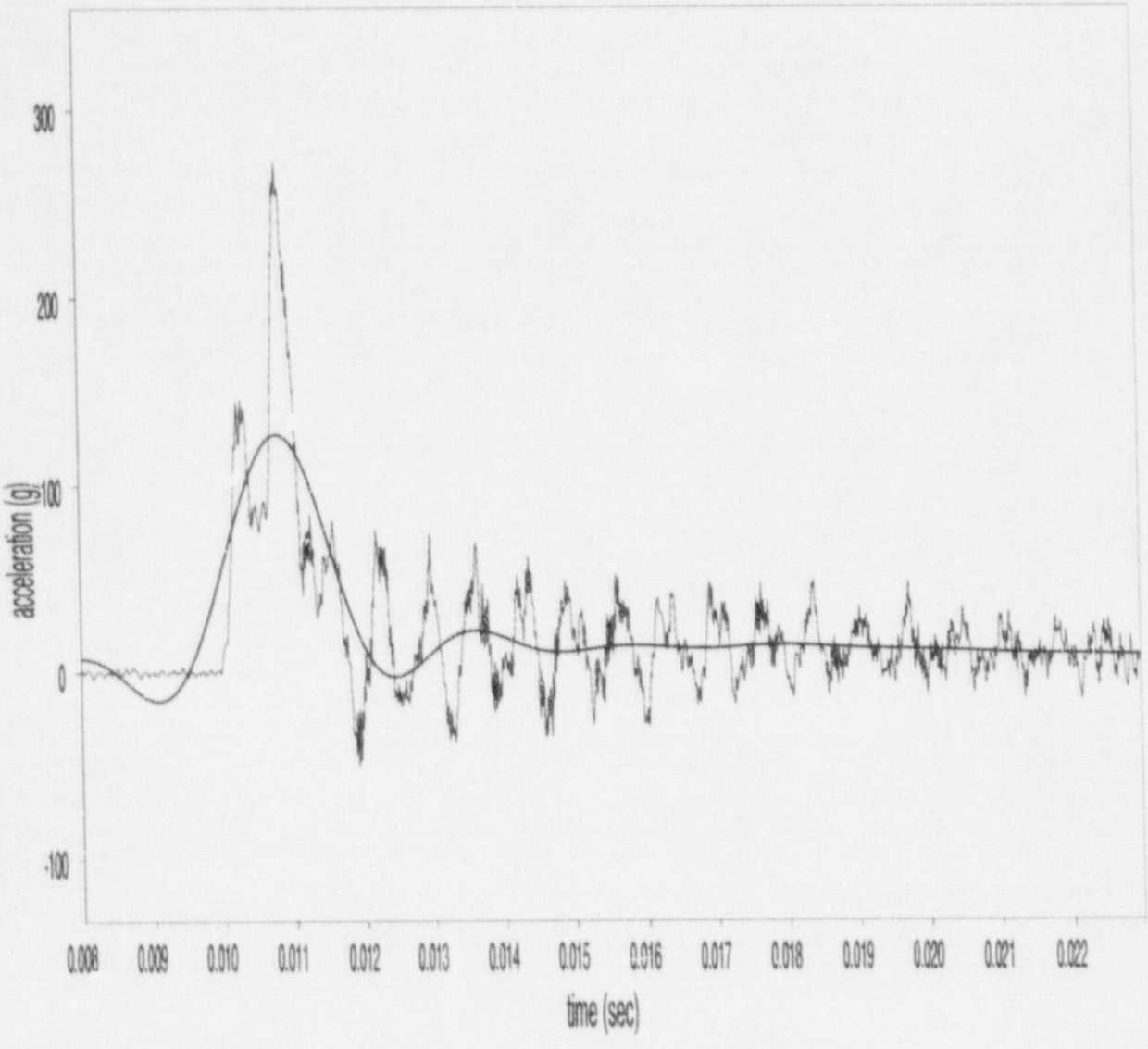

Figure A-27 SNL Test #228, Gauge A5 (45.7-cm (45.7-cm (18-inch)) end drop, filter cutoff: 450Hz, max. acceleration: 127.0g)

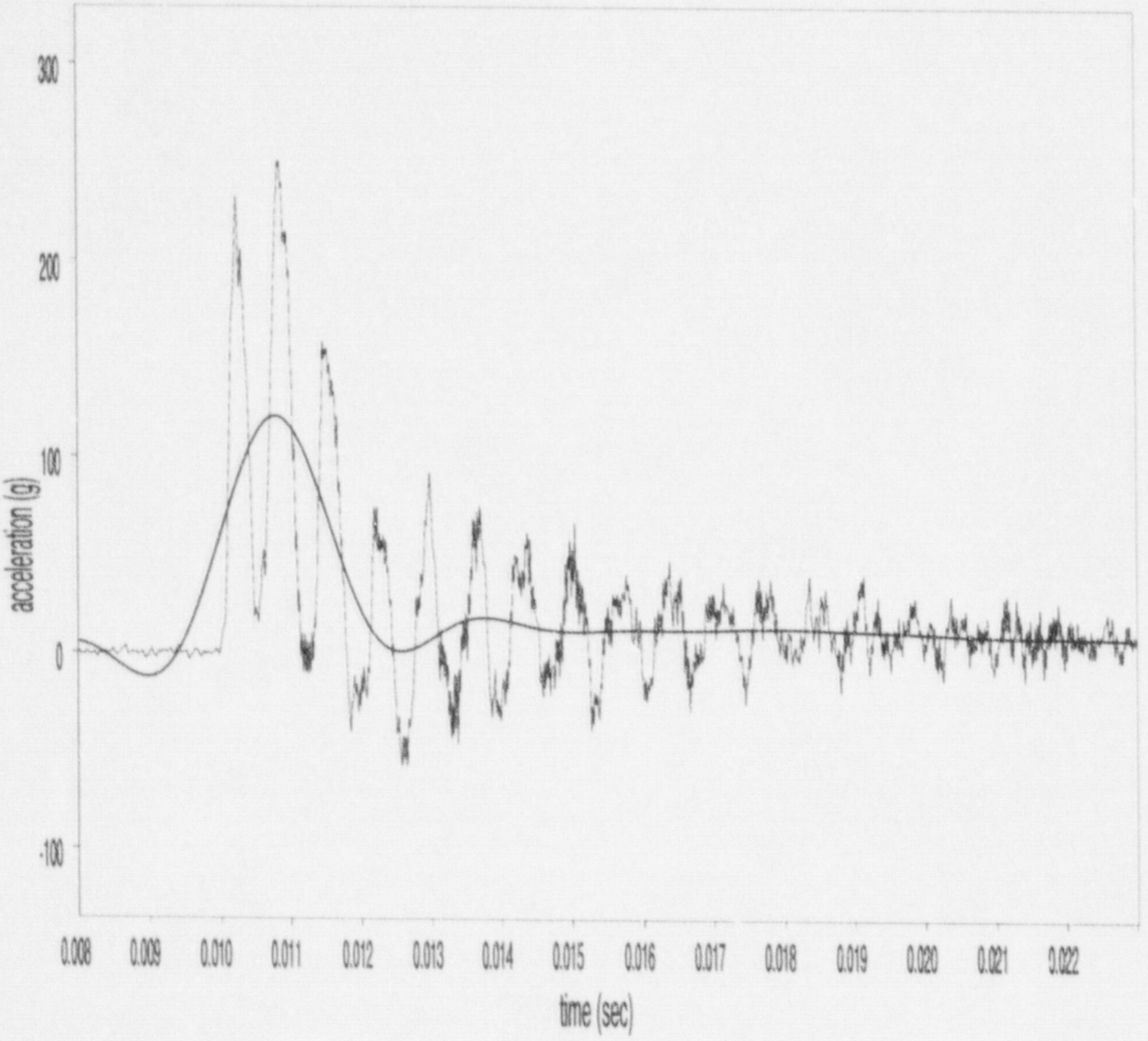

Figure A-28 SNL Test #228, Gauge A6 (45.7-cm (45.7-cm (18-inch)) end drop, filter cutoff: 450Hz, max. acceleration: 120.8g)

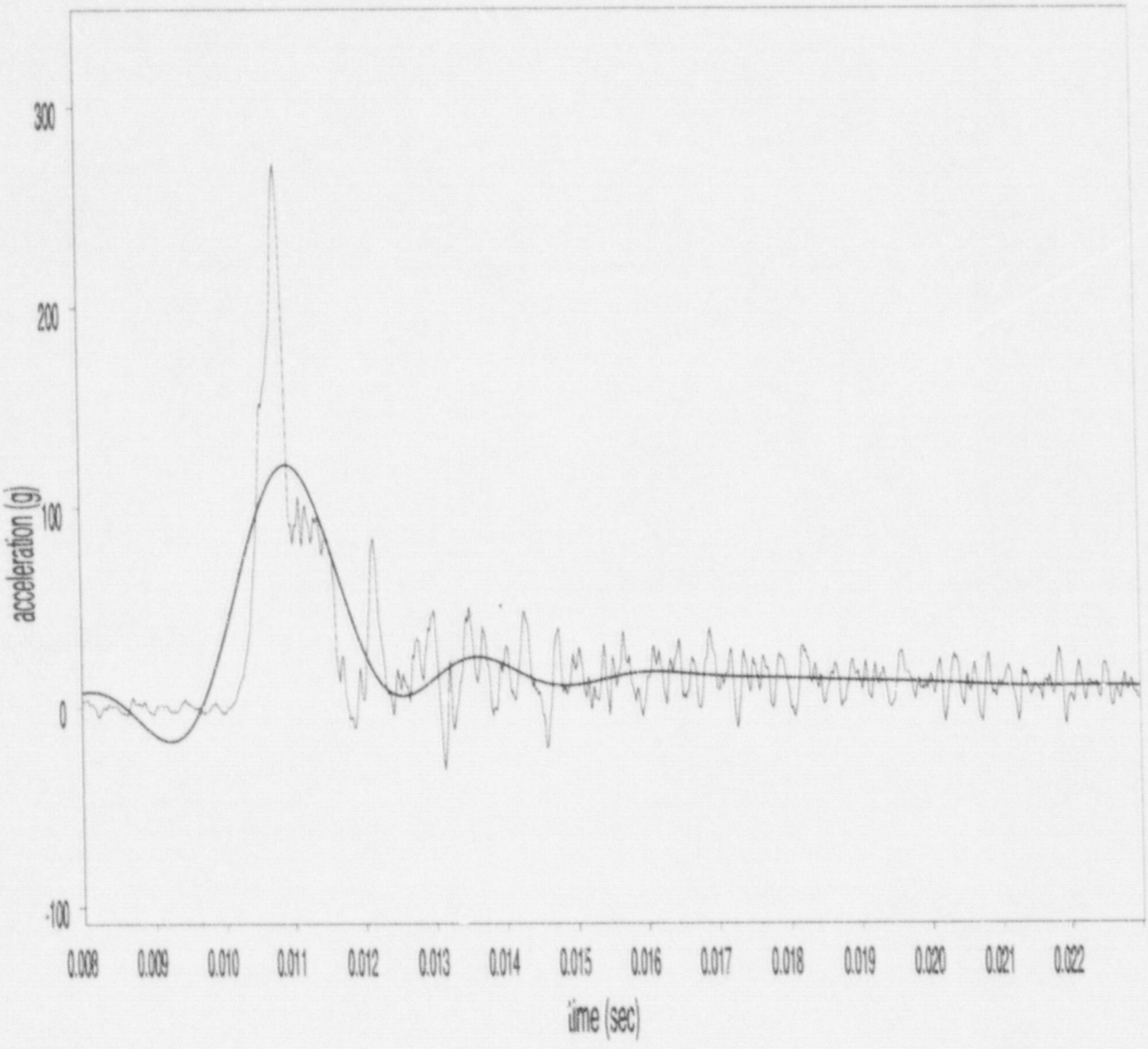

Figure A-29 SNL Test #229, Gauge A1 (45.7-cm (18-inch) end drop, filter cutoff: 450Hz, max. acceleration: 121.4g)

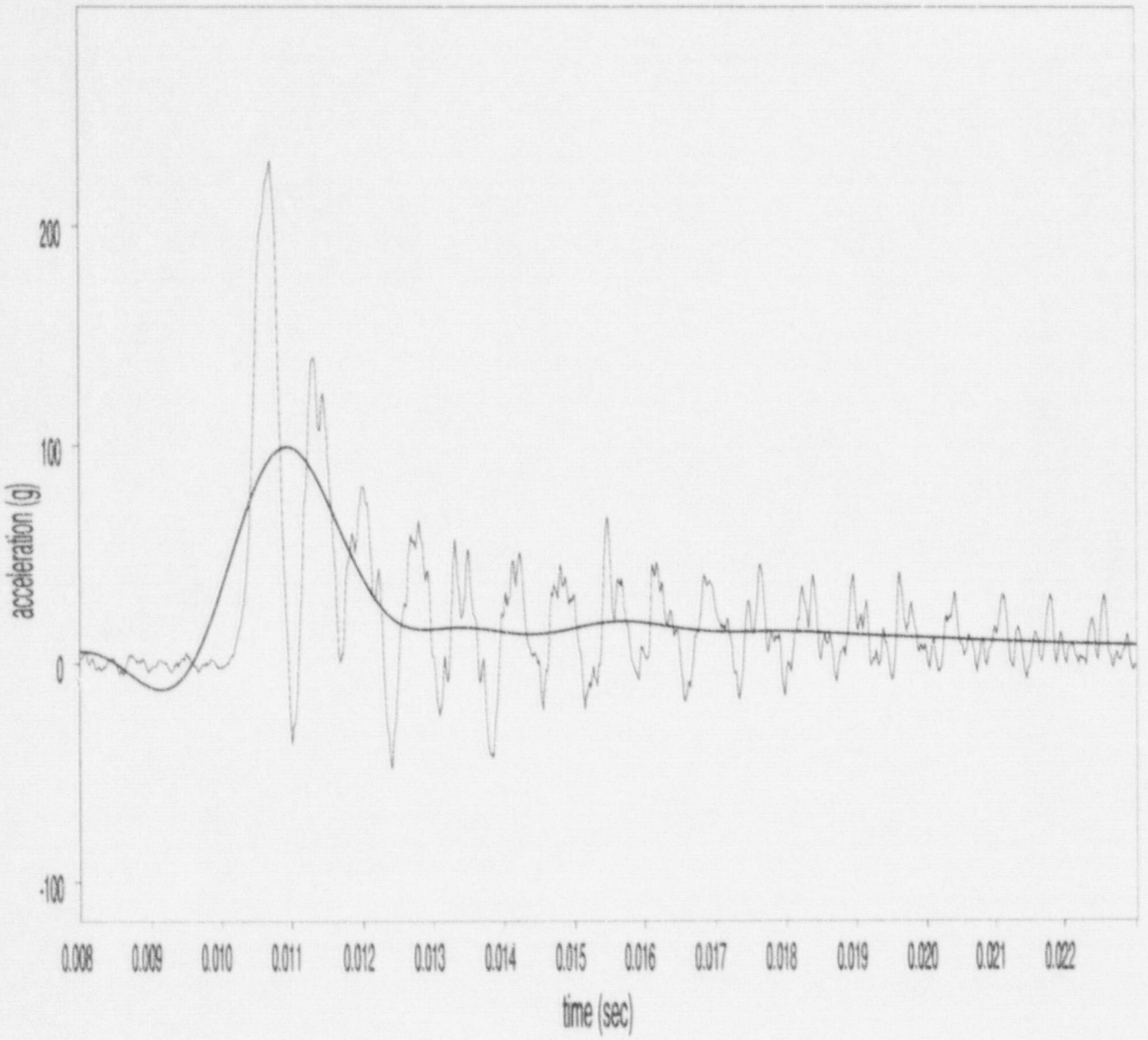

Figure A-30 SNL Test #229, Gauge A2 (45.7-cm (18-inch) end drop, filter cutoff: 450Hz, max. acceleration: 99.2g)

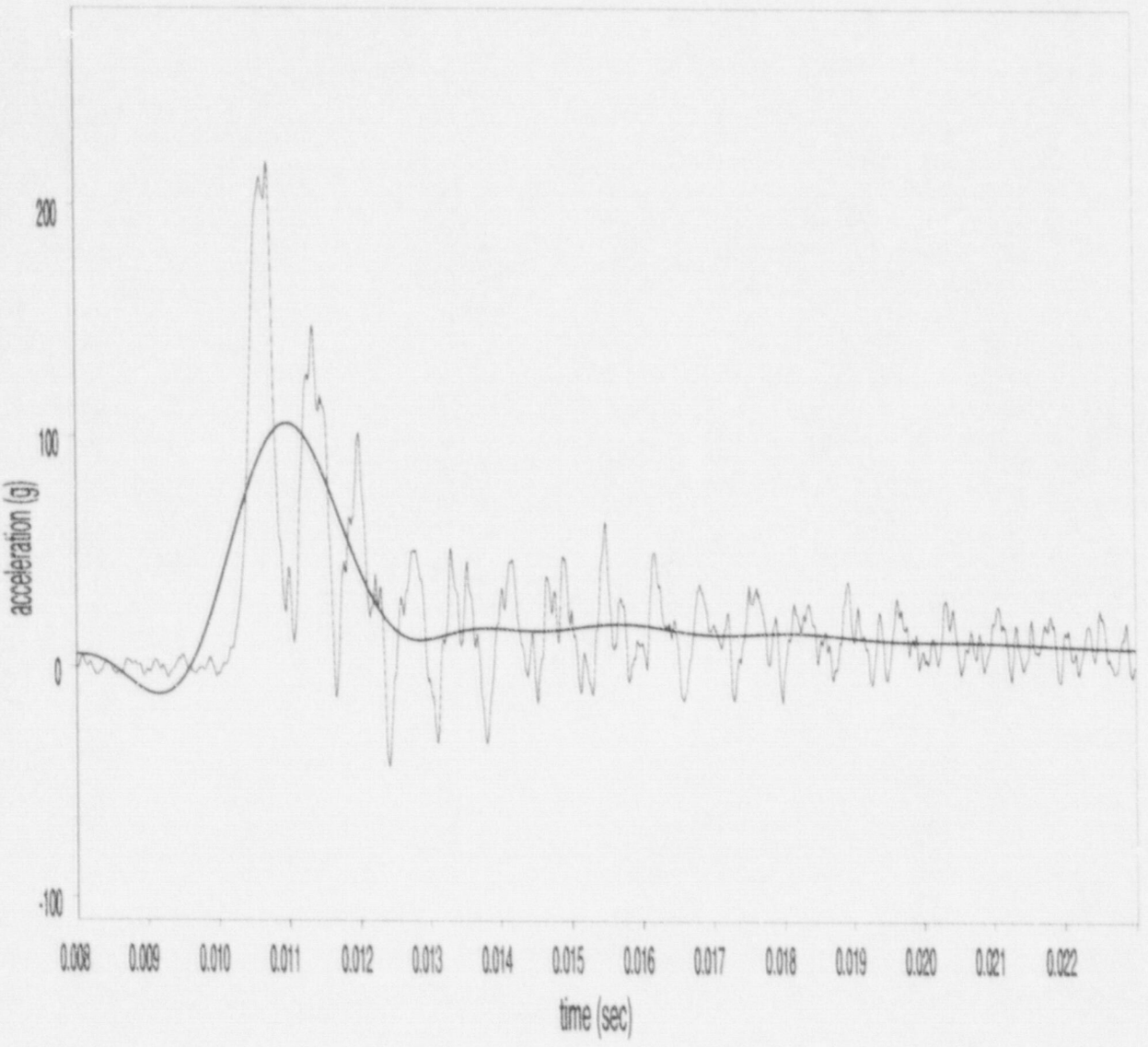

Figure A-31 SNL Test #229, Gauge A3 (45.7-cm (18-inch) end drop, filter cutoff: 450Hz, max. acceleration: 105.6g)

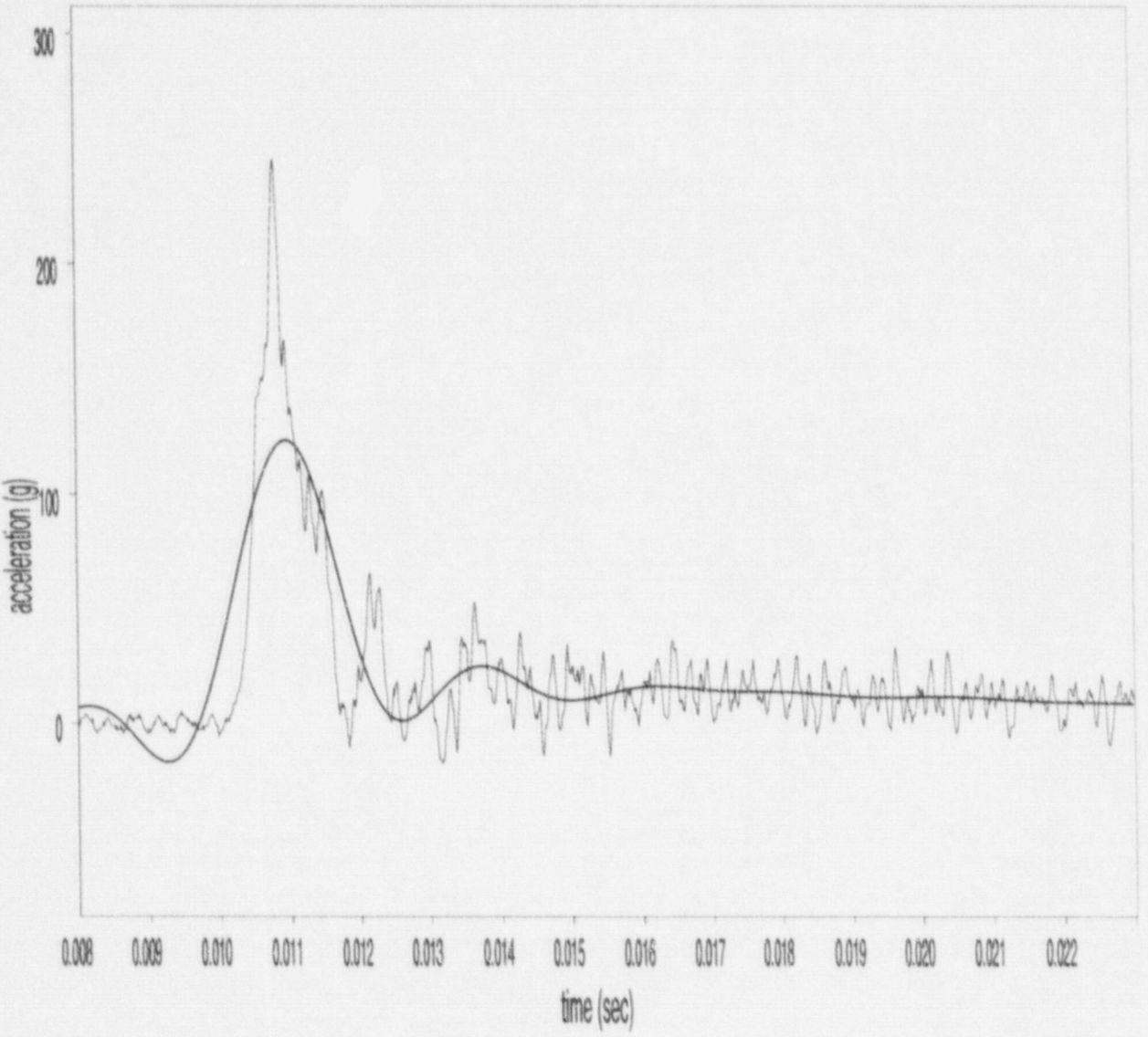

Figure A-32 SNL Test #229, Gauge A4 (45.7-cm (18-inch) end drop, filter cutoff: 450Hz, max. acceleration: 123.4g)

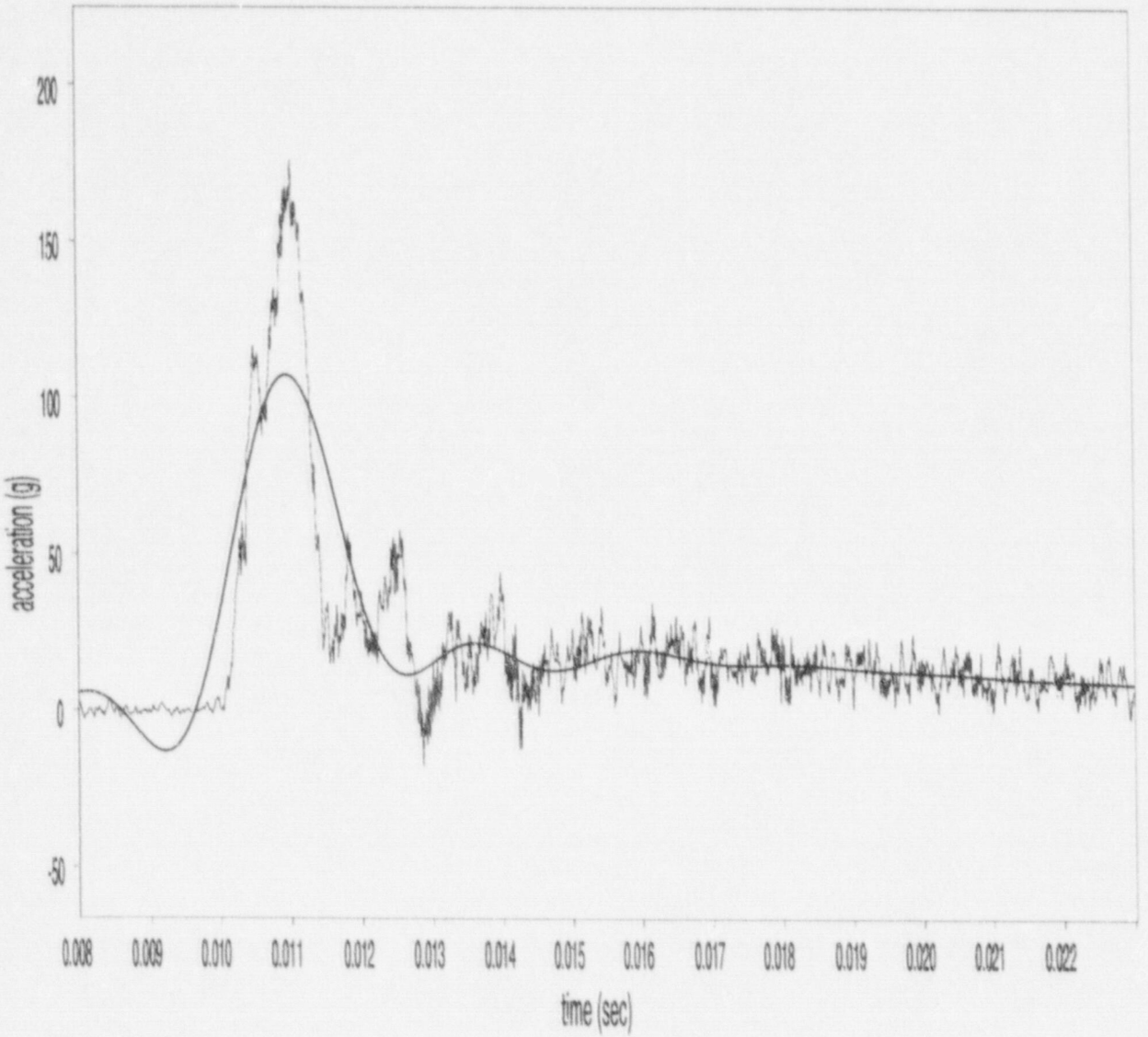

Figure A-33 SNL Test #229, Gauge A5 (45.7-cm (18-inch) end drop, filter cutoff: 450Hz, max. acceleration: 107.3g)

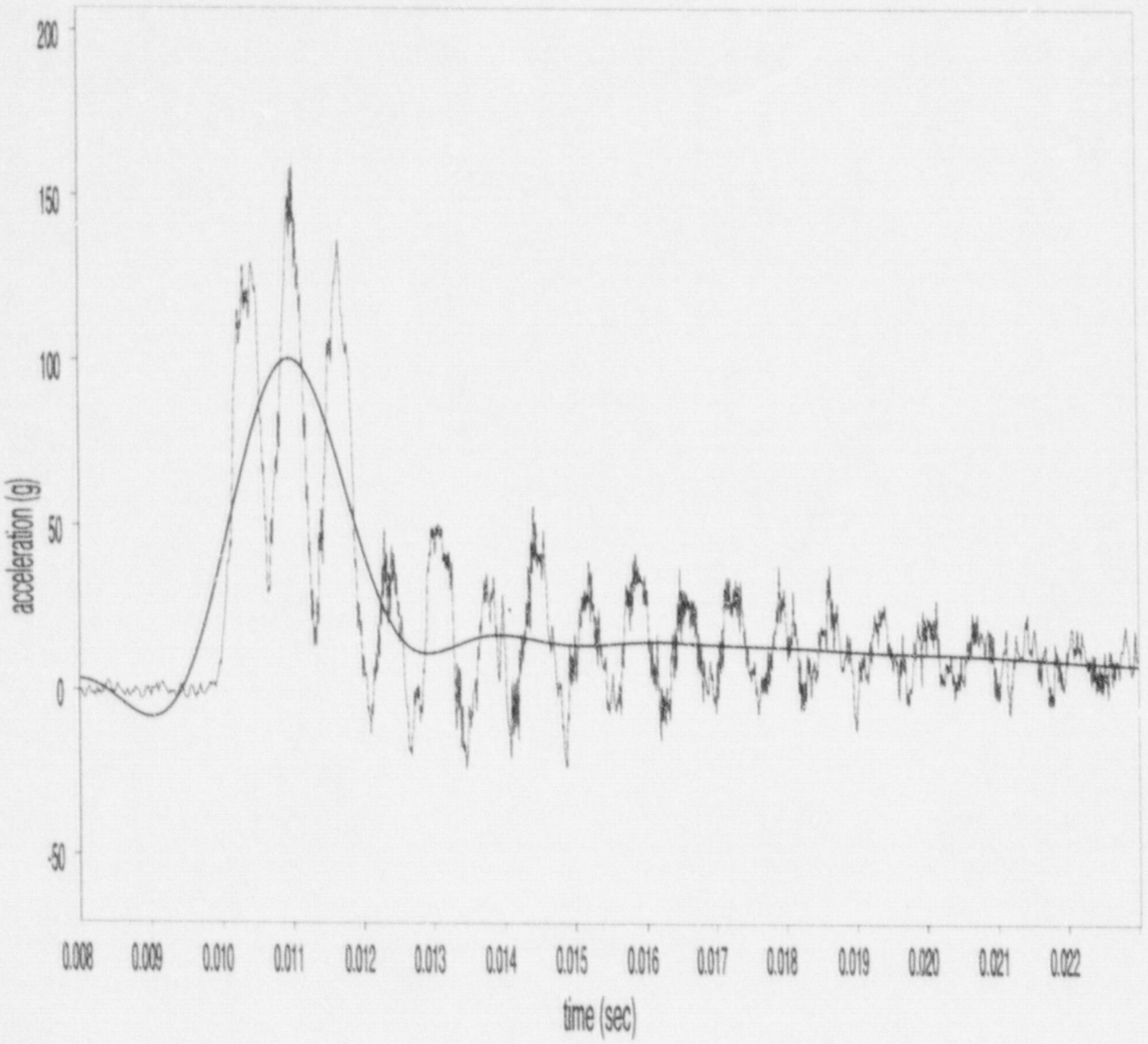

Figure A-34 SNL Test #229, Gauge A6 (45.7-cm (18-inch) end drop, filter cutoff: 450Hz, max. acceleration: 100.5g)

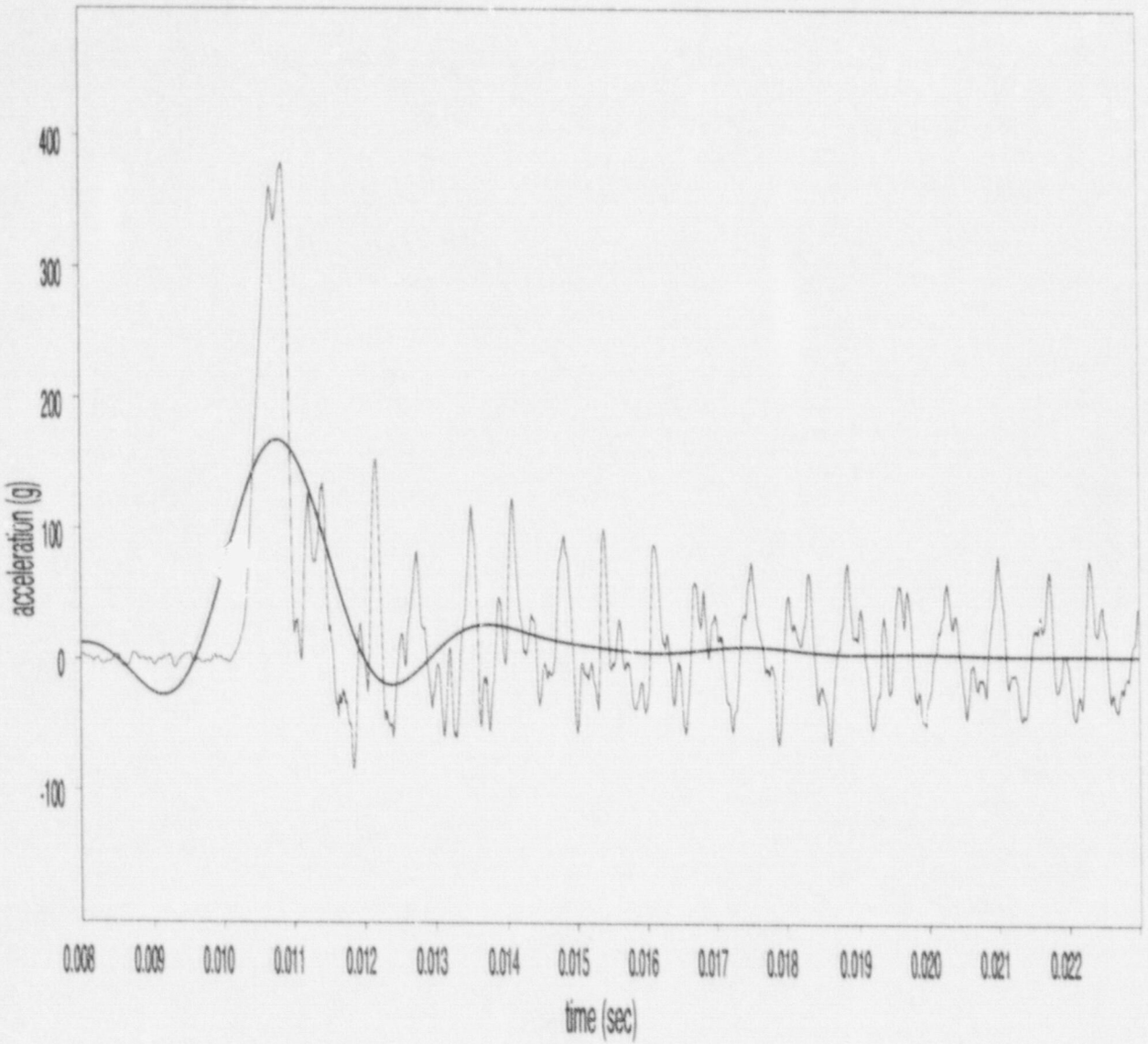

Figure A-35 SNL Test #230, Gauge A1 (45.7-cm (18-inch) end drop, filter cutoff: 450Hz, max. acceleration: 167.9g)

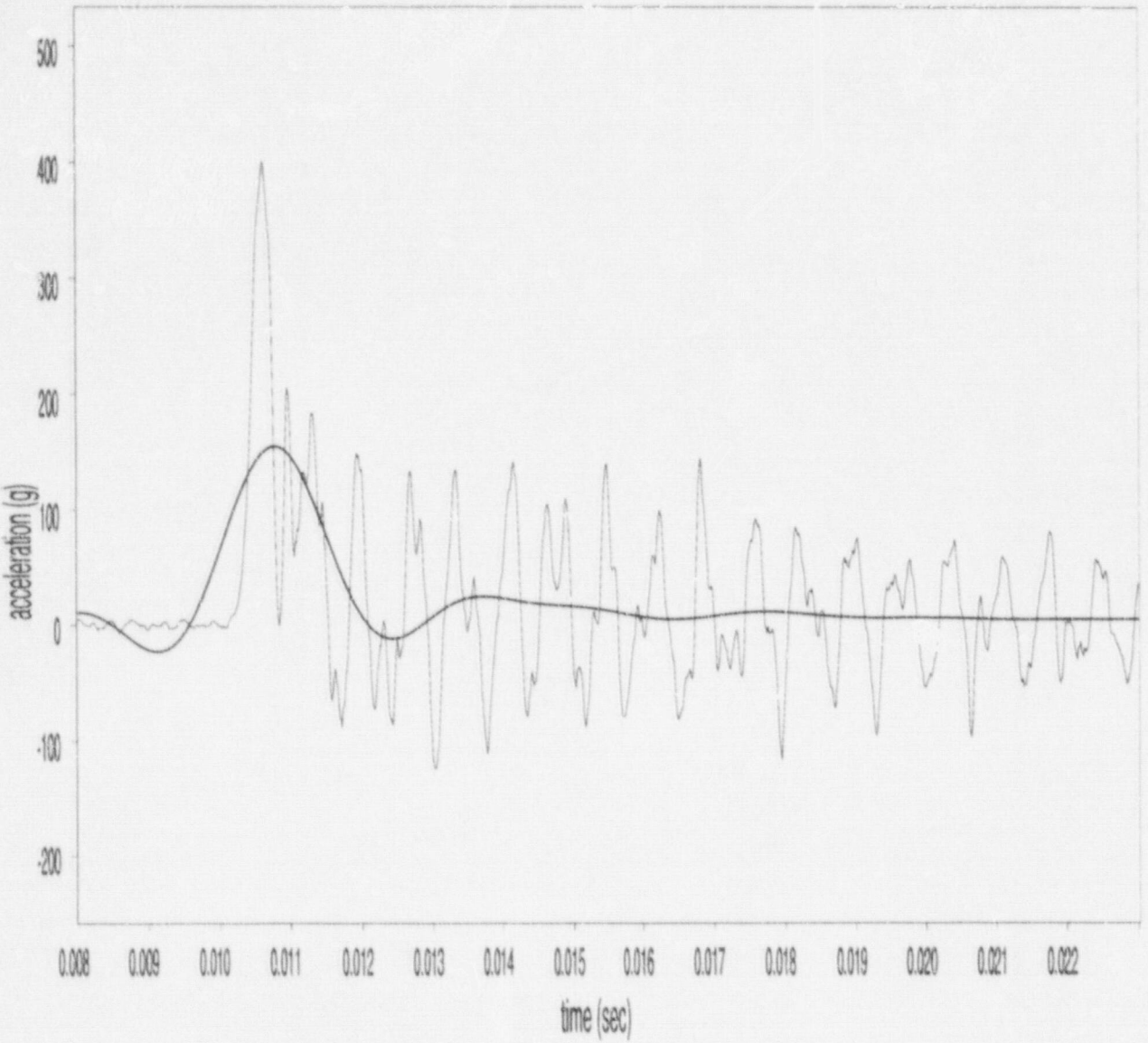

Figure A-36 SNL Test #230, Gauge A2 (45.7-cm (18-inch) end drop, filter cutoff: 450Hz, max. acceleration: 154.5g)

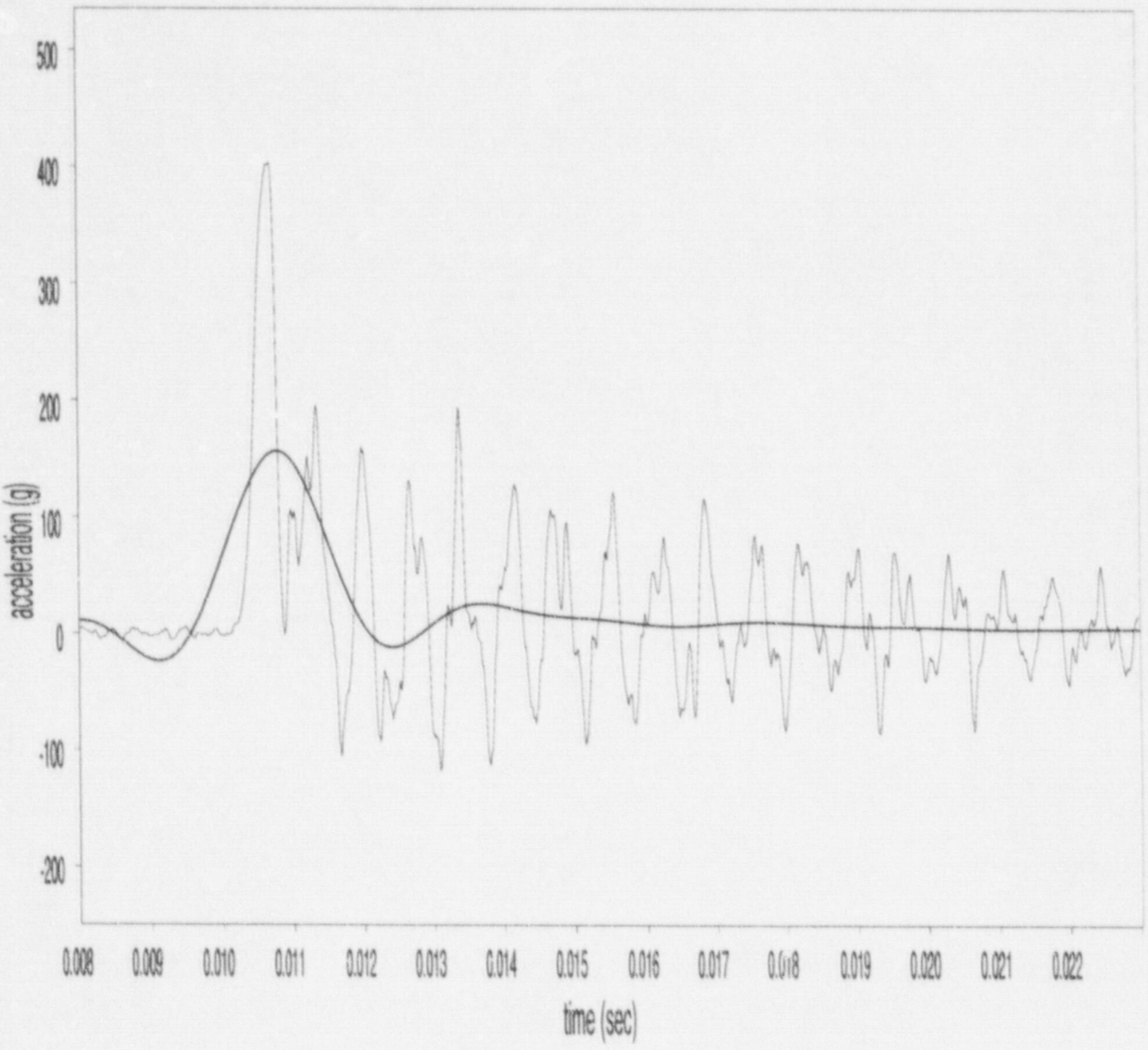

Figure A-37 SNL Test #230, Gauge A3 (45.7-cm (18-inch) end drop, filter cutoff: 450Hz, max. acceleration: 156.4g)

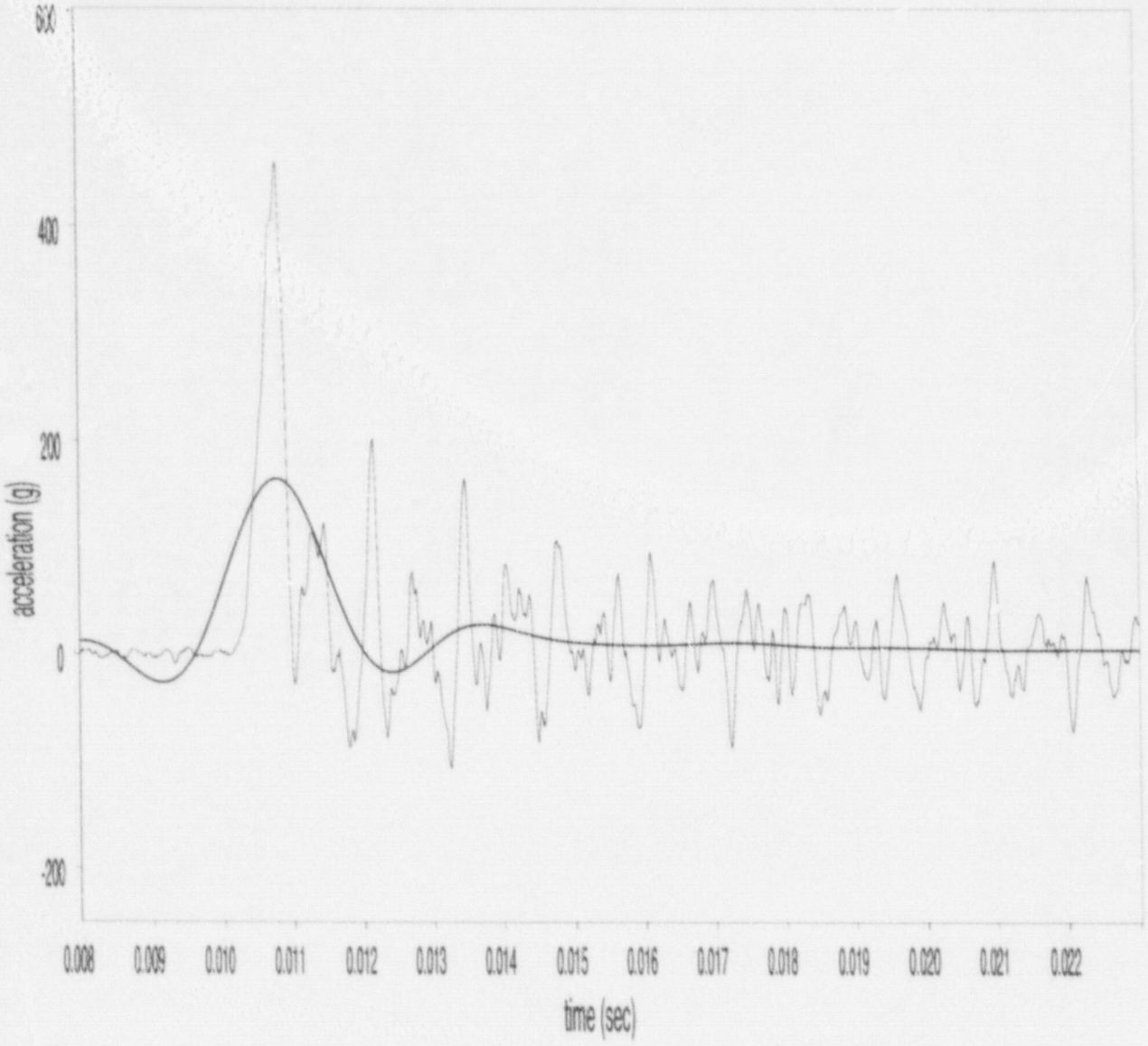

Figure A-38 SNL Test #230, Gauge A4 (45.7-cm (18-inch) end drop, filter cutoff: 450Hz, max. acceleration: 164.0g)

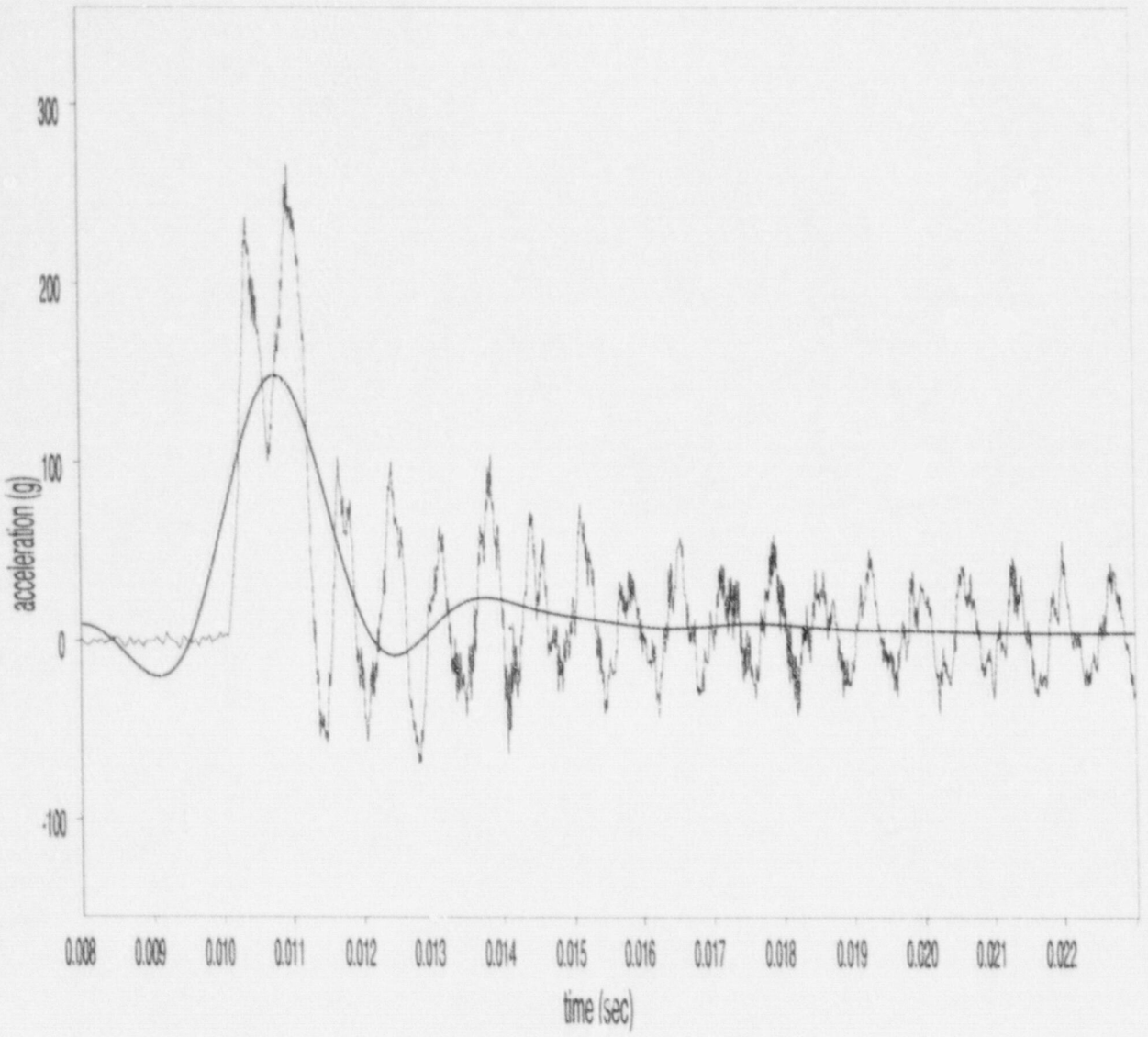

Figure A-39 SNL Test #230, Gauge A5 (45.7-cm (18-inch) end drop, filter cutoff: 450Hz, max. acceleration: 148.6g)

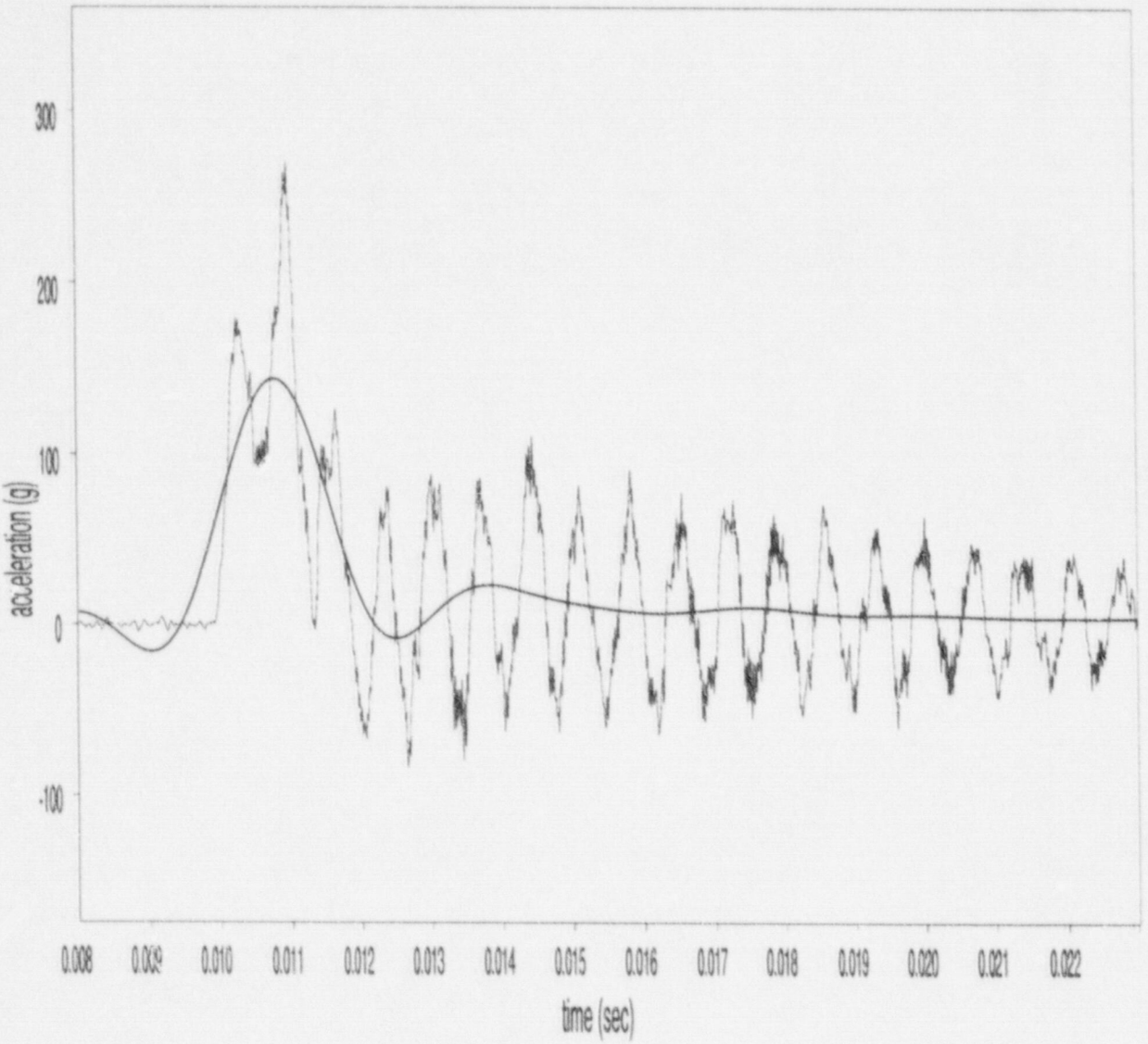

Figure A-40 SNL Test #230, Gauge A6 (45.7-cm (18-inch) end drop, filter cutoff: 450Hz, max. acceleration: 143.7g)

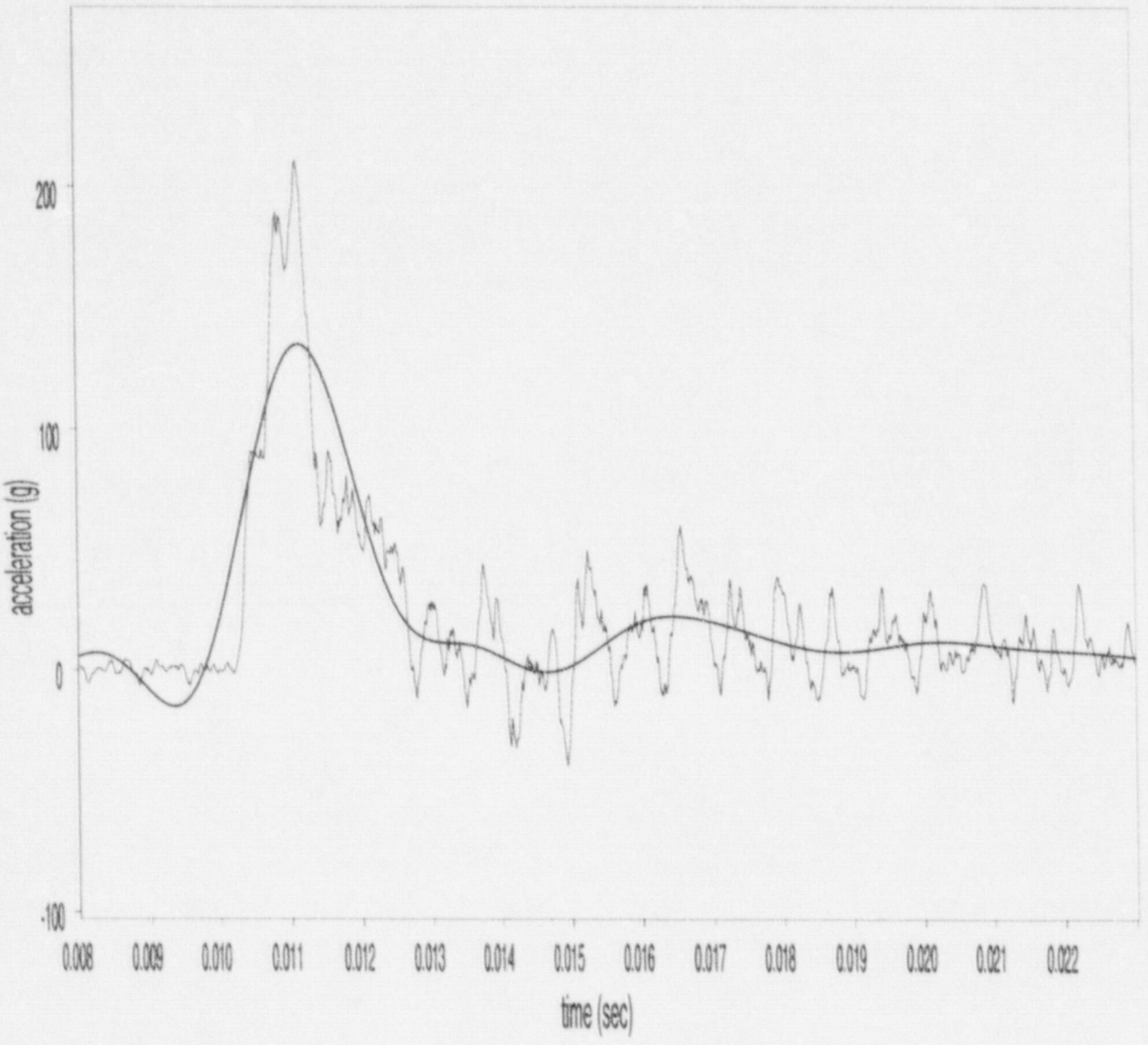

Figure A-41 SNL Test #231, Gauge A1 (45.7-cm (18-inch) end drop, filter cutoff: 450Hz, max. acceleration: 134.8g)

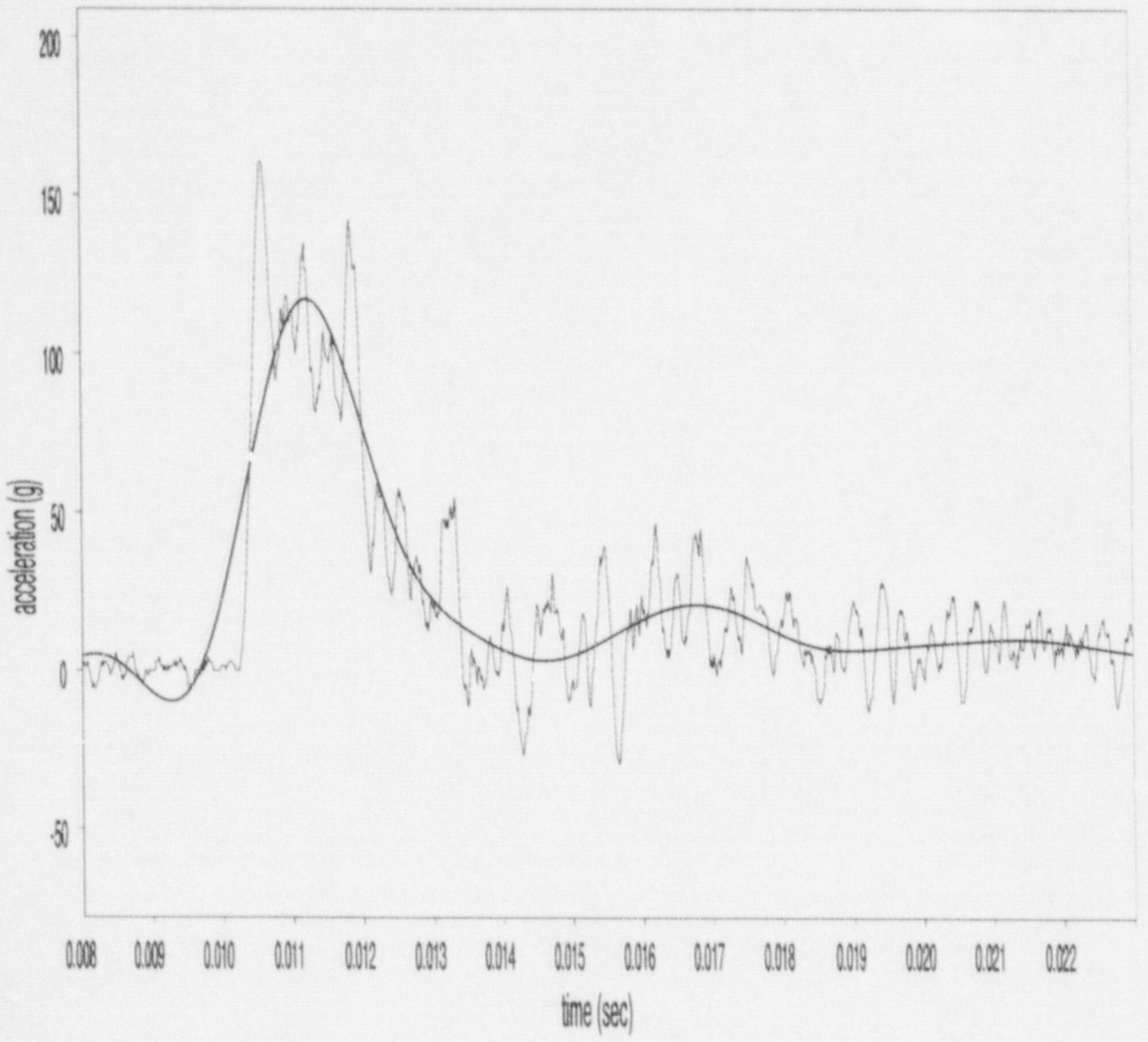

Figure A-42 SNL Test #231, Gauge A2 (45.7-cm (18-inch) end drop, filter cutoff: 450Hz, max. acceleration: 117.1g)

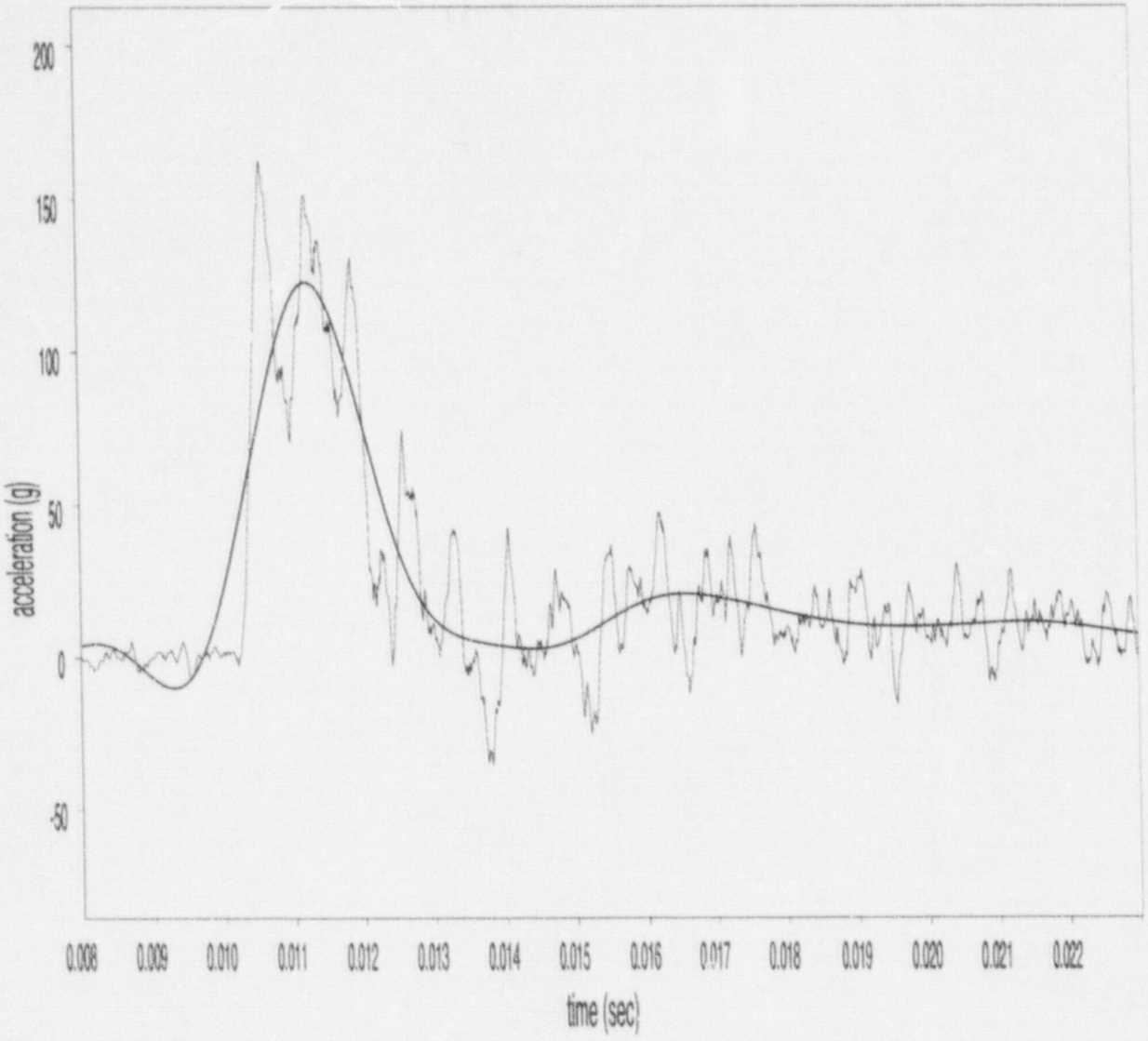

Figure A-43 SNL Test #231, Gauge A3 (45.7-cm (18-inch) end drop, filter cutoff: 450Hz, max. acceleration: 122.7g)

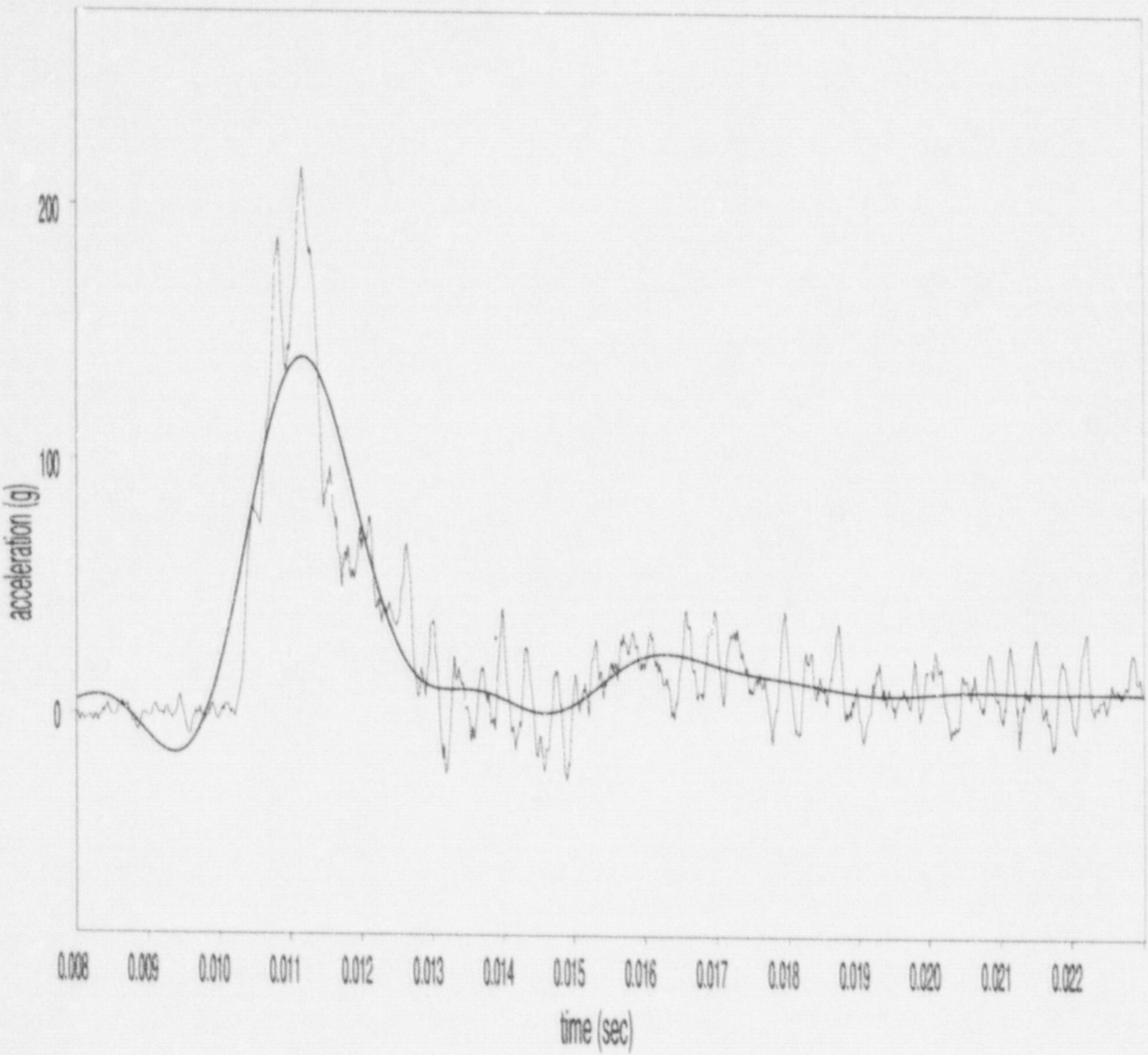

Figure A-44 SNL Test #231, Gauge A4 (45.7-cm (18-inch) end drop, filter cutoff: 450Hz, max. acceleration: 140.2g)

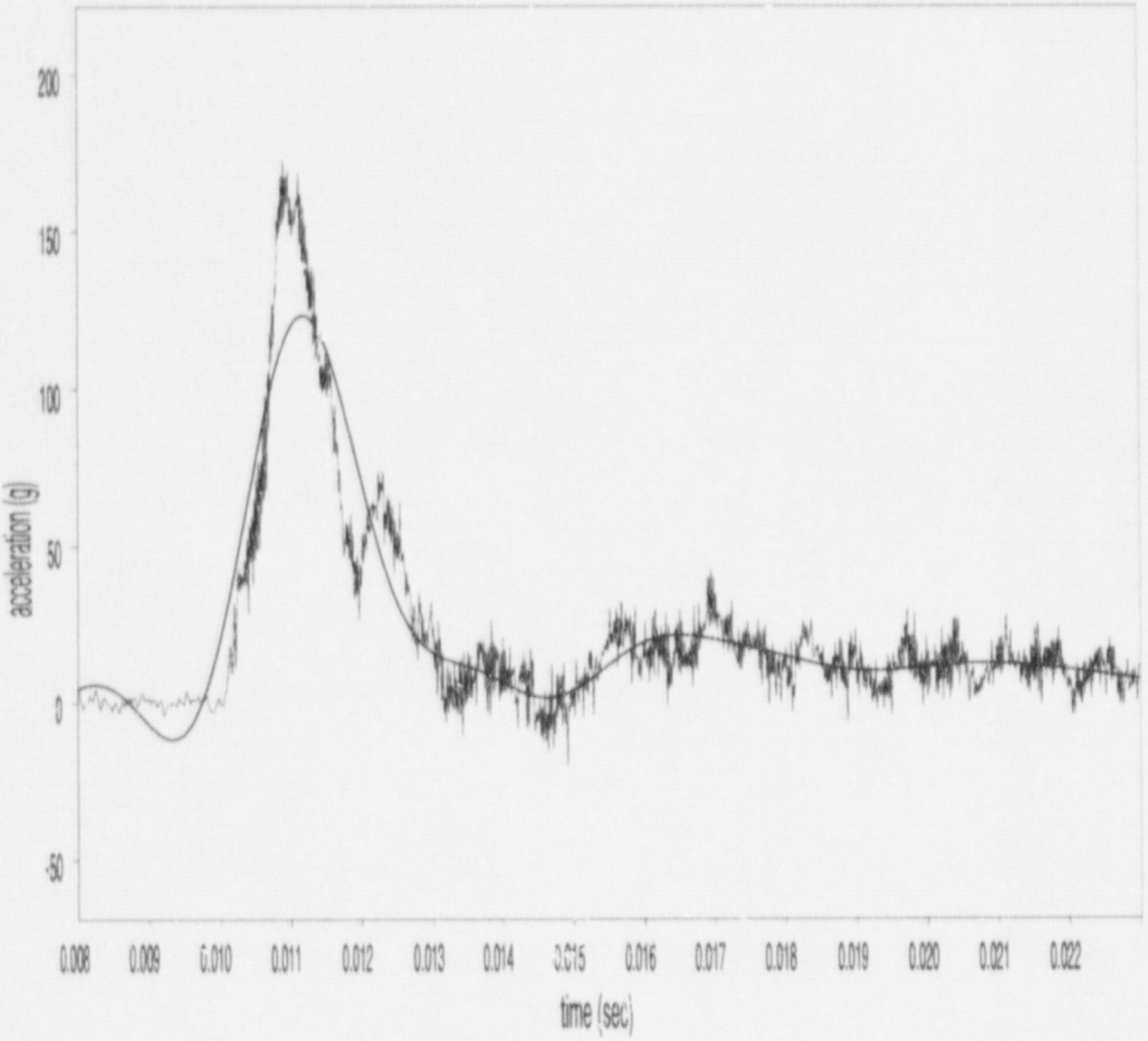

Figure A-45 SNL Test #231, Gauge A5 (45.7-cm (18-inch) end drop, filter cutoff: 450Hz, max. acceleration. 123.2g)

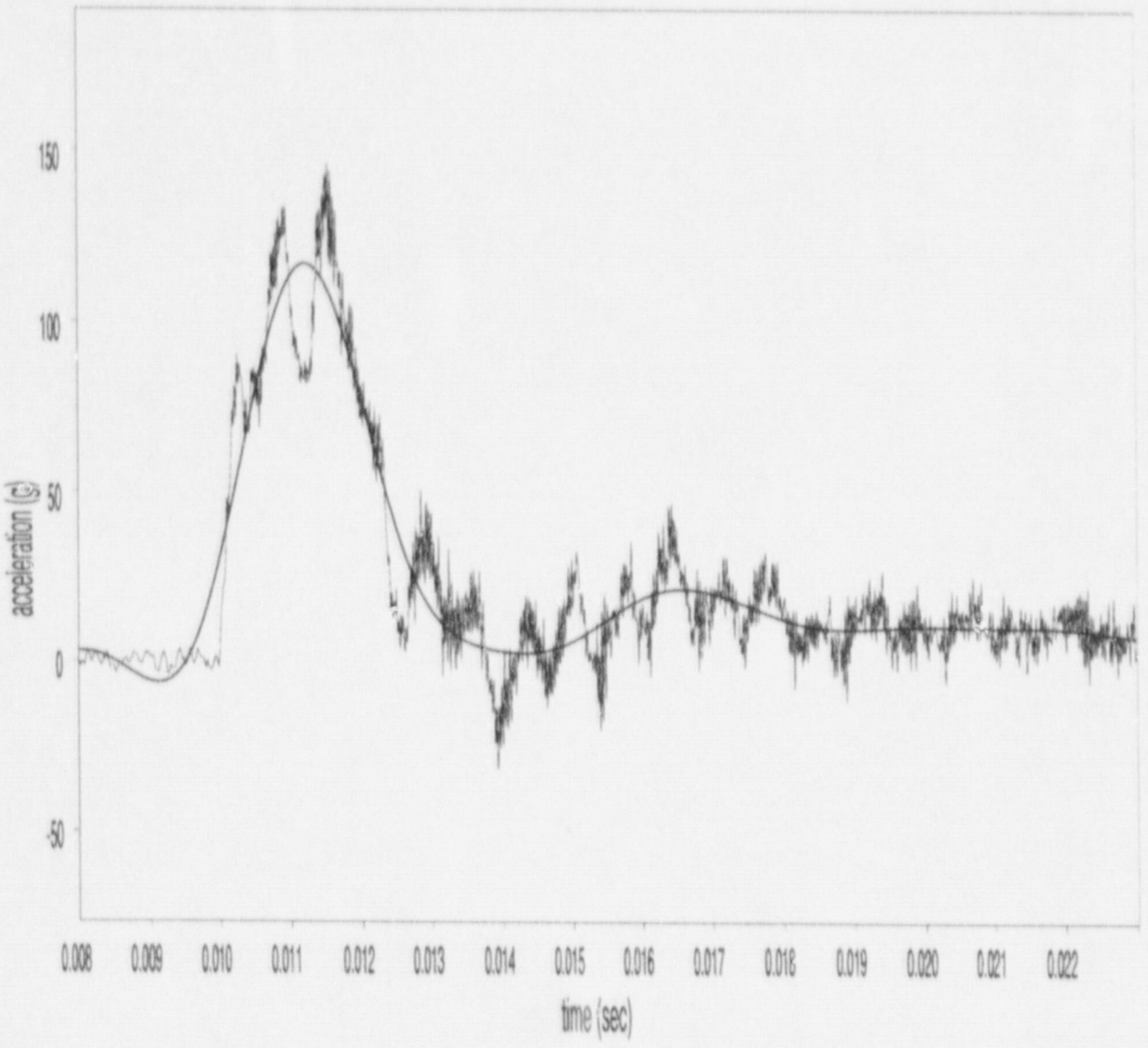

Figure A-46 SNL Test #231, Gauge A6 (45.7-cm (18-inch) end drop, filter cutoff: 450Hz, max. acceleration: 116.8g)

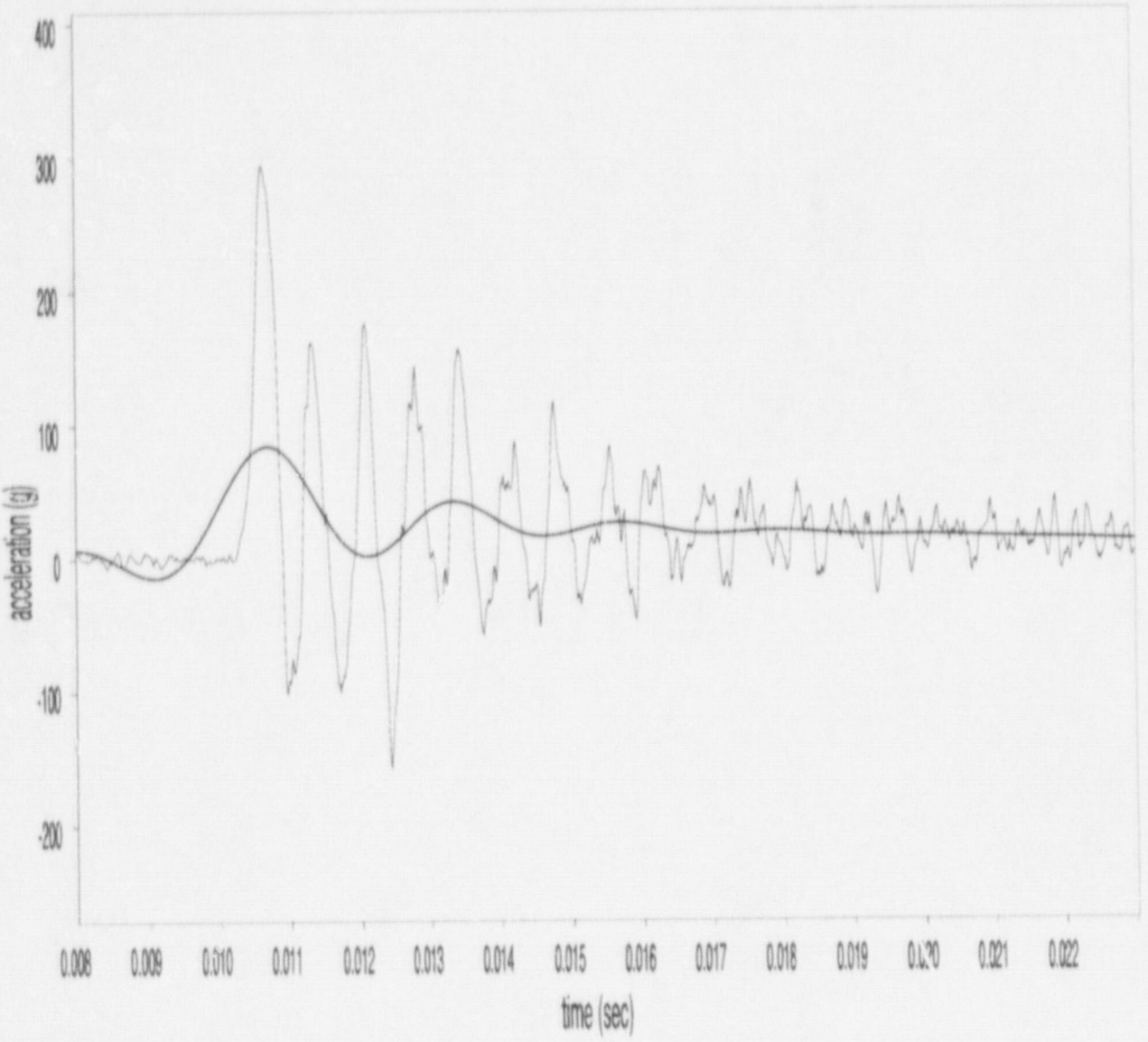

Figure A-47 SNL Test #232, Gauge A1 (45.7-cm (18-inch) end drop, filter cutoff: 450Hz, max. acceleration: 84.0g)

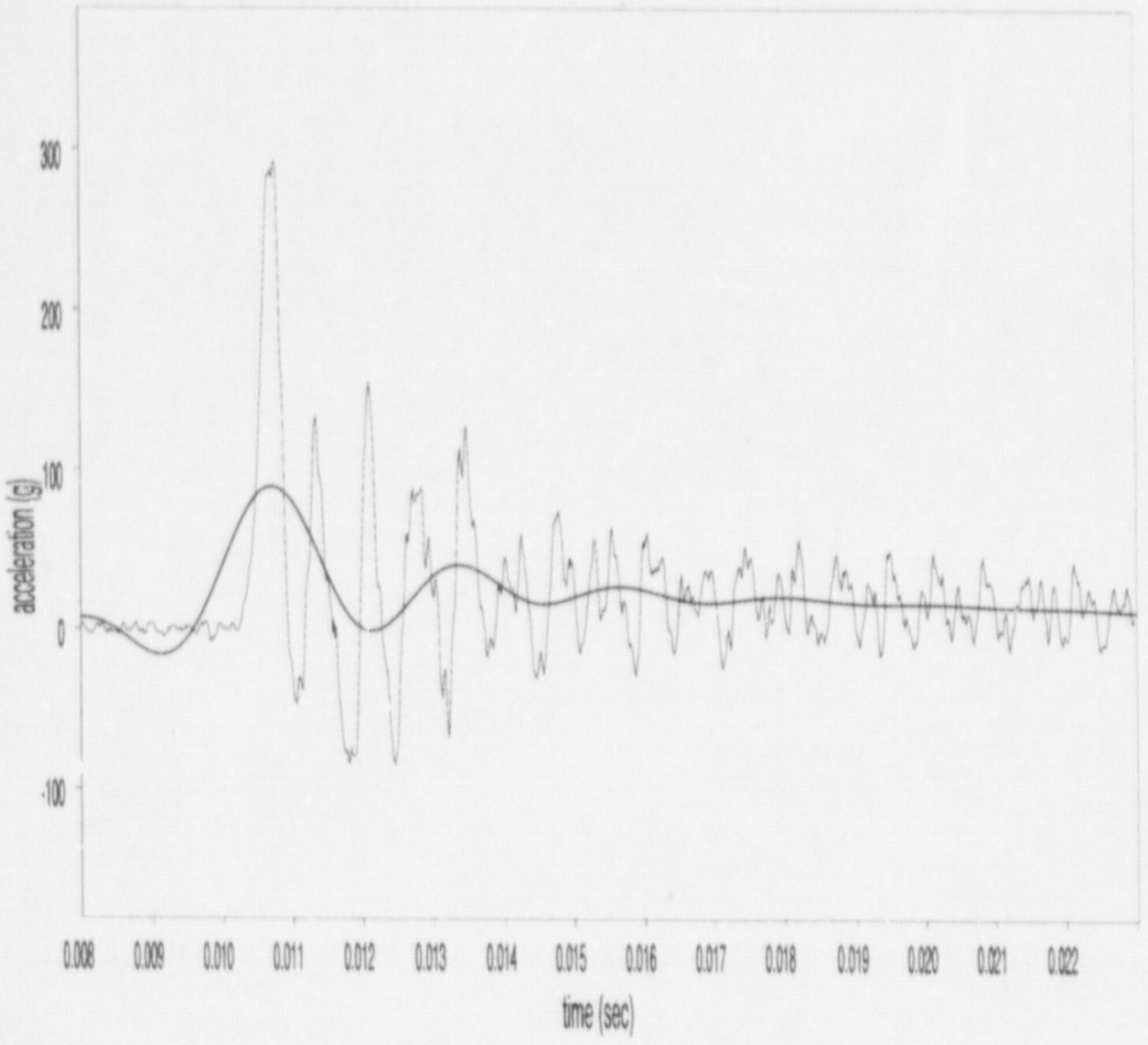

Figure A-48 SNL Test #232, Gauge A2 (45.7-cm (18-inch) end drop, filter cutoff: 450Hz, max. acceleration: 89.5g)

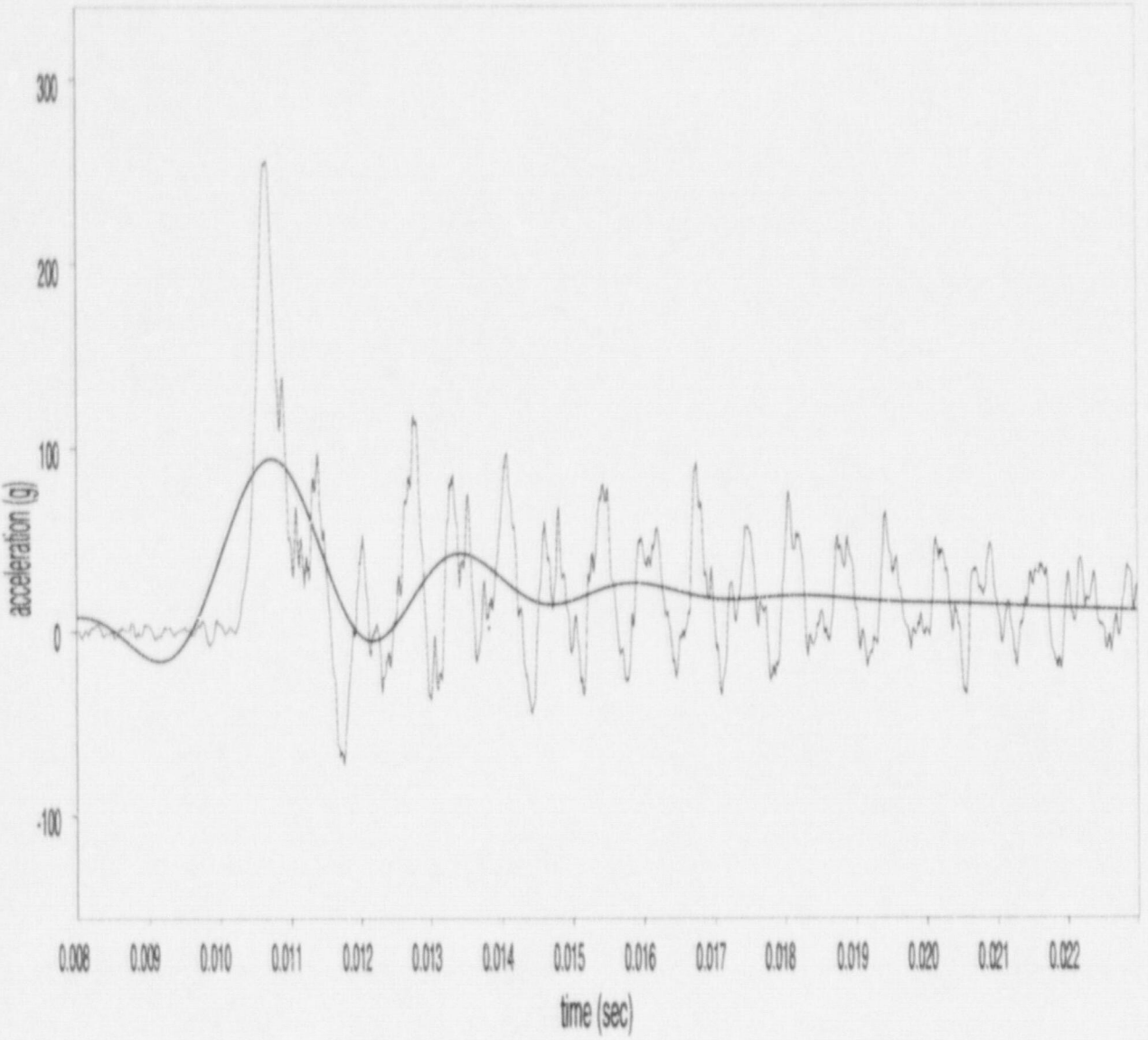

Figure A-49 SNL Test #232, Gauge A3 (45.7-cm (18-inch) end drop, filter cutoff: 450Hz, max. acceleration: 93.8g)

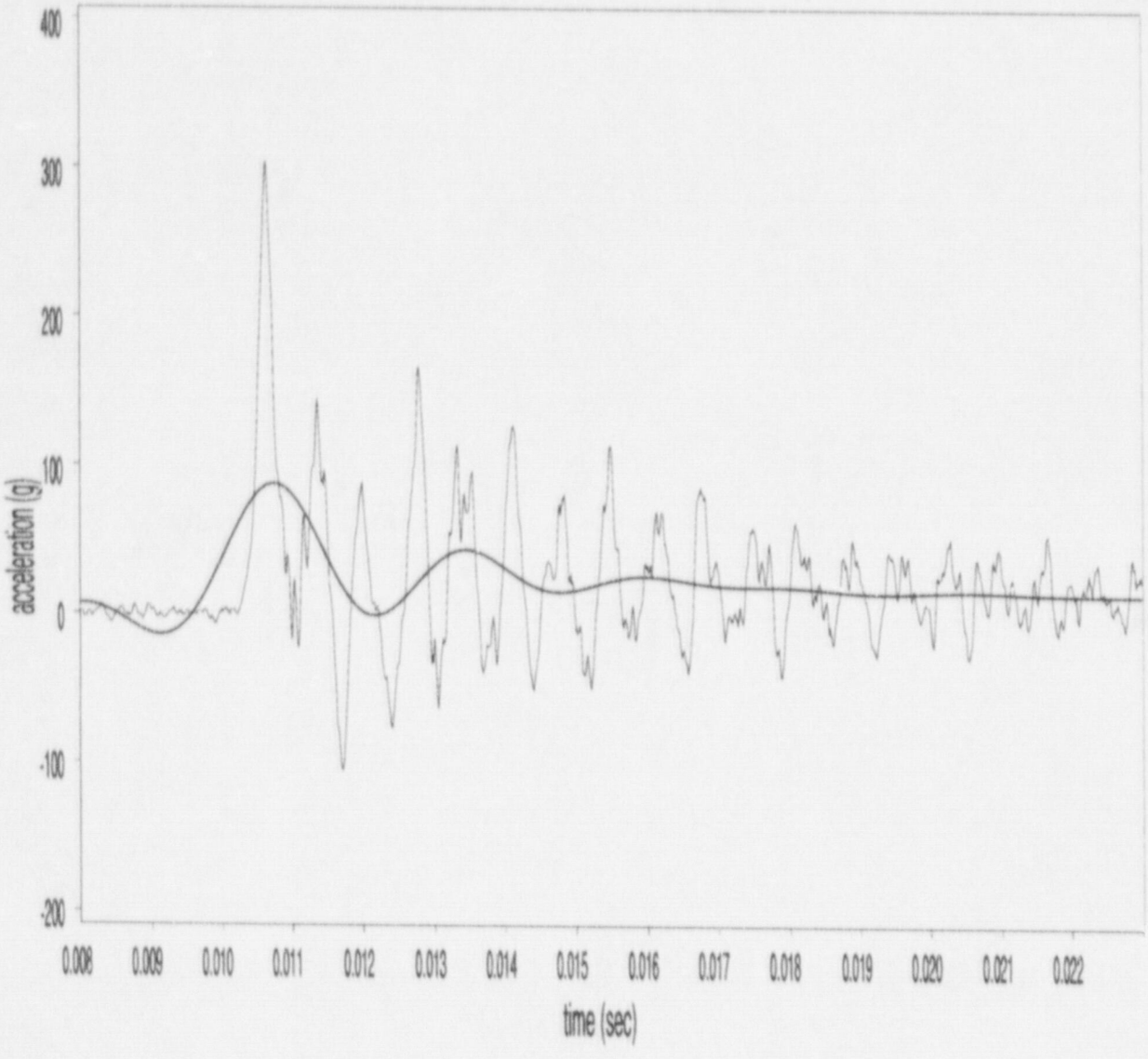

Figure A-50 SNL Test #232, Gauge A4 (45.7-cm (18-inch) end drop, filter cutoff: 450Hz, max. acceleration: 87.5g)

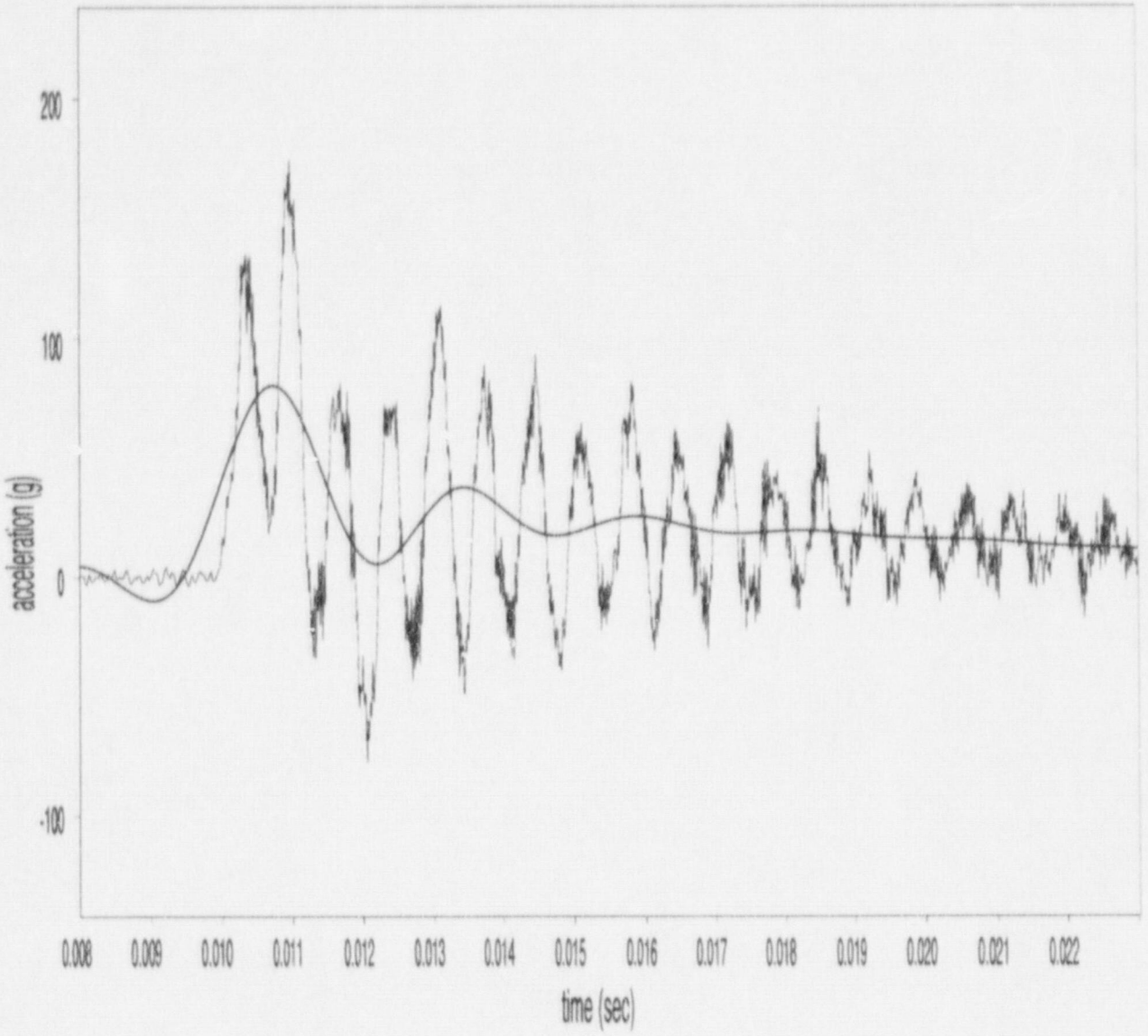

Figure A-51 SNL Test #232, Gauge A5 (45.7-cm (18-inch) end drop, filter cutoff: 450Hz, max. acceleration: 80.1g)

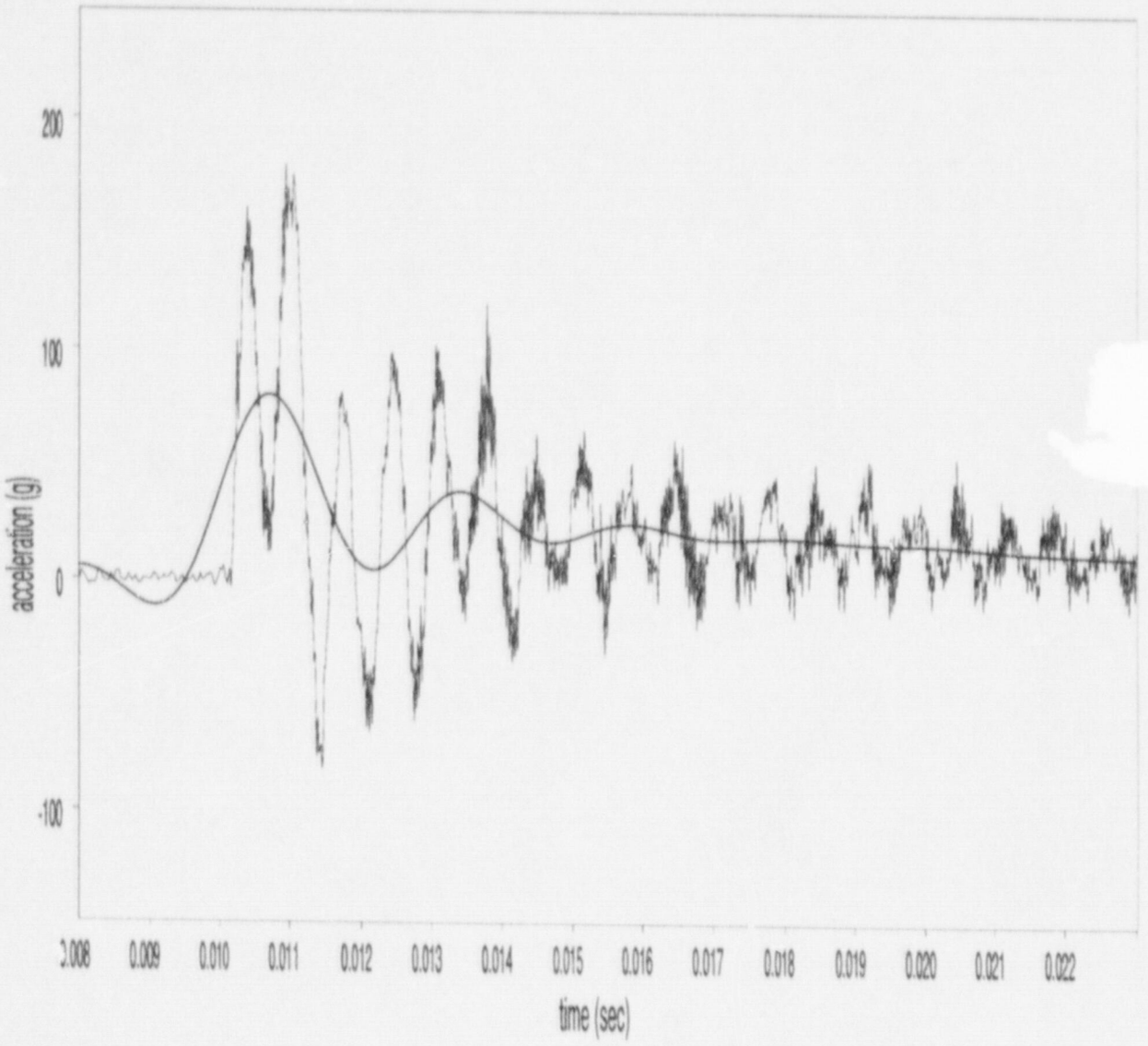

Figure A-52 SNL Test #232, Gauge A6 (45.7-cm (18-inch) end drop, filter cutoff: 450Hz, max. acceleration: 80.1g)

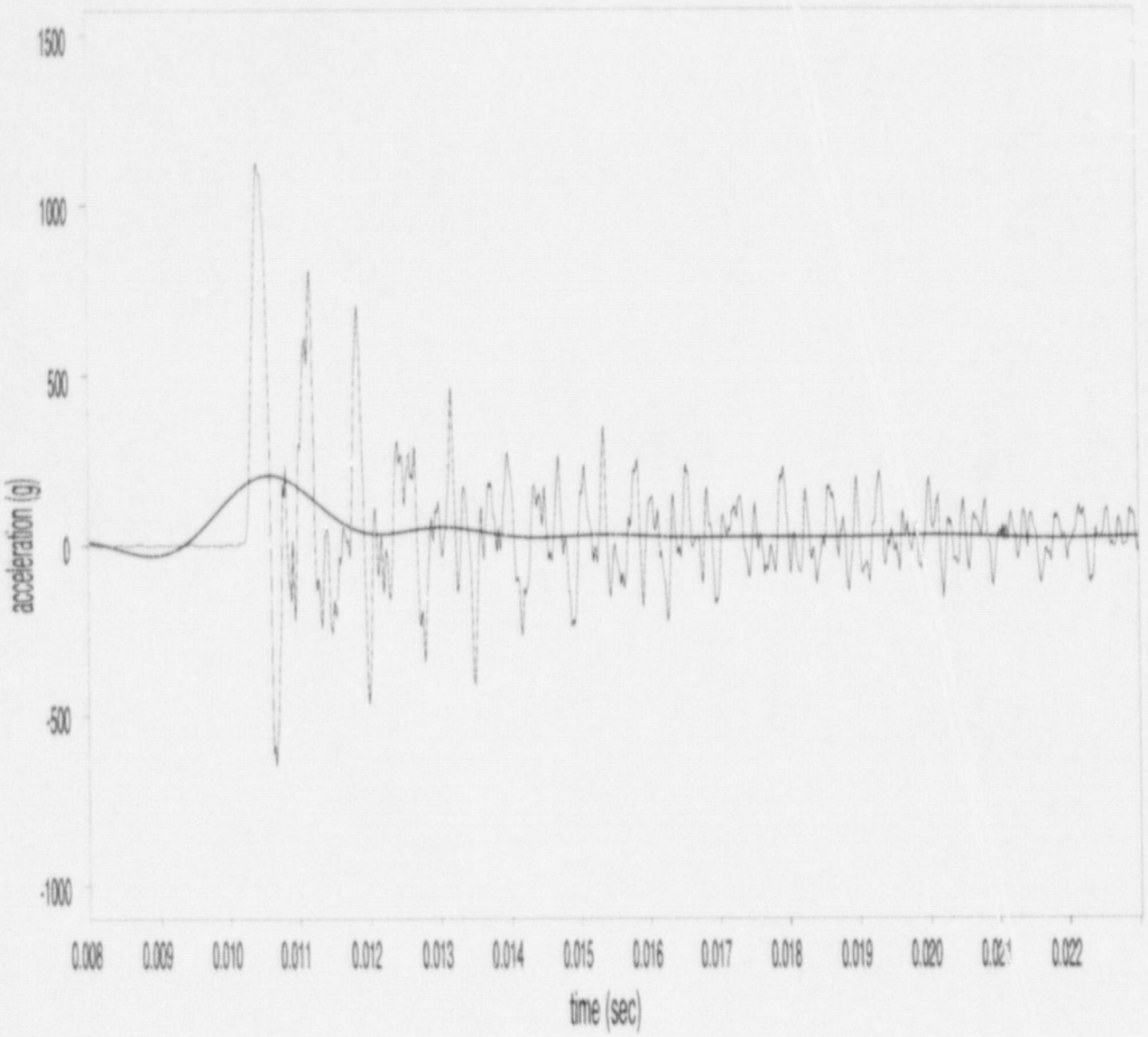

Figure A-53 SNL Test #233, Gauge A1 (1.83-meter (72-inch) end drop, filter cutoff: 450Hz, max. acceleration: 205.2g)

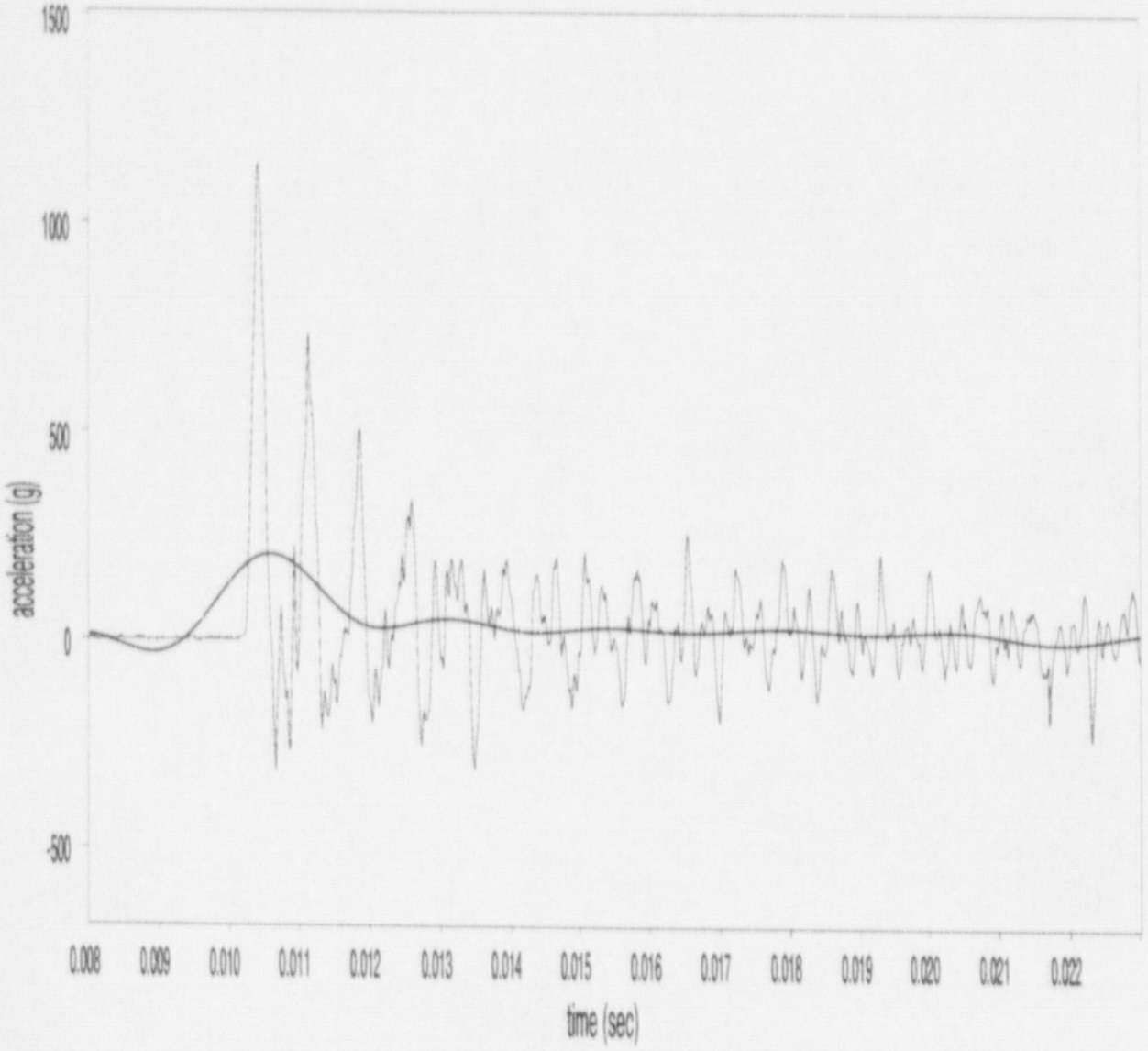

Figure A-54 SNL Test #233, Gauge A2 (1.83-meter (72-inch) end drop, filter cutoff: 450Hz, max. acceleration: 205.7g)

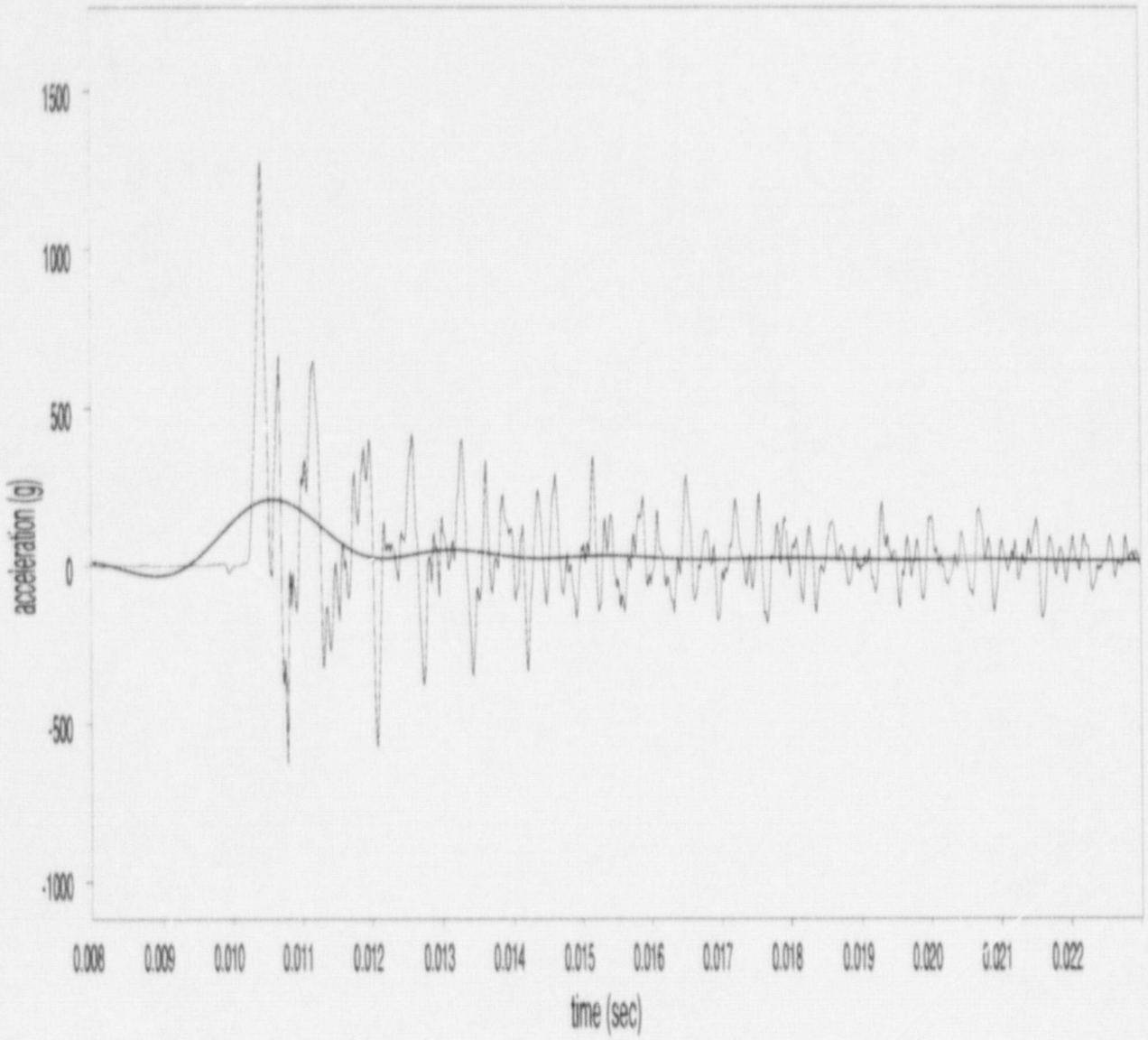

Figure A-55 SNL Test #233, Gauge A3 (1.83-meter (72-inch) end drop, filter cutoff: 450Hz, max. acceleration: 210.2g)

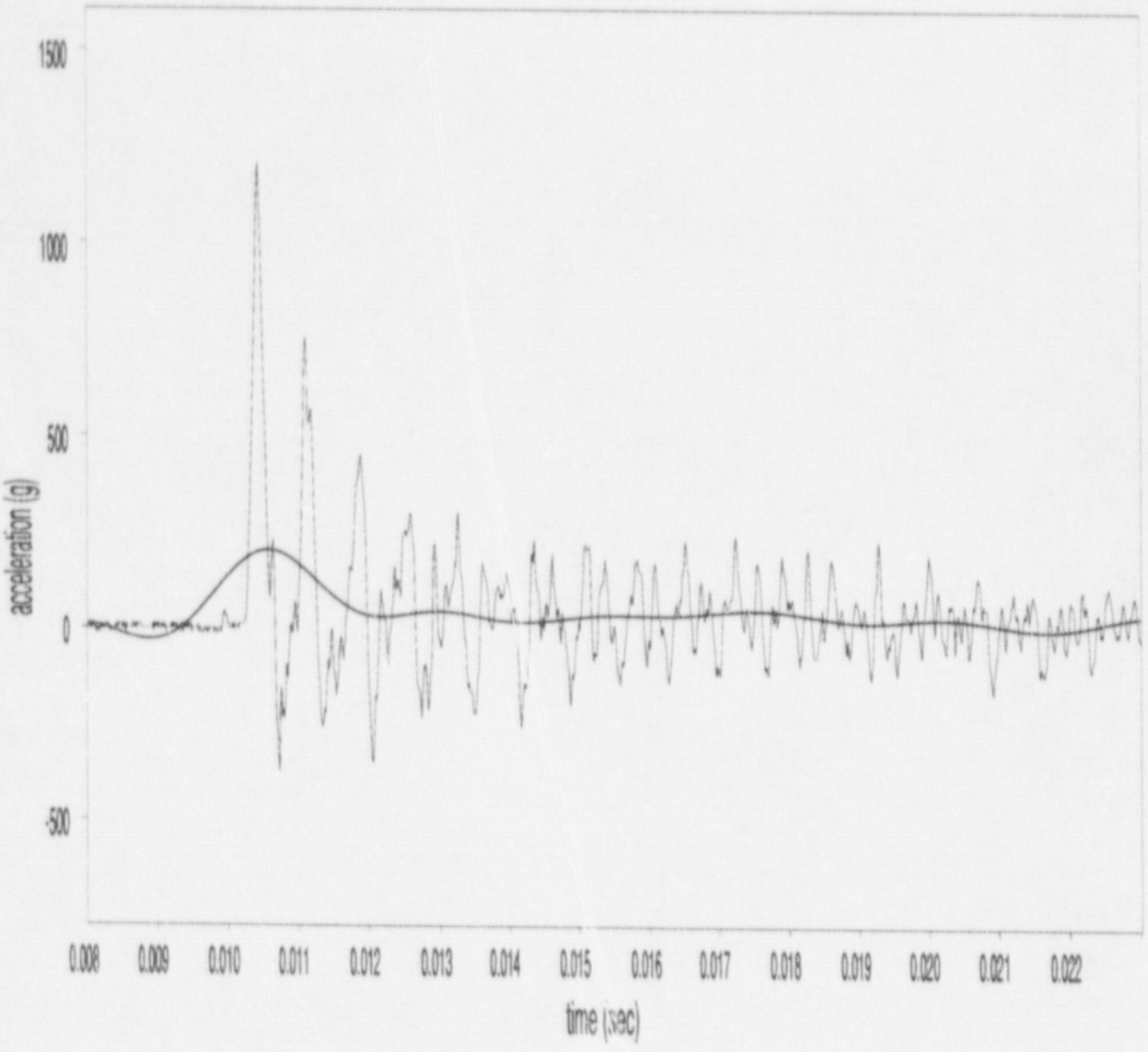

Figure A-56 SNL Test #233, Gauge A4 (1.83-meter (72-inch) end drop, filter cutoff: 450Hz, max. acceleration: 202.4g)

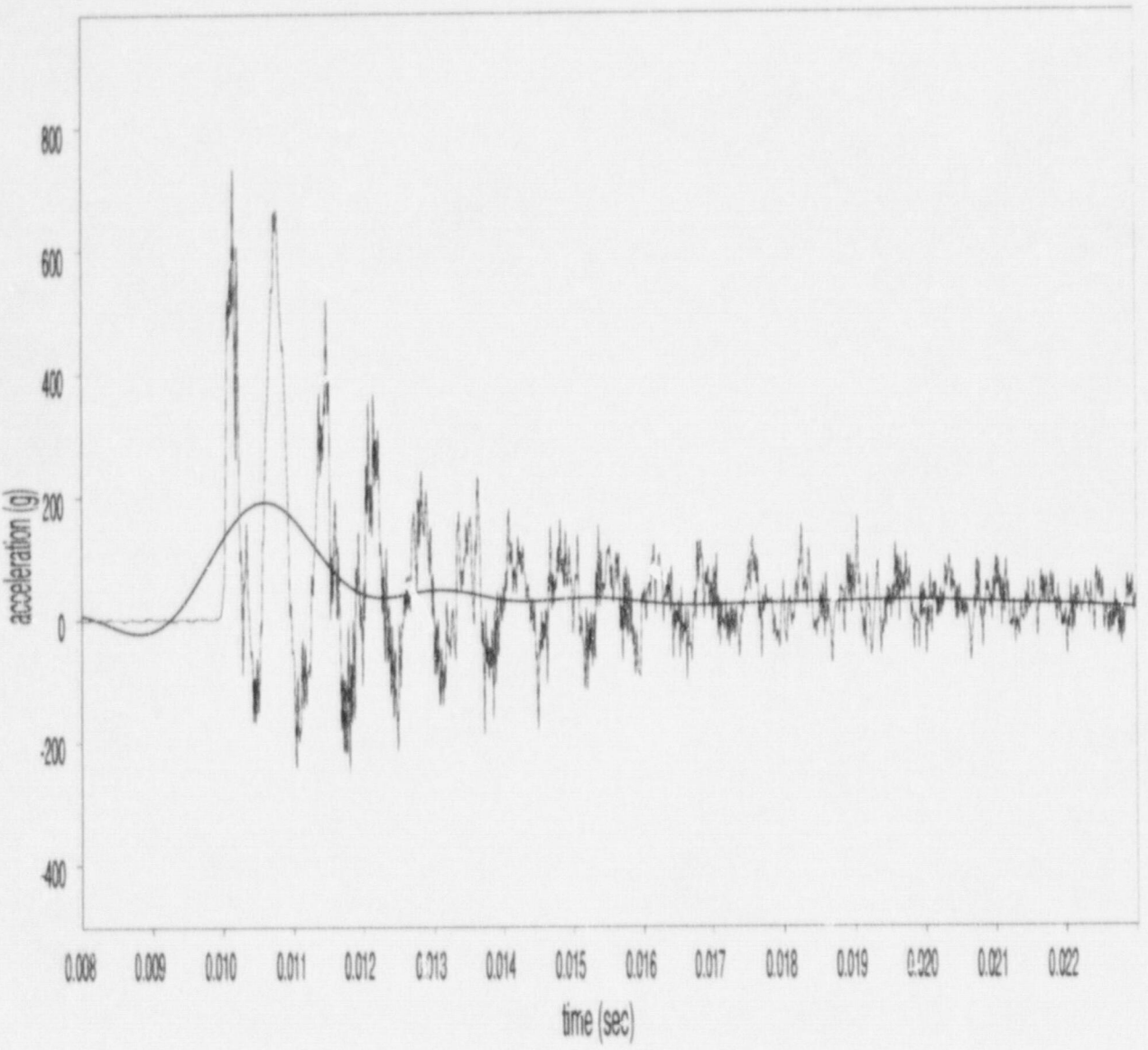

Figure A-57 SNL Test #233, Gauge A5 (1.83-meter (72-inch) end drop, filter cutoff: 450Hz, max. acceleration: 191.0g)

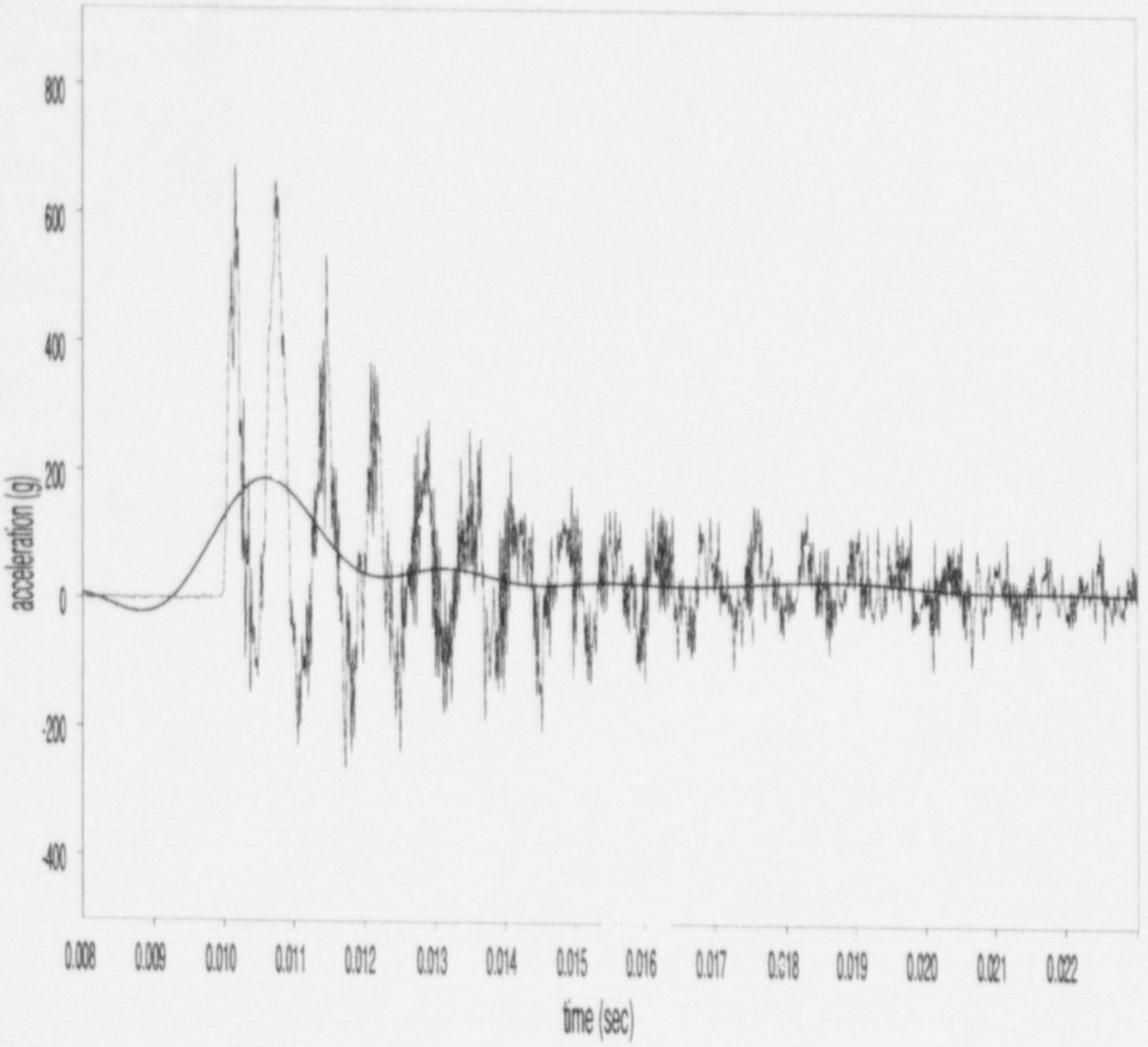

Figure A-58 SNL Test #233, Gauge A6 (1.83-meter (72-inch) end drop, filter cutoff: 450Hz, max. acceleration: 187.4g)

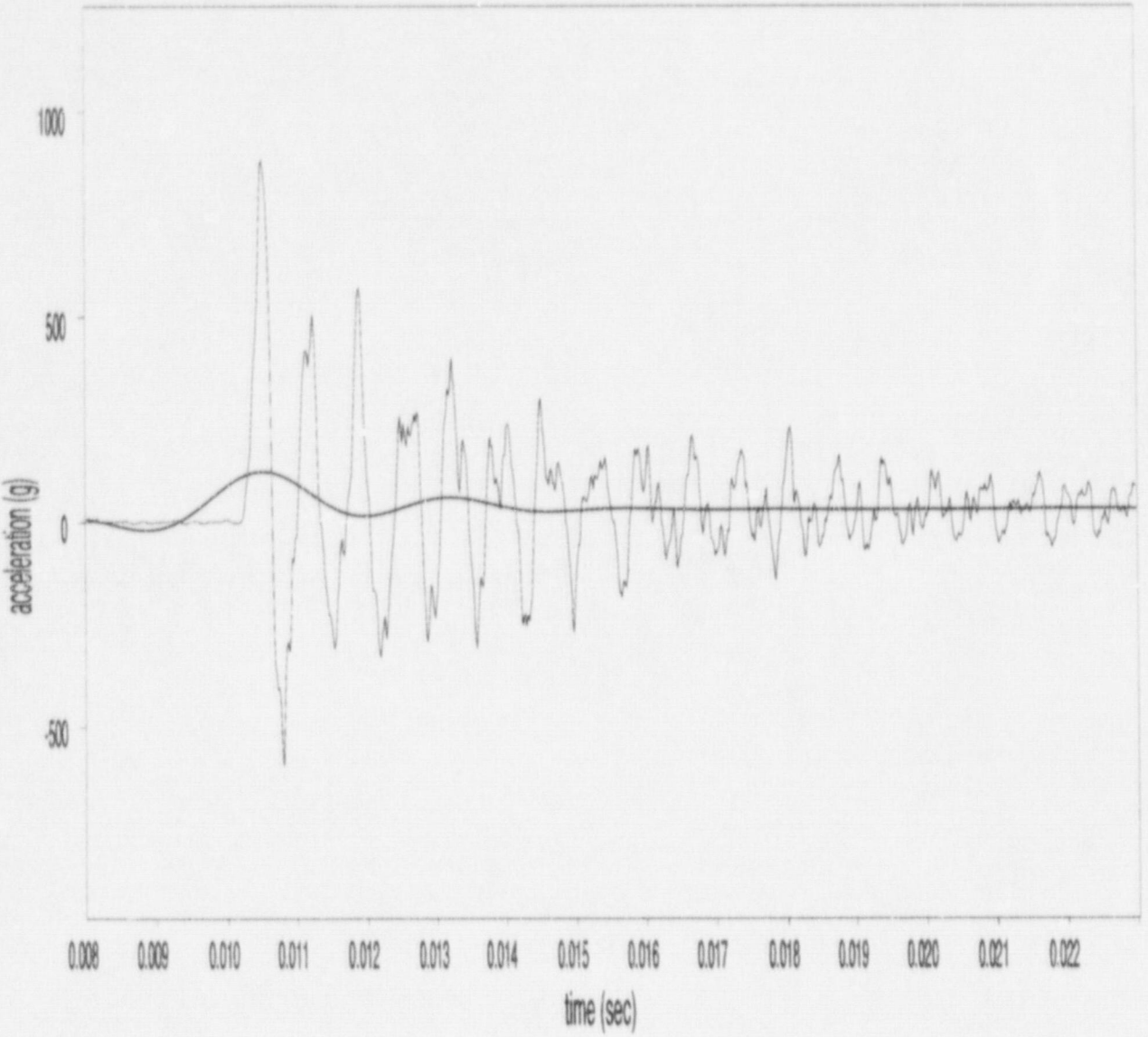

Figure A-59 SNL Test #234, Gauge A1 (1.83-meter (72-inch) end drop, filter cutoff: 450Hz, max. acceleration: 123.0g)

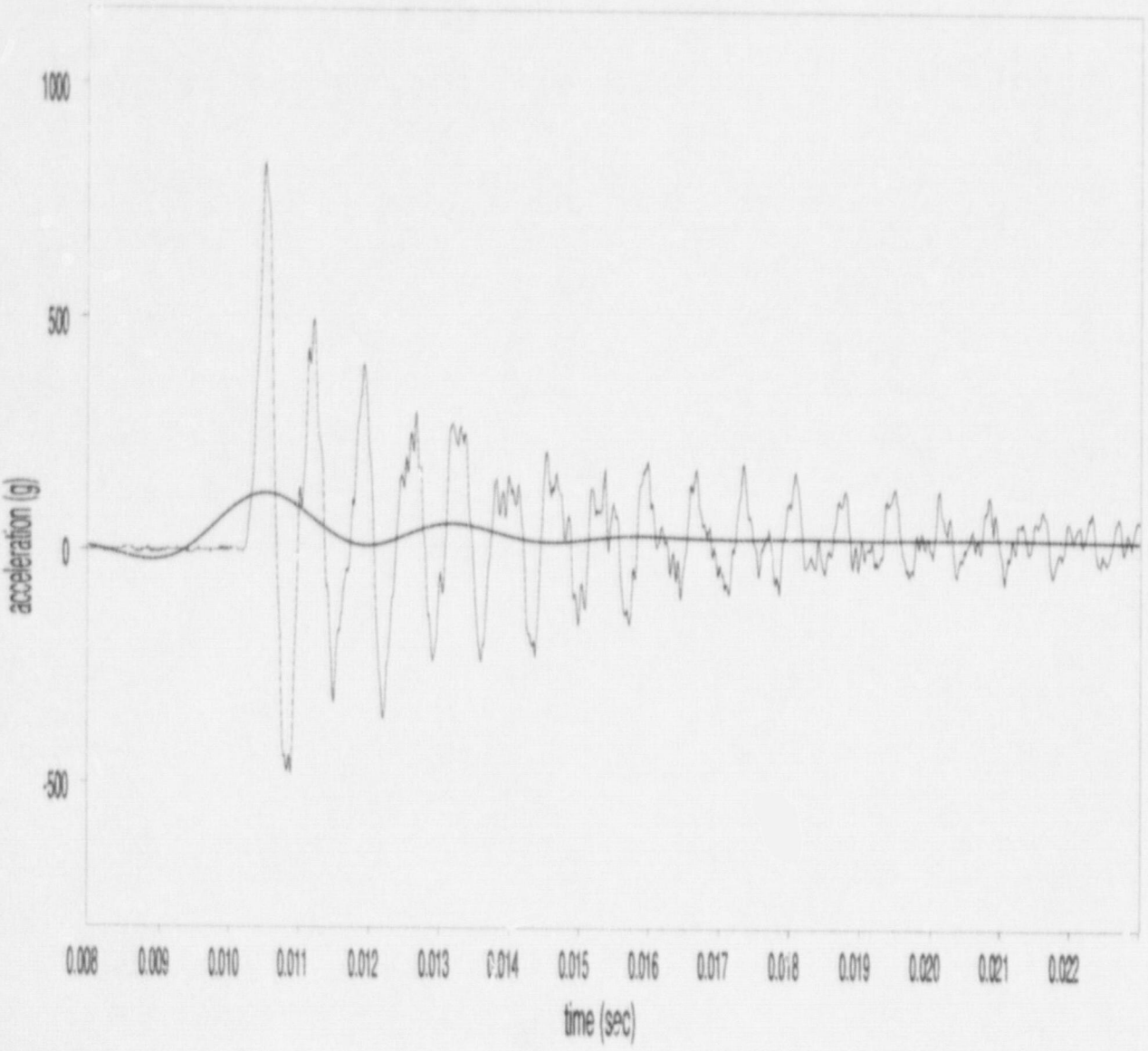

Figure A-60 SNL Test #234, Gauge A2 (1.83-meter (72-inch) end drop, filter cutoff: 450Hz, max. acceleration: 122.3g)

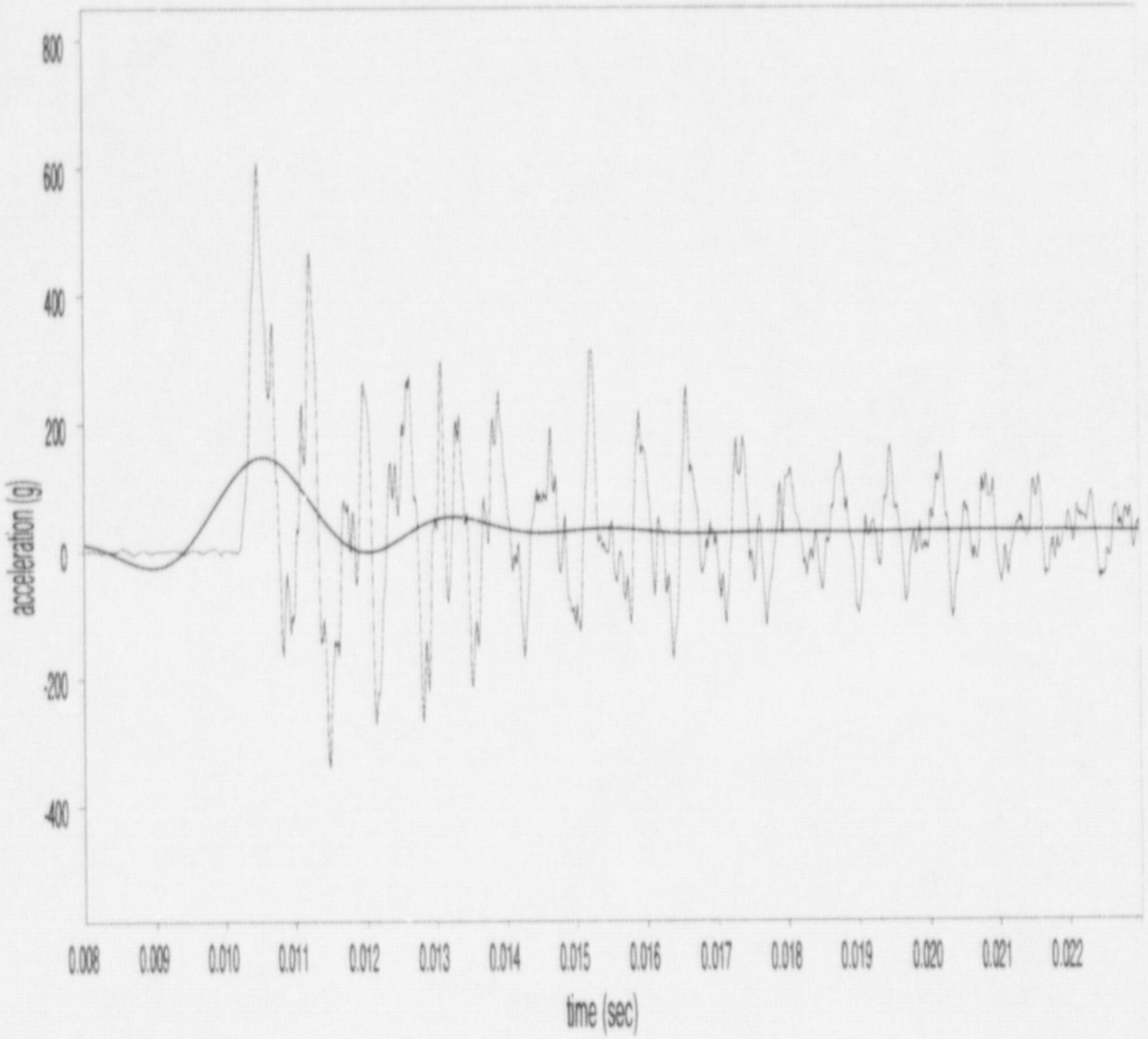

Figure A-61 SNL Test #234, Gauge A3 (1.83-meter (72-inch) end drop, filter cutoff: 450Hz, max. acceleration: 147.3g)

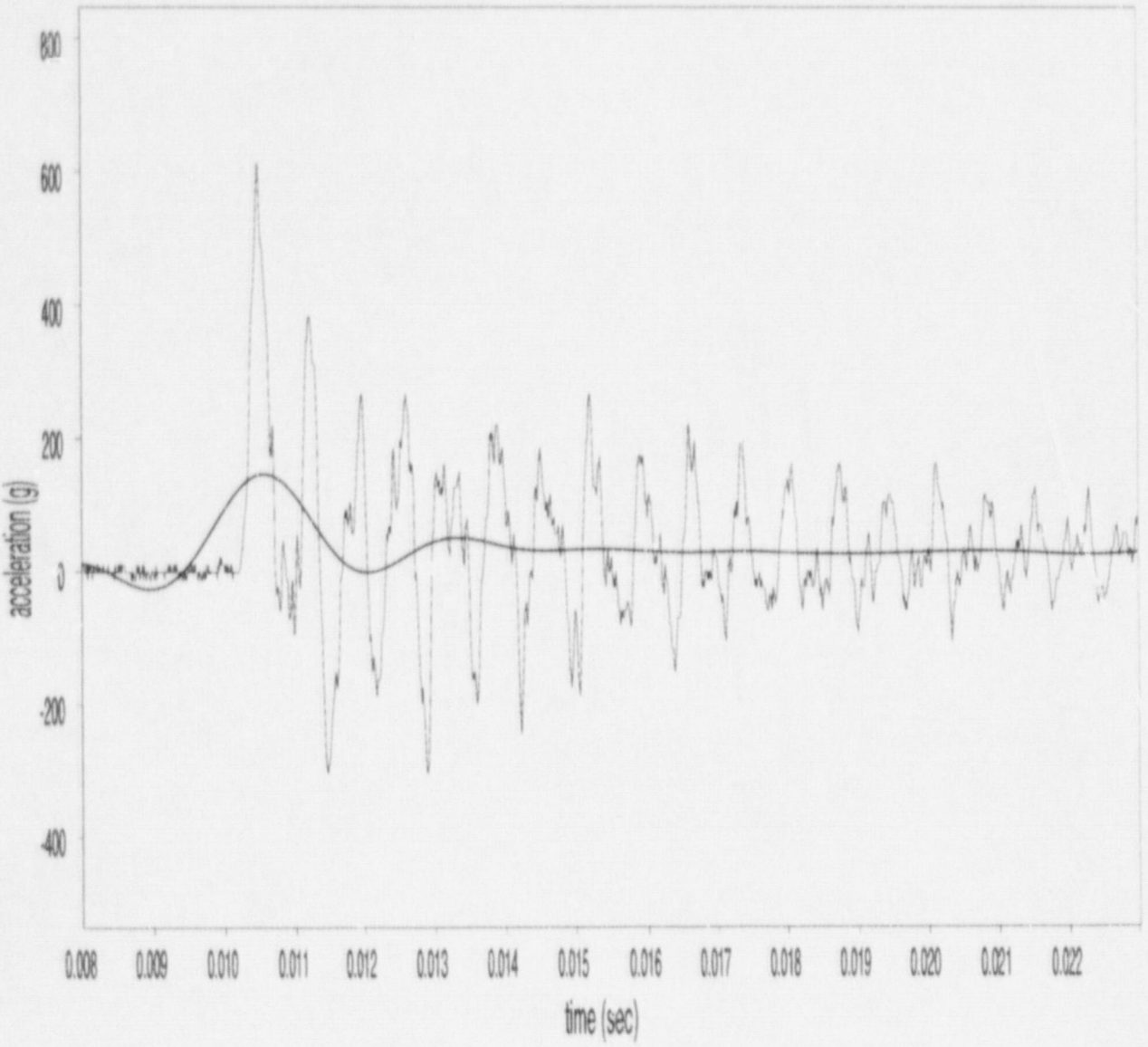

Figure A-62 SNL Test #234, Gauge A4 (1.83-meter (72-inch) end drop, filter cutoff: 450Hz, max. acceleration: 146.3g)

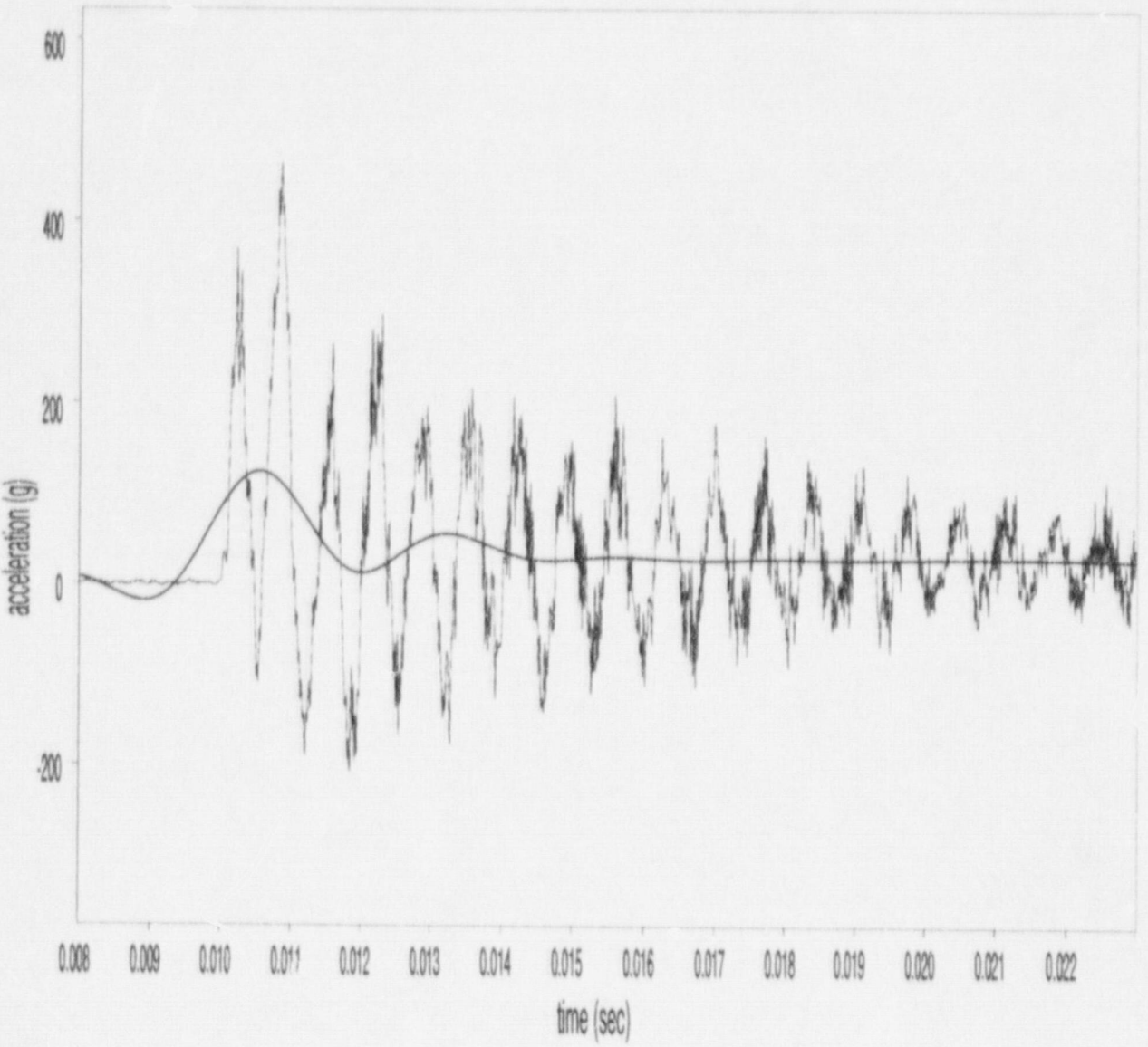

Figure A-63 SNL Test #234, Gauge A5 (1.83-meter (72-inch) end drop, filter cutoff: 450Hz, max. acceleration: 123.7g)

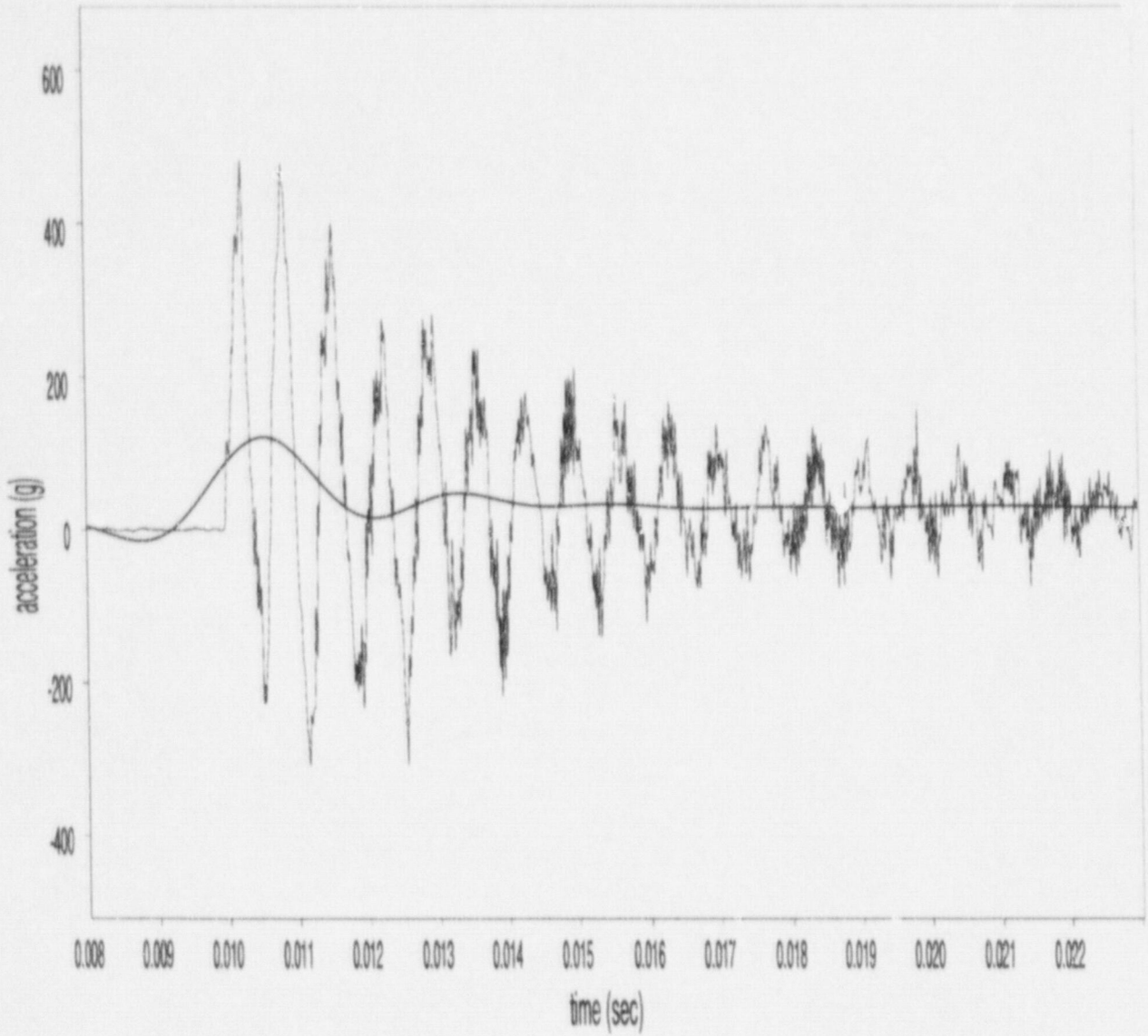

Figure A-64 SNL Test #234, Gauge A6 (1.83-meter (72-inch) end drop, filter cutoff: 450Hz, max. acceleration: 120.6g)

APPENDIX B. ACCELERATION TRACES, FILTERED AND UNFILTERED, FOR LLNL TESTS

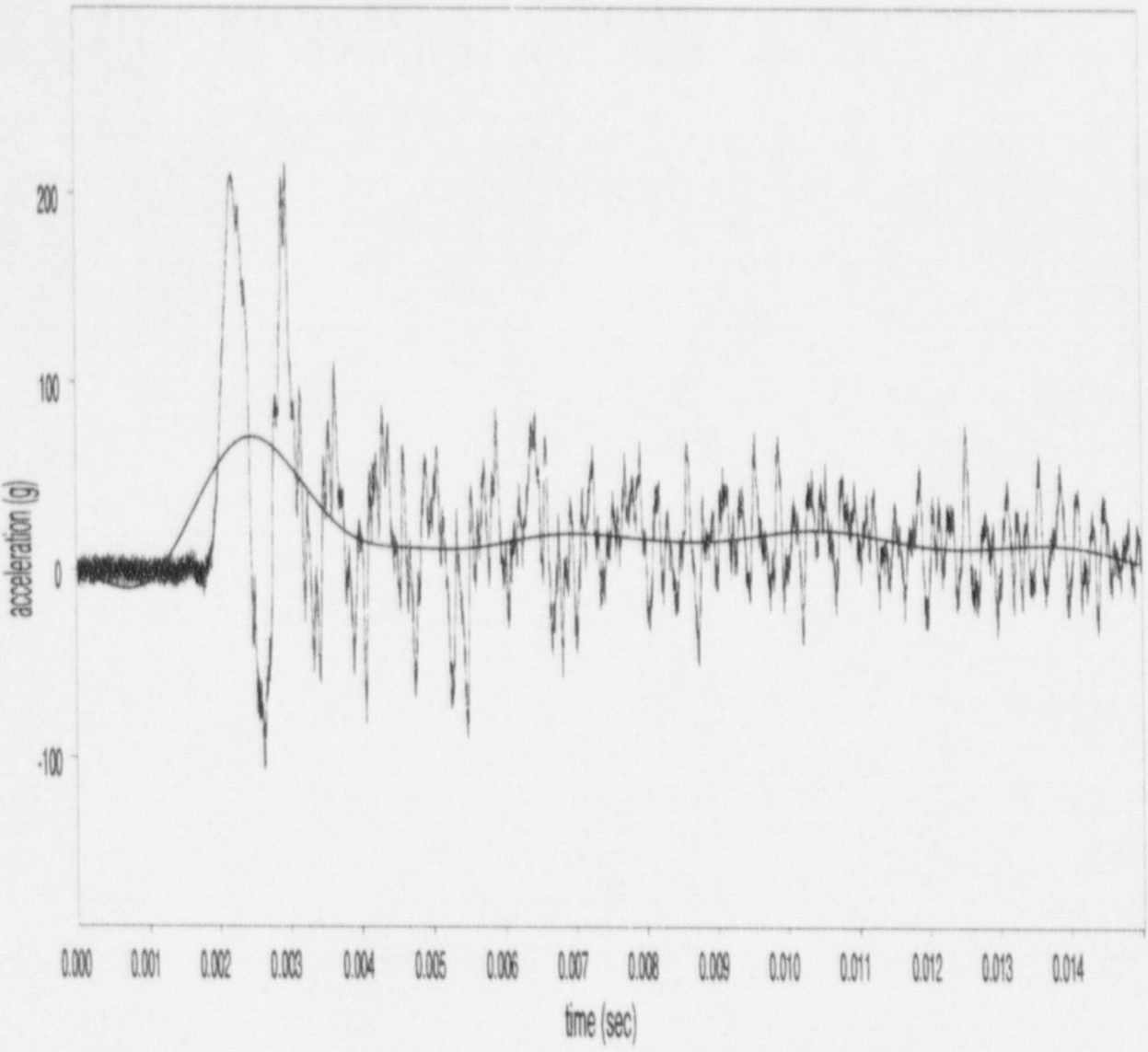

Figure B-1 LLNL Test #1, Gauge A1 (45.7-centimeter (18-inch) end drop, filter cutoff: 450 Hz, maximum acceleration: 70.8g)

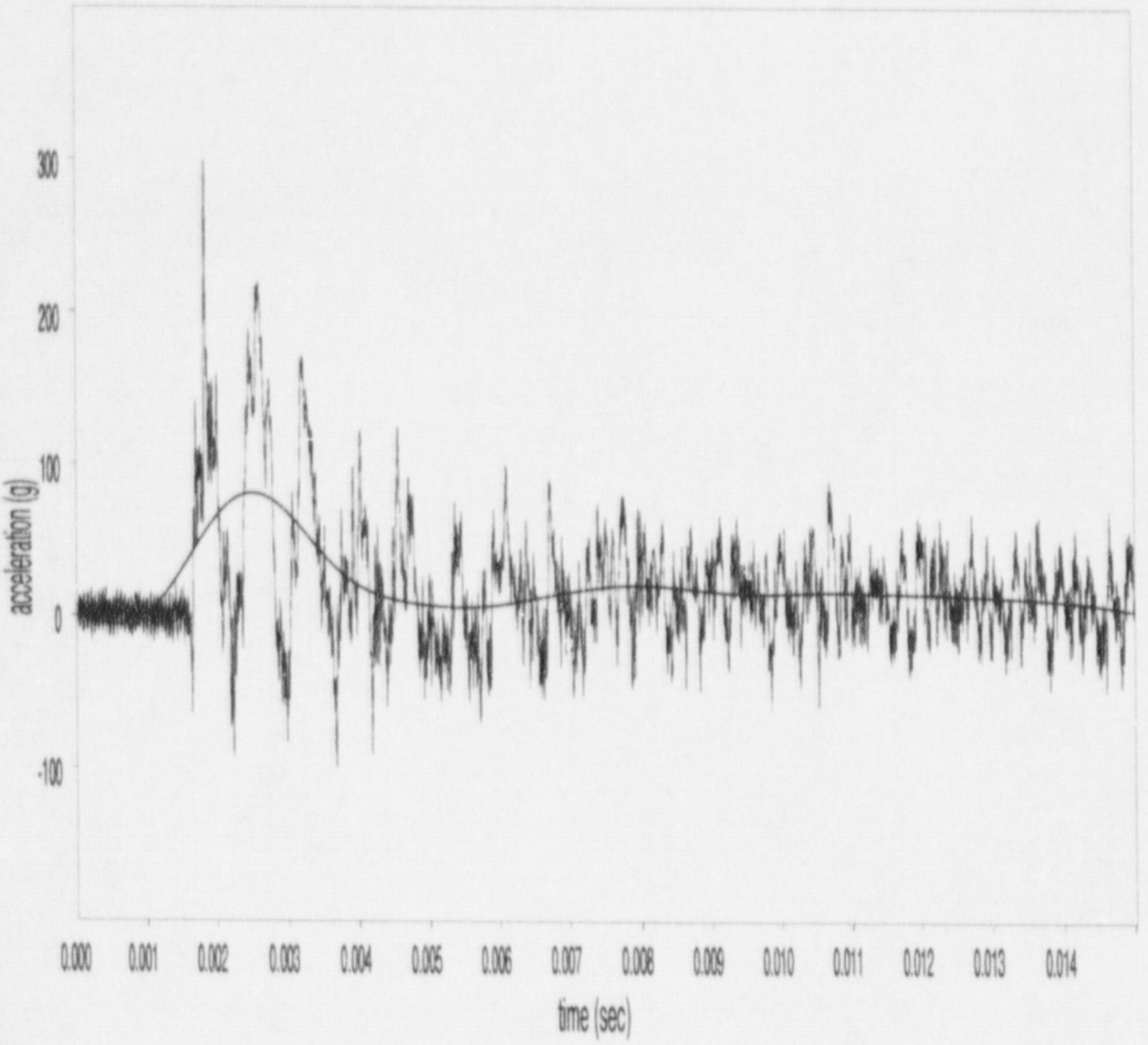

Figure B-2 LLNL Test #1, Gauge A2 (45.7-centimeter (18-inch) end drop, filter cutoff: 450 Hz, maximum acceleration: 80.7g)

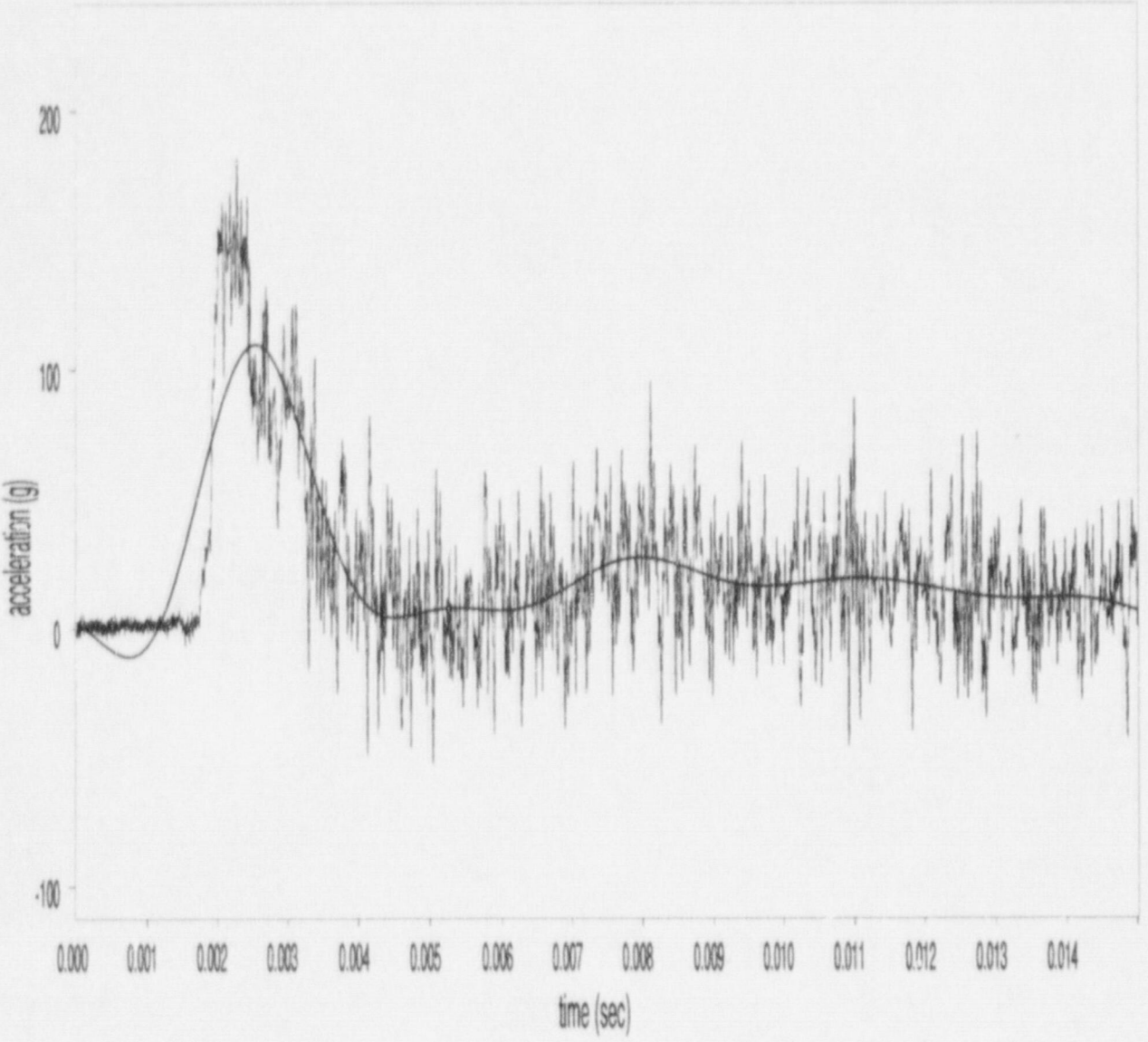

Figure B-3 LLNL Test #1, Gauge A3 (45.7-centimeter (18-inch) end drop, filter cutoff: 450 Hz, maximum acceleration: 109.5g)

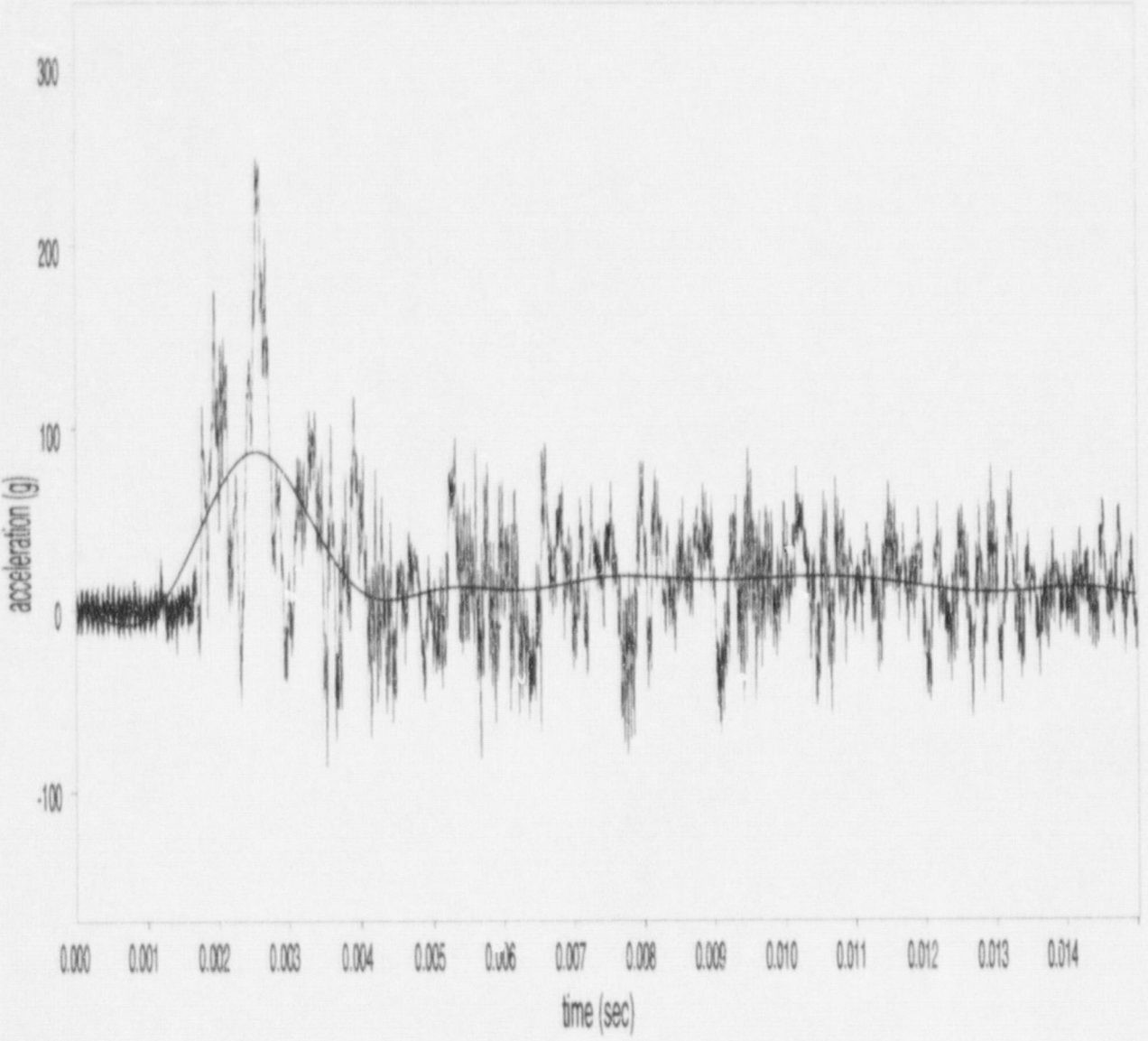

Figure B-4 LLNL Test #1, Gauge A4 (45.7-centimeter (18-inch) end drop, filter cutoff: 450 Hz, maximum acceleration: 87.2g)

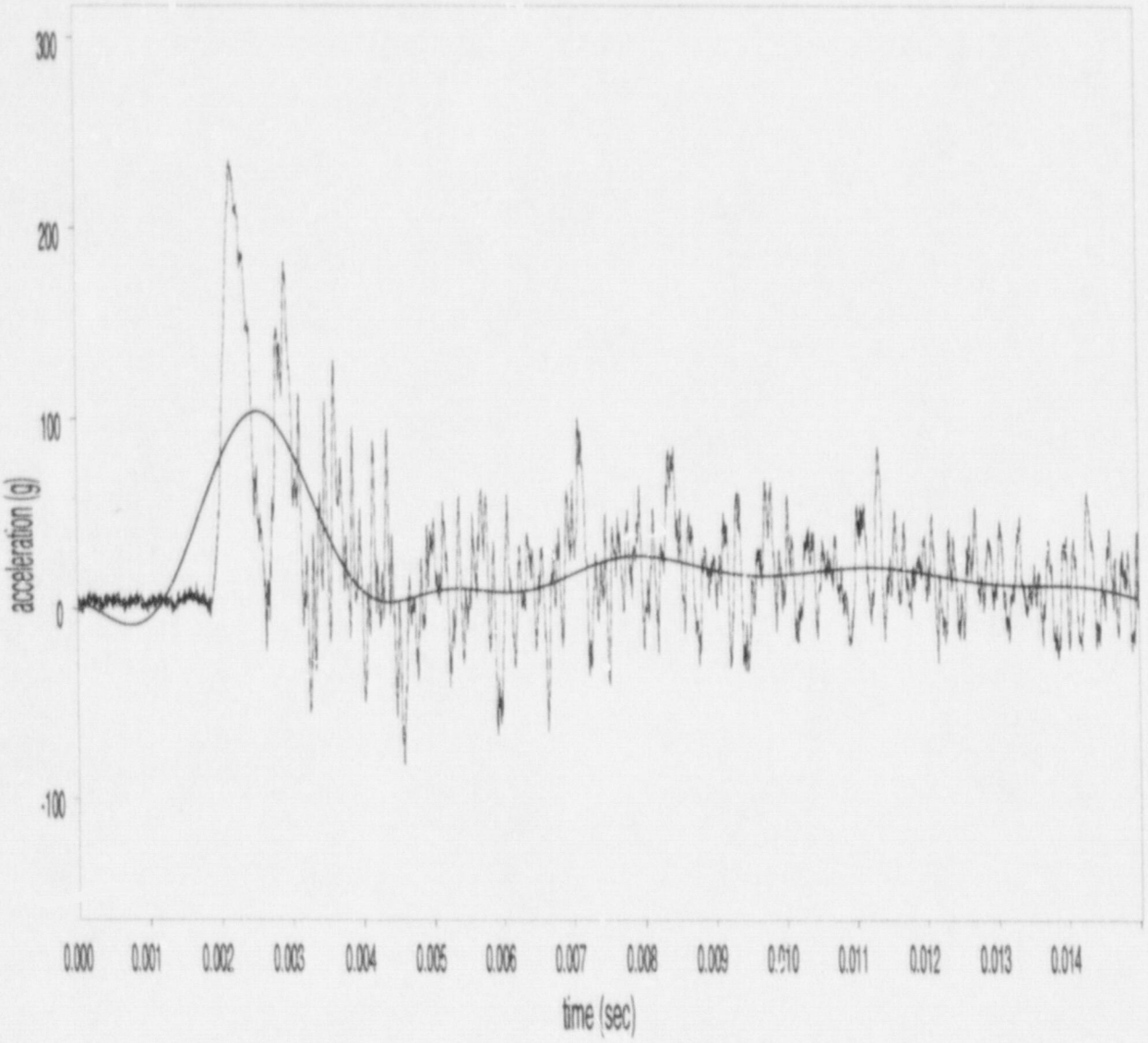

Figure B-5 LLNL Test #1, Gauge A5 (45.7-centimeter (18-inch) end drop, filter cutoff: 450 Hz, maximum acceleration: 103.3g)

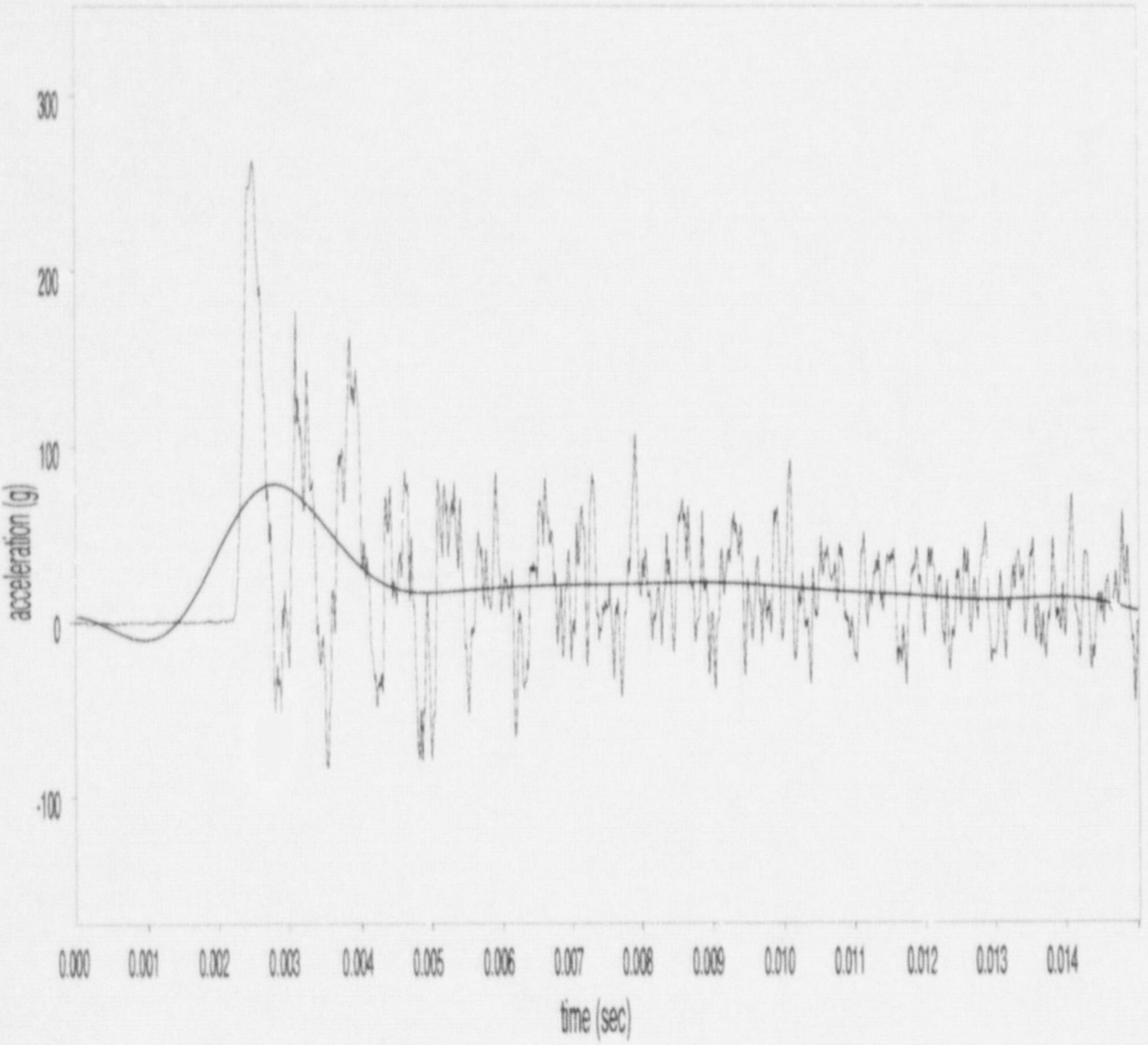

Figure B-6 LLNL Test #2, Gauge A1 (45.7-centimeter (18-inch) end drop, filter cutoff: 450 Hz, maximum acceleration: 78.7g)

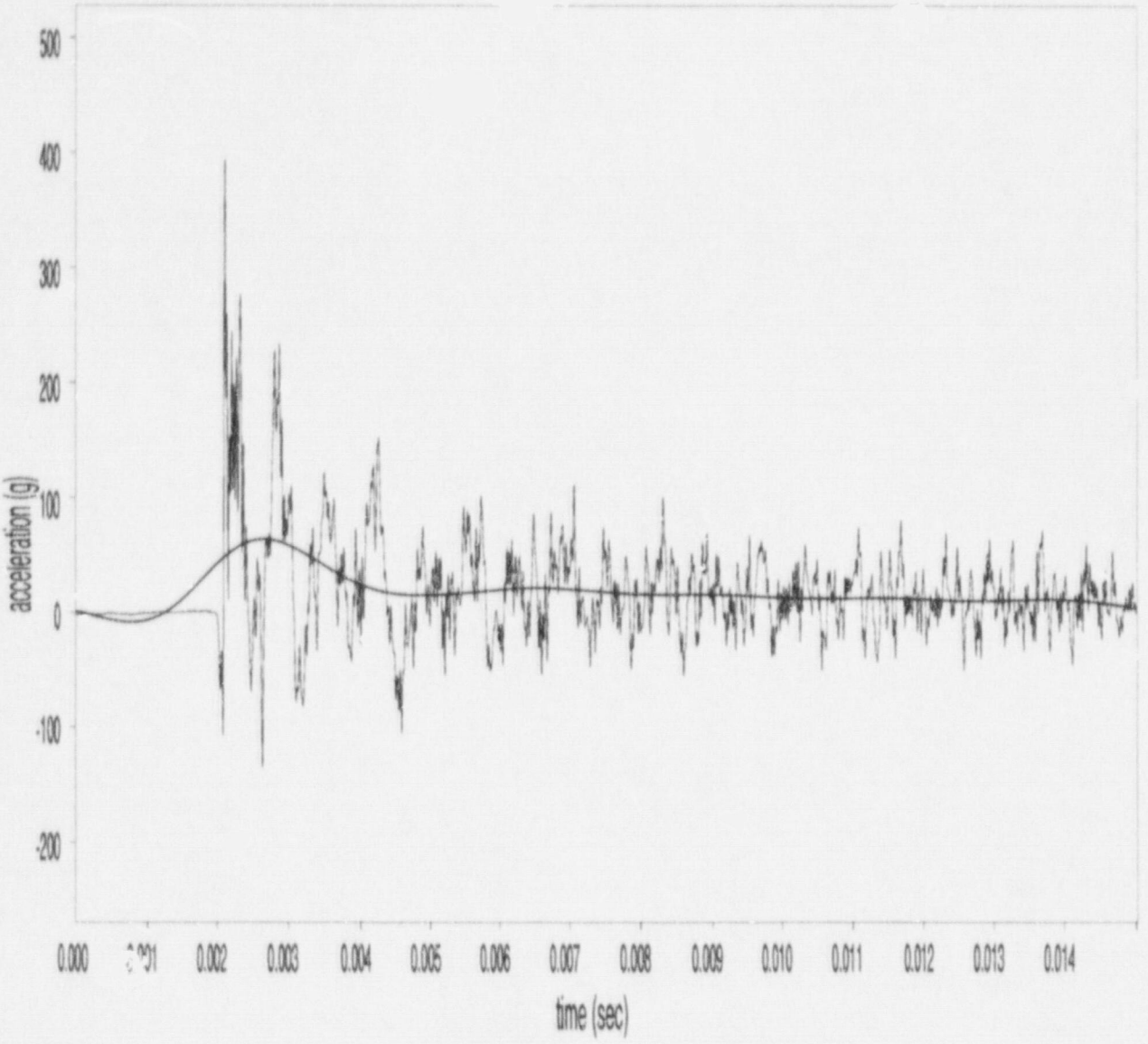

Figure B-7 LLNL Test #2, Gauge A2 (45.7-centimeter (18-inch) end drop, filter cutoff: 450 Hz, maximum acceleration: 63.6g)

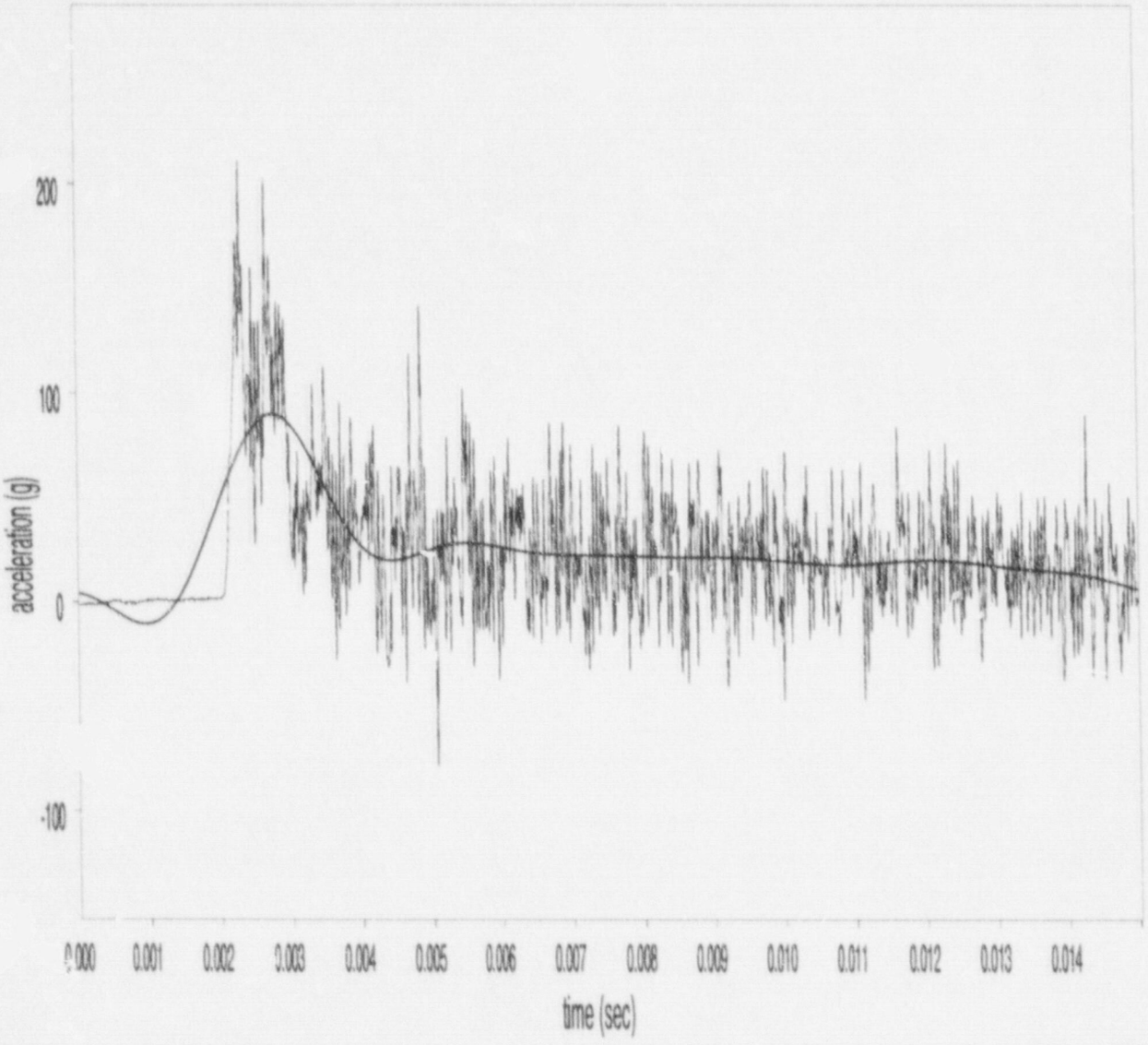

Figure B-8 LLNL Test #2, Gauge A3 (45.7-centimeter (18-inch) end drop, filter cutoff: 450 Hz, maximum acceleration: 89.8g)

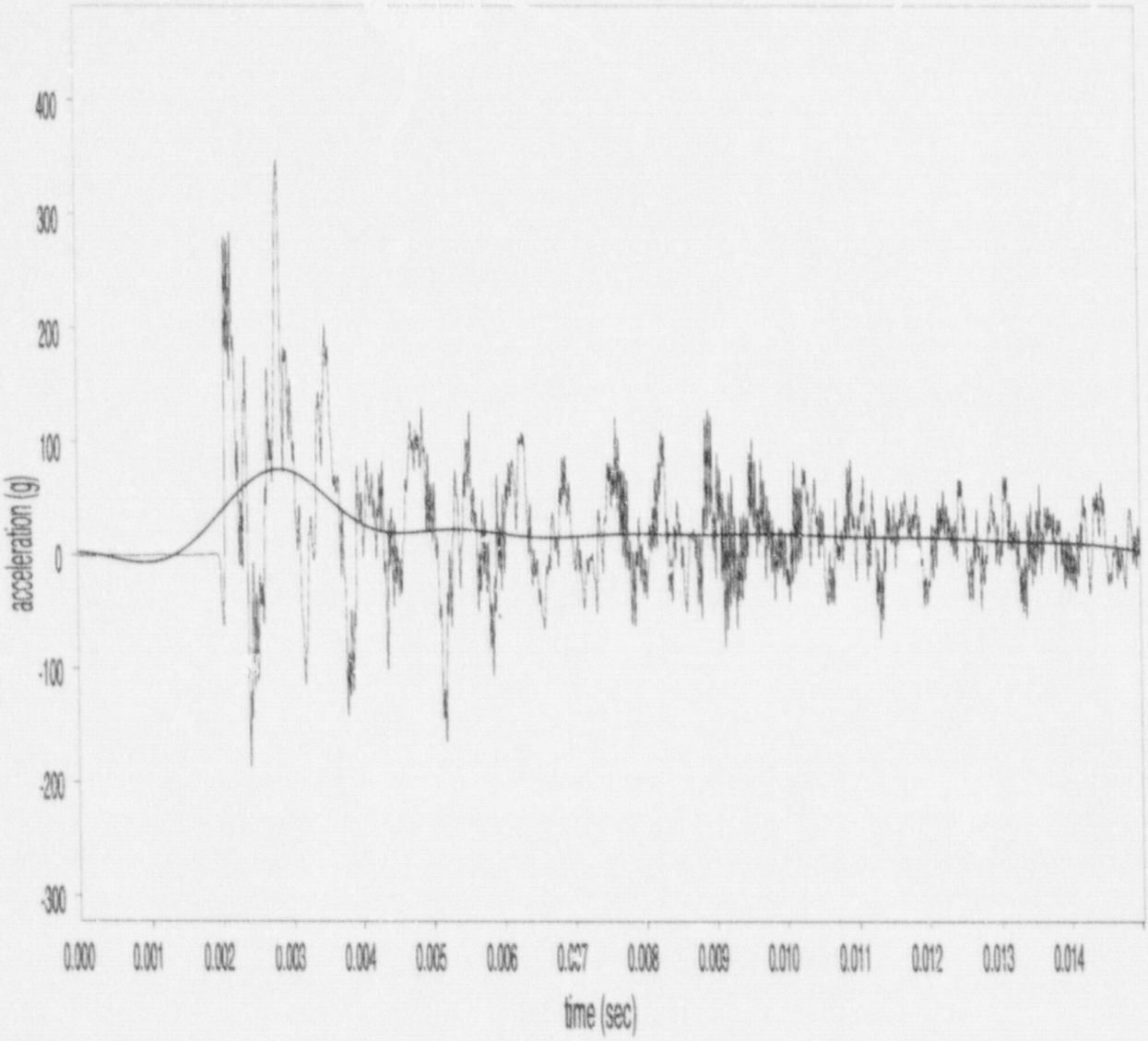

Figure B-9 LLNL Test #2, Gauge A4 (45.7-centimeter (18-inch) end drop, filter cutoff: 450 Hz, maximum acceleration: 75.4g)

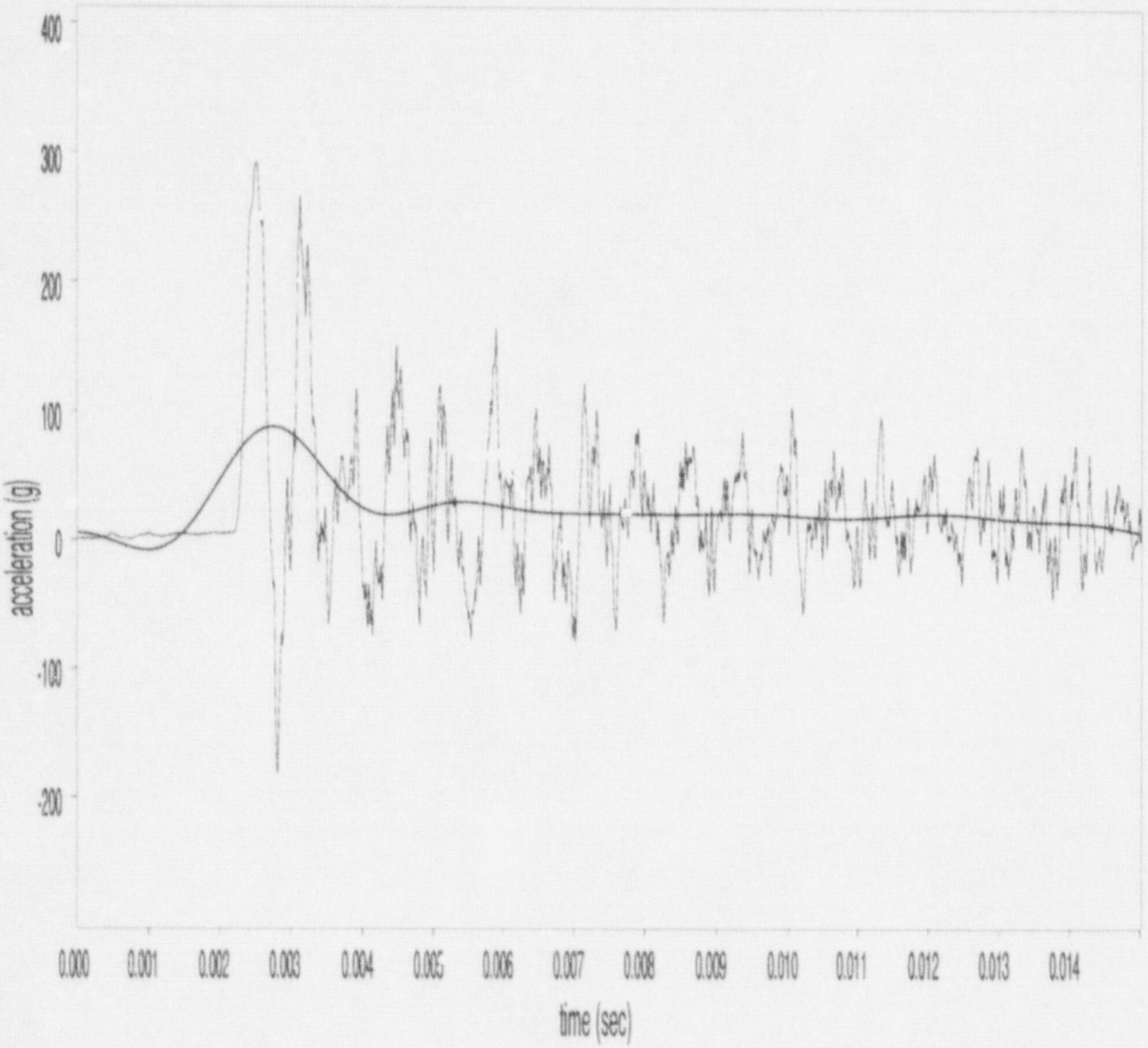

Figure B-10 LLNL Test #2, Gauge A5 (45.7-centimeter (18-inch) end drop, filter cutoff: 450 Hz, maximum acceleration: 88.0g)

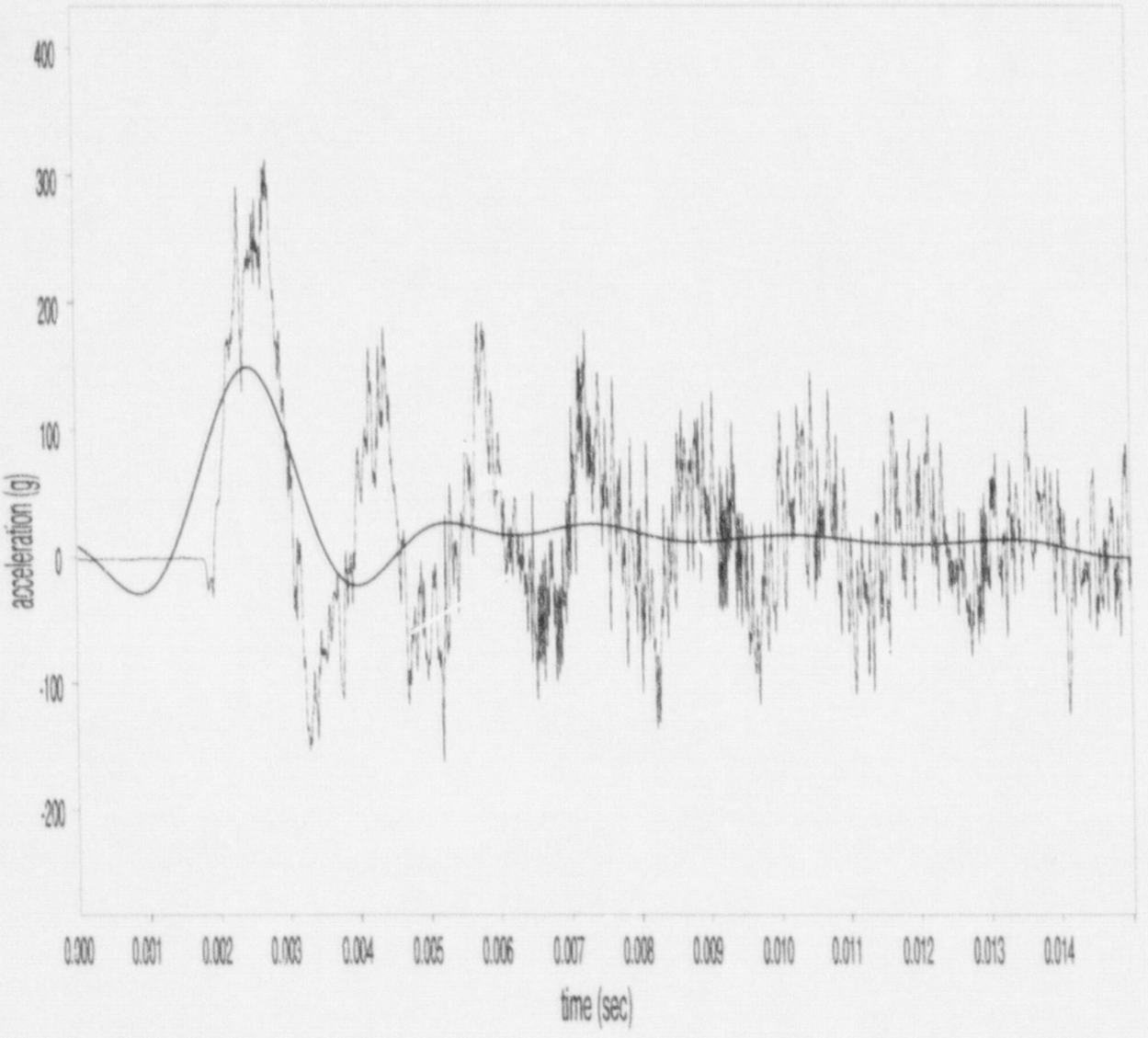

Figure B-11 LLNL Test #3, Gauge A1 (45.7-centimeter (18-inch) side drop, filter cutoff: 450 Hz, maximum acceleration: 148.8g)

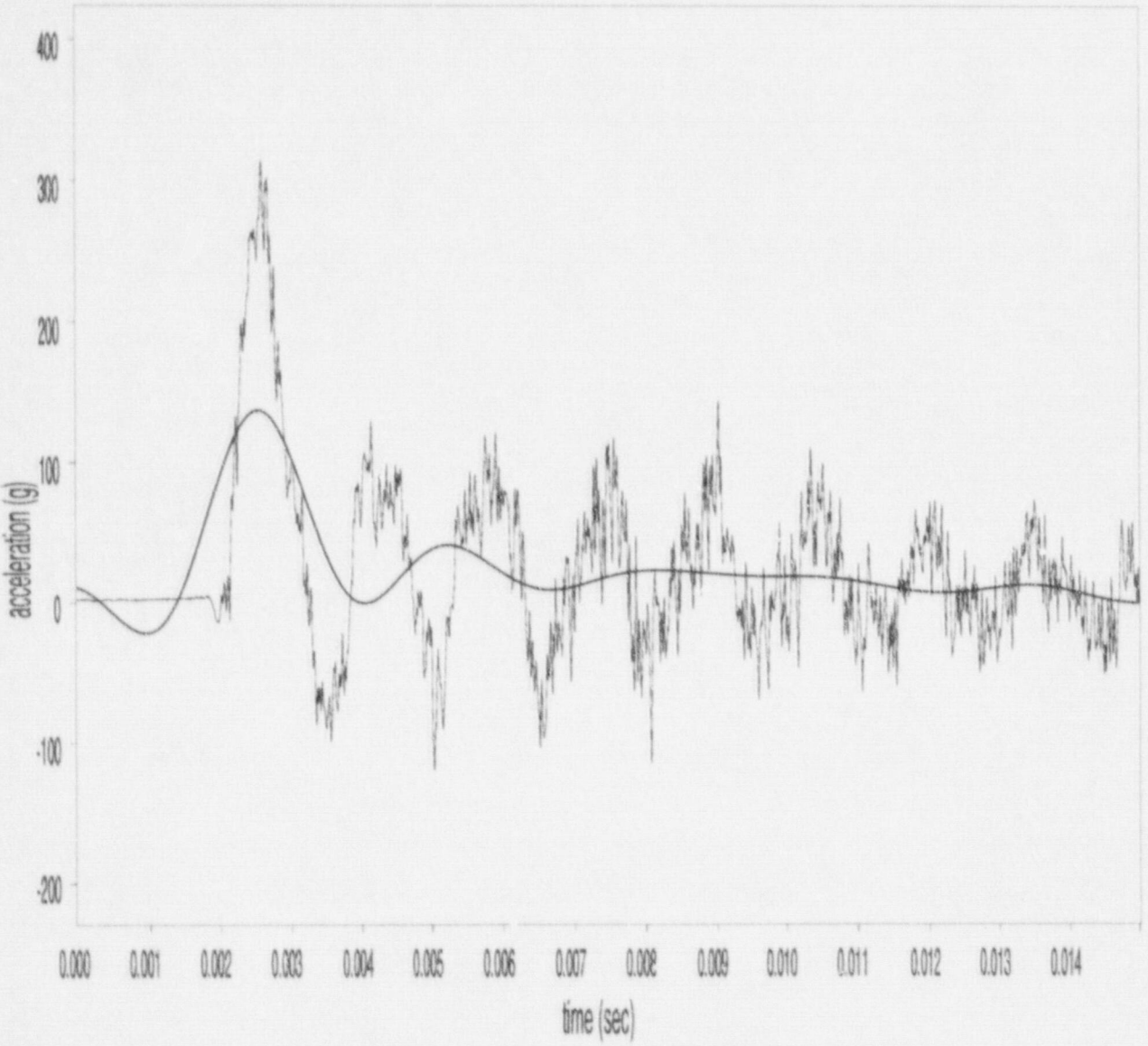

Figure B-12 LLNL Test #3, Gauge A2 (45.7-centimeter (18-inch) side drop, filter cutoff: 450 Hz, maximum acceleration: 136.9g)

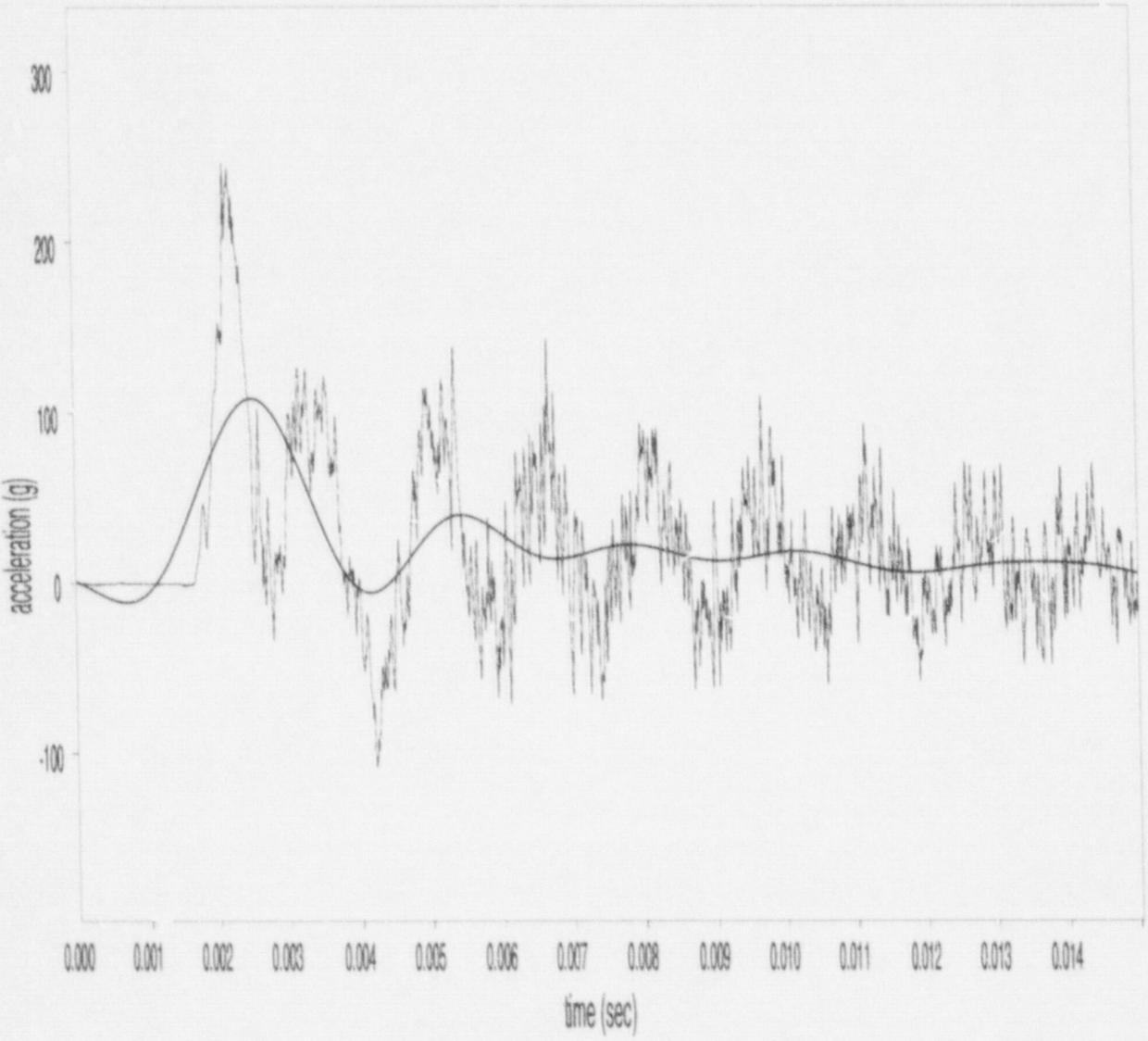

Figure B-13 LLNL Test #3, Gauge A3 (45.7-centimeter (18-inch) side drop, filter cutoff: 450 Hz, maximum acceleration: 108.2g)

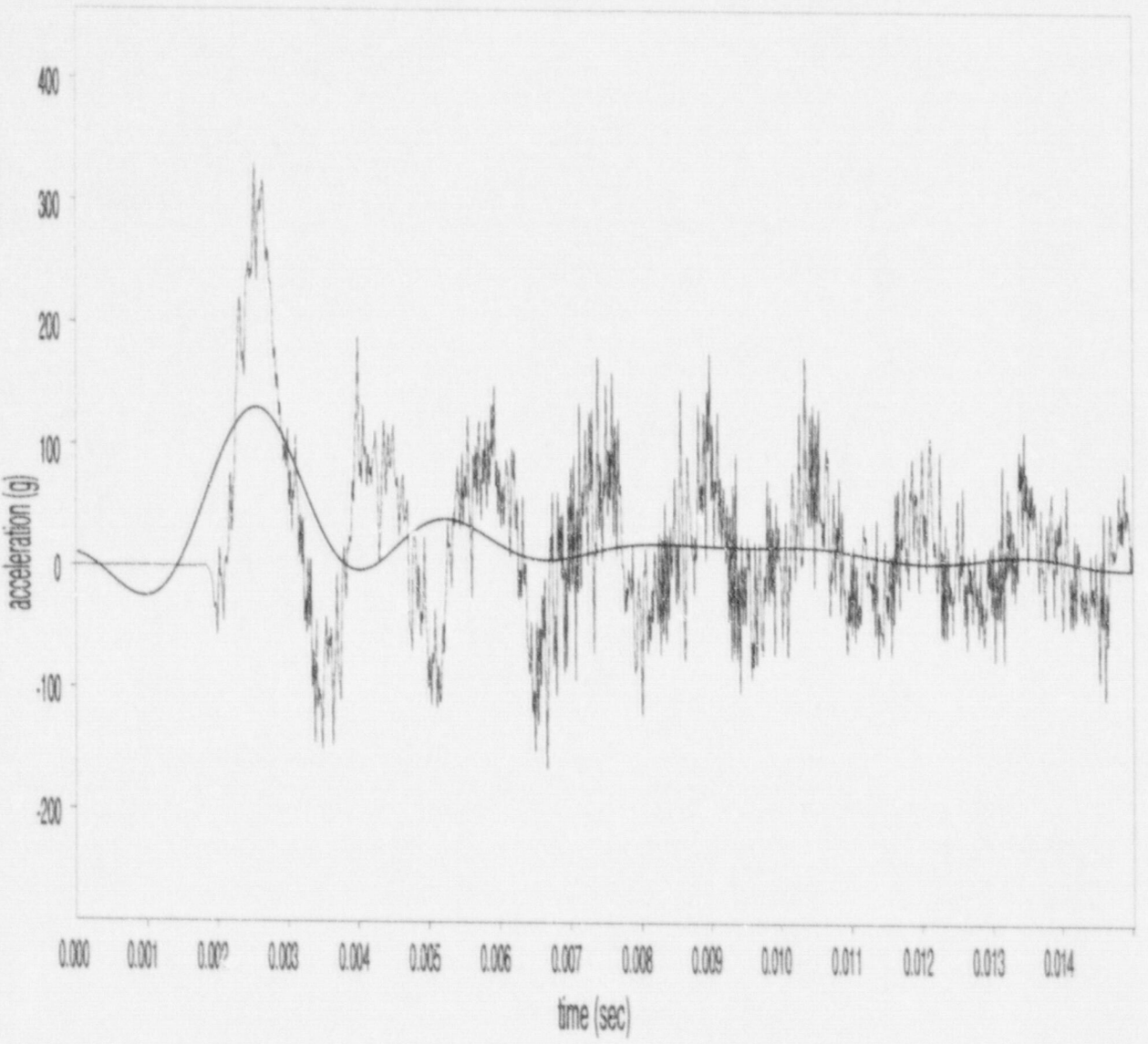

Figure B-14 LLNL Test #3, Gauge A4 (45.7-centimeter (18-inch) side drop, filter cutoff: 450 Hz, maximum acceleration: 129.9g)

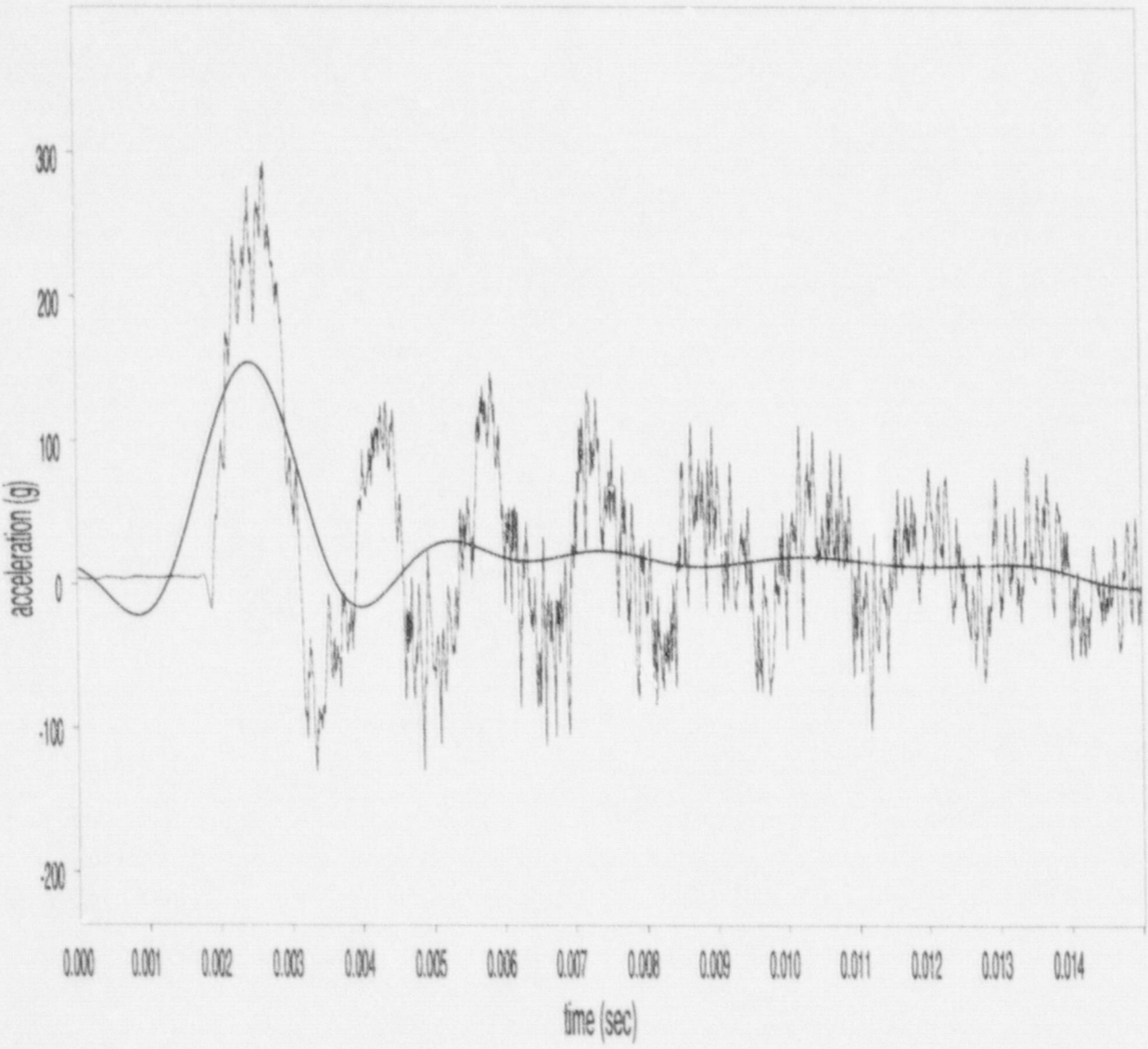

Figure B-15 LLNL Test #3, Gauge A5 (45.7-centimeter (18-inch) side drop, filter cutoff: 450 Hz, maximum acceleration: 154.0g)

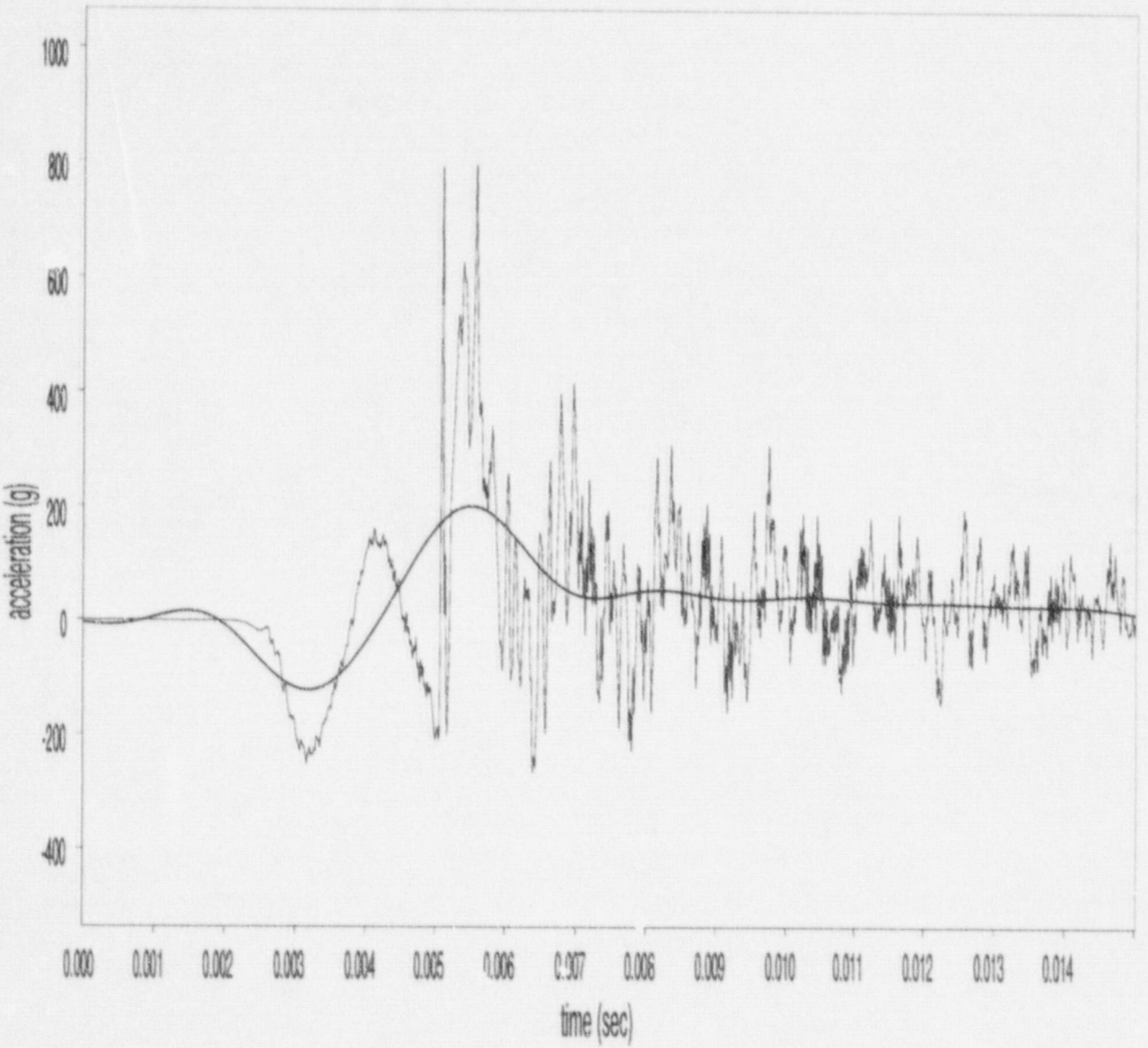

Figure B-16 LLNL Test #4, Gauge A1 (91.4-centimeter (36-inch) side drop, filter cutoff: 450 Hz, maximum acceleration: 200.0g)

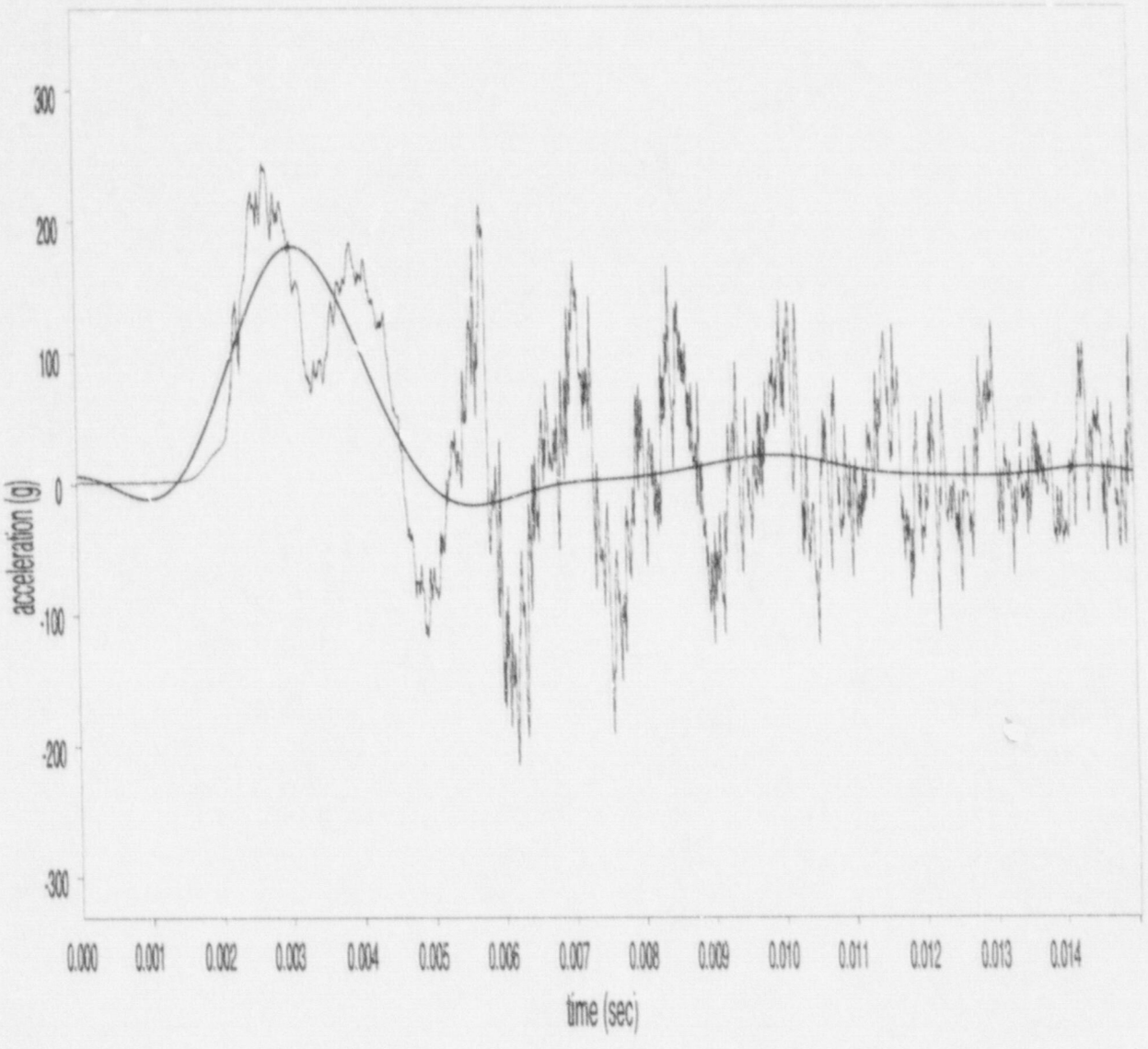

Figure B-17 LLNL Test #4, Gauge A2 (91.4-centimeter (36-inch) side drop, filter cutoff: 450 Hz, maximum acceleration: 180.7g)

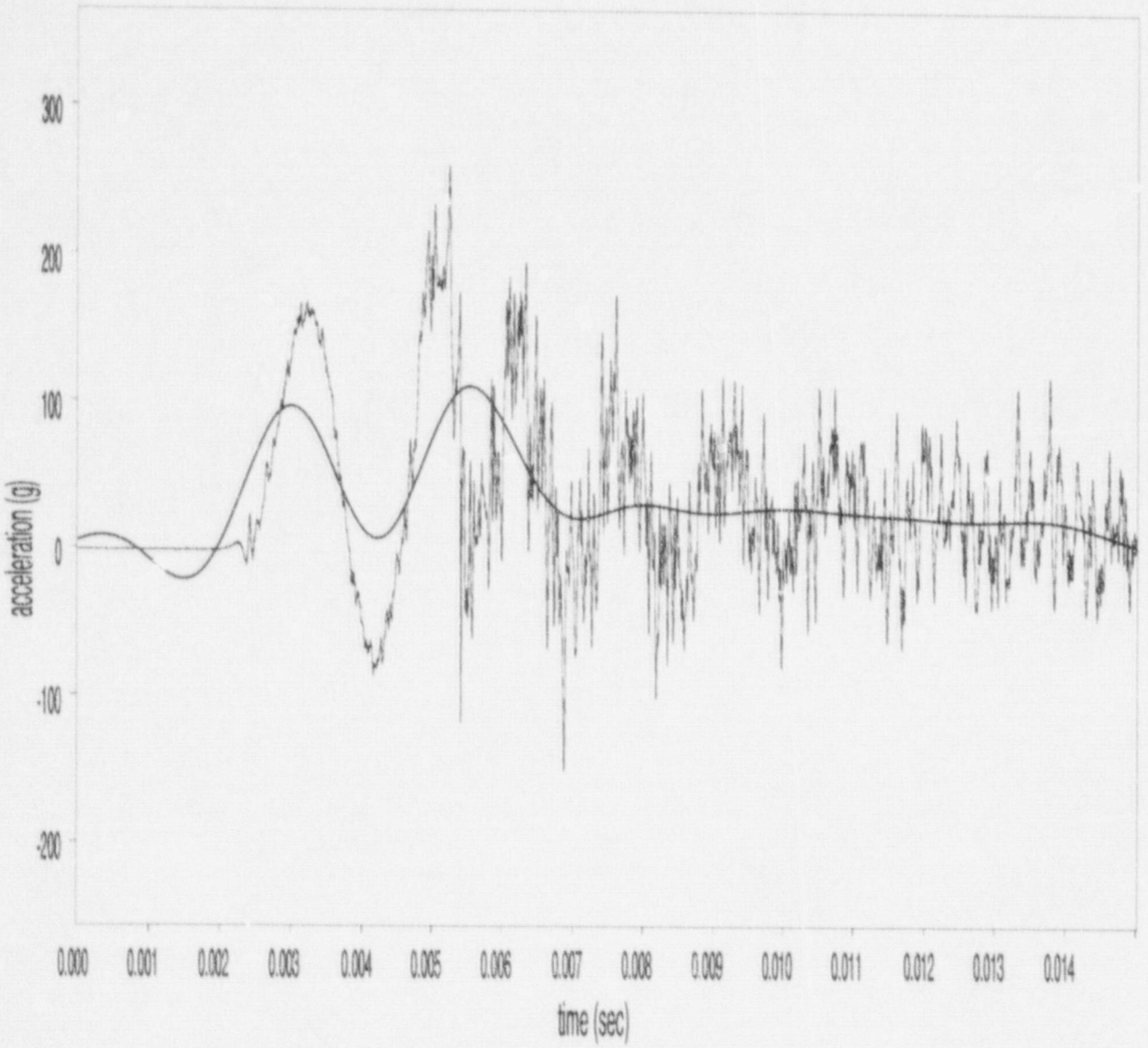

Figure B-18 LLNL Test #4, Gauge A3 (91.4-centimeter (36-inch) side drop, filter cutoff: 450 Hz, maximum acceleration: 110.0g)

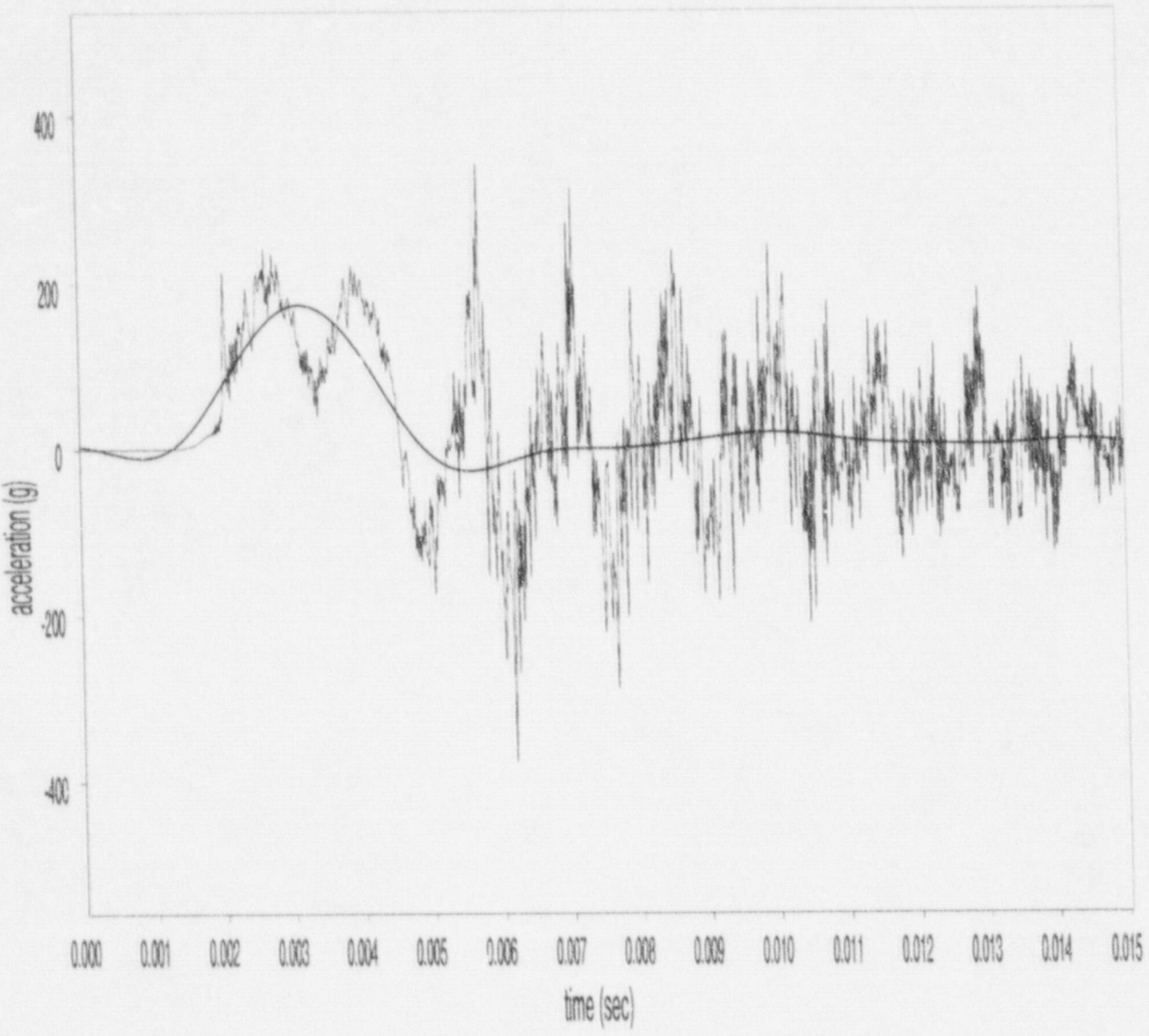

Figure B-19 LLNL Test #4, Gauge A4 (91.4-centimeter (36-inch) side drop, filter cutoff: 450 Hz, maximum acceleration: 173.1g)

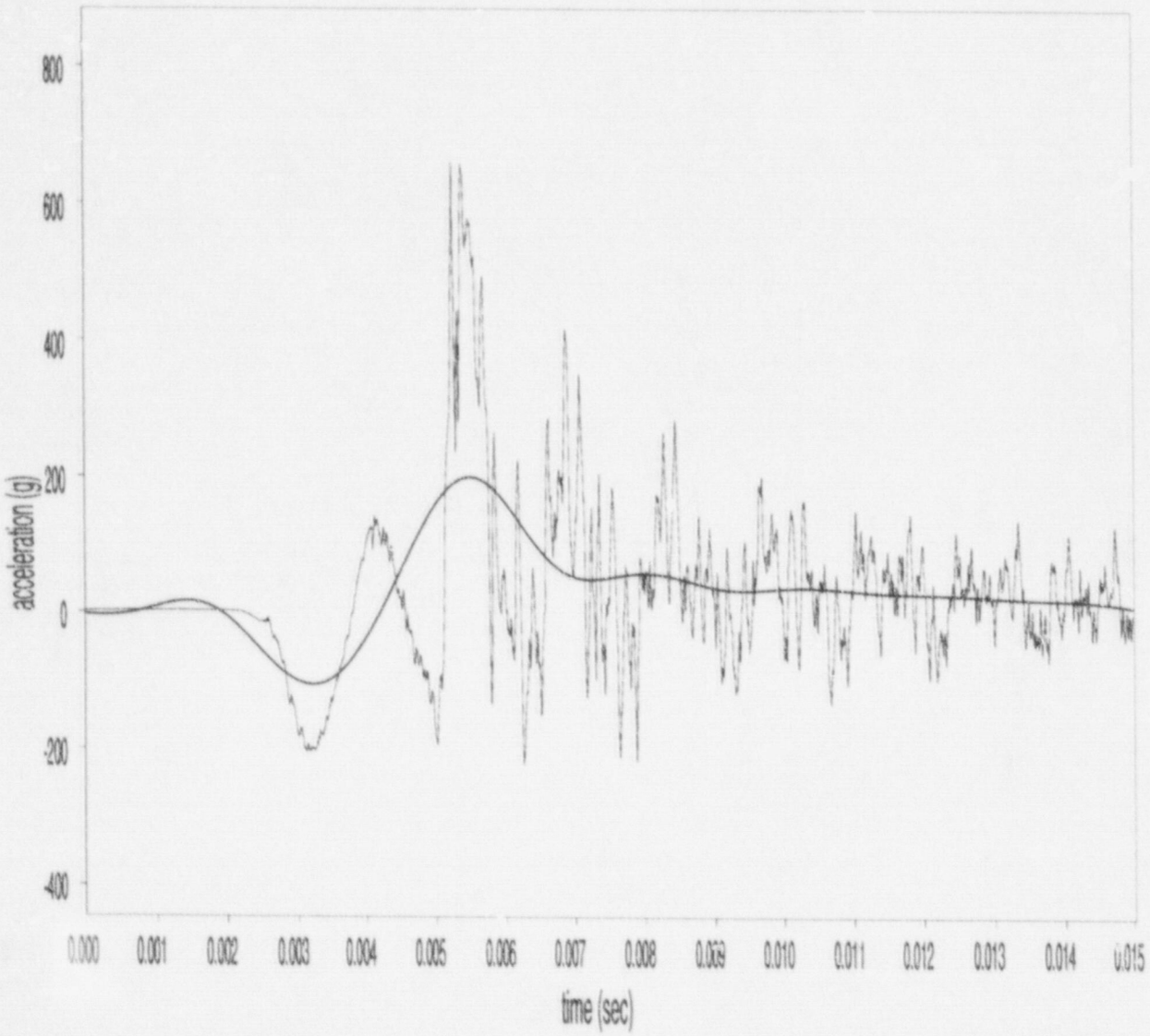

Figure B-20 LLNL Test #4, Gauge A5 (91.4-centimeter (36-inch) side drop, filter cutoff: 450 Hz, maximum acceleration: 198.7g)

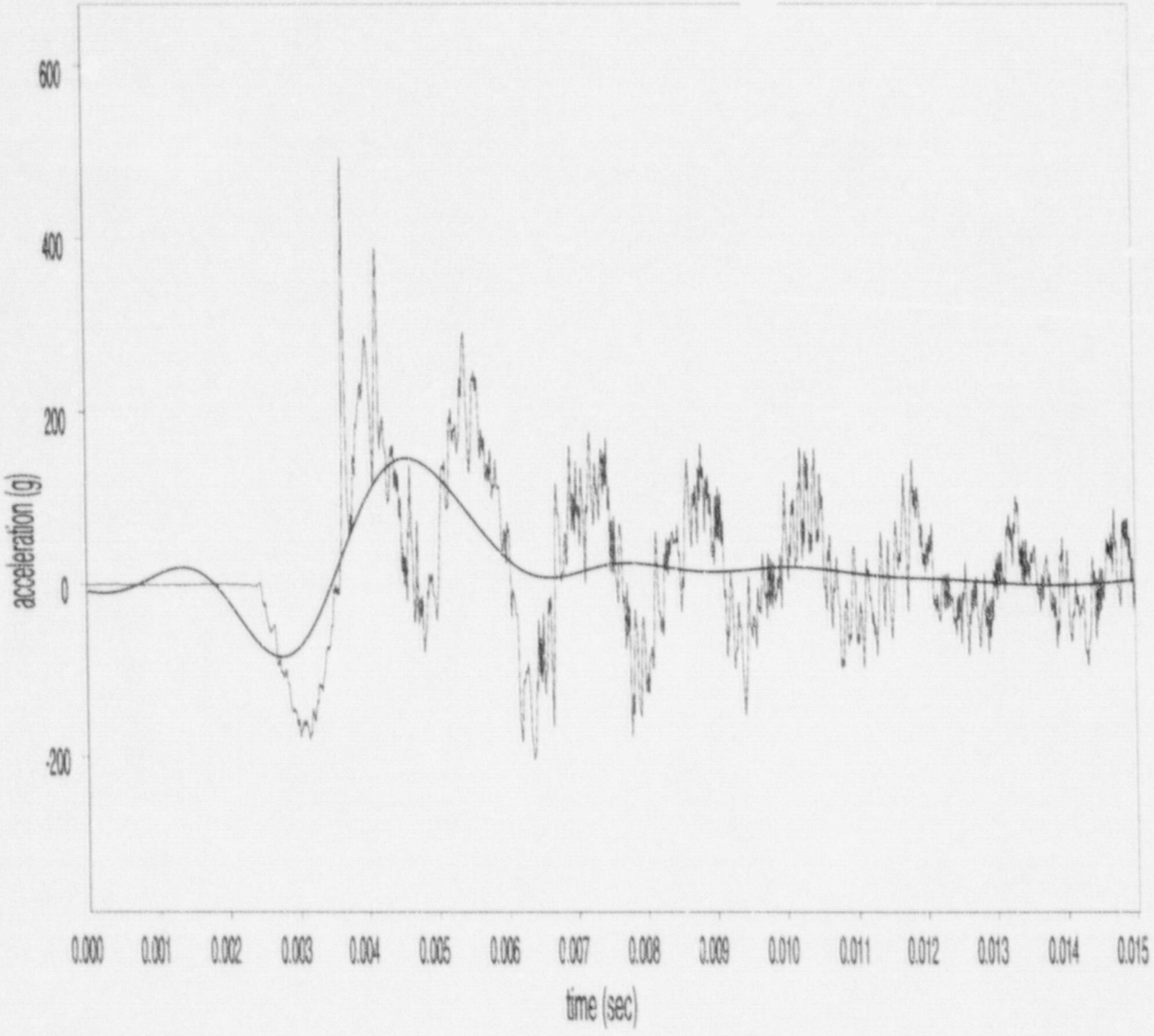

Figure B-21 LLNL Test #5, Gauge A1 (45.7-centimeter (18-inch) side drop, filter cutoff: 450 Hz, maximum acceleration: 145.8g)

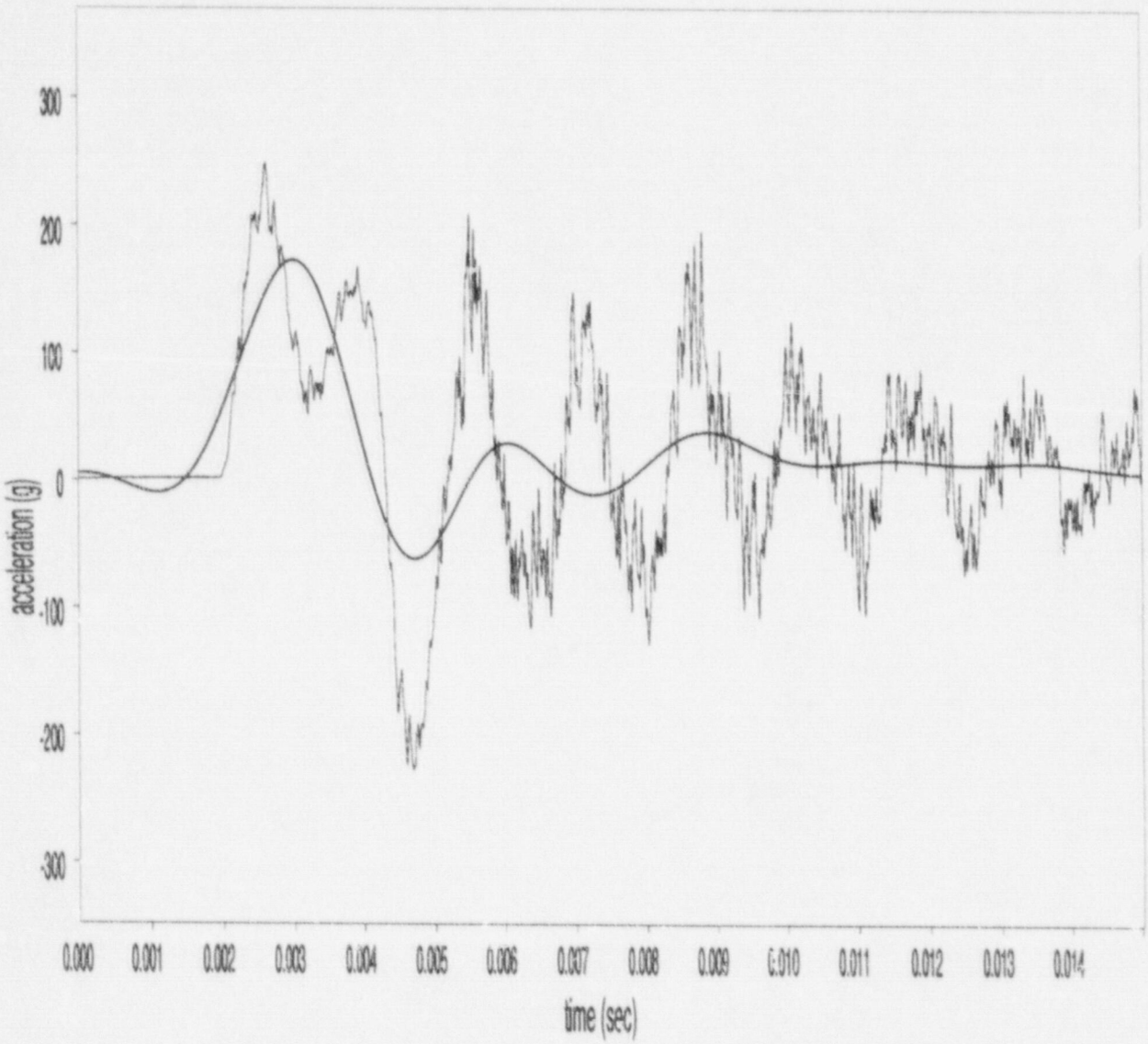

Figure B-22 LLNL Test #5, Gauge A2 (45.7-centimeter (18-inch) side drop, filter cutoff: 450 Hz, maximum acceleration: 172.4g)

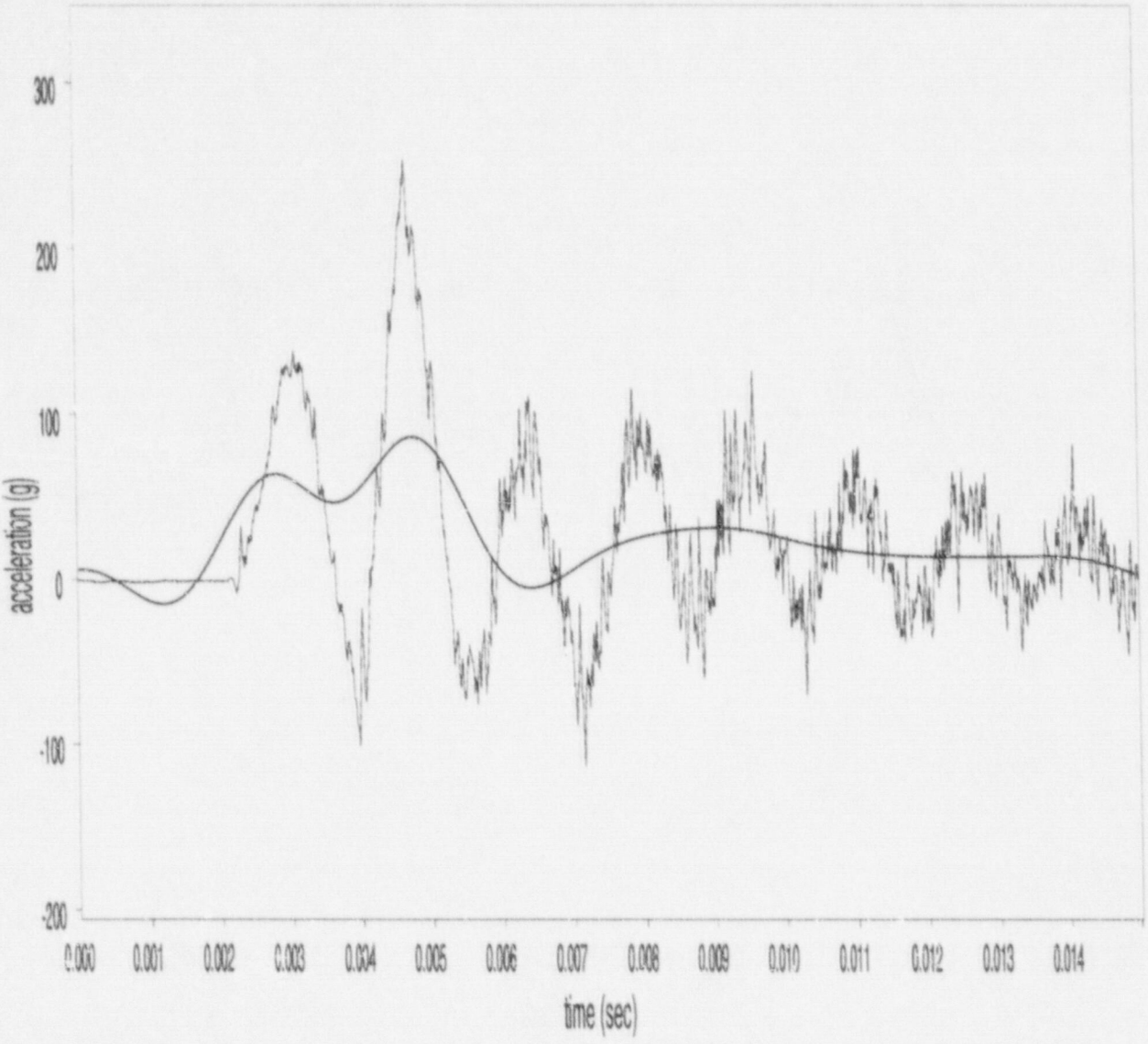

Figure B-23 LLNL Test #5, Gauge A3 (45.7-centimeter (18-inch) side drop, filter cutoff: 450 Hz, maximum acceleration: 86.0g)

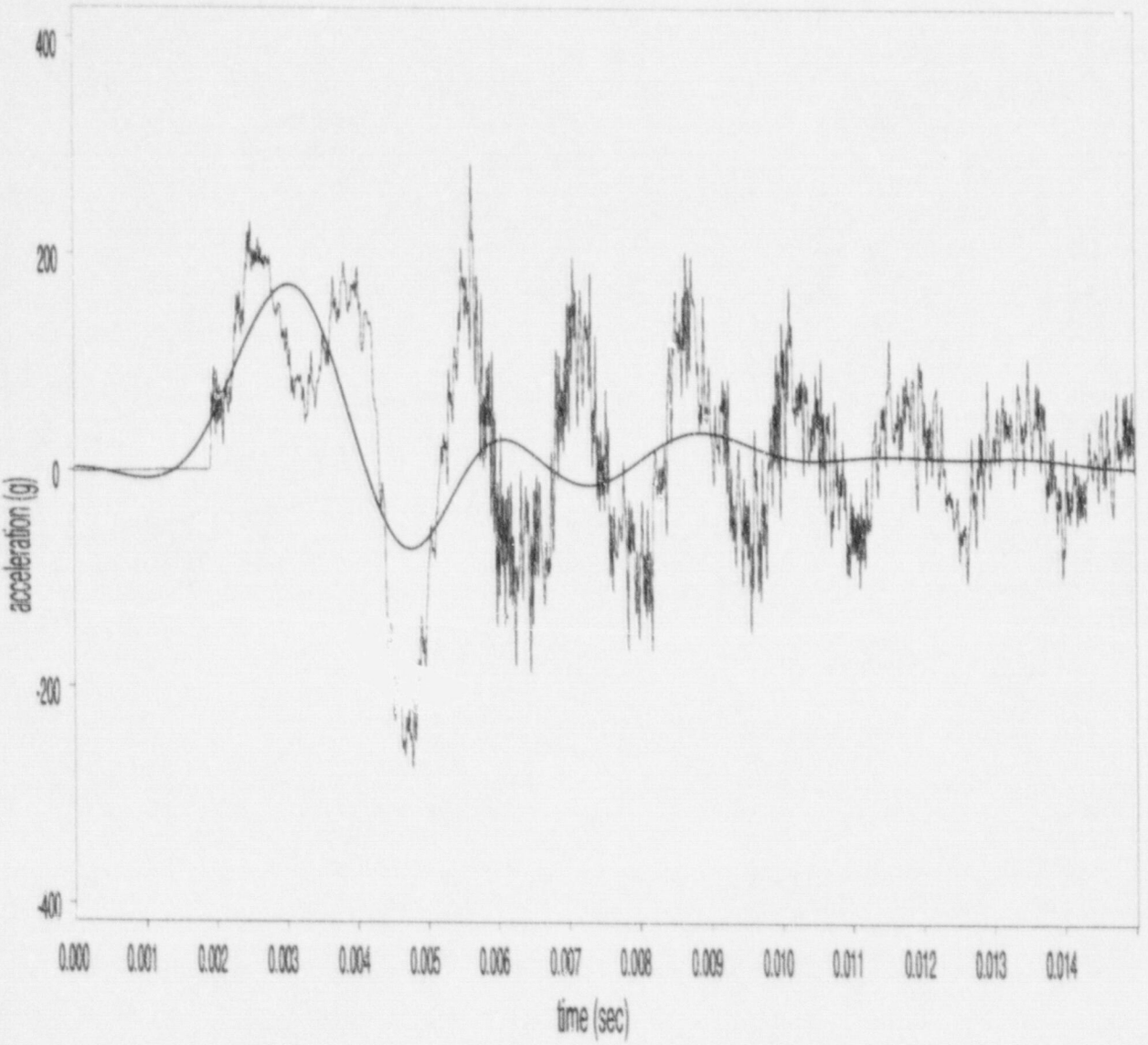

Figure B-24 LLNL Test #5, Gauge A4 (45.7-centimeter (18-inch) side drop, filter cutoff: 450 Hz, maximum acceleration: 171.2g)

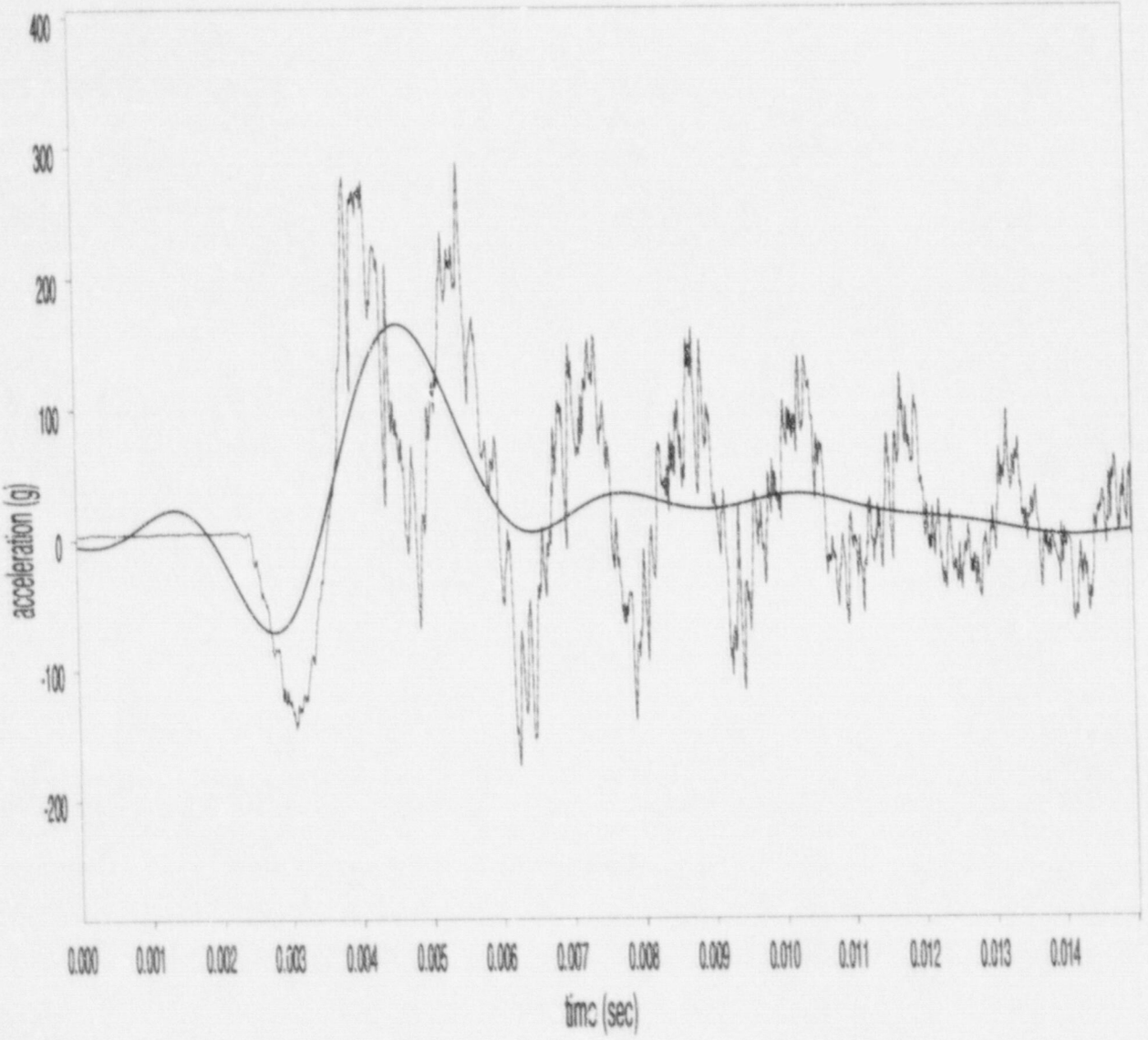

Figure B-25 LLNL Test #5, Gauge A5 (45.7-centimeter (18-inch) side drop, filter cutoff: 450 Hz, maximum acceleration: 164.4g)

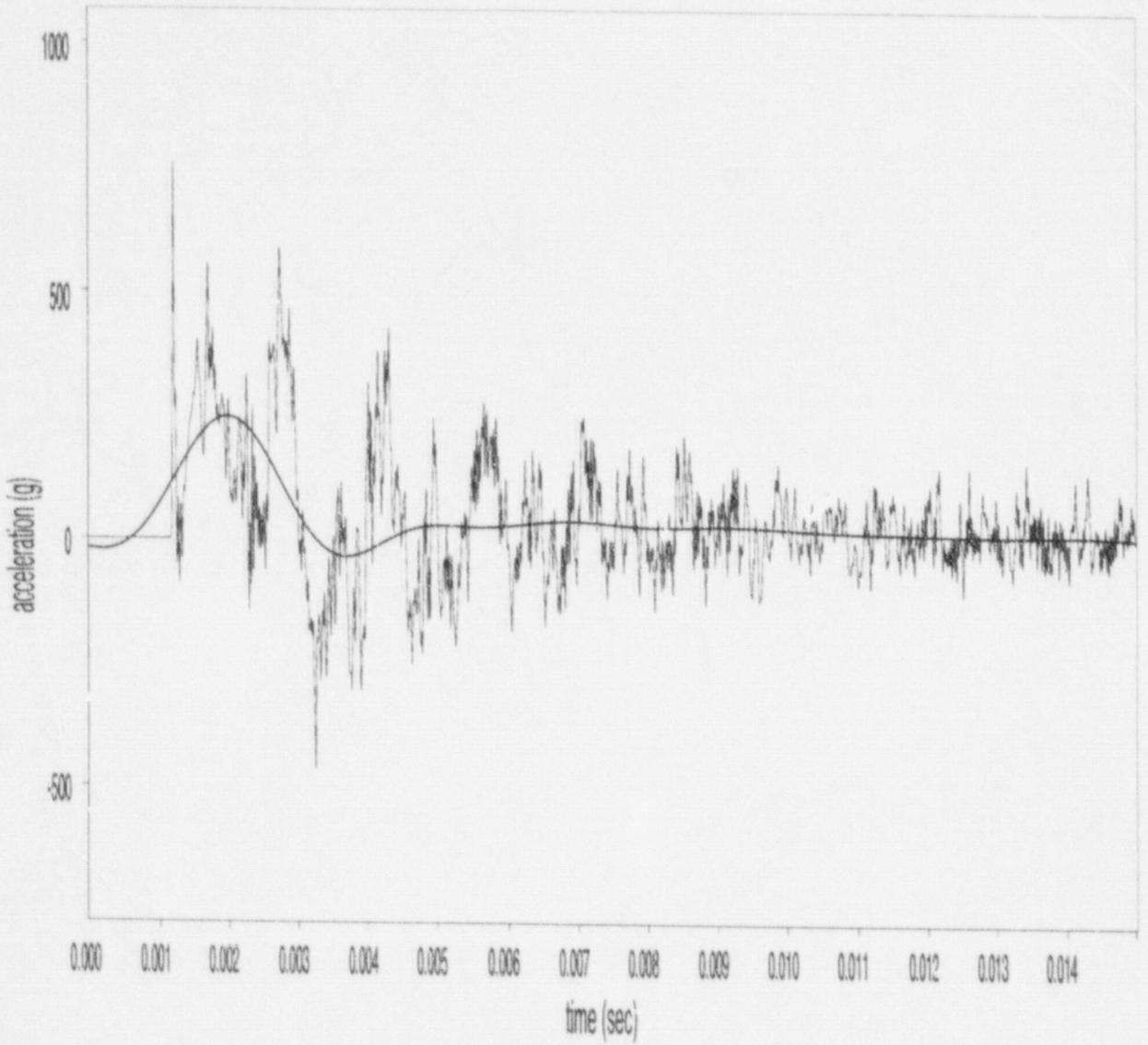

Figure B-26 LLNL Test #6, Gauge A1 (1.83-meter (72-inch) side drop, filter cutoff: 450 Hz, maximum acceleration: 246.3g)

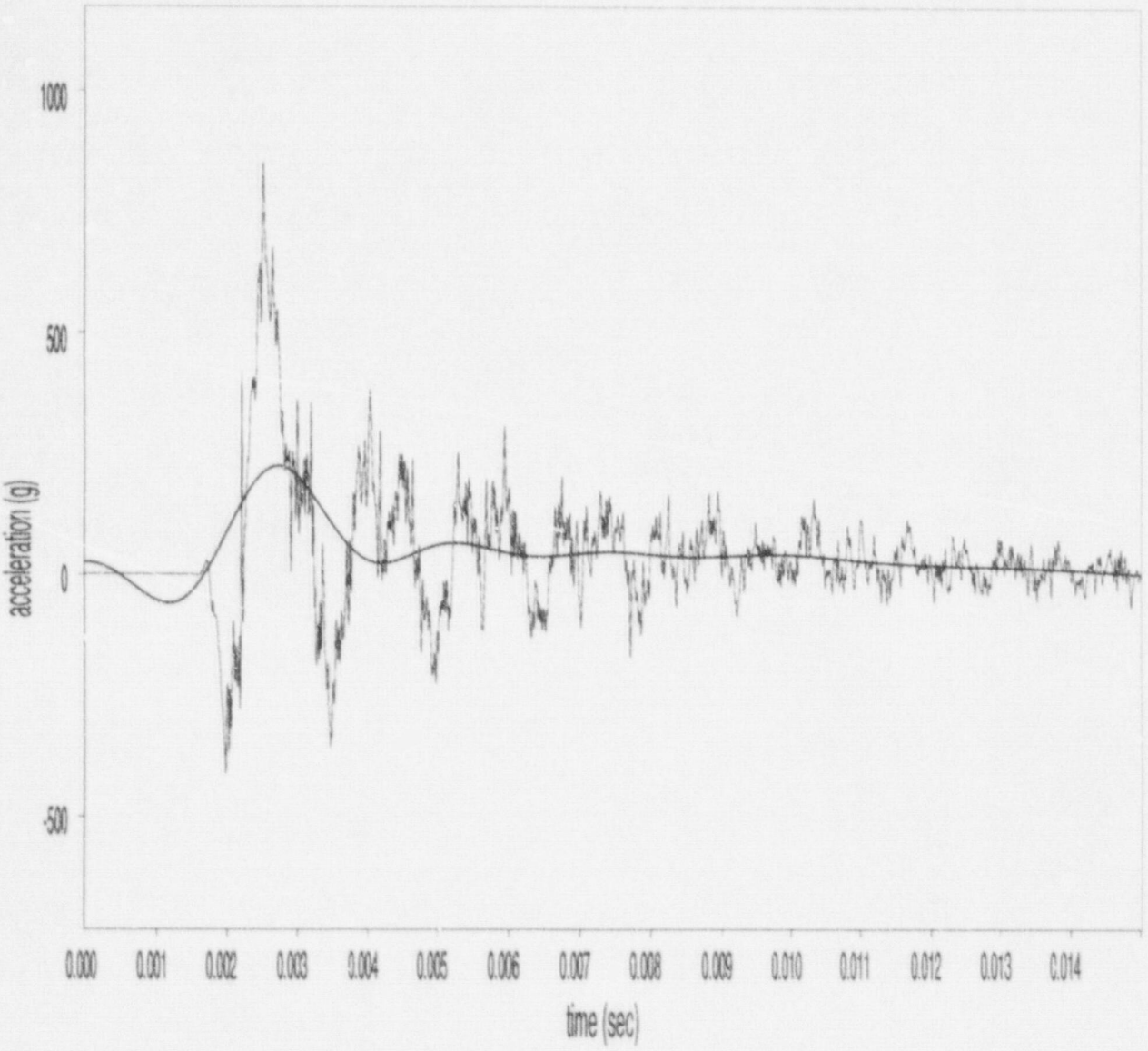

Figure B-27 LLNL Test #6, Gauge A2 (1.83-meter (72-inch) side drop, filter cutoff: 450 Hz, maximum acceleration: 225.7g)

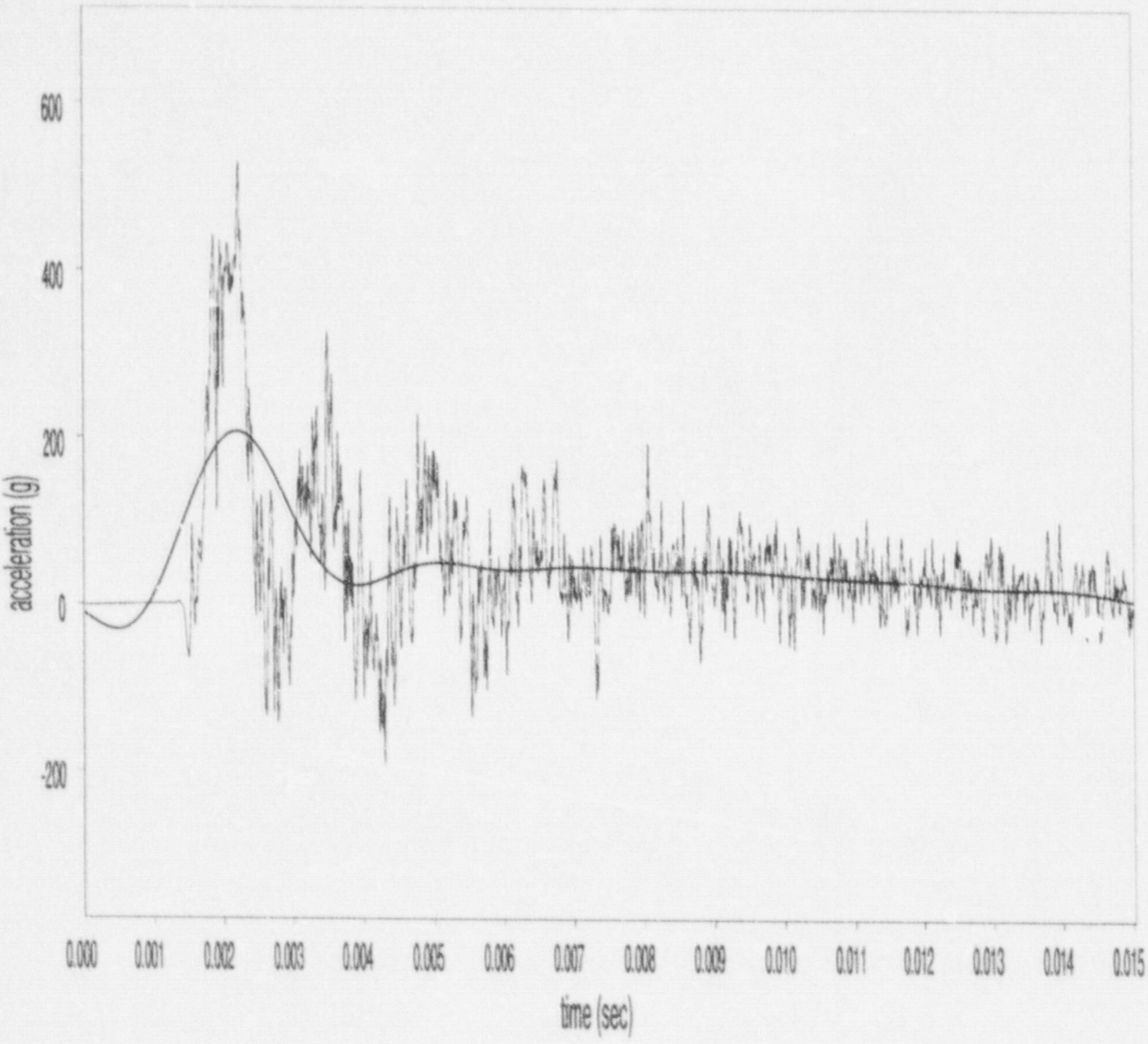

Figure B-28 LLNL Test #6, Gauge A3 (1.83-meter (72-inch) side drop, filter cutoff: 450 Hz, maximum acceleration: 206.7g)

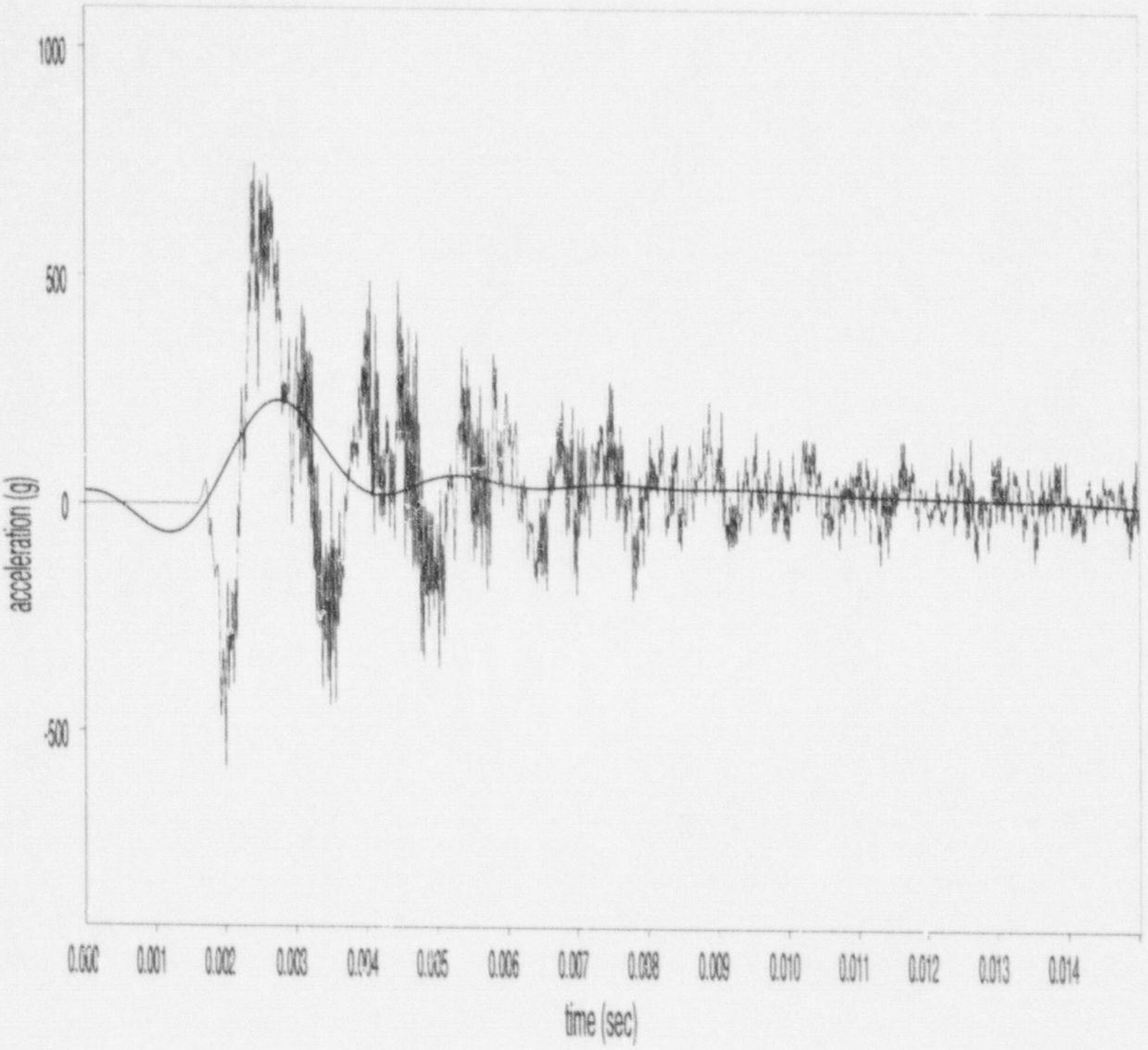

Figure B-29 LLNL Test #6, Gauge A4 (1.83-meter (72-inch) side drop, filter cutoff: 450 Hz, maximum acceleration: 227.0g)

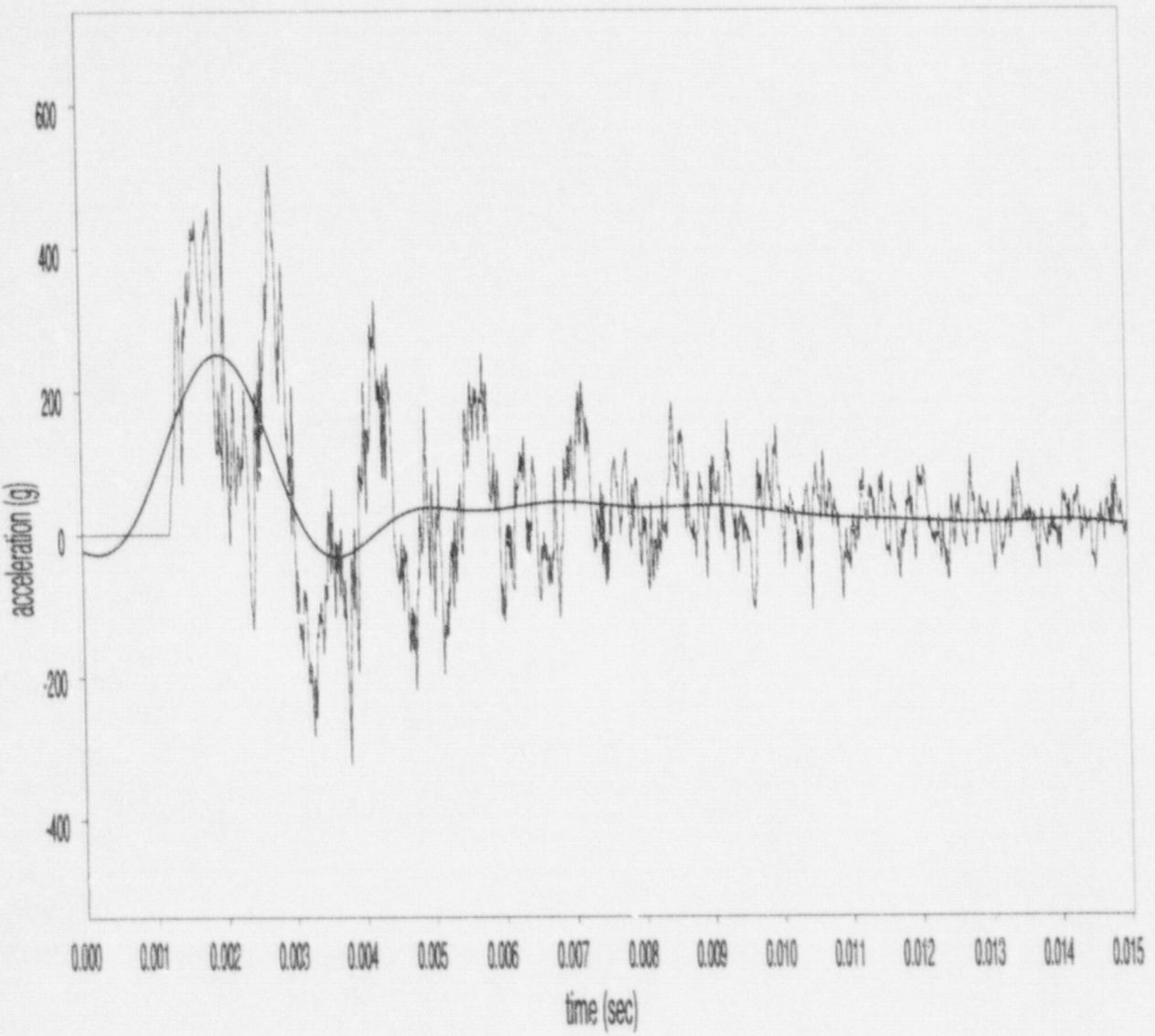

Figure B-30 LLNL Test #6, Gauge A5 (1.83-meter (72-inch) side drop, filter cutoff: 450 Hz, maximum acceleration: 251.5)

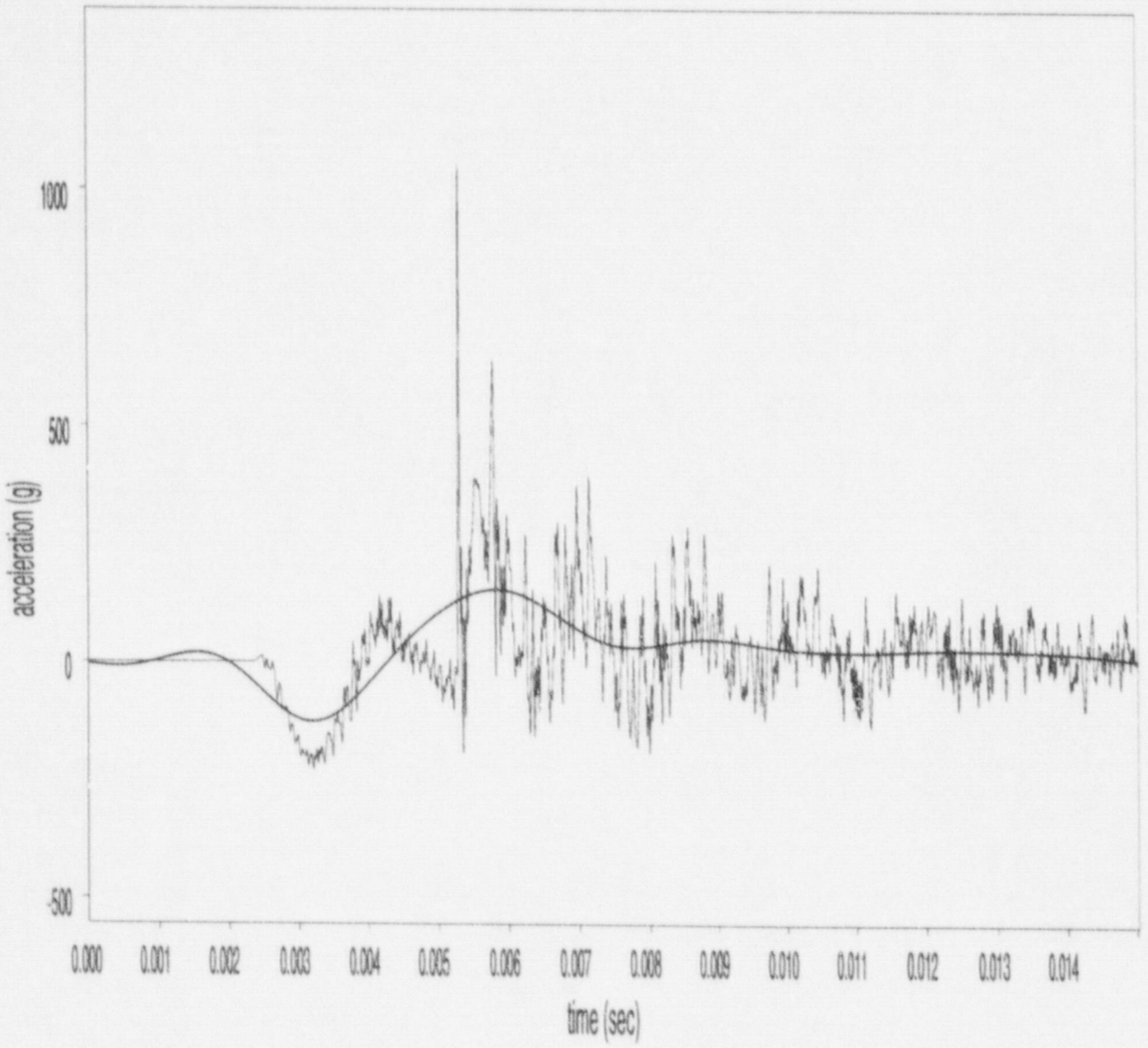

Figure B-31 LLNL Test #7, Gauge A1 (91.4-centimeter (36-inch) side drop, filter cutoff: 450 Hz, maximum acceleration: 154.2g)

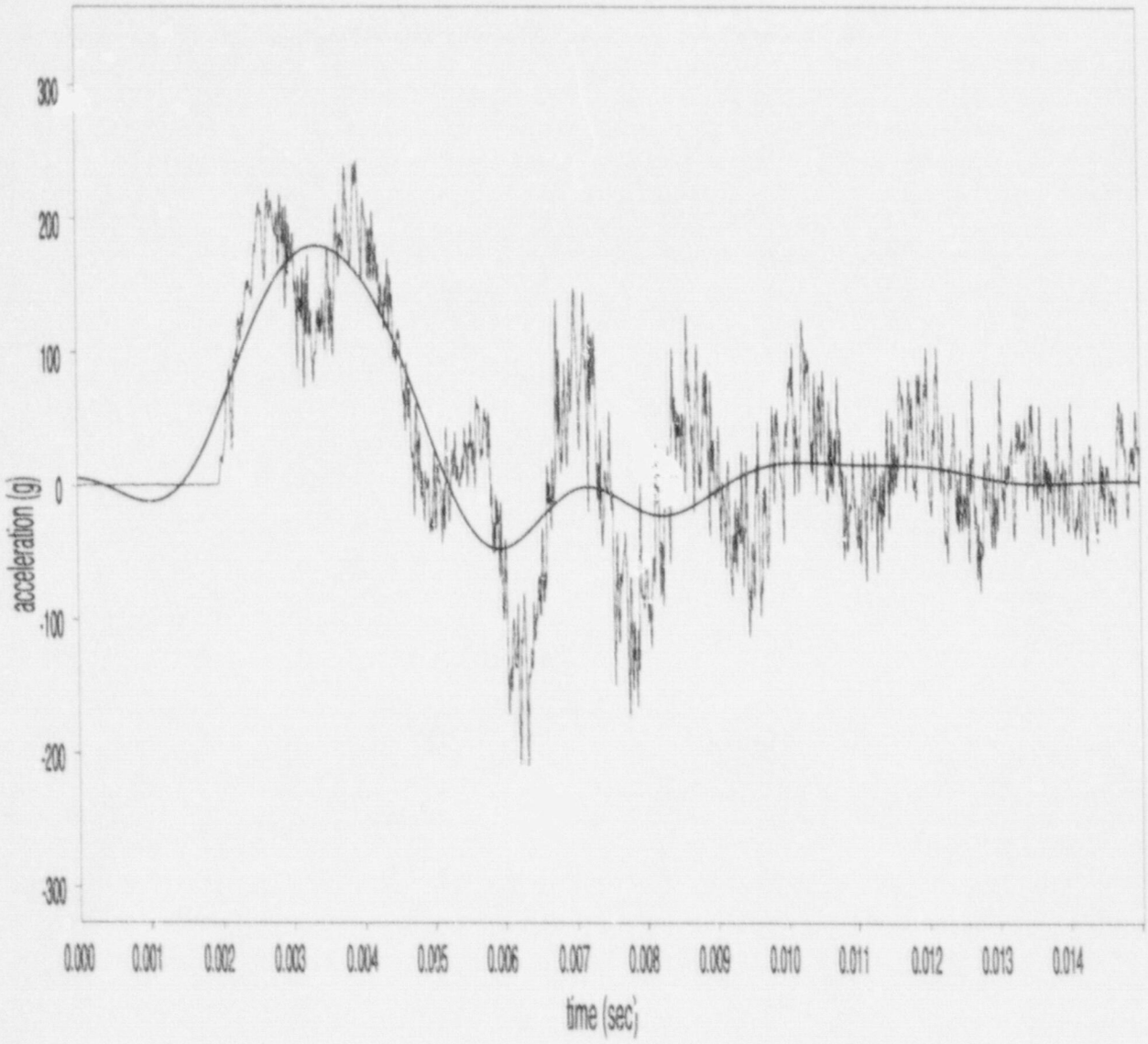

Figure B-32 LLNL Test #7, Gauge A2 (91.4-centimeter (36-inch) side drop, filter cutoff: 450 Hz, maximum acceleration: 179.5g)

LLNL Test #7, Gauge A3. Accelerometer did not function.

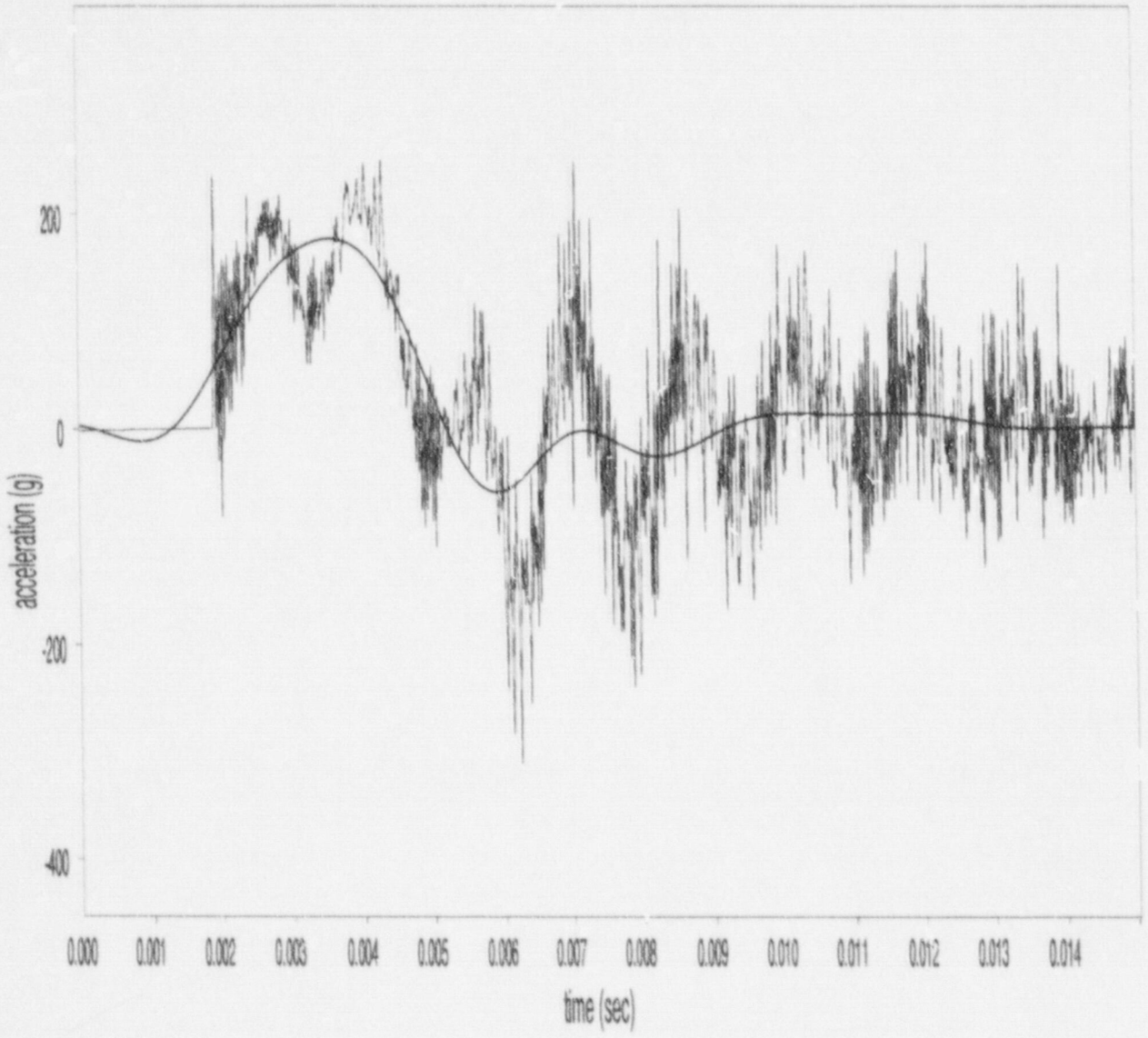

Figure B-33 LLNL Test #7, Gauge A4 (91.4-centimeter (36-inch) side drop, filter cutoff: 450 Hz, maximum acceleration: 176.8g)

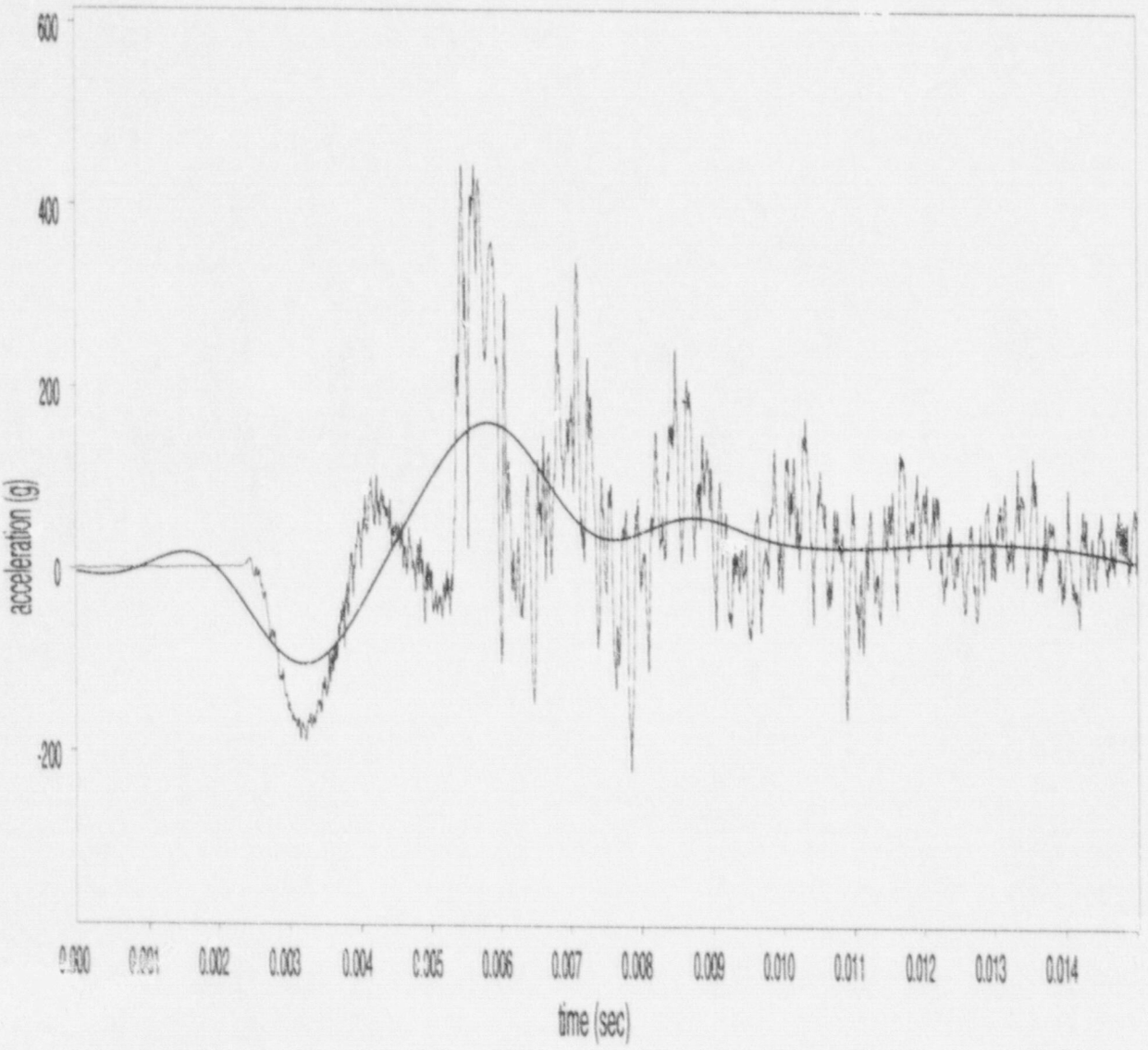

Figure B-34 LLNL Test #7, Gauge A5 (91.4-centimeter (36-inch) side drop, filter cutoff: 450 Hz, maximum acceleration: 162.0g)

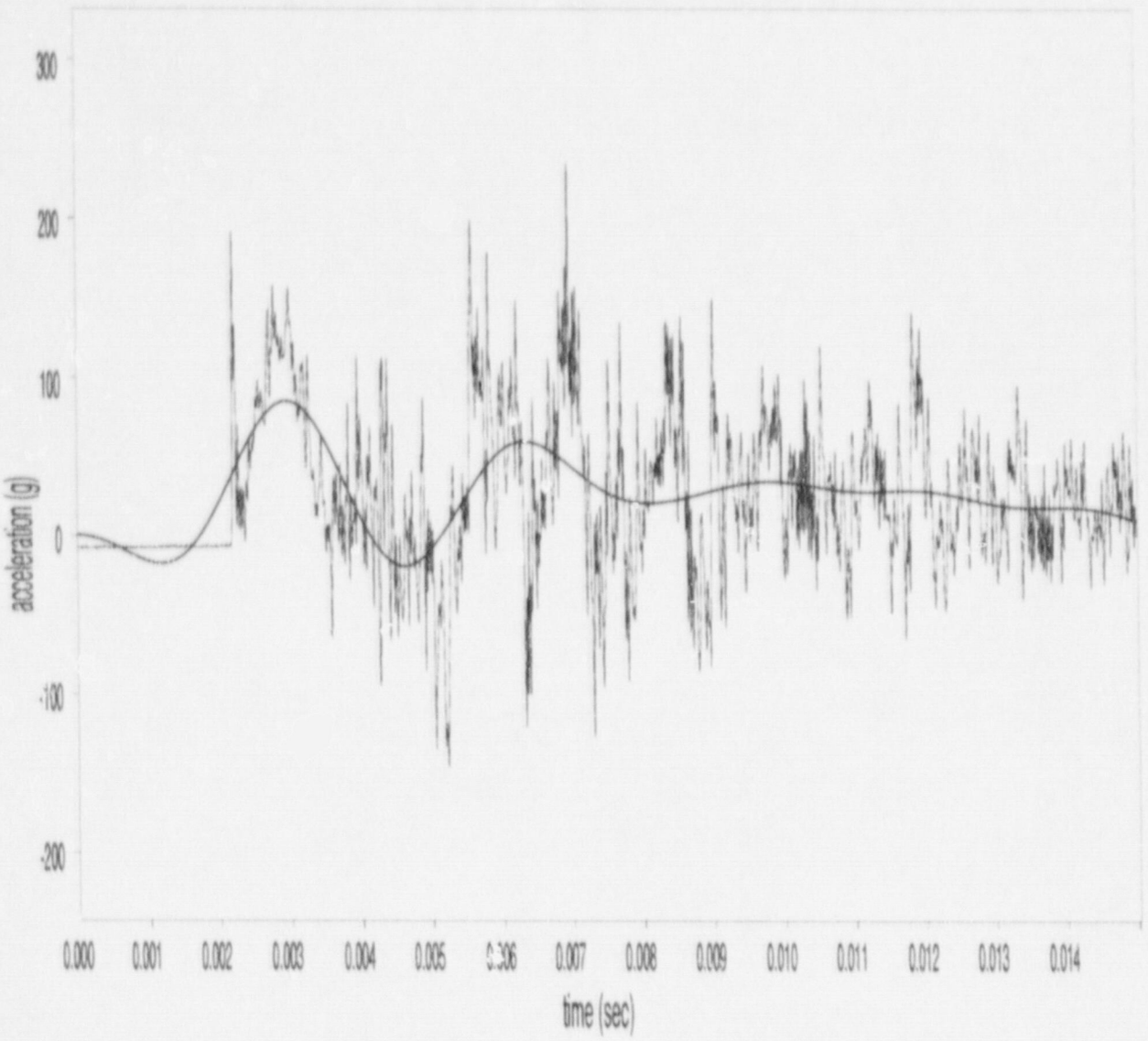

Figure B-35 Test #8, Gauge A1 (1.83-meter (72-inch) side drop, filter cutoff: 450 Hz, maximum acceleration: 84.9g)

LLNL Test #8, Gauge A2. Accelerometer did not function.

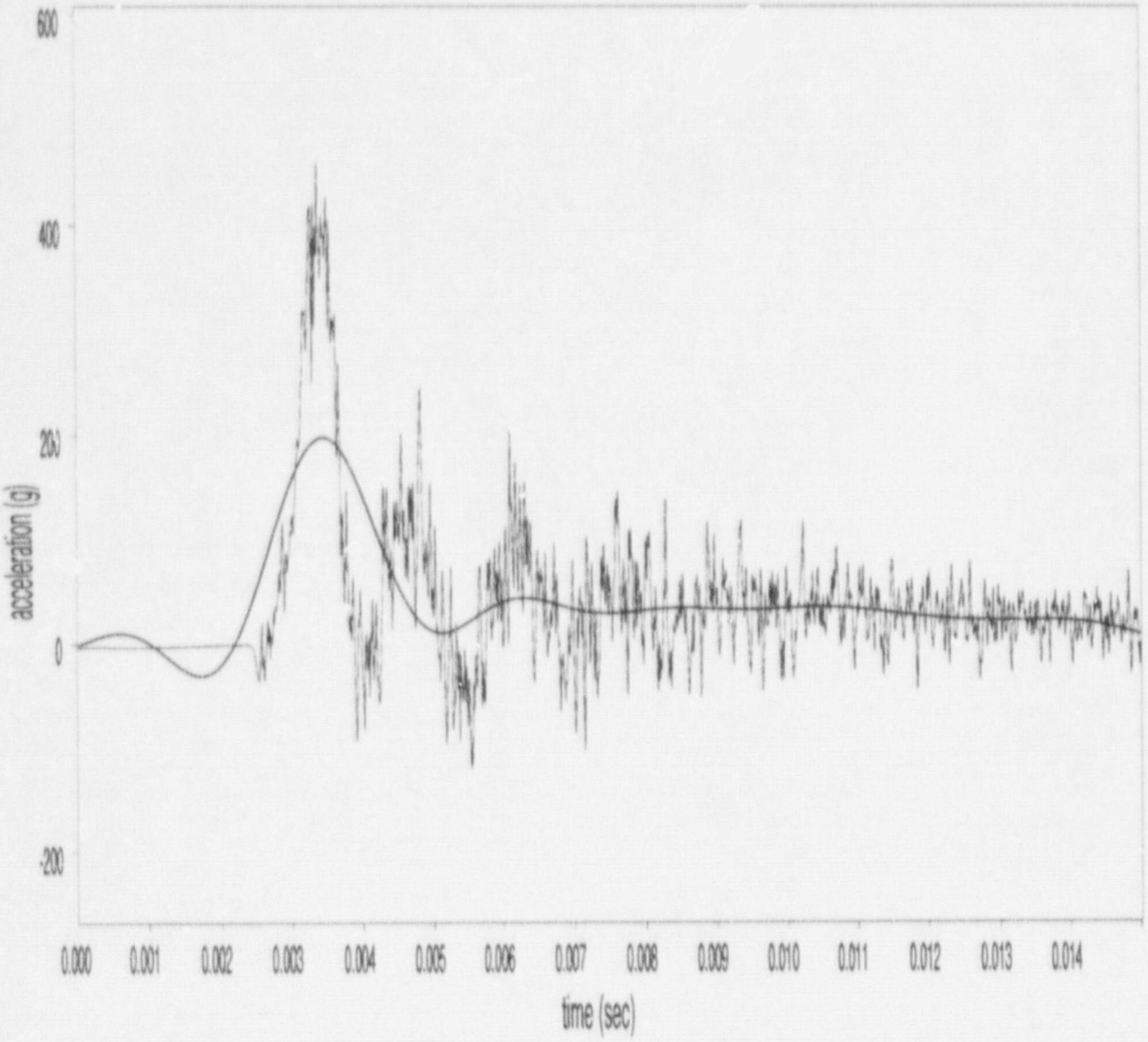

Figure B-36 Test #8, Gauge A3 (1.83-meter (72-inch) side drop, filter cutoff: 450 Hz, maximum acceleration: 197.0g)

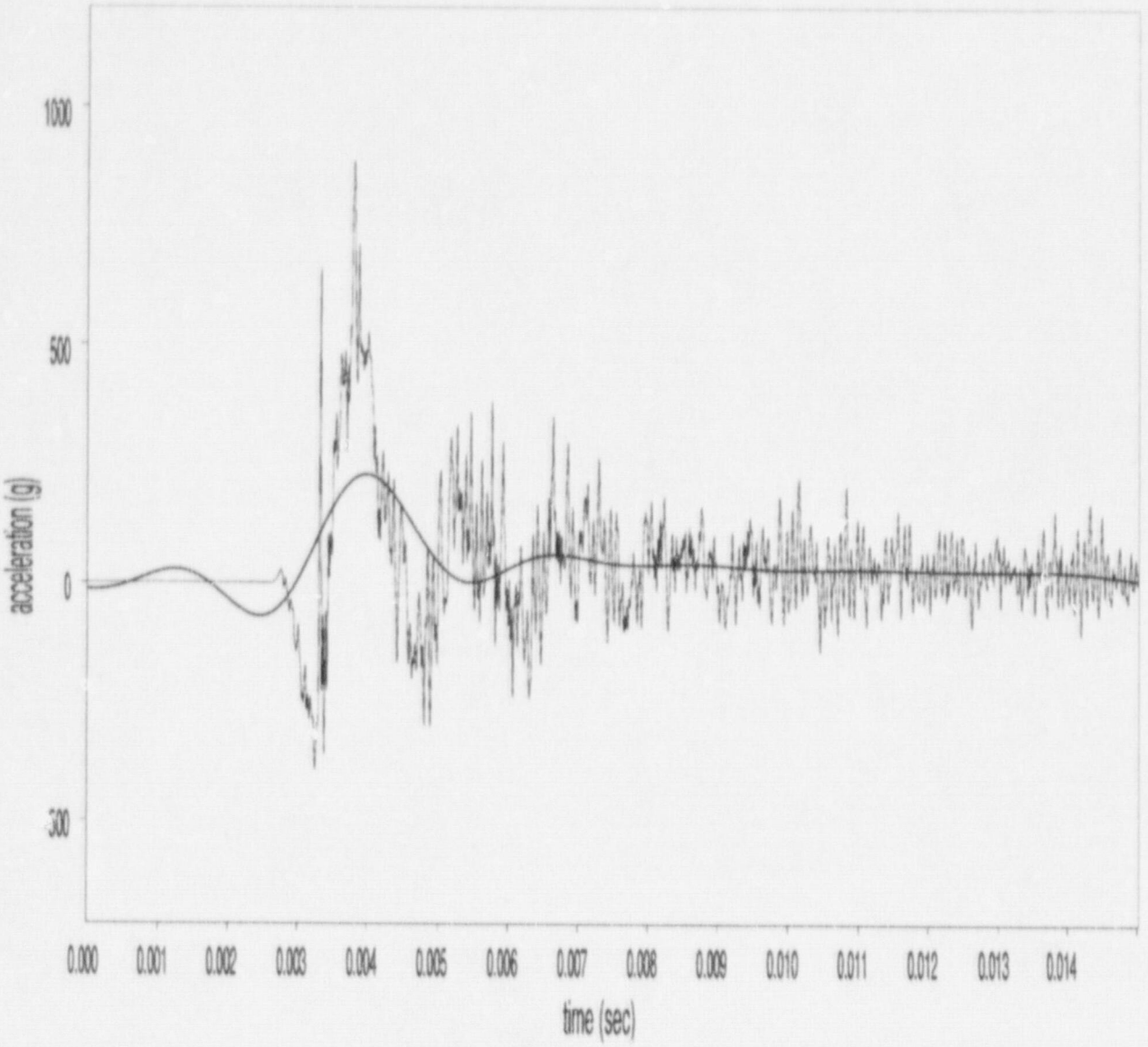

Figure B-37 Test #8, Gauge A4 (1.83-meter (72-inch) side drop, filter cutoff: 450 Hz, maximum acceleration: 227.9g)

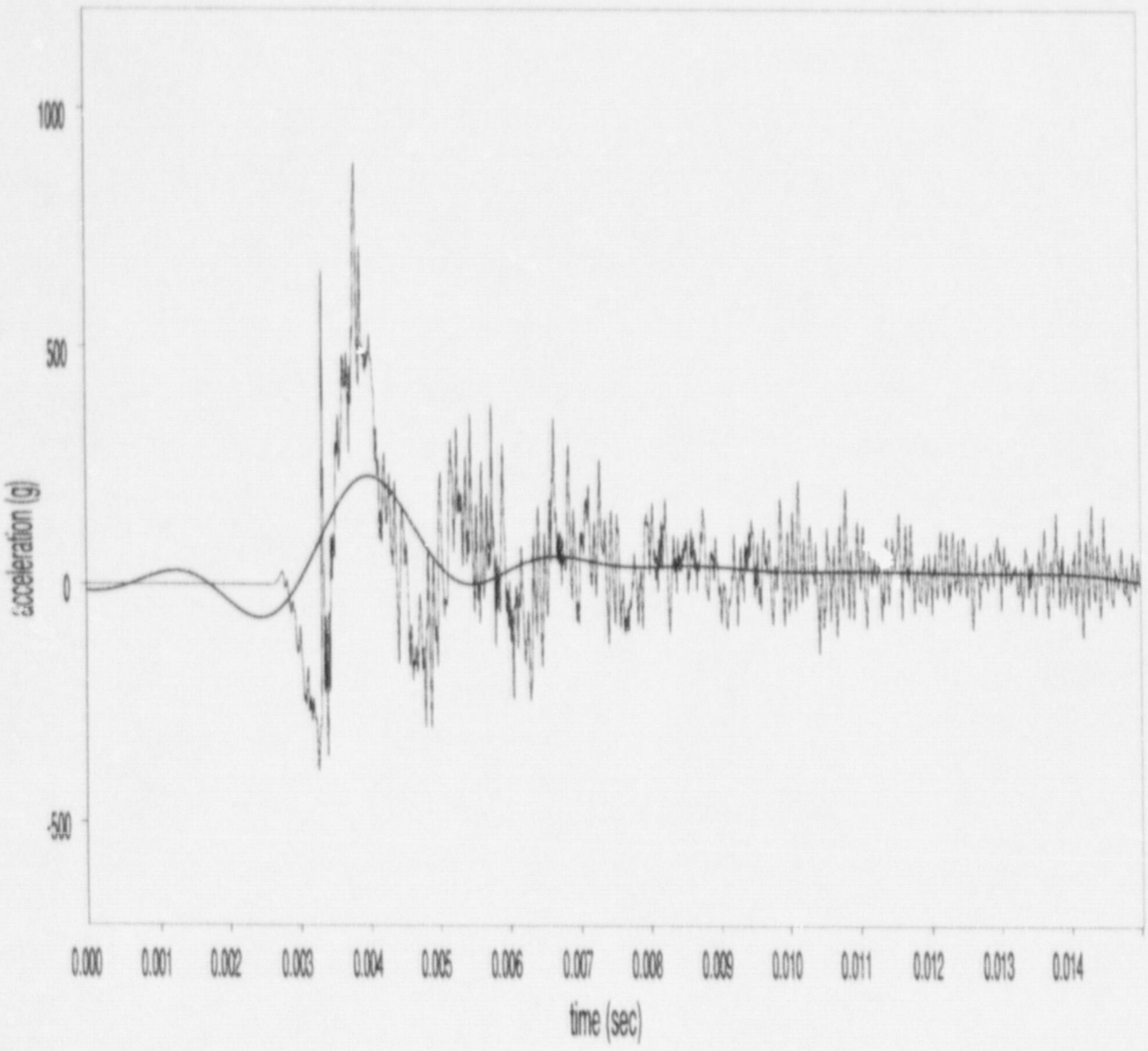

Figure B-38 Test #8, Gauge A5 (1.83-meter (72-inch) side drop, filter cutoff: 450 Hz, maximum acceleration: 255.1g)

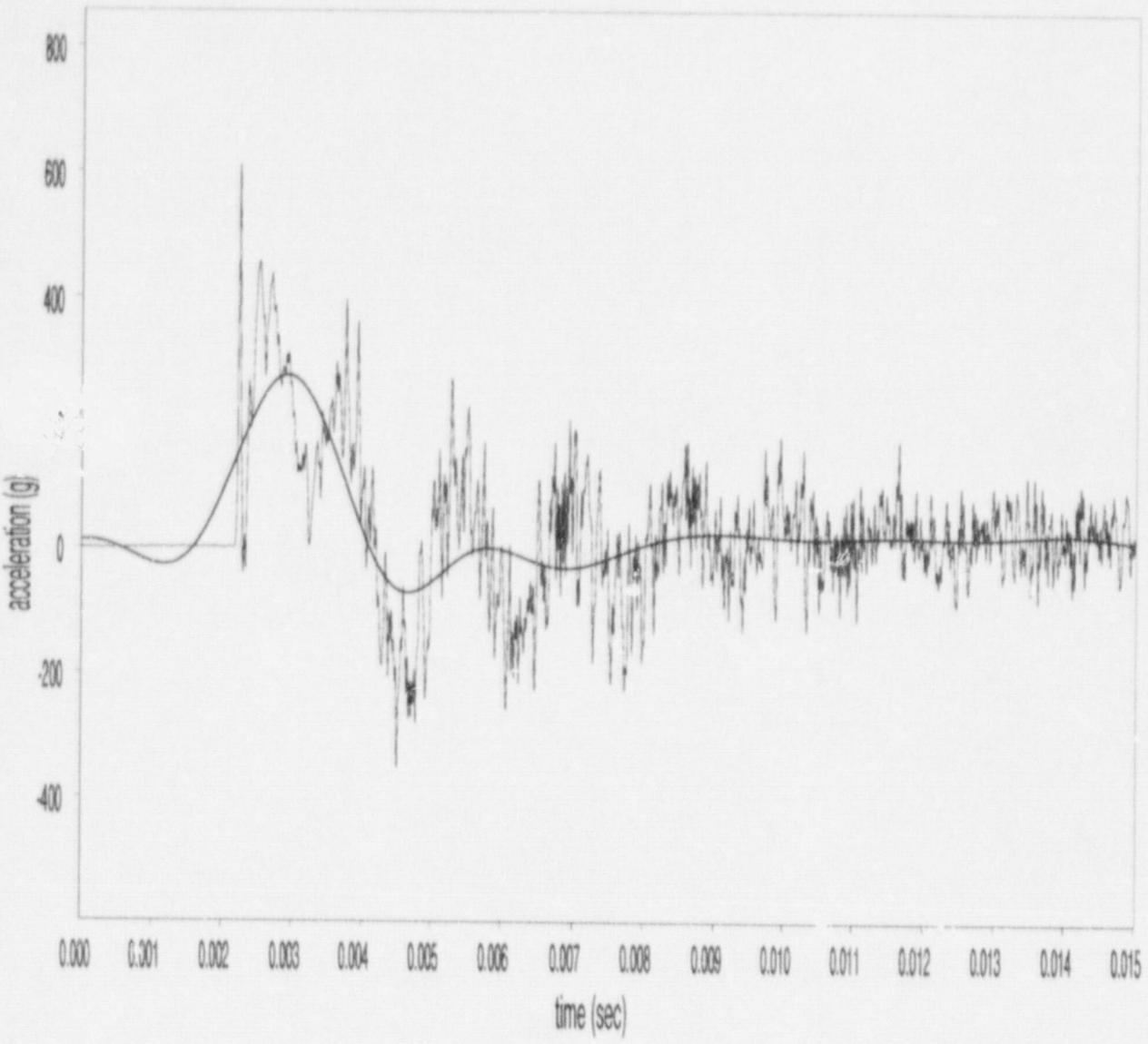

Figure B-39 Test #9, Gauge A1 (91.4-centimeter (36-inch) side drop, filter cutoff: 450 Hz, maximum acceleration: 274.9g)

LLNL Test #9, Gauge A2. Accelerometer did not function.

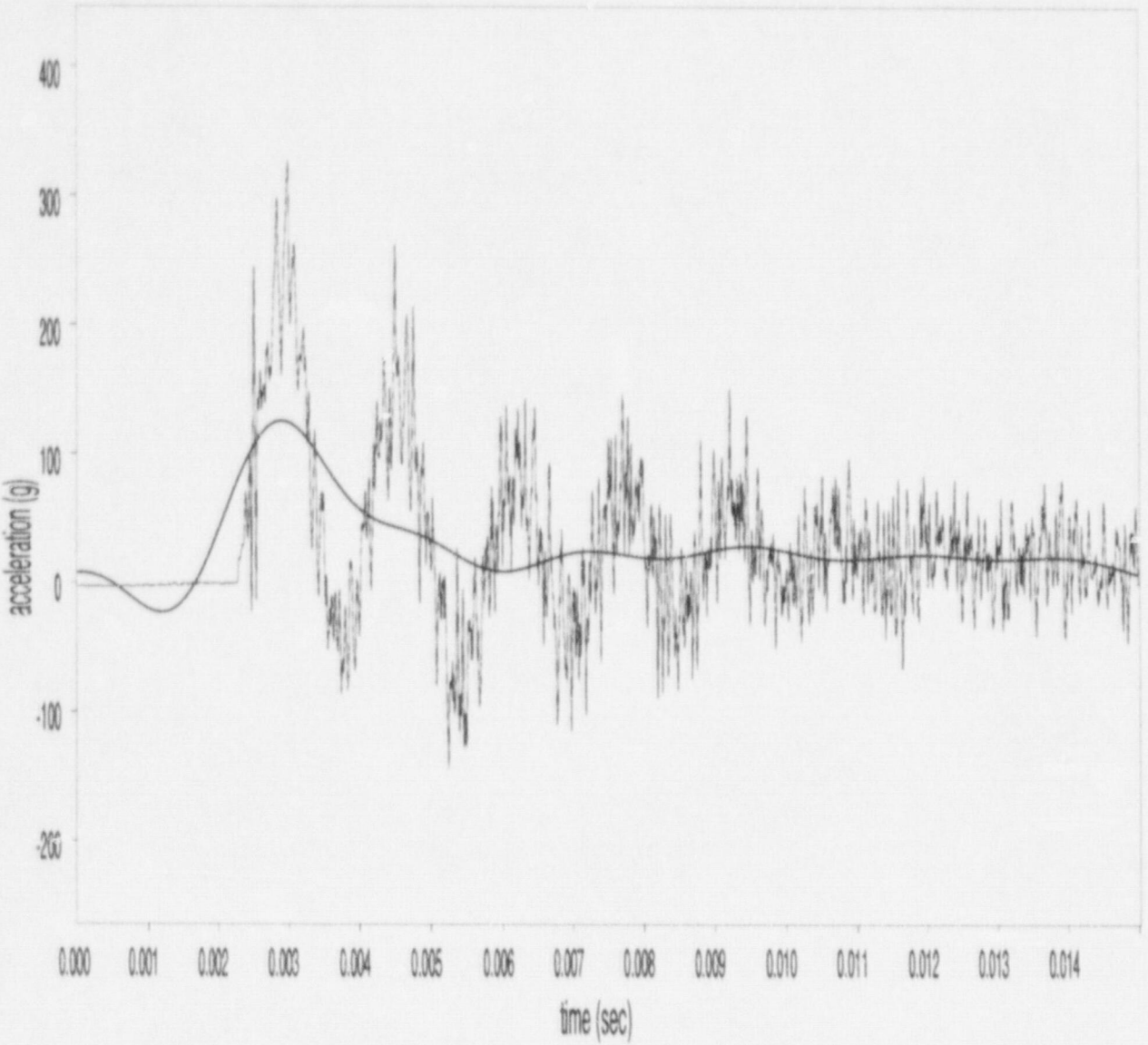

Figure B-40 Test #9, Gauge A3 (91.4-centimeter (36-inch) side drop, filter cutoff: 450 Hz, maximum acceleration: 125.2g)

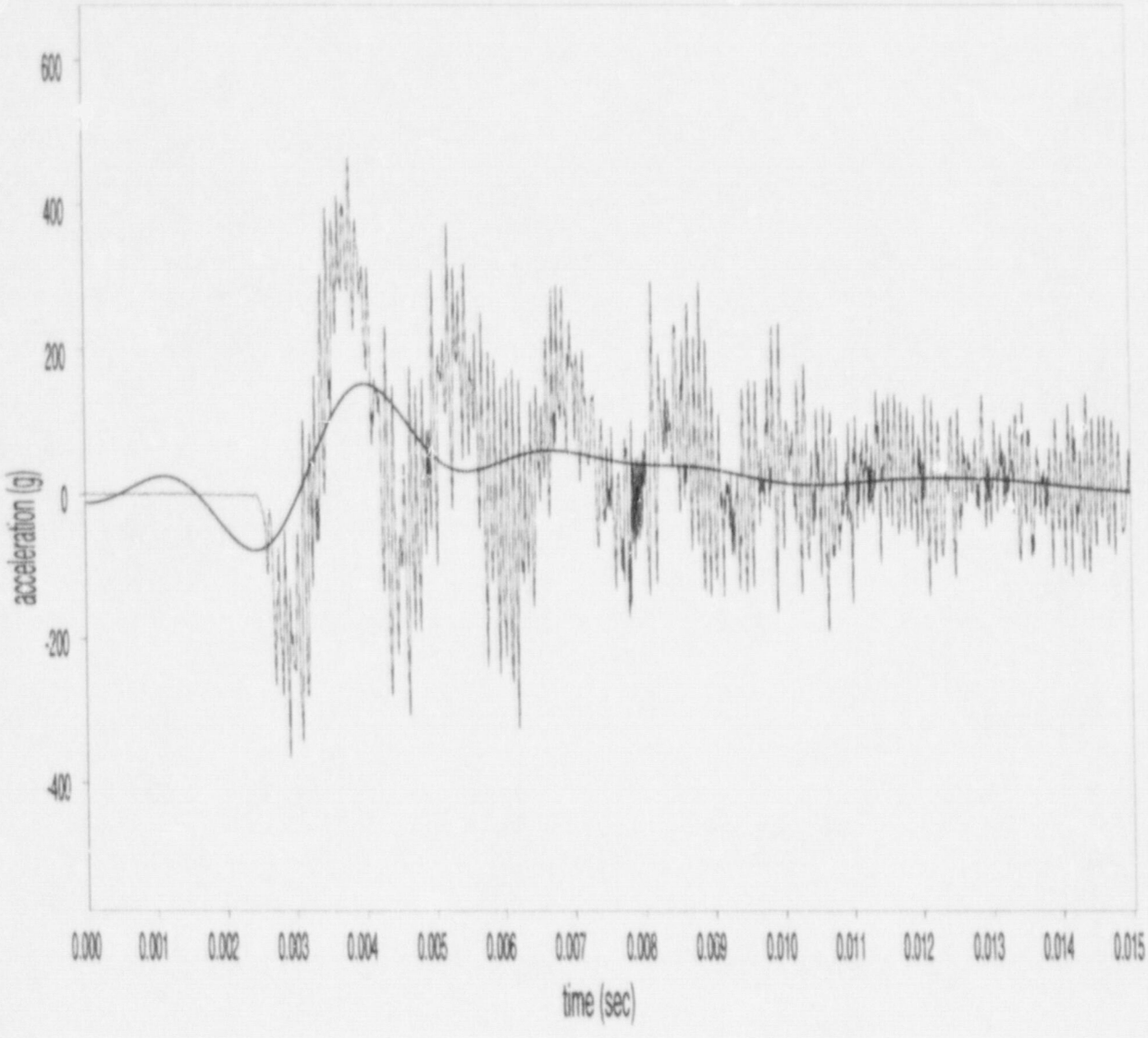

Figure B-41 Test #9, Gauge A4 (91.4-centimeter (36-inch) side drop, filter cutoff: 450 Hz, maximum acceleration: 152.5g)

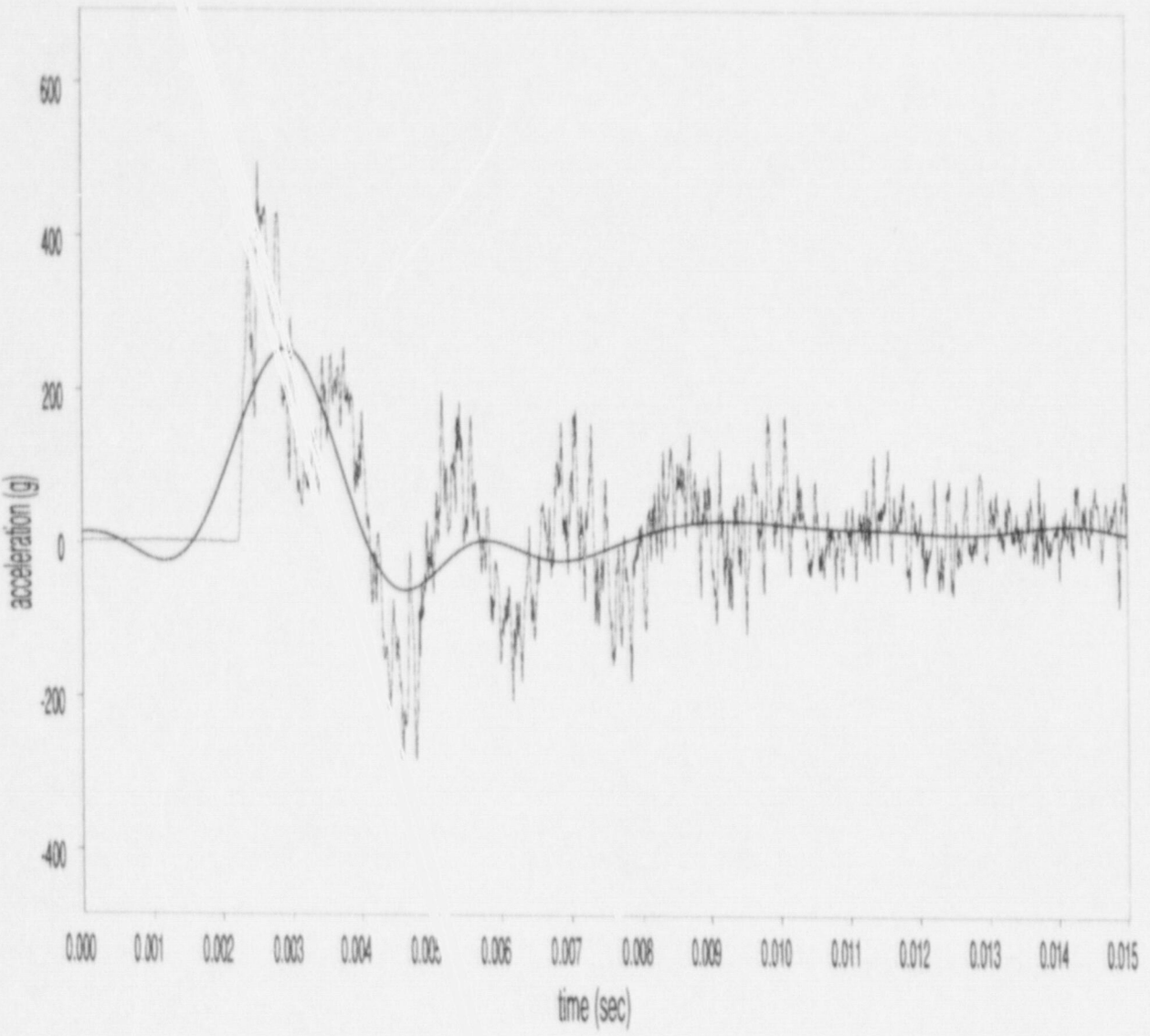

Figure B-42 Test #9, Gauge A5 (91.4-centimeter (36-inch) side drop, filter cutoff: 450 Hz, maximum acceleration: 253.5g)

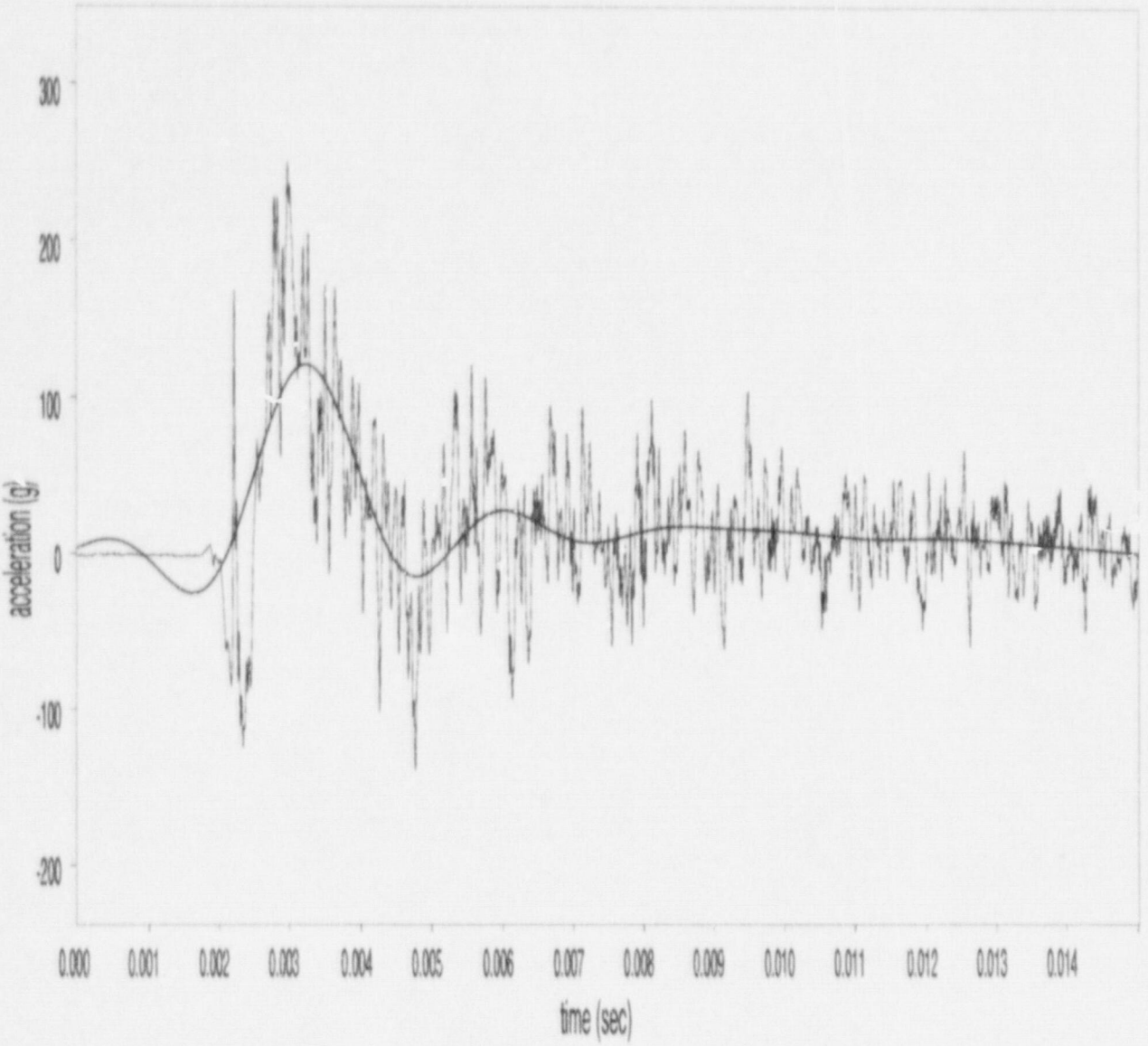

Figure B-43 Test #10, Gauge A1 (45.7-centimeter (18-inch) side drop, filter cutoff: 450 Hz, maximum acceleration: 120.6g)

LLNL Test #10, Gauge A2. Accelerometer did not function.

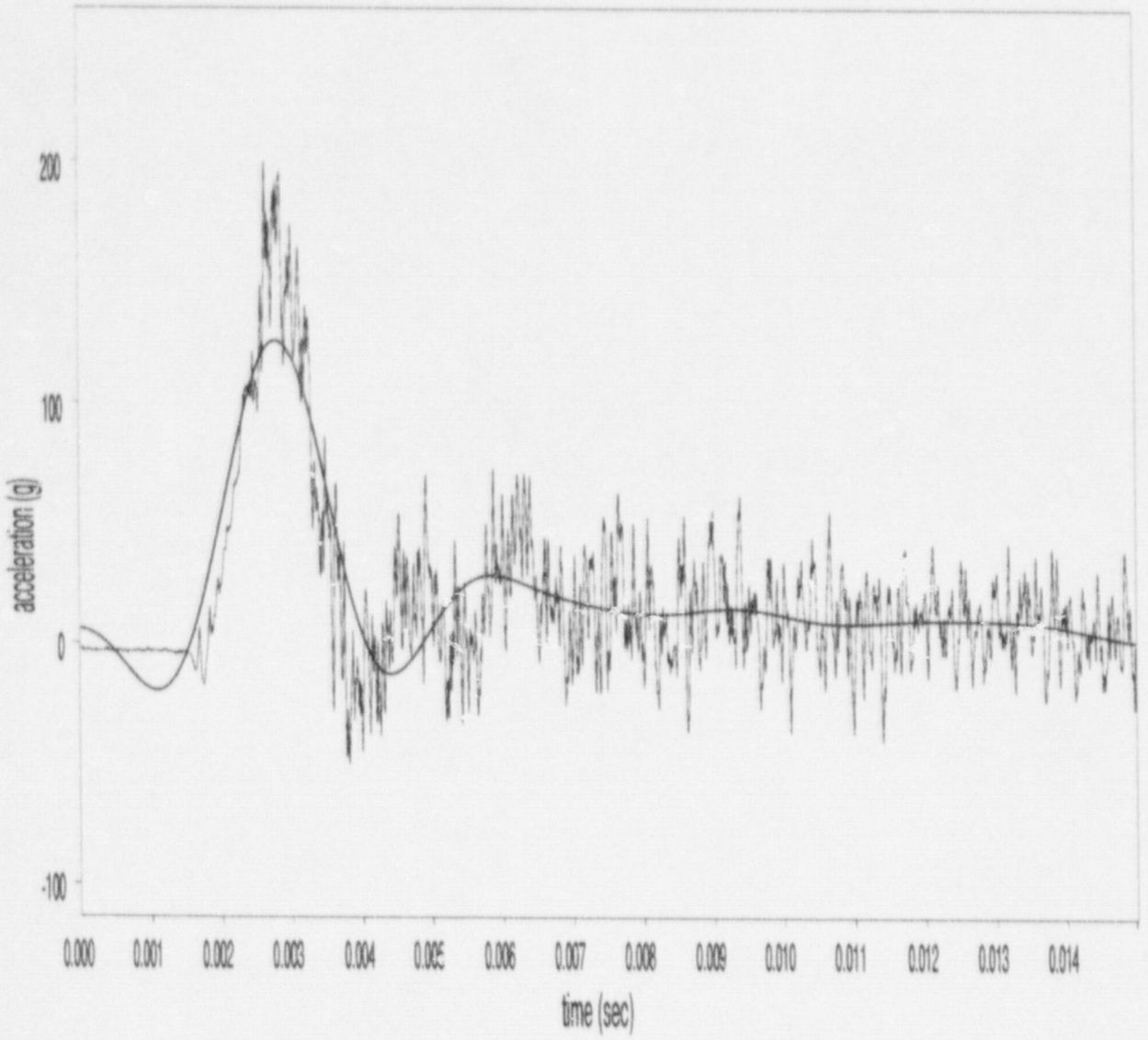

Figure B-44 Test #10, Gauge A3 (45.7-centimeter (18-inch) side drop, filter cutoff: 450 Hz, maximum acceleration: 125.5g)

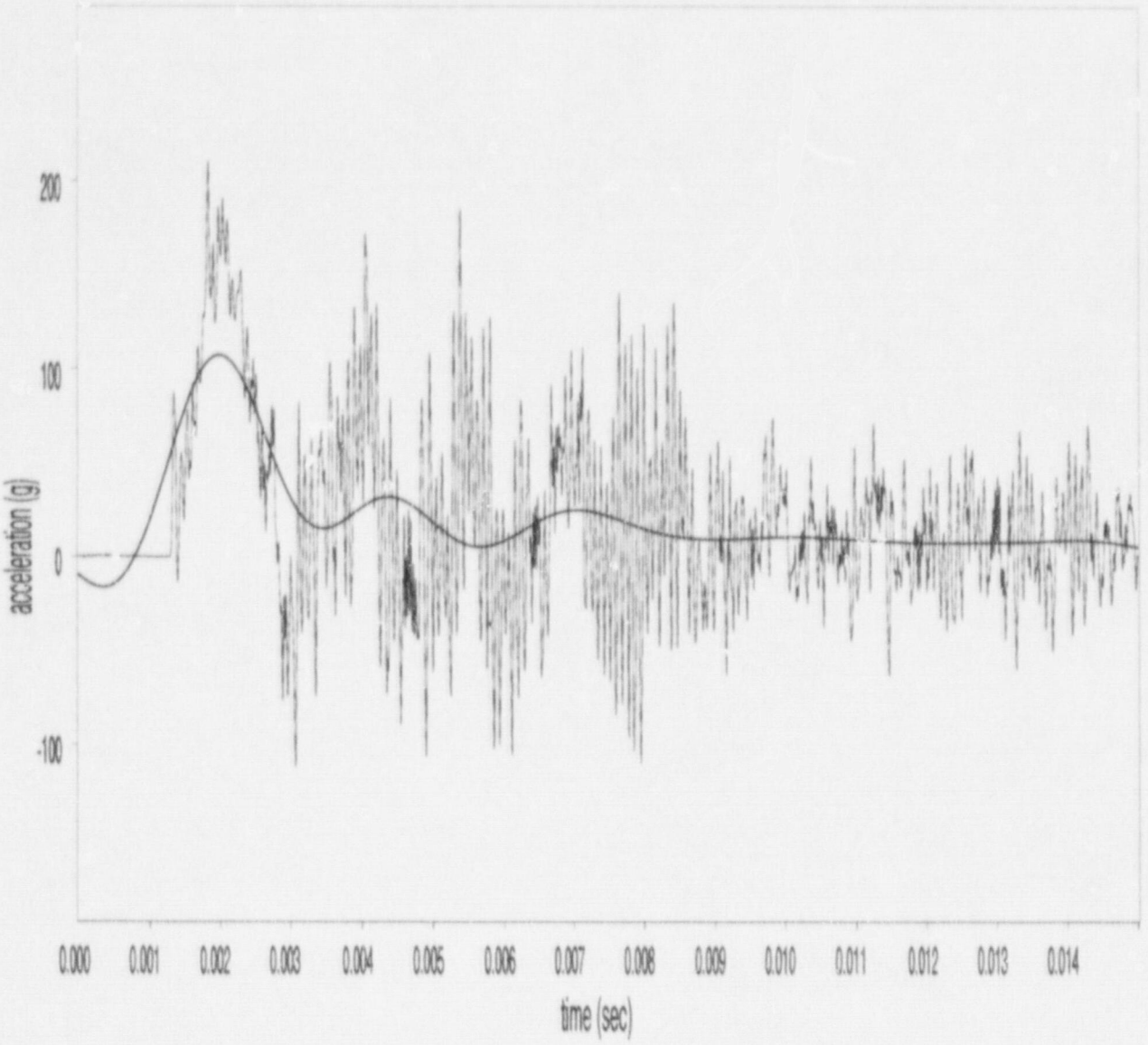

Figure B-45 Test #10, Gauge A4 (45.7-centimeter (18-inch) side drop, filter cutoff: 450 Hz, maximum acceleration: 107.0g)

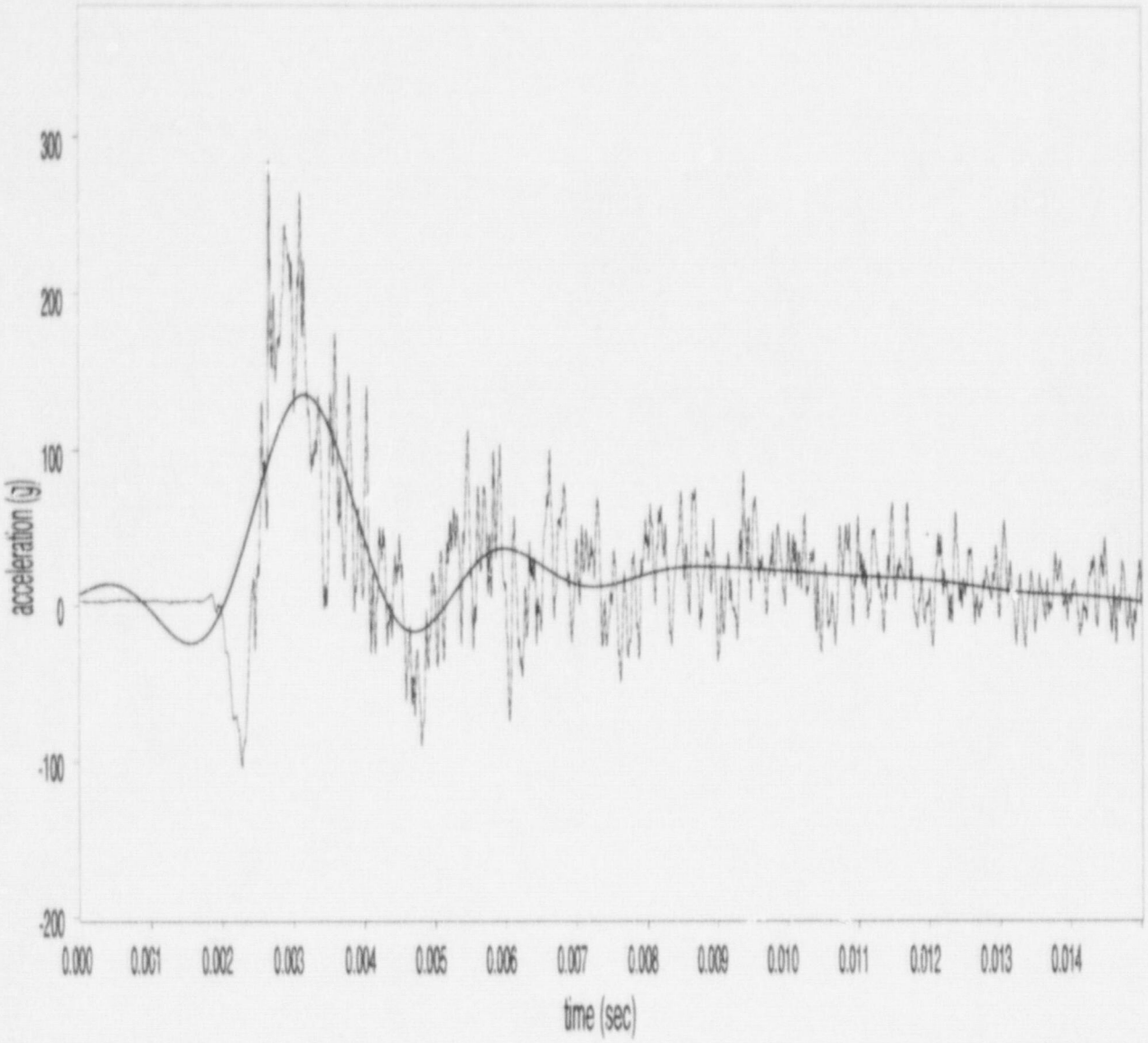

Figure B-46 Test #10, Gauge A5 (45.7-centimeter (18-inch) side drop, filter cutoff: 450 Hz, maximum acceleration: 135.3g)

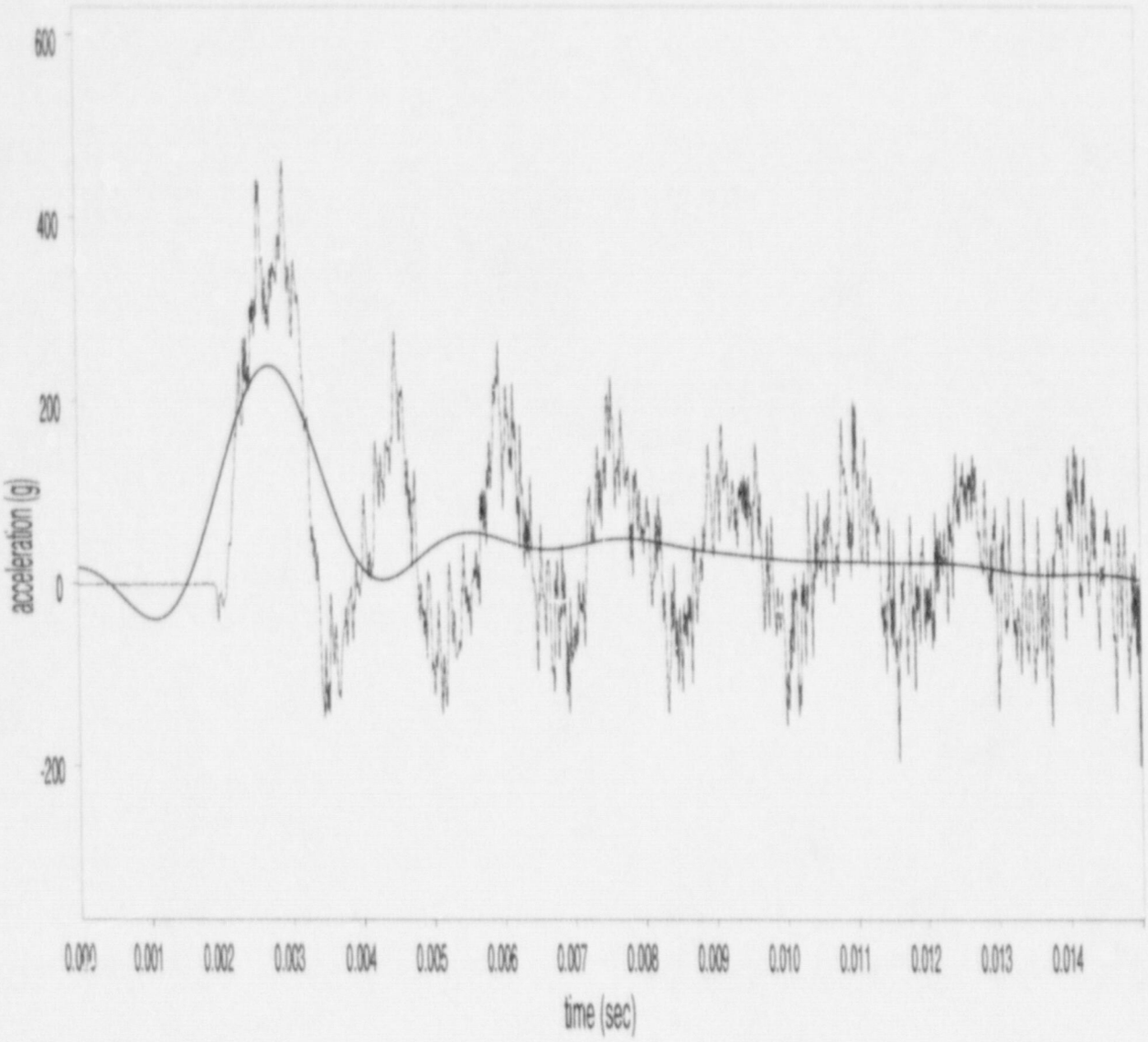

Figure B-47 Test #11, Gauge A1 (tipover, filter cutoff: 450 Hz, maximum acceleration: 237.5g)

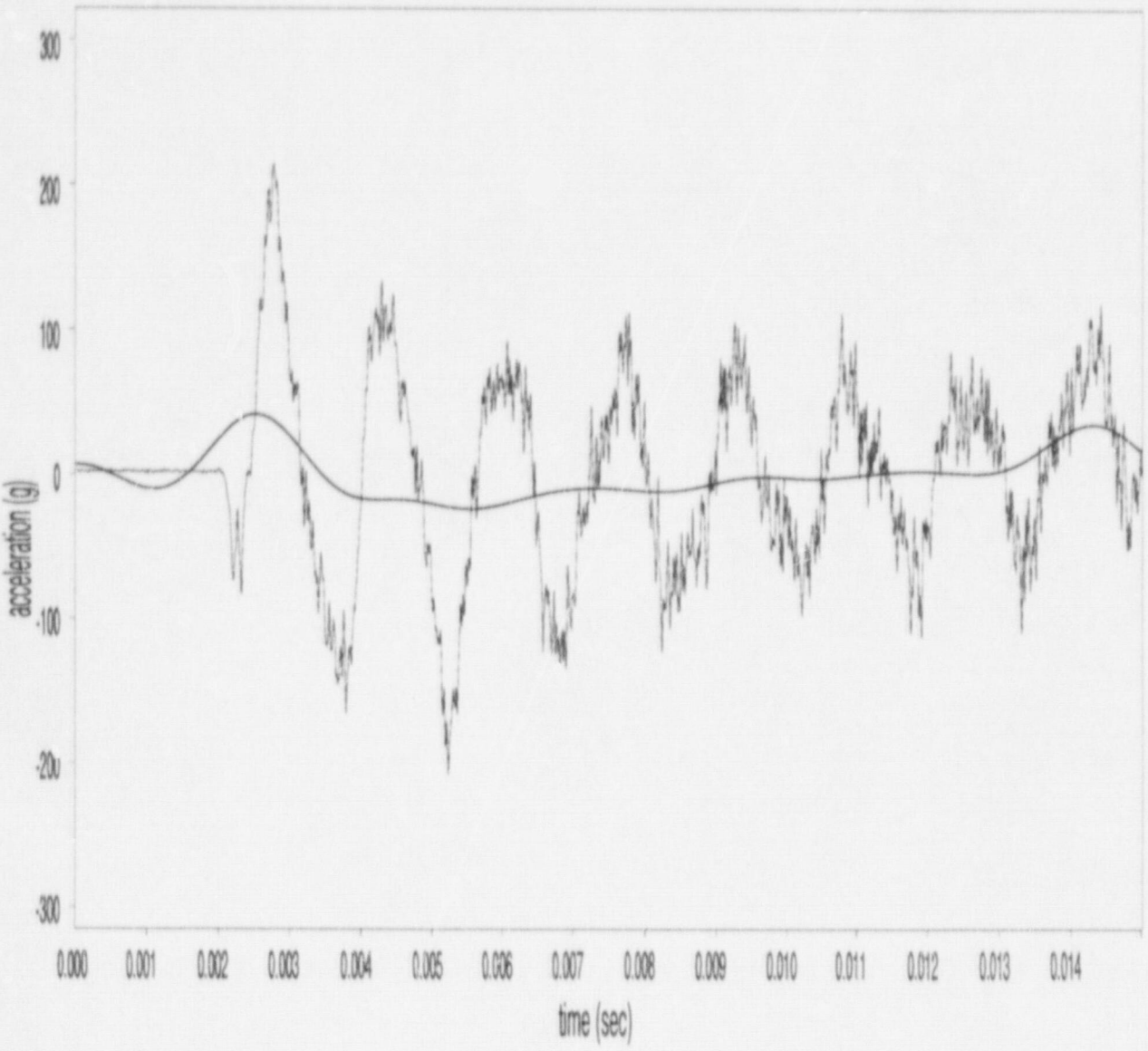

Figure B-4ª Test #11, Gauge A2 (tipover, filter cutoff: 450 Hz, maximum acceleration: 41.5g)

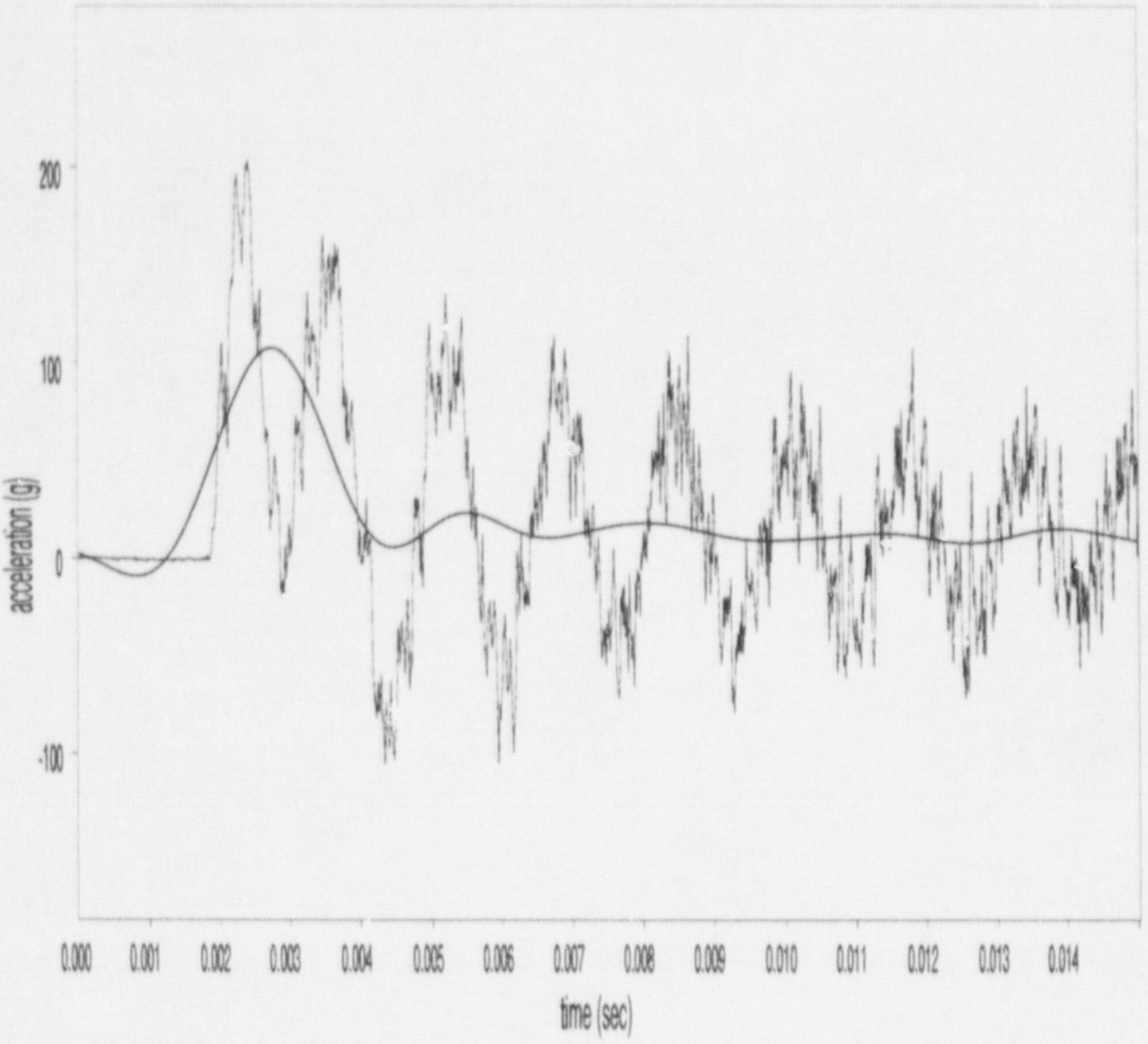

Figure B-49 Test #11, Gauge A3 (tipover, filter cutoff: 450 Hz, maximum acceleration: 107.3g)

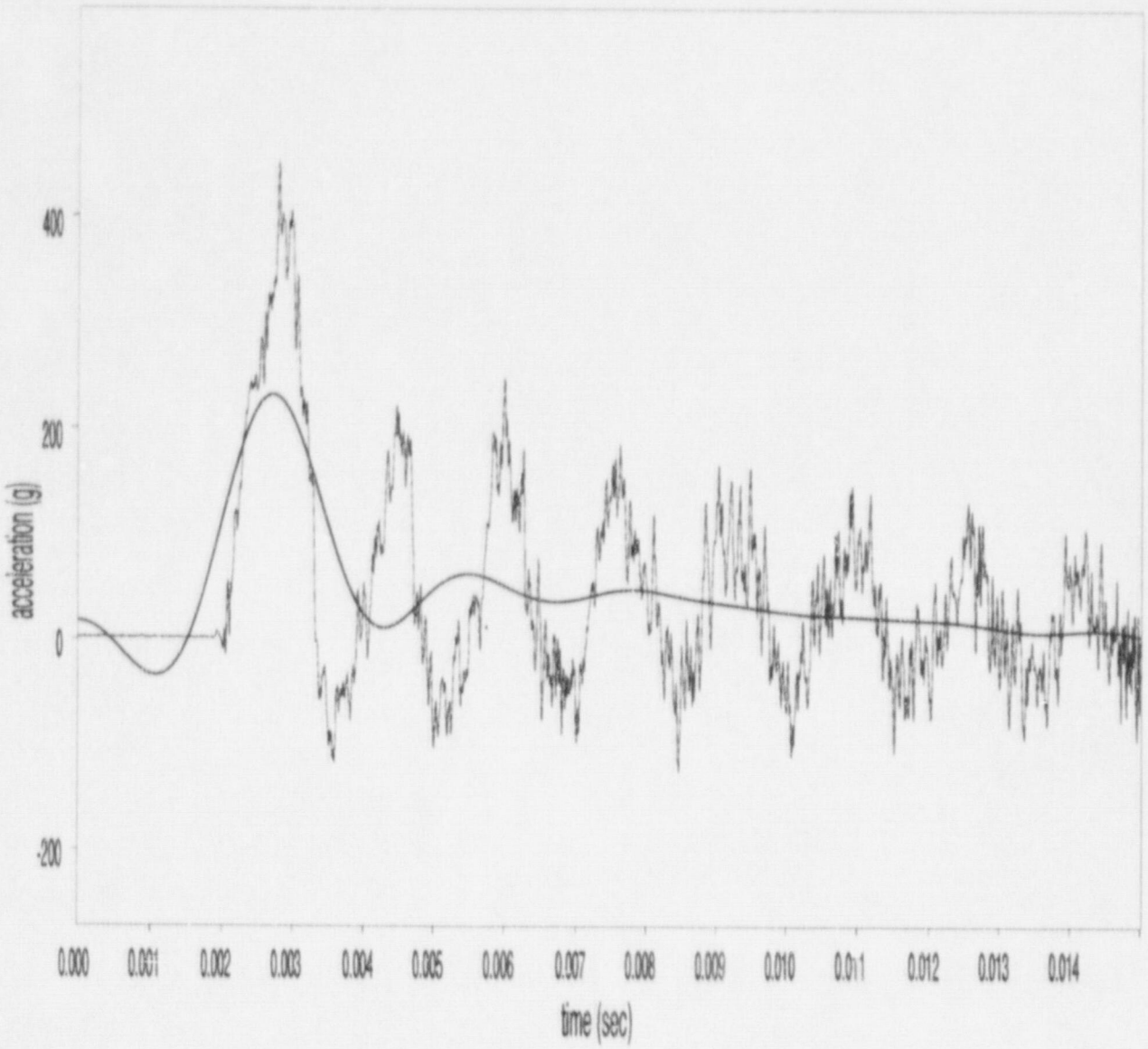

Figure B- 50 Test #11, Gauge A5 (tipover, filter cutoff: 450 Hz, maximum acceleration: 231.5g)

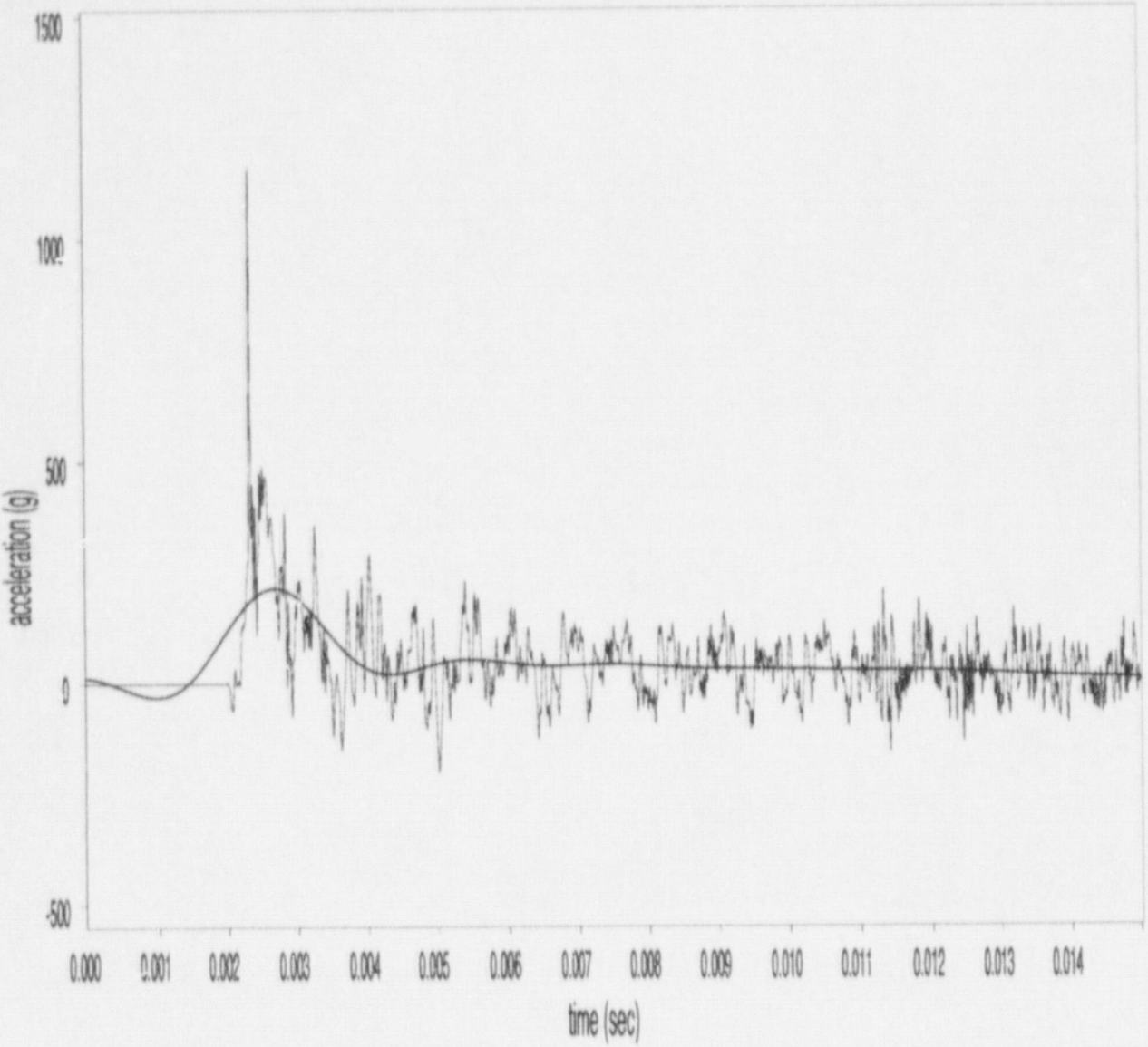

Figure B-51 Test #12, Gauge A1 (tipover, filter cutoff: 450 Hz, maximum acceleration: 213.6g)

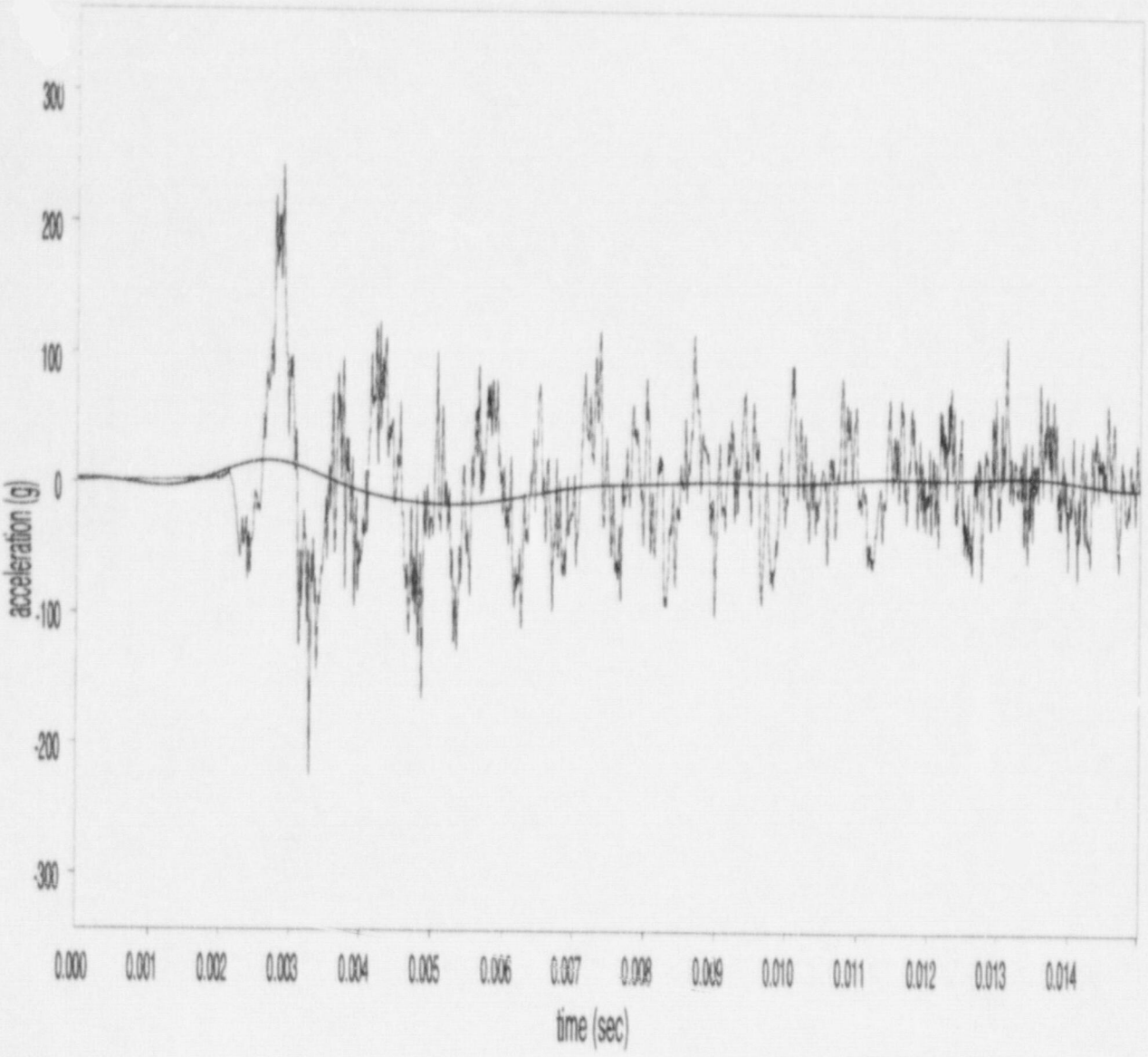

Figure B-52 Test #12, Gauge A2 (tipover, filter cutoff: 450 Hz, maximum acceleration: 17.1g)

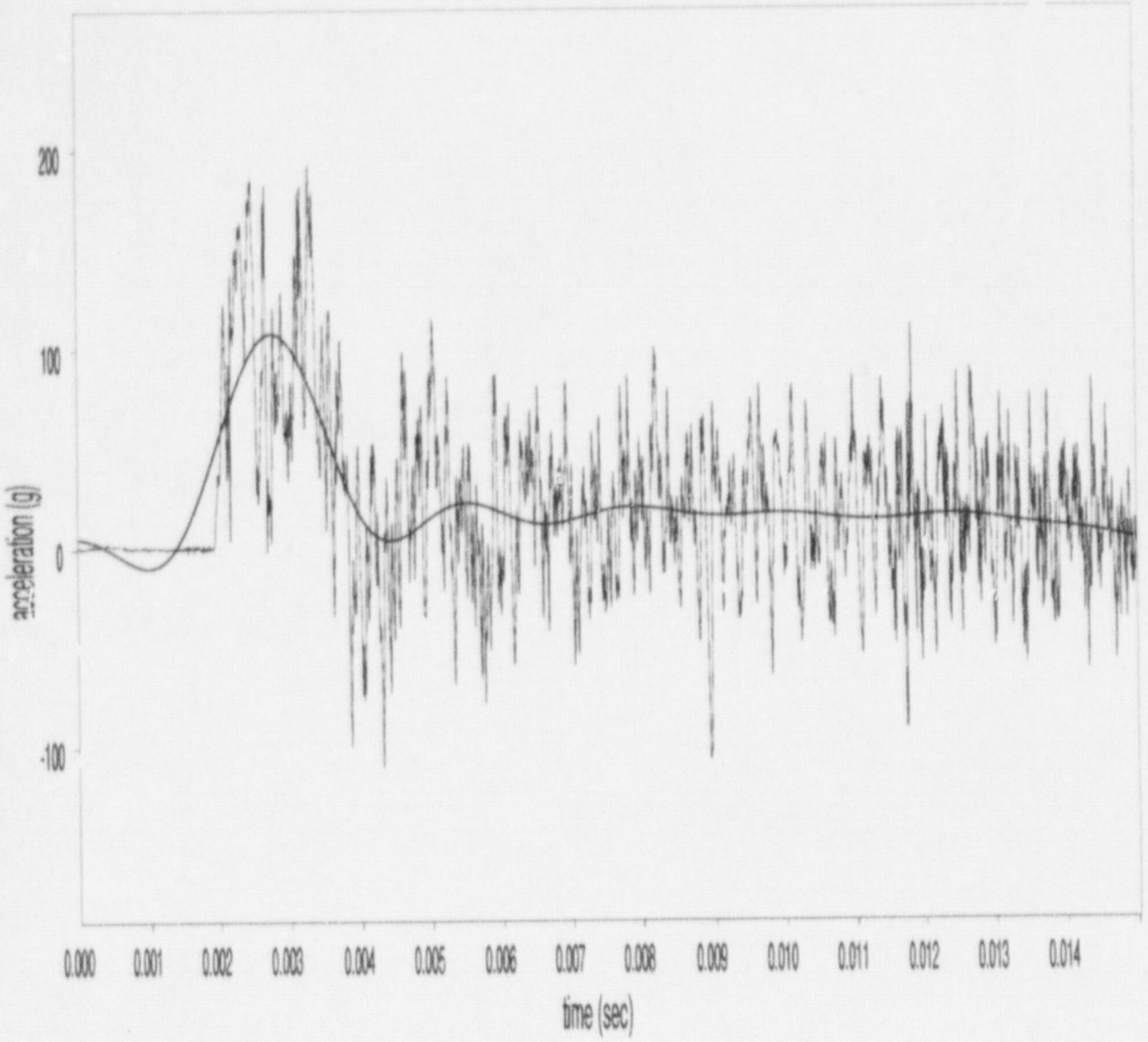

Figure B-53 Test #12, Gauge A3 (tipover, filter cutoff: 450 Hz, maximum acceleration: 107.8g)

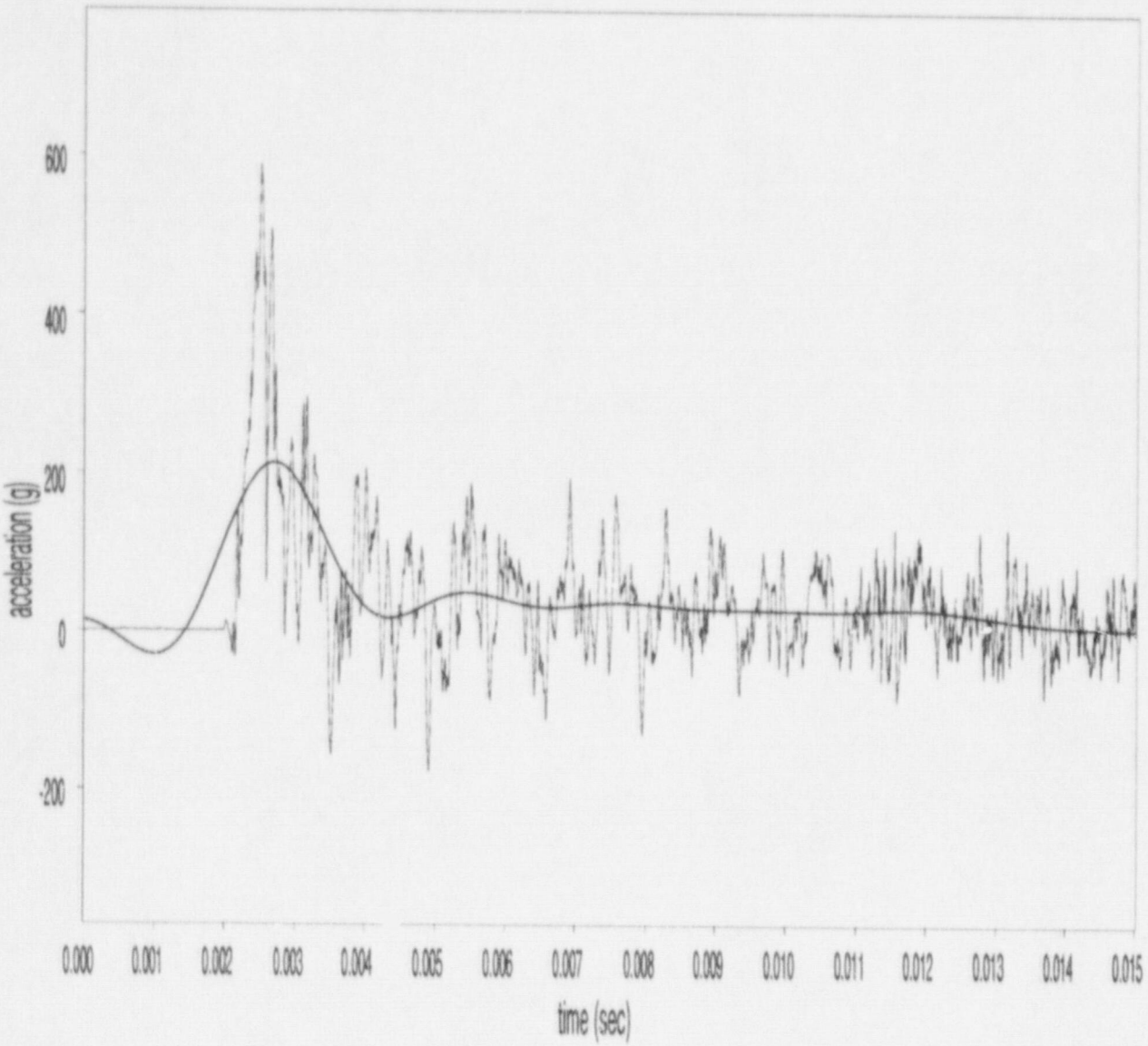

Figure B-54 Test #12, Gauge A5 (tipover, filter cutoff: 450 Hz, maximum acceleration: 213.0$_g$)

APPENDIX C. DETAILS OF CONCRETE MODEL

DYNA3D has an option for a concrete constitutive model known as Material Model 16, which was developed to give provide concrete and geologic material modeling capabilities to DYNA. For the finite element simulation described in this report, Mode II B was the option selected within Material Model 16, which was used with Equation of State Form 8. This option provides two yield vs. pressure curves, so that once the material has failed in compression, the model skips to the lower yield vs. pressure curve. The two yield-vs.-pressure curves are defined as the upper, or undamaged, curve, represented by

$$\sigma_{max} = \mathbf{a}_0 + \frac{\mathbf{P}}{\mathbf{a}_1 + \mathbf{a}_2\mathbf{P}},$$

where

σ_{max} = the material yield stress at the undamaged state

P = pressure

a_0, a_1, a_2 = material constants that characterize the yield-vs.-pressure relationship in the undamaged state

and the lower, or failed (damaged), curve is represented by

$$\sigma_{\mathbf{failed}} = \mathbf{a}_{0f} + \frac{\mathbf{P}}{\mathbf{a}_{1f} + \mathbf{a}_2\mathbf{P}},$$

where

σ_{failed} = the material yield stress at the damaged state

a_{0f}, a_{1f}, a_2 = material constants that characterize the yield-vs.-pressure relationship in the damaged state.

After defining these two curves and introducing an appropriate "damage" scale factor, η, the following equation is used

$$\sigma_{\mathbf{yield}} = \sigma_{\mathbf{failed}} + \eta\left(\sigma_{max} - \sigma_{\mathbf{failed}}\right),$$

to describe either a hardening or a softening phenomenon as commonly observed in the concrete material according to the amount of plastic strain produced in the material. The pressure-volumetric strain relationship of the material is treated independently of its deviatoric behavior and can be described by using a tabulated equation-of-state form. The volumetric strain, ε_V, is defined as the natural logarithm of the relative volume: $\varepsilon_V = \ln (V/V_0)$, and is negative in compression.

The maximum principal stress at tensile failure is set at an 870-psi cutoff. Since data on strain rate effects were unavailable, a constant load curve multiplier of unity was used.

Included below is a summary of the required input for DYNA3D used for the finite element simulations described in this report.[1]

mass density = 2.09675E-4 lb sec^2 / in^4

Poisson's ratio = .22

cohesion (a_0)= 2000 psi

pressure hardening coefficient (a_1)= 0.418

pressure hardening coefficient (a_2)= 0.0000835

pressure hardening coefficient for failed material (a1f)= 0.385

The effective plastic strain vs. η is shown below:

Effective Plastic Strain	Scale factor, η
0.0	0.0
0.00094	0.289
0.00296	0.465
0.00837	0.629
0.01317	0.774
0.0234	0.893
0.04034	1.0
1.0	1.0

[1] Note that values with English units are provided , since these are the values which were used in the described finite element simulations.

The pressure-volume behavior of the concrete is modeled in Equation of State Form 8 with a tabulated pressure-vs.-volumetric strain relationship:

Volumetric strain (ε_v)	Pressure (psi)
0.0	0.0
-0.006	4600
-0.0075	5400
-0.01	6200
-0.012	6600
-0.02	7800
-0.038	10000
-0.06	12600
-0.0755	15000
-0.097	18700

The unloading bulk modulus, K, is assumed to be a constant 700 ksi at any volumetric strain.

The material constants that characterize the yield-vs.-pressure relationship for the concrete in the damaged state and the "damage" scale factor are parameters described in the DYNA3D User's Manual for the specific material model employed.

APPENDIX D. ACCELERATION TRACES, FILTERED AND UNFILTERED, FOR FINITE ELEMENT ANALYSIS SIMULATION

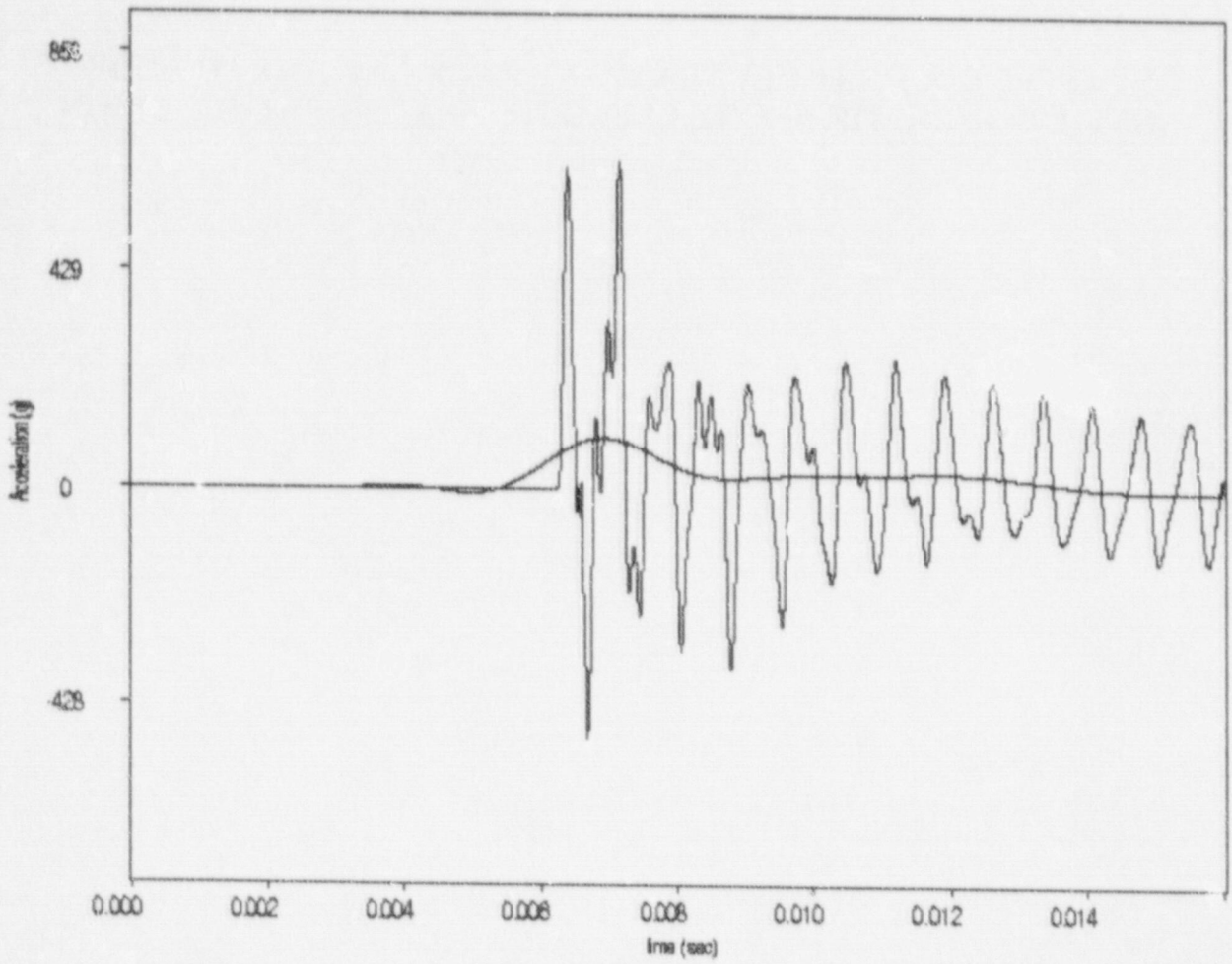

Figure D-1 Finite Element Analysis, Billet (45.7-centimeter (18-inch) end drop, filter cutoff: 450Hz, max. acceleration: 99.5g)

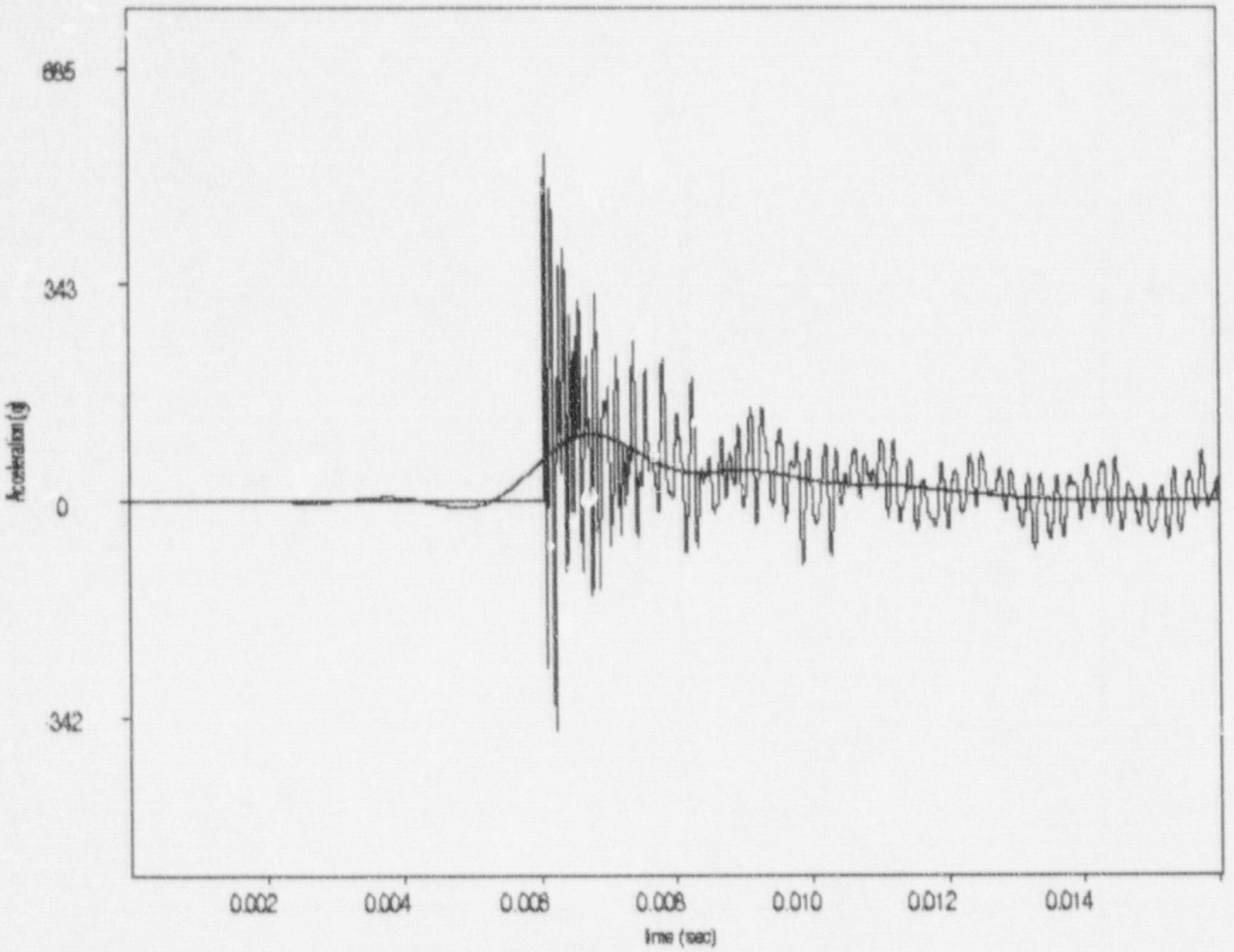

Figure D-2 Finite Element Analysis, Billet (45.7-centimeter (18-inch) side drop, filter cutoff: 450Hz, max. acceleration: 105g)

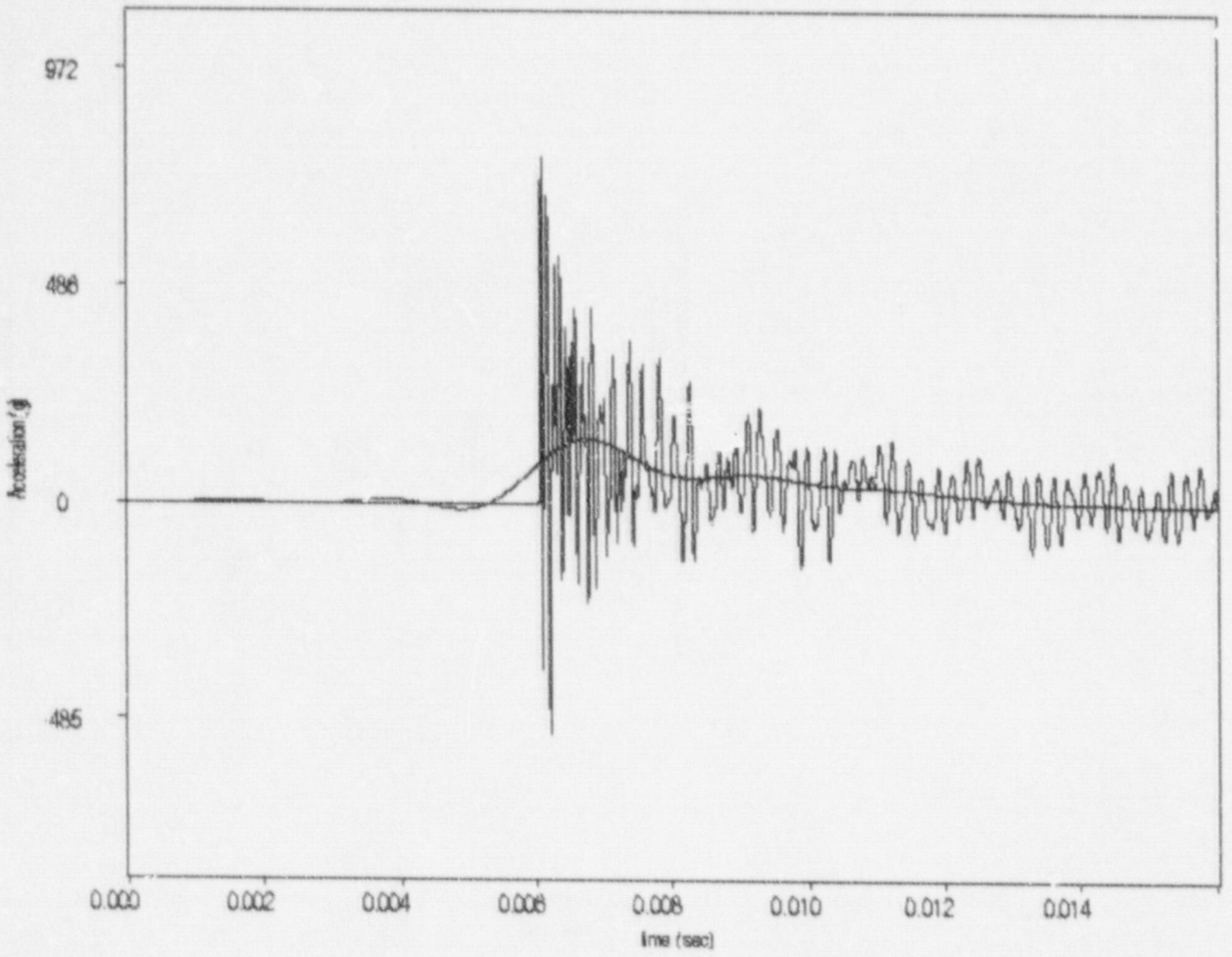

Figure D-3 Finite Element Analysis, Billet (91.4-centimeter (36-inch) side drop, filter cutoff: 450Hz, max. acceleration: 142.7g)

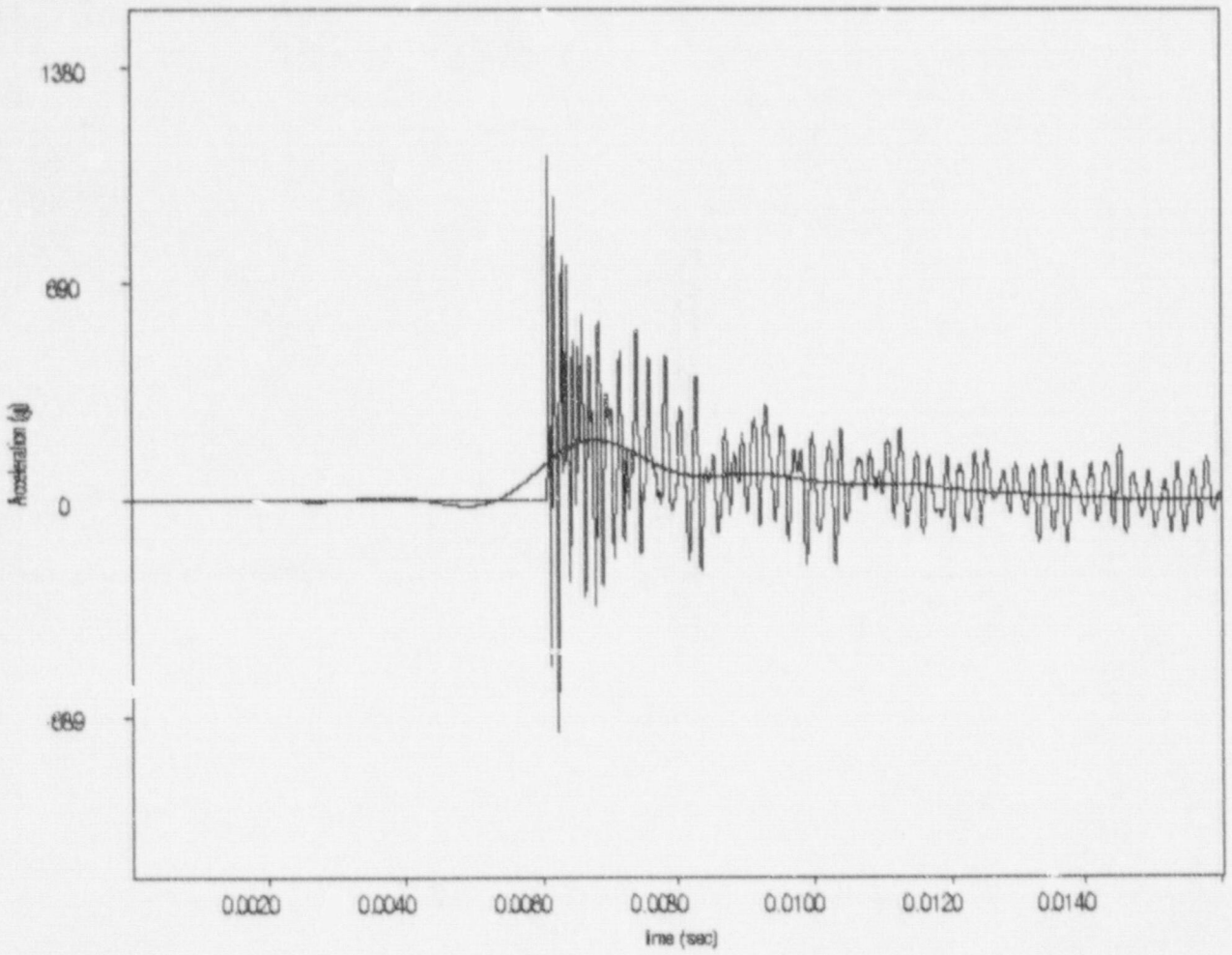

Figure D-4 Finite Element Analysis, Billet (1.83-meter (72-inch) side drop, filter cutoff: 450Hz, max. acceleration: 190.1g)

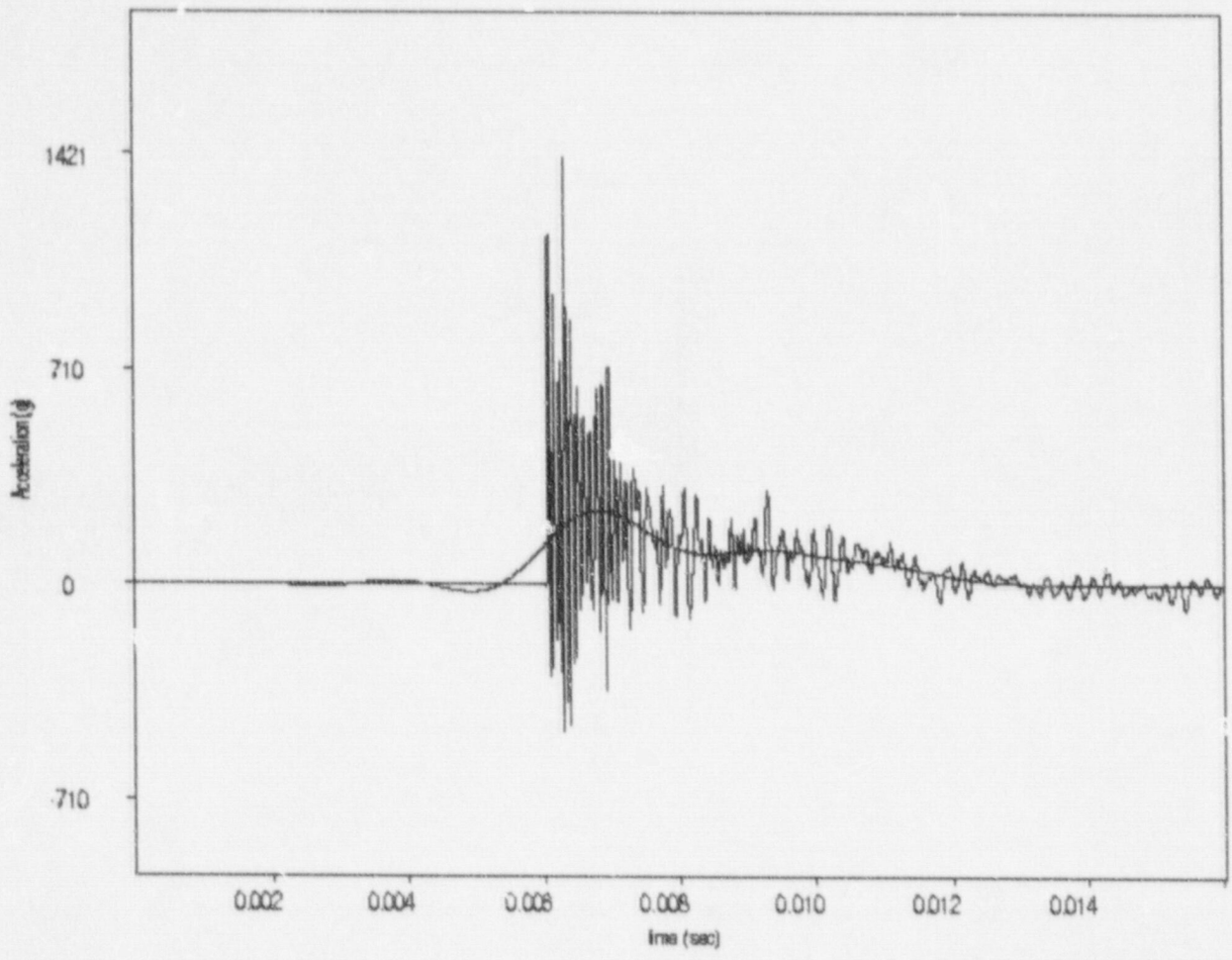

Figure D-5 Finite Element Analysis, Billet (tipover, filter cutoff: 450Hz, max. acceleration: 244.7g)

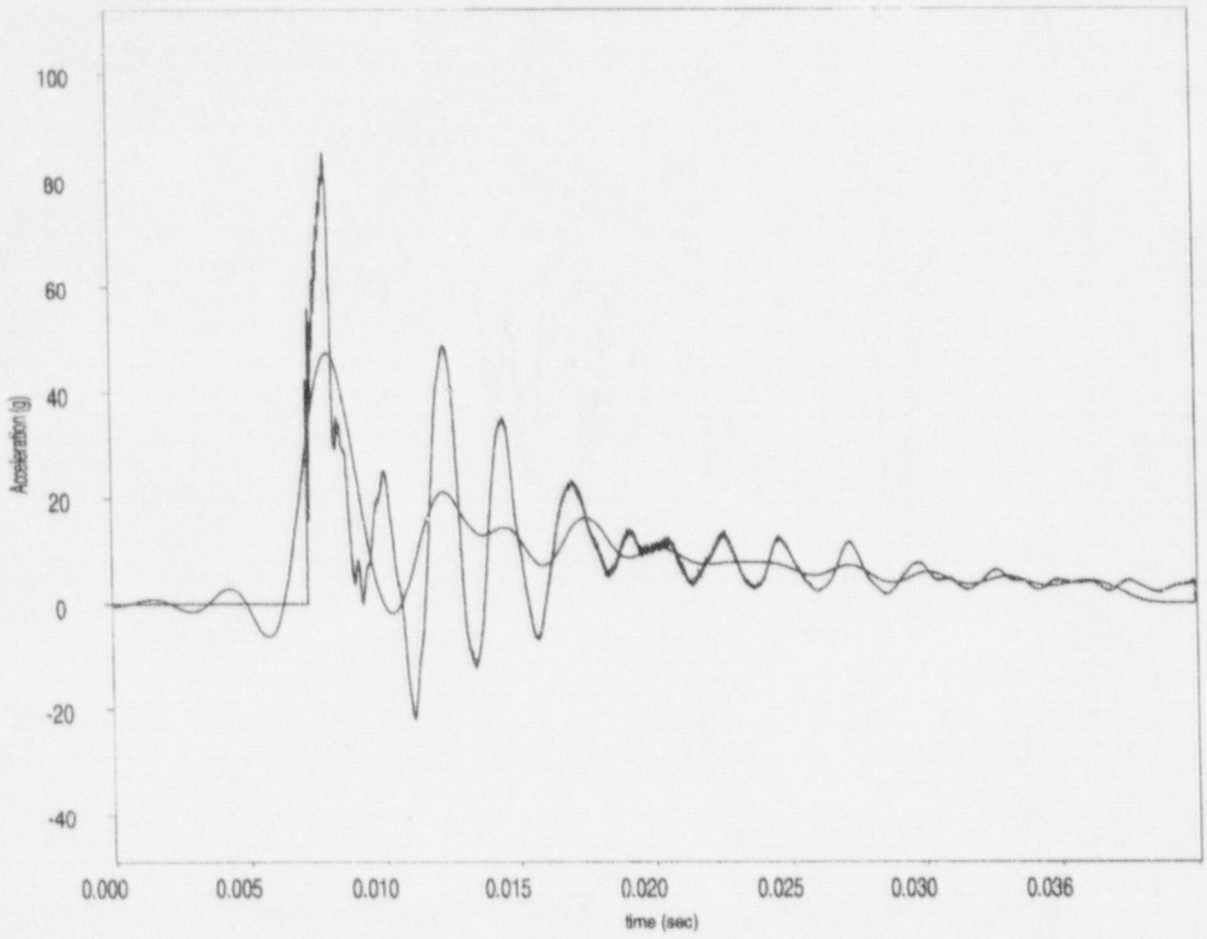

Figure D-6 Finite Element Analysis, Generic Cask (45.7-centimeter (18-inch) end drop, filter cutoff: 350Hz, max. acceleration: 47.3g averaged through the cask wall)

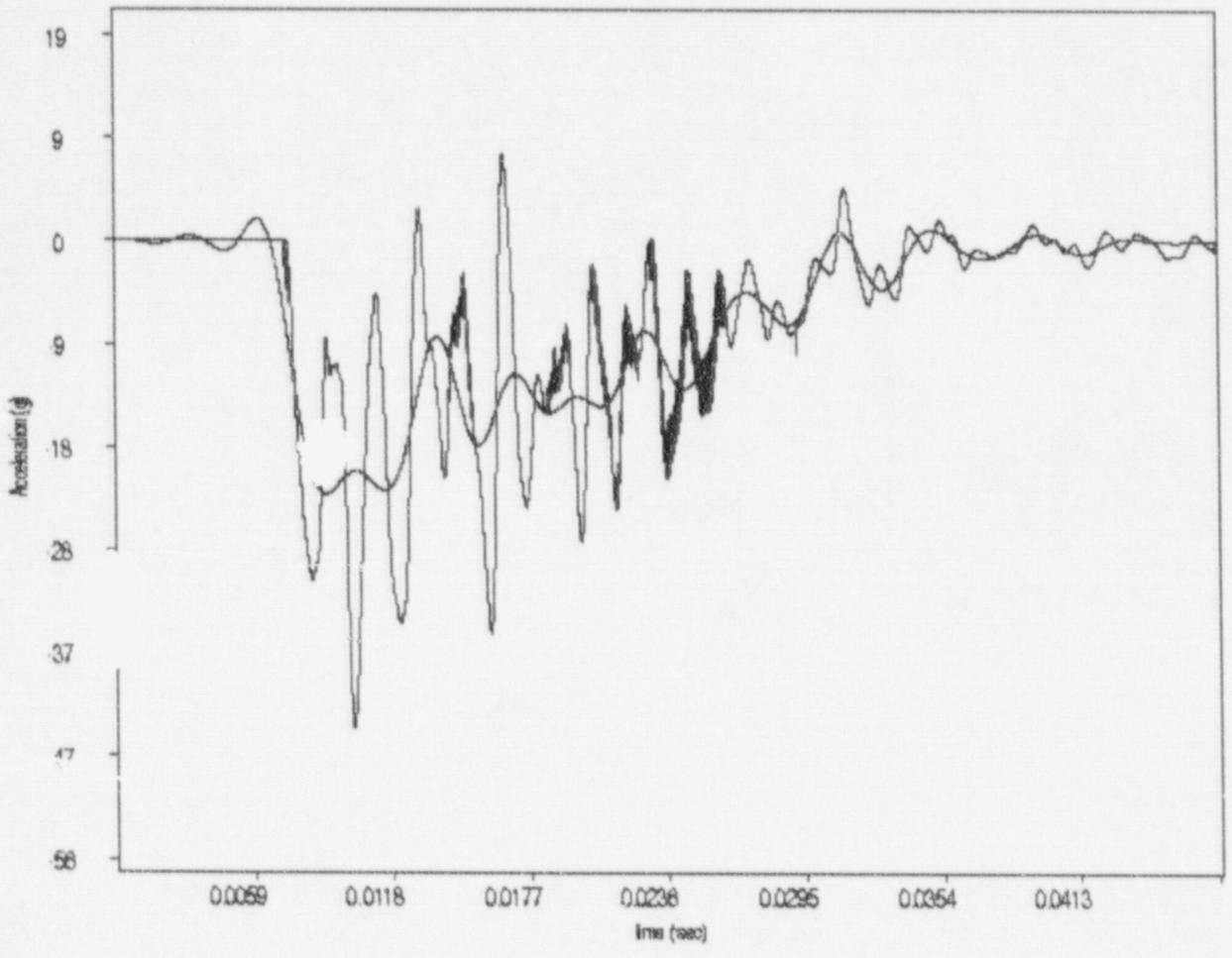

Figure D-7 Finite Element Analysis, Generic Cask (45.7-centimeter (18-inch) side drop, filter cutoff: 350 Hz, max. acceleration: 23.2g)

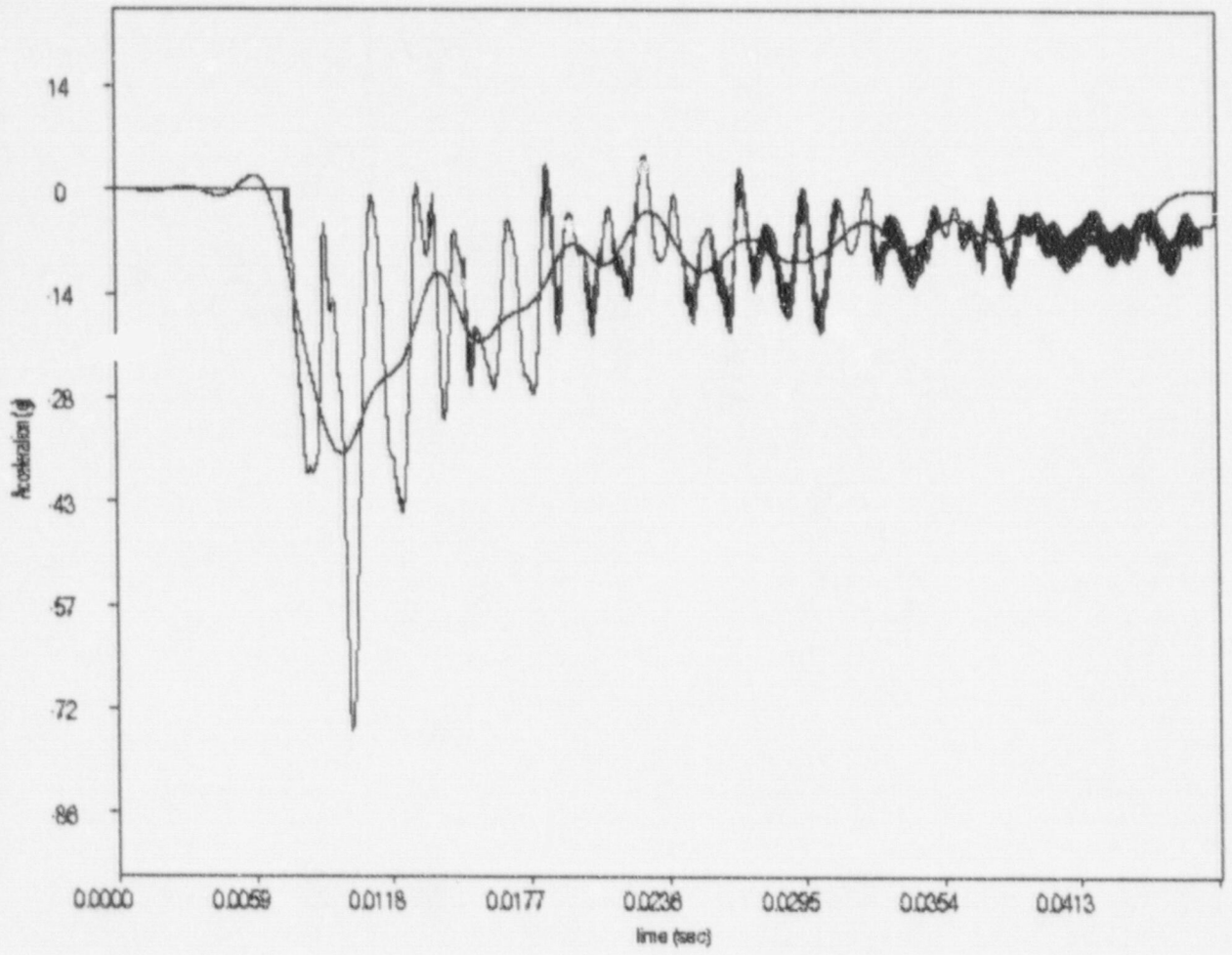

Figure D-8 Finite Element Analysis, Generic Cask (91.4-centimeter (36-inch) side drop, filter cutoff: 350Hz, max. acceleration: 36.5g)

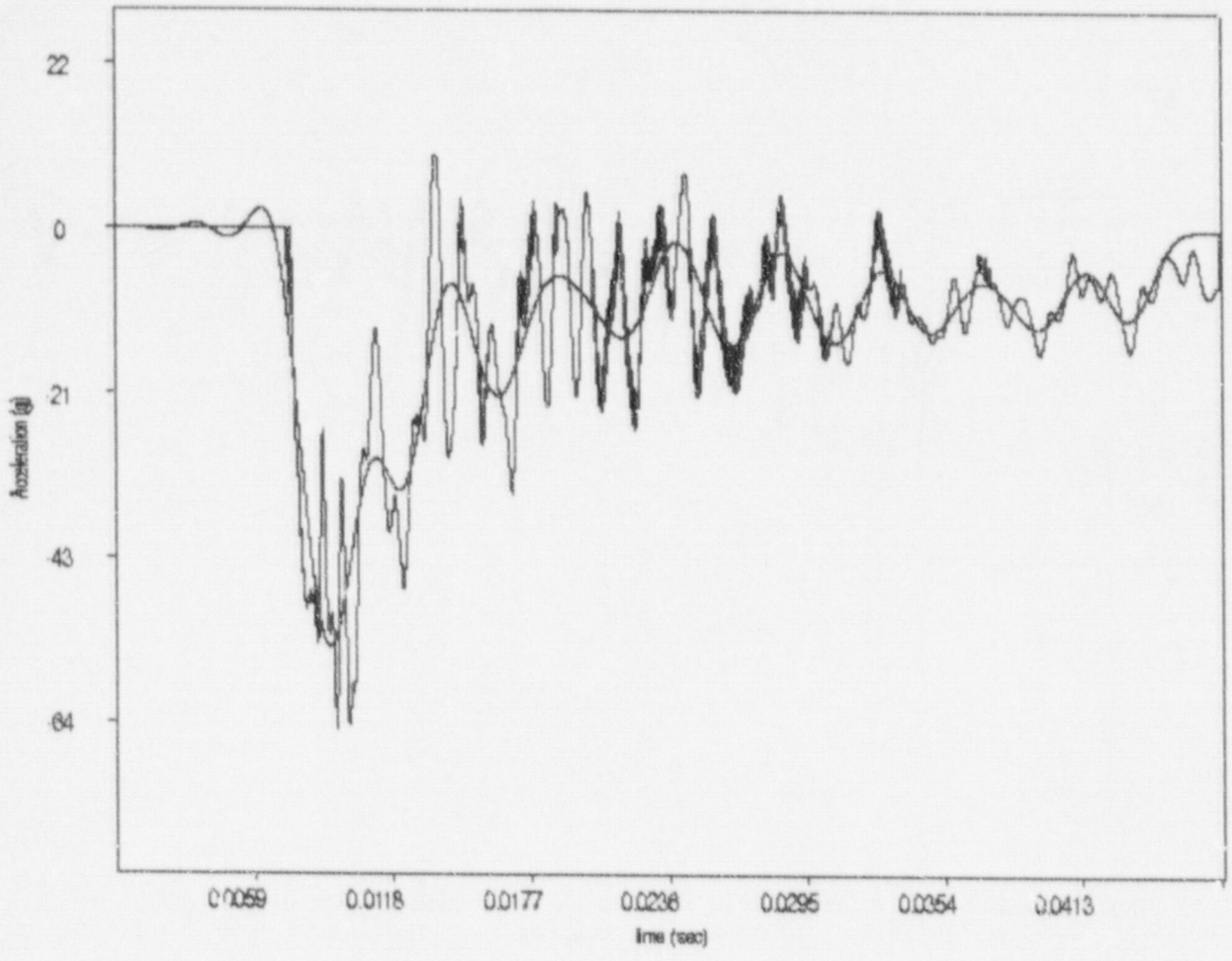

Figure D-9 Finite Element Analysis, Generic Cask (1.83-meter (72-inch) side drop, filter cutoff: 350Hz, max. acceleration: 54.8g)

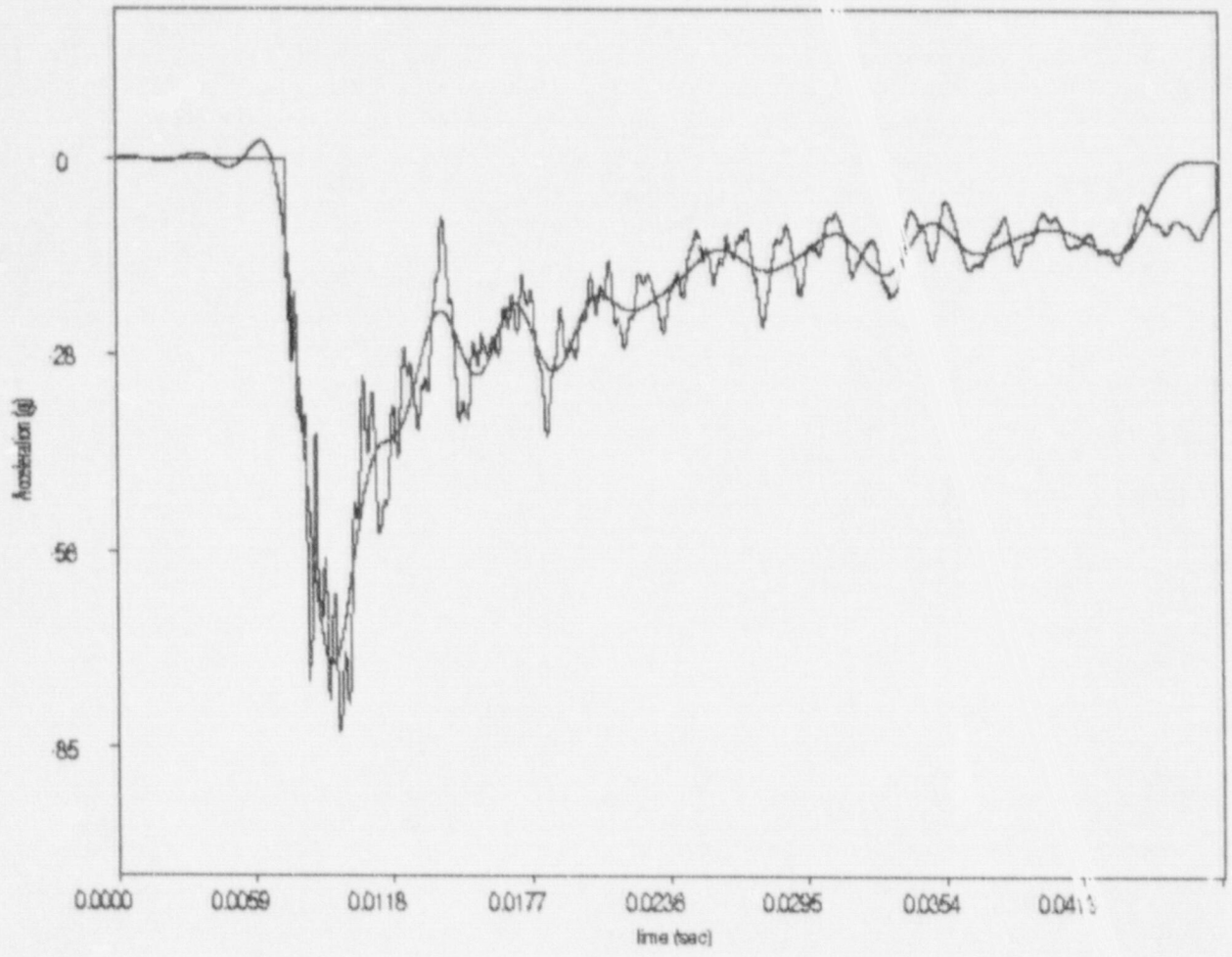

Figure D-10 Finite Element Analysis, Generic Cask (tipover, filter cutoff: 350Hz, max. acceleration: 73.2g)

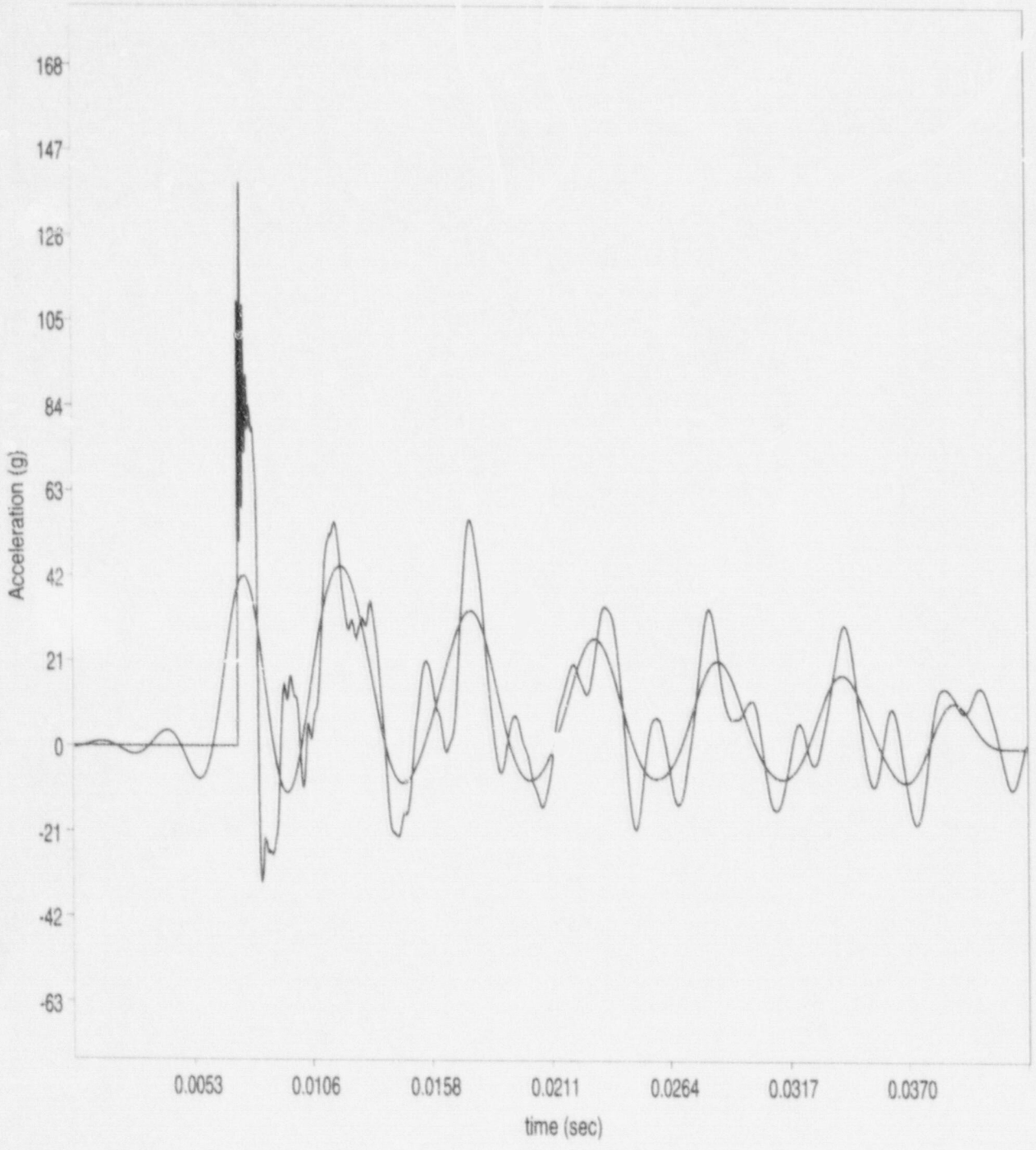

Figure D-11 Finite Element Analysis, Generic Cask Hollow Model (18-in end drop, filter cutoff: 350Hz, max. acceleration: 44.5g averaged through the end cap)

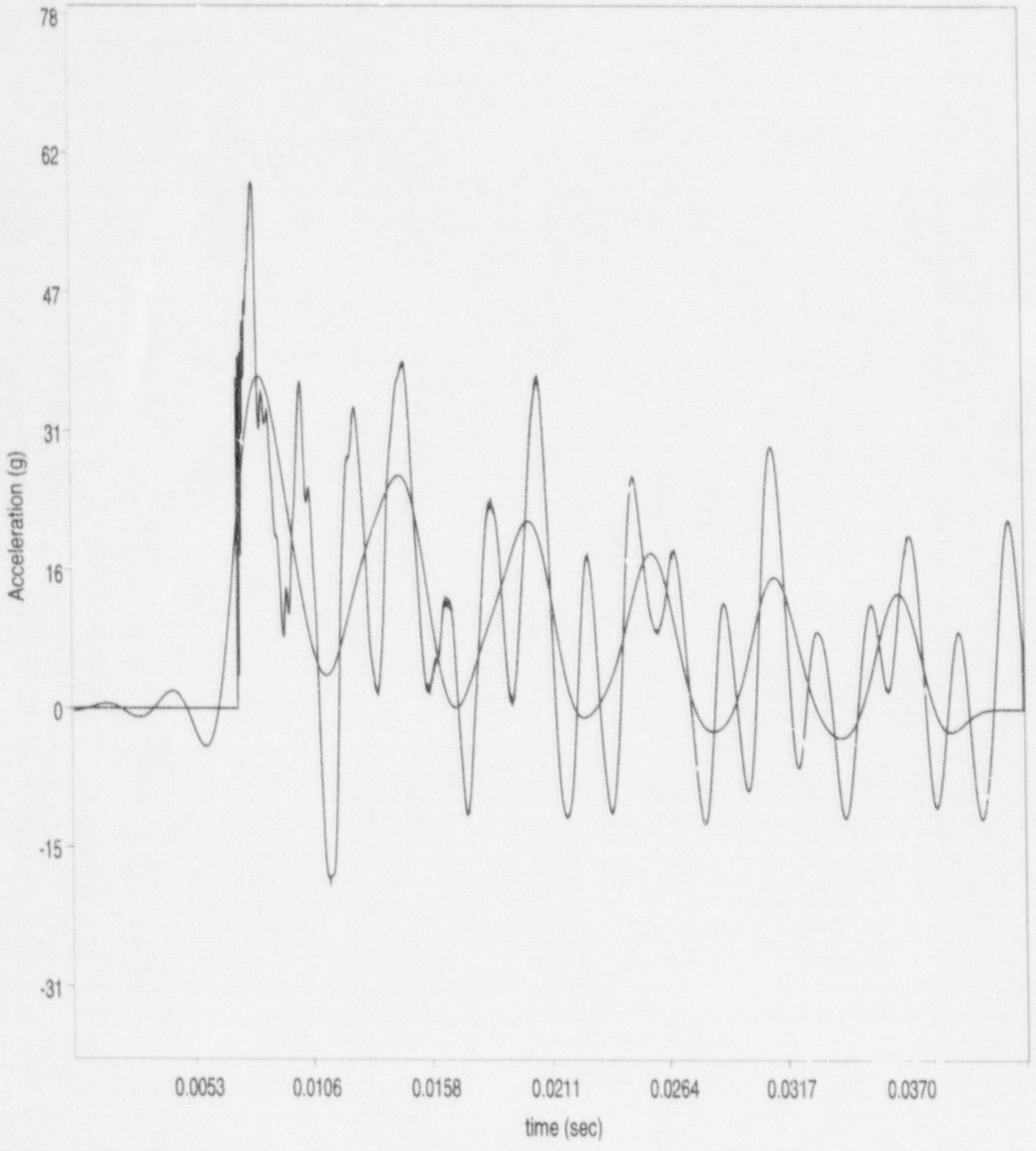

Figure D-12 Finite Element Analysis, Generic Cask Hollow Model (18-in end drop, filter cutoff: 350Hz, max. acceleration: 37.1g averaged through the cask wall)

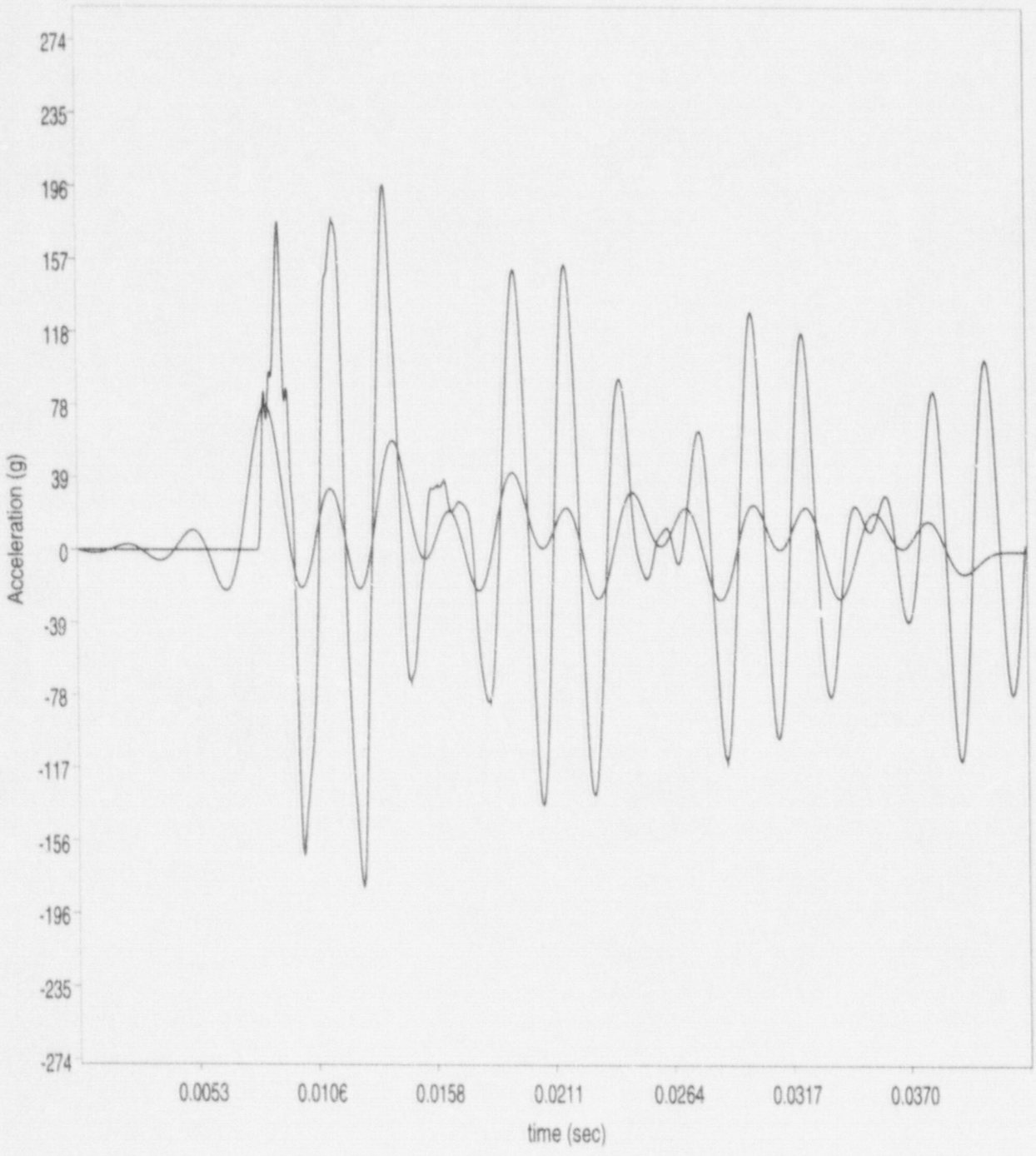

Figure D-13 Finite Element Analysis, Generic Cask Hollow Model (18-in end drop, filter cutoff: 350Hz, max. acceleration: 78.0g averaged through the cask lid)

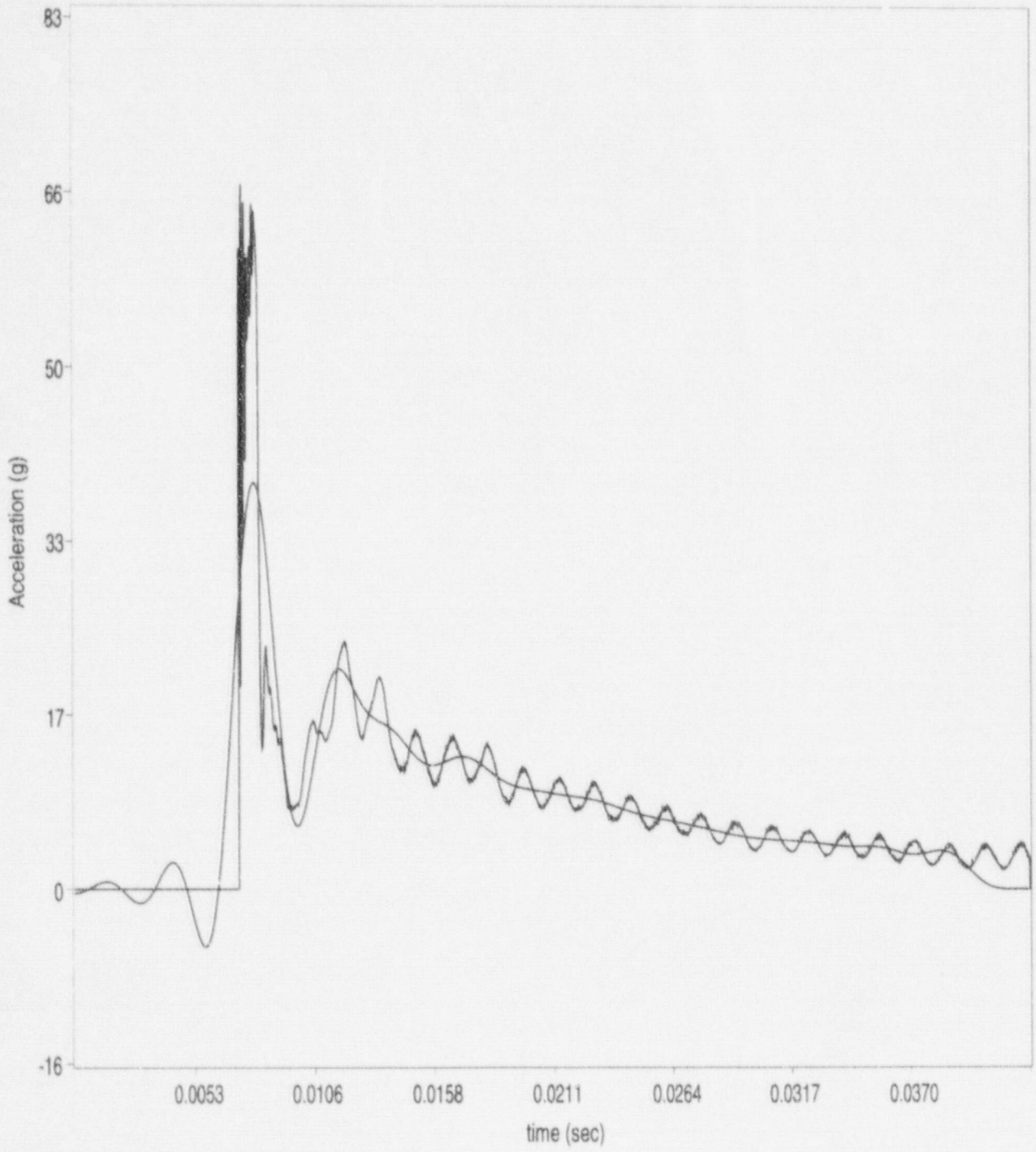

Figure D-14 Finite Element Analysis, Generic Cask Solid Homogeneous Model (18-in end drop, filter cutoff: 350Hz, max. acceleration: 38.6g averaged through the cask body)

NRC FORM 335 (2-89) NRCM 1102, 3201, 3202

U.S. NUCLEAR REGULATORY COMMISSION

BIBLIOGRAPHIC DATA SHEET

(See instructions on the reverse)

1. REPORT NUMBER (Assigned by NRC, Add Vol., Supp., Rev., and Addendum Numbers, if any.)

NUREG/CR-6608
UCRL-i29211

2. TITLE AND SUBTITLE

Summary and Evaluation of Low-Velocity Impact Test of Solid Steel Billet Onto Concrete Pads

3. DATE REPORT PUBLISHED

MONTH	YEAR
February	1998

4. FIN OR GRANT NUMBER

A0293

5. AUTHOR(S)

M. C. Witte, J. Hovingh, G. C. Mok,
S. S. Murty, T. F. Chen, L. E. Fischer

6. TYPE OF REPORT

Final

7. PERIOD COVERED (Inclusive Dates)

8. PERFORMING ORGANIZATION – NAME AND ADDRESS (If NRC, provide Division, Office or Region, U.S. Nuclear Regulatory Commission, and mailing address; if contractor, provide name and mailing address.)

Lawrence Livermore National Laboratory
7000 East Ave.
P.O. Box 808, L-631
Livermore, CA 94550

9. SPONSORING ORGANIZATION – NAME AND ADDRESS (If NRC, type "Same as above"; if contractor, provide NRC Division, Office or Region, U.S. Nuclear Regulatory Commission, and mailing address.)

Spent Fuel Project Office
Office of Nuclear Material Safety and Safeguards
U.S. Nuclear Regulatory Commission
Washington, DC 20555-0001

10. SUPPLEMENTARY NOTES

D. T. Tang, NRC Technical Monitor

11. ABSTRACT (200 words or less)

Spent fuel storage casks intended for use at independent spent fuel storage installations are evaluated during the application and review process for low-velocity impacts representative of possible handling accidents. In the past, the analyses involved in these evaluations have assumed that the casks dropped or tipped onto an unyielding surface—a conservative and simplifying assumption. Applicants are currently seeking a more realistic model for the analyses to predict the effect of a cask dropping onto a reinforced concrete pad, including energy absorbing aspects such as cracking and flexure. To develop data suitable for benchmarking these analyses, the NRC has conducted several series of drop-test studies of a solid steel billet and of a near-full-scale empty cask. This report contains a summary and evaluation of all steel billet testing conducted by Sandia National Laboratories and Lawrence Livermore National Laboratory. A series of finite element analyses of the billet testing is described and benchmarked against the test data. A method to apply the benchmarked finite element model of the soil and concrete pad to an analysis of a full-size storage cask is provided. In addition, an application to a "generic" full-size cask is presented for side and end drops, and tipover events.

12. KEY WORDS/DESCRIPTORS (List words or phrases that will assist researchers in locating the report.)

cask storage
drop tests
10 CFR 72
Billet drop tests

13. AVAILABILITY STATEMENT

unlimited

14. SECURITY CLASSIFICATION

(This Page)
unclassified
(This Report)
unclassified

15. NUMBER OF PAGES

16. PRICE

Federal Recycling Program

UNITED STATES
NUCLEAR REGULATORY COMMISSION
WASHINGTON, DC 20555-0001

OFFICIAL BUSINESS
PENALTY FOR PRIVATE USE, $300

SPECIAL STANDARD MAIL
POSTAGE AND FEES PAID
USNRC
PERMIT NO. G-67

120555154486 1 1AN1RW155156
US NRC-OIRM
TPS-PDR-NUREG
2WFN-6E7
WASHINGTON DC 20555

UNITED STATES
NUCLEAR REGULATORY COMMISSION
WASHINGTON, DC 20555-0001

OFFICIAL BUSINESS
PENALTY FOR PRIVATE USE, $300

SPECIAL STANDARD MAIL
POSTAGE AND FEES PAID
USNRC
PERMIT NO. G-67

1205551544B6 1 1ANIRW155150
US NRC-OIRM
TPS-PDR-NUREG
2WFN-6E7
WASHINGTON DC 20555